Modelling the fate of secondary inorganic aerosol and its precursors over Europe

Dissertation

zur Erlangung des akademischen Grades
Doktor der Naturwissenschaften
am Fachbereich Geowissenschaften
der Freien Universität Berlin

Vorgelegt von
Sabine Banzhaf

Mai 2014

Gutachter:
Prof. Dr. Peter Builtjes
Prof. Dr. Uwe Ulbrich

Tag der Disputation: 20.06.2014

Table of Contents

List of Figures

List of Tables

Summary

Secondary inorganic aerosol (SIA), which are sulphate, nitrate and ammonium, is involved in the eutrophication and acidification of ecosystems, the formation of health relevant particulate matter (PM) and climate change by affecting the radiation balance of the earth. A thorough understanding of the SIA budget is of scientific interest and is required to be able to devise emission mitigation strategies that are effective for biodiversity, climate change and human health. SIA concentrations and the deposition of sulphur and nitrogen compounds show non-linear responses to emission changes of sulphur dioxide, nitrogen oxides and ammonia. At the start of this study CTMs did not incorporate all processes leading to these non-linearities and previous studies highlighted that the performance of these models showed clear deficiencies in comparison to observations. Within the here presented study the process description of SIA formation and wet removal is improved within two state-of-the-art regional CTMs followed by a comprehensive operational and dynamic evaluation of the models against observations with the focus on the non-linearity aspects.

The chemical transport model REM-Calgrid (RCG) has been improved by the implementation of pH dependent aqueous-phase sulphate formation. Furthermore, a new wet deposition scheme including cloud liquid water content dependent in-cloud scavenging and pH dependent droplet saturation has been incorporated. A model sensitivity study varying cloud and rain droplet pH within atmospheric ranges has revealed a significant impact on resultant SIA air concentrations and wet deposition fluxes of sulphur and nitrogen compounds. It was found that the effect on sulphate formation in clouds in between precipitation events and prior to rain out dominates the impact of pH variations. Furthermore, a model run using modelled droplet pH has been performed and compared to a model run applying a constant pH of 5 and to observations. The results have revealed that using a modelled droplet pH is preferable to using a constant pH leading to an increased model performance and better consistency concerning air concentrations and wet deposition fluxes.

Using the improved RCG model system two PM episodes over Central Europe characterized by a high SIA contribution have been analysed. The model performed well in

capturing the temporal variation of the SIA concentrations and was successfully used to analyse the origin, development and characteristics of the episodes. To investigate the response of SIA concentrations to precursor emission changes several model runs for different emission scenarios varying emissions of sulphur dioxide, nitrogen dioxide and ammonia have been performed. The results confirmed that the response of SIA concentrations and sulphur and nitrogen deposition fluxes to precursor emission changes is non-linear. The deviation from linearity was found to be lower for total deposition fluxes than for SIA concentrations. Furthermore, it was shown that the incorporation of the pH dependent aqueous phase chemistry adds non-linear responses to the system and significantly modifies the models' response to precursor emission variations compared to when using a constant droplet pH. The analysis of emission reduction scenario runs performed on a domain covering Germany and a domain covering Europe has demonstrated that next to European-wide emission reductions, additional national ammonia emission measures in Germany are more effective in reducing SIA concentrations and deposition fluxes than additional national measures on sulphur dioxide and nitrogen dioxide.

Finally, a dynamic model evaluation over Europe from 1990 to 2009 has been performed using observations at European rural background sites. Therefore, the improved aqueous phase chemistry scheme was implemented in the LOTOS-EUROS model as the latter includes a source apportionment module that enables the analysis of changes in SIA formation efficiency over time. The analysis of the observed trends has confirmed former studies showing that the trends in sulphate and total nitrate concentrations from 1990 to 2009 are significantly lower than the trends in precursor emissions and precursor concentrations. The model was able to capture these non-linear responses to the emission changes. Using the source apportionment module trends in SIA formation efficiency have been quantified for four European regions/countries ('The Netherlands and Belgium', 'Baltic Sea', 'Czech Republic' and 'Romania'). Increases in formation efficiency have been found for sulphate in all regions (increases of about 20-60%) and for nitrate in the Benelux region and Czech Republic (increases of up to 20%) showing that changes in the formation efficiency due to changes in the chemical regime from 1990 to 2009 are at the basis of the observed non-linearity.

With this modelling study, added knowledge and an improved understanding has been obtained with respect to the non-linearity between emissions of sulphur and nitrogen compounds and the resulting concentrations and deposition fluxes.

Zusammenfassung

Sekundäre anorganische Aerosole (= Sulfat, Nitrat und Ammonium, aus dem Englischen zusammengefasst unter der Abkürzung SIA) tragen zur Versauerung und Eutrophierung von Ökosystemen bei, bedingen einen bedeutenden Anteil von PM_{10} (= Partikel mit einem aerodynamischen Durchmesser kleiner 10 μm) und tragen durch ihre Beeinflussung des Strahlungshaushaltes der Erde zum Klimawandel bei. Ein detailliertes Verständnis des SIA Budgets ist von wissenschaftlichem Interesse und nötig, um Emissionsminderungsstrategien zur effektiven Reduzierung von SIA zu entwickeln, um die negativen Auswirkungen auf Umwelt und Mensch einzudämmen. SIA Konzentrationen und die Depositionen von Schwefel- und Stickstoffverbindungen verhalten sich nichtlinear zu Emissionsänderungen der Vorläuferstoffe Schwefeldioxid, Stickstoffoxiden und Ammoniak. Zu Beginn der vorliegenden Studie wurden nicht alle Prozesse, die zu diesen Nichtlinearitäten führen in state-of-the-art Chemie-Transportmodellen berücksichtigt. Des Weiteren belegten mehrere vorausgehenden Studien, dass Ergebnisse dieser Modelle bei Vergleichen mit Beobachtungen deutlich von diesen abwichen. Innerhalb der hier präsentierten Studie wurde daher die Prozessbeschreibung der Bildung von SIA in der Atmosphäre und der Auswaschung von SIA aus der Atmosphäre innerhalb zweier regionaler Chemie-Transportmodelle verbessert. Anschließend wurden die Ergebnisse der Modelle anhand einer operationellen und einer dynamischen Evaluation mit Beobachtungen verglichen. Hierbei lag der Fokus auf dem Aspekt der Nichtlinearität.

Das Chemie-Transportmodell REM-Calgrid (RCG) wurde durch den Einbau einer pH-Wert abhängigen Sulfatbildung in der Flüssigphase weiterentwickelt. Des Weiteren wurde eine neue Routine zur Berechnung der nassen Deposition implementiert. Diese berücksichtigt eine vom Flüssigwassergehalt abhängige Auswaschung innerhalb der Wolke und eine vom pH-Wert abhängige Tropfensättigung bei der Auswaschung von Gasen innerhalb und unterhalb der Wolke. Eine Modellsensitivitätsstudie, in welcher der pH-Wert von Wolken- und Regentropfen zwischen 4.5 und 6.5 variiert wurde, hat einen deutlichen Einfluss der pH-Wert Variationen auf die Konzentrationen von SIA und auf die nassen Depositionsflüsse von Schwefel- und Stickstoffverbindungen ergeben. Ferner wurden die Ergebnisse eines Modelllaufs, in welchem der pH-Wert der Wolken- und Regentropfen modelliert wurde

mit denen eines Modelllaufes, in welchem ein konstanter Tropfen-pH-Wert angenommen wurde, verglichen. Außerdem wurden Messungen von Konzentrationen und der nassen Deposition zum Vergleich herangezogen. Die Ergebnisse haben gezeigt, dass die Verwendung eines modellierten pH-Wertes von Wolken- und Regentropfen der Verwendung eines konstanten pH-Wertes vorzuziehen ist, da dies zu einer verbesserten Modellgüte und Modellkonsistenz bezüglich der Konzentrationen und der Depositionen führt.
Des Weiteren wurde die weiterentwickelte Version des RCG Modells für die Analyse zweier, durch hohe SIA Anteile charakterisierte, PM_{10} Episoden über Zentraleuropa verwendet. Das Modell konnte die zeitliche Variation der SIA Konzentrationen gut wiedergeben und wurde daher zur Untersuchung des Ursprungs, der Entwicklung und der Charakteristik der Episoden herangezogen. Um die Reaktion der SIA Konzentrationen und Depositionen auf Emissionsvariationen zu untersuchen, wurden anschließend mehrere Modellläufe für verschiedene Emissionsszenarien durchgeführt. Hierfür wurden die Emissionen der Vorläuferstoffe Schwefeldioxid, Stickstoffdioxid und Ammoniak variiert. Die Ergebnisse haben das nichtlineare Verhalten der SIA Konzentrationen und Depositionen gegenüber Variationen der Vorläuferemissionen bestätigt. Die Ergebnisse haben demonstriert, dass die Abweichung von der Linearität für die Deposition geringer ist als für die Konzentrationen. Es hat sich außerdem gezeigt, dass der Einbau der pH-Wert abhängigen Flüssigphasenchemie das nichtlineare Verhalten des Systems verstärkt und die Reaktion des Modellsystems auf Emissionsvariationen deutlich modifiziert. Eine Reihe von Emissionsminderungsszenarien wurde sowohl für ein Modellgebiet über Deutschland, als auch für ein Modellgebiet über ganz Europa durchgeführt. Diese Studie ergab, dass in Deutschland neben europaweiten Emissionsminderungsmaßnahmen zusätzliche Maßnahmen zur Minderung von Ammoniakemissionen auf nationaler Ebene zu höheren SIA Konzentrationsminderungen führen, als zusätzliche nationale Minderungen von Schwefeldioxid und Stickstoffdioxid Emissionen.
Abschließend wurde eine dynamische Modellevaluation über Europa für die Jahre 1990 bis 2009 anhand von Messungen an europäischen ländlichen Hintergrundstationen durchgeführt. Für diese Studie wurde das LOTOS-EUROS Modell verwendet, da es ein sogenanntes 'source apportionment' Modul enthält, mit welchem zeitliche Änderungen in der Effizienz der SIA-Bildung analysiert werden können. In einem ersten Schritt wurde zunächst die neu entwickelte Routine zur Beschreibung der Flüssigphasenchemie in dieses Modell implementiert. Die Analyse der beobachteten Trends hat die Ergebnisse früherer Studien darin bestätigt, dass die Trends in Sulfat- und Nitratkonzentrationen von 1990 bis 2009 einen geringeren Rückgang aufweisen, als die Trends in den Emissionen und Konzentrationen der Vorläuferstoffe. Das Modell hat diesen nichtlinearen Zusammenhang zwischen Vorläuferemission und SIA Konzentration gut wiedergegeben. Mit Hilfe des 'source appotionment' Moduls wurden die Trends in der Effizienz der SIA-Bildung von 1990 bis

2009 für vier Regionen/Länder in Europa quantifiziert ('Die Niederlande und Belgien', 'Ostsee', 'Tschechien' und 'Rumänien'). Die Ergebnisse zeigen für Sulfat in allen untersuchten Regionen einen Anstieg in der Bildungseffizienz (20-60%) und für Nitrat einen Anstieg in den Benelux Staaten und in Tschechien (bis zu 20%). Dies verdeutlicht, dass die Änderungen in der Effizienz der SIA-Bildung aufgrund der Änderungen des chemischen Regimes von 1990 bis 2009, die Basis für den beobachteten nichtlinearen Zusammenhang zwischen den SIA Konzentrationen und den Emissionen der Vorläuferstoffe bilden.
Mit dieser Modellstudie wurde neues Wissen und ein verbessertes Verständnis in Bezug auf das nichtlineare Verhältnis zwischen Emissionen schwefel- und stickstoffhaltiger Vorläuferstoffe und den daraus resultierenden SIA Konzentrationen und Depositionsflüssen gewonnen.

Chapter 1

Introduction

An aerosol is defined as a suspension of fine solid and/or liquid particles in gas. However, within atmospheric science it is common to use the term aerosol just for the solid or liquid particles and neglect the carrier gas. Particles with diameters within the range of a few nanometers to around 100 micrometers are considered as aerosols. Aerosol particles can exist in diverse mixing states consisting of various compounds. They can change their size and composition by condensation of vapor species or by evaporation, by chemical reaction or by coagulating with other particles, or by activation in the presence of water supersaturation to become cloud droplets (Seinfeld and Pandis, 1998).
Aerosols can be of anthropogenic or of natural origin stemming from either direct emissions or from gas-to-particle conversion of precursor gases. Since the Industrial Revolution in the 19th century the amount of airborne aerosols has significantly increased and aerosol composition has significantly changed in the industrialised regions of the Northern Hemisphere. However, the latter modifications are not restricted to industrialised regions. The lifetime of aerosols in the troposphere varies from a few days to a few weeks. Considering that within the aerosol lifetime air masses can travel up to several thousand kilometers, there are no places on earth where the quantity and composition of aerosols is still pristine (Andreae, 2007) .
Atmospheric aerosols affect the radiation budget of the earth (Forster et al., 2007) through direct and indirect effects, impact atmospheric visibility (Bäumer et al., 2008), are linked to acidification and eutrophication of ecosystems (Bobbink et al., 1998) and have adverse impact on human health (Pope et al., 2009). Hence, studies on atmospheric aerosols strongly vary in time-scale (from centuries to years to seconds) and length-scale (from global to regional to local) and various atmospheric sciences are involved. The investigations concentrate on the overall atmospheric aerosol, on aerosols of concrete size ranges like PM_{10} or $PM_{2.5}$ (particles smaller than 10 or 2.5 μm, respectively) or on specific aerosol compounds.

This thesis focuses on secondary inorganic aerosol (SIA) which is sulphate, nitrate and ammonium because of the non-linear relation between SIA and its precursor emissions and the unresolved aspects of that relation. The description of SIA is improved within two state-of-the-art chemistry transport models (CTMs) and its observed and modelled responses to emission changes over Europe are investigated. In the following subsections ambient atmospheric aerosols and in particular SIAs are introduced. Furthermore, concise summaries of the application of models to simulate SIA concentrations and its precursors and mitigation of precursor emissions in Europe are given. In the last subsection of Chapter 1 the research aims and thesis outline are presented. In Chapter 2 the applied methods, models and observations are described. Chapters 3, 4 and 5 contain three scientific publications composed within the study. Finally, in Chapter 6 the overall conclusions and an outlook are given.

1.1 Ambient aerosol size distribution

As the size of particles which spans over four orders of magnitude affects their physical and chemical properties and their lifetime in the atmosphere we need to mathematically characterise their size distribution making use of a number of modes. According to their diameter, atmospheric aerosol particles are assigned to different modes:

Nucleation mode: 10^{-3} μm - 10^{-2} μm
Aitken mode: 10^{-2} μm - 0.1 μm
Accumulation mode: 0.1 μm - 2.5 μm
Coarse mode: Particles $>$ 2.5 μm

Aerosol particles with diameters lower than 2.5 μm are also referred to as "fine" fraction and those greater than 2.5 μm as "coarse" fraction. When dealing with size distributions we can distinguish between the number size distribution and the mass or volume size distribution. While the fine fraction dominates the number size distribution of airborne particles the mass distribution of airborne particles is dominated by the coarse fraction. In general, fine and coarse mode particles have different sources and different physical-chemical origin, are transformed separately, are of different composition, have different optical properties, are removed from the atmosphere by different mechanisms and differ in their deposition pattern in the respiratory tract (Seinfeld and Pandis, 1998) and hence their characterisation by size is fundamental.
The above is summarized in Table 1.1. Therein Nucleation and Aitken mode are combined to one Ultrafine mode. The Ultrafine mode particles are formed from the nucleation of

	Fine (≤2.5 μm)		Coarse (2.5 – 10 μm)
	Ultrafine (<0.1 μm)	**Accumulation (0.1 – 2.5 μm)**	
Formed from:	Combustion, high-temperature processes, and atmospheric reactions		Break-up of large solids/droplets
Formed by:	Nucleation Condensation Coagulation	Condensation Coagulation Evaporation of fog and cloud droplets in which gases have dissolved and reacted	Mechanical disruption (crushing, grinding, and abrasion of surfaces) Evaporation of sprays Suspension of dusts Reactions of gases in or on particles
Composed of:	Sulfate, $SO_4^=$ Black carbon Metal compounds Low-volatility organic compounds	Sulfate, $SO_4^=$ Nitrate, NO_3^- Ammonium, NH_4^+ Hydrogen ion, H^+ Black carbon Large variety of organic compounds Metals: compounds of Pb, Cd, V, Ni, Cu, Zn, Mn, Fe, etc. Particle-bound water	Suspended soil or street dust Fly ash from uncontrolled combustion of coal, oil, and wood Nitrates and chlorides from HNO_3 and HCl Oxides of crustal elements (Si, Al, Ti, and Fe) $CaCO_3$, NaCl, and sea salt Pollen, mold, and fungal spores Plant and animal fragments Tire, brake-pad, and road-wear debris
Typical Atmospheric half-life:	Minutes to hours	Days to weeks	Minutes to hours
Important Removal processes:	Growth into accumulation mode Wet and dry deposition	Wet and dry deposition	Wet and dry deposition
Typical Travel distance:	<1 to 10s of km	100s to 1000s of km	<1 to 10s of km (100s to 1000s in dust storms)
Source: Adapted from Wilson and Suh (1997).			

Table 1.1 Illustration of ambient particle fractions adopted from McMurry et al. (2004).

atmospheric species to form new particles, during combustion processes from condensation of hot vapors or from atmospheric reactions. Furthermore, they may coagulate forming larger particles. Other than the Ultrafine mode, the accumulation mode does contribute a considerable part of the total aerosol mass. Particles in the accumulation mode are formed from coagulation of particles in the Ultrafine mode, from condensation of vapors on existing particles, from combustion processes, from atmospheric reactions or are released from evaporated cloud or fog droplets in which gases have dissolved and reacted. Most important removal processes are wet and dry deposition. Coarse particles are mostly formed by reactions of gases in or on particles, break-up of large solids, evaporation of sprays or mechanical processes like suspension of dust.

For all modes the most important removal processes are wet and dry deposition. Ultrafine particles may also coagulate with larger particles growing into the accumulation mode.

Eye-catching in Table 1.1 is that the typical atmospheric lifetime is highest for particles in the accumulation mode resulting also in the longest typical travel distance for these particles. This is because particle removal processes are least efficient for particles of the accumulation mode.

1.2 Composition of the tropospheric aerosol over Europe

Together with the aerosol size the chemical composition of the aerosol determines the aerosols' effects on climate, ecosystems and human health. Furthermore, the composition of the aerosol reveals its various sources. Among the diverse aerosol compounds (some examples are given in 1.1), SIA, carbonaceous matter, sea-salt and mineral dust are the principle components contributing to a large part of the particulate matter (PM) mass. The different contributions vary over Europe depending on the aerosol size and the location. (Putaud et al., 2004; Putaud et al., 2010).
A distinction can be made between primary aerosols which are directly emitted into the atmosphere and secondary aerosols which are formed in the atmosphere from oxidation or transformation of precursor gases. However, as already stated aerosols exist in diverse mixing states and typically consist of primary and secondary compounds. Furthermore, one can distinguish between aerosols of anthropogenic and aerosols of natural origin. Anthropogenic sources of primary aerosols or precursor gases of secondary aerosols are e.g. combustion of coal, oil, gasoline, diesel or wood or resuspension of industrial dust, tire or brake-pad. Examples of natural sources are suspension of soil, ocean spray, volcanic activity or forest fires.
The aerosol composition can be measured by sampling and subsequent analysis. As an example, Figure 1.1 shows the average compositional distribution of PM_{10} (measured between August 2007 and 4 September 2008), which is PM with an aerodynamic diameter < 10 μm, at the rural background measurement site Hellendoorn in the eastern part of The Netherlands. The figure was created using data from Weijers et al. (2011).

The chemically analysed fraction accounts for 74% of the observed PM mass at Hellendoorn. The remaining 26% include the non-measured oxides present in PM, as well as the contribution of non-carbon atoms (e.g. H, O, N) in organic material and elements contributing to mineral dust (Schaap et al., 2010). An additional part of the "not analysed" mass may be explained by water that is bound to particles and contributes to the PM mass measurement.

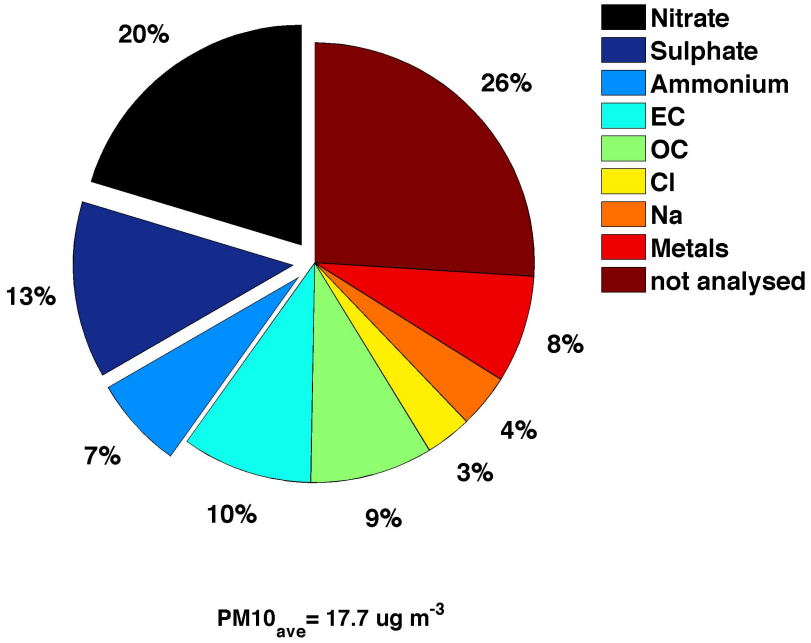

Figure 1.1 Observed relative chemical distribution of PM_{10} at the Dutch rural background site Hellendoorn. Data from Weijers et al. (2011).

Metals form 8% of the PM_{10} at Hellendoorn. Metals originate from a vast range of abrasion processes and the metallurgical industry (Schaap et al., 2010). Mechanically or wind-blown suspended soil containing e.g. Si, Al, Fe, Ca and K may also contribute to metal concentrations.

Sodium (Na) and chloride (Cl) together contribute to 7% of the PM mass. Both are tracers associated with sea salt. Sodium can be used to estimate the sea-salt contribution as there are no losses due to depletion while in the case of chloride, reactions in the atmosphere may occur with any present sulphuric and nitric acid, resulting in the loss of chloride in the aerosol.

A substantial fraction of the PM mass can be attributed to the carbonaceous aerosols elemental carbon (EC) (=10%) and organic carbon (OC) (=9%). Elemental carbon is also denoted as black carbon (BC) depending on the instrumental method utilized for its measurement. Elemental carbon is a primary aerosol and is formed by incomplete combustion of fossil fuels and biomass (e.g. wood burning). Organic carbon can be of primary or of secondary origin. The organic component of ambient aerosols is a complex mixture of hundreds to thousands of organic compounds (Seinfeld and Pandis, 1998) including mainly carbon, hydrogen, oxygen and nitrogen. The main sources of primary

organic aerosol are biomass burning, fossil fuel combustion, meat cooking, suspended road dust and biological materials (e.g. pollen and spores). Secondary organic aerosol (SOA) is formed by chemical reaction and gas-to-particle conversion of volatile organic compounds (VOCs). These precursors can be of anthropogenic (e.g. fossil fuel combustion) or biogenic (e.g. plants and trees) origin, whereas the latter biogenic share is presently postulated to be the major contributor to atmospheric SOA (e.g. Simpson et al., 2007). The contribution of SOA to aerosol mass is uncertain, as the major formation routes are still not well known (Weijers et al., 2011).
Finally, the SIA compounds sulphate (13%), nitrate (20%) and ammonium (7%) together account for 40% of the observed PM_{10} mass dominating the PM_{10} composition at Hellendoorn. At European rural background sites the SIA contribution to PM_{10} mass is on average 25-50% (Putaud et al., 2010). The secondary components sulphate, nitrate and ammonium are formed in the atmosphere from their precursor gases sulphur dioxide, nitrogen oxides and ammonia, respectively. Over Europe the sources of the SIA precursors are mainly of anthropogenic origin stemming from power plants, traffic and agricultural activity. The formation of SIA and its precursors' sources will be addressed in more detail in the following sections.

As already stated above the composition of atmospheric aerosols varies depending on the location and on the aerosol size. At a site close to the sea the mass contributions of sodium and chloride is increased compared to their contributions at a site of continental character. At an urban site the elemental carbon fraction is increased compared to its fraction at a rural background site. Furthermore, all components are present in both the fine and the coarse fractions, but their contributions in each fraction are often different. Mineral dust and sea salt contribute more to the coarse fraction, whereas SIA, organic carbon and elemental carbon contribute more to the fine fraction (Putaud et al., 2004).

1.3 The role of SIA in air pollution and impact on climate

1.3.1 Impact on ecosystems

Trace gases and PM are removed from the atmosphere by dry and wet deposition. Dry deposition includes the sedimentation of particles or the adsorption or diffusion of gases or aerosols onto surfaces without the involvement of precipitation whereas wet deposition encompasses all processes by which the airborne gases and aerosols are transferred onto

the surface in aqueous form (Seinfeld and Pandis, 1998). The latter processes involve dissolution of atmospheric gases in airborne droplets (cloud, rain or fog droplets), removal of atmospheric particles when they serve as cloud condensation nuclei (CCN) and removal of atmospheric particles when the particle collides with a cloud, fog or rain droplet.
The wet and dry deposition of sulphur and nitrogen components decreases biodiversity in vulnerable terrestrial and aquatic ecosystems through eutrophication and acidification of soils and fresh water (Bobbink et al., 1998). Acidifying deposition reduces the pH of soils and waters affected and causes leaching of aluminium, threatening the vitality of forests and fish stocks (Kangas and Syri, 2002). Eutrophying deposition alters the species composition and causes leaching of nitrogen to surface and ground waters.
The major sources of sulphur and nitrogen in the atmosphere are the emissions of sulphur dioxide, nitrogen oxides and ammonia through fossil fuel combustion and agricultural activities. These primary gases may themselves be removed from the atmosphere by deposition processes endangering ecosystems. However, sulphur dioxide, nitrogen oxides and ammonia are also the precursor gases for SIA providing a means for long-range transport of these components on a continental scale as the tropospheric lifetime of SIA is considerably longer (several days to weeks) than that of its precursor gases (several hours to a few days) (Seinfeld and Pandis, 1998). Hence, the deposition of SIA causes negative impact on ecosystems also far away from the major source areas and therewith considerably enhances the circumference of acidification and eutrophication.

1.3.2 SIA as constituent of PM

According to epidemiological studies (e.g. Eeftens et al., 2012 and references therein), severe health effects can be attributed to PM. Based on long-term studies, there is strong evidence that there are associations between long-term exposure to ambient particulates and elevated cases of cardiovascular problems, respiratory morbidity and mortality. However, from a toxicological point of view it is not yet clear which constituents are responsible for these adverse effects (WHO, 2007).
Sulphate, nitrate and ammonium are the major inorganic ions in atmospheric PM forming a substantial fraction of the total PM mass throughout the European domain. The few currently available toxicological studies do not support a role for SIA in adverse health outcomes noted in epidemiological studies (Schlesinger and Cassee, 2003; Reiss et al., 2007). However, the authors of these studies highlight that the exact physicochemical characteristics of the PM in the epidemiological studies and the one to which human populations are normally exposed may differ from those used in the controlled toxicological studies. Furthermore, possible indirect adverse effects of SIA within the PM mixture

in the atmosphere are highlighted, including (1) potential increase in bioavailability of metallic species, (2) enhancement of lung deposition of more toxic compounds, and (3) catalysis of organic aerosol formation (Reiss et al., 2007). These mechanisms will need further research.

As there is no conclusive evidence which components are most relevant for deteriorating human health, the European air quality standards currently focus on PM_{10} and $PM_{2.5}$. The European Union has fixed daily and annual limit values for PM_{10} (PM < 10 μm) (EC, 2001) and an annual limit value for $PM_{2.5}$ (PM < 2.5 μm) will be implemented from 2015 on (EC, 2008). These implemented or to be implemented limit values for PM_{10} and $PM_{2.5}$ are not yet achieved at many European observational sites (EEA, 2012). The SIA contribution has been found to be particularly enhanced on days with PM_{10} concentrations up to or above the EU daily limit value (e.g. Weijers et al., 2010). Therefore, comprehensive knowledge on the spatial and temporal variability of SIA and atmospheric conditions influencing SIA formation is important within the assessment of the effects of abatement strategies.

1.3.3 Impact on climate

Since the Industrial Revolution the levels of green house gases (GHGs) and aerosols in the troposphere have risen interfering with the radiation balance of the earth. While GHGs result in a warming effect of the troposphere (= positive radiative forcing) aerosols result in an overall cooling effect of the troposphere (= negative radiative forcing) Boucher et al. (2013). However, the radiative forcing of different aerosol compounds differs in sign and magnitude. While GHGs have lifetimes of decades or longer and are therefore uniformly distributed over the globe, aerosols have lifetimes of days to weeks and their mass, number concentration and composition strongly varies over the globe in time and space (Seinfeld and Pandis, 1998). The latter complicates the assessment of the aerosol radiative forcing (Schaap, 2003).

SIA are involved in climate change by affecting the radiation balance of the earth (Forster et al., 2007; Boucher et al., 2013). For sulphate this has been long known as even the first estimate of the direct aerosol effect in the early 1990s by Charlson et al. (1991) was limited to sulphate aerosols (Myhre et al., 2013). Within the IPCC Fourth and Fifth Assessment Reports (AR4 and AR5) the direct radiative forcing of sulphate was estimated with -0.4 $\pm$ 0.2 W m^{-2} (Forster et al., 2007; Boucher et al., 2013). Note that although the sulphate direct forcing has been studied since the early 1990s, the uncertainty is still $\pm$ 50%. The AR4 was the first IPCC report giving a direct radiative forcing estimate also for nitrate. A direct radiative forcing of -0.10 $\pm$ 0.1 W m^{-2} was adopted, but it was acknowledged

that the number of studies performed was insufficient for accurate characterization of its magnitude and uncertainty (Forster et al., 2007). Within AR5 the radiative forcing of nitrate was re-evaluated to be stronger with -0.15 ± 0.1 W m^{-2} (Boucher et al., 2013). However, the models used to assess the latter value still widely differ. As atmospheric ammonium nitrate aerosol forms when sulphate aerosol is fully neutralised and there is further excess of ammonia, the weakening of the radiative forcing of sulphate aerosol in many regions due to reduced emissions may be partially balanced by increases in the radiative forcing of nitrate aerosol (Liao and Seinfeld, 2005; Adams et al., 2001). The latter enhances the need of further studies on the impact of nitrate on the earths' radiation balance.

The direct radiative forcing of sulphate and nitrate are negative, implicating a cooling effect, which may mask some of the warming from e.g. BC estimated with a direct radiative forcing of 0.3 ± 0.2 W m^{-2} within AR5 (Boucher et al., 2013). An important consideration in evaluating present-day short term climate mitigation is that sulphate and nitrate precursors may arise in the same combustion sources that produce BC. Recent studies show that short term climate mitigation aimed at reducing BC may only be effective provided that the climate impact of the co-emitted SIA precursors does not cause a net cooling impact (Bond et al., 2013).

Next to the direct aerosol forcing also semi-direct and indirect effects in which aerosols modify the microphysical and hence the radiative properties, and the amount and lifetime of clouds have been identified (e.g. Ramanathan et al., 2001; Haywood and Boucher, 2000). Key parameters for determining the indirect effect are the effectiveness of an aerosol particle to act as a cloud condensation nucleus (Forster et al., 2007) , which is amongst others a function of the size and chemical composition (e.g. McFiggans et al., 2006). Within the AR4 and AR5 published model studies on the indirect radiative forcing are summerised showing that the numbers widely differ between the different studies (Forster et al., 2007; Boucher et al., 2013). The SIA indirect effect has not yet been quantified within the AR4 or AR5.

1.4 SIA sources, formation and sinks

1.4.1 Emission sources of the precursor gases

The gaseous precursors of SIA are sulphur dioxide, nitrogen oxides and ammonia. Anthropogenic emission sources of sulphur dioxide are coal-burning power plants, shipping, cement industry, smelters, industrial boilers, biomass burning and oil refineries. Natural sources are e.g. volcanic activity and natural biomass burning (e.g. forest fires). Anthro-

pogenic emissions account for about 90% of the sulphur dioxide emissions (Seinfeld and Pandis, 1998). The major emission sources for nitrogen oxides are fossil fuel combustion in traffic, ships, power plants and industries. In Europe these anthropogenic emissions are at least four times larger than the natural emissions from lightning, soil emissions and forest fires (Vestreng et al., 2009). Ammonia is mainly emitted through agricultural activity. In Europe, the latter accounts for more than 90% of ammonia emissions (Amann et al., 2012). Small contributions can be attributed to biomass burning, oil refineries or fuel combustion and natural sources like oceans, wild animals or natural biomass burning.

SIA is dominated by ammonium sulfate and ammonium nitrate salts (Putaud et al., 2010). In the following subsections the formation of SIA from its precursor gases is described following Seinfeld and Pandis (1998), Schaap (2003) and Weijers et al. (2010).

1.4.2 Sulphate formation

Sulphate is formed by oxidation of sulphur dioxide (SO_2) by gas-phase or aqueous-phase reactions. In case of the gas-phase pathway sulphur dioxide is converted into sulphuric acid gas (H_2SO_4) by reacting with hydroxyl radicals ($OH\cdot$), oxygen (O_2) and water vapor (H_2O):

$$OH\cdot + SO_2 \rightarrow HSO_3 \tag{1.1}$$

$$HSO_3 + O_2 \rightarrow HO_2 + SO_3 \tag{1.2}$$

$$SO_3 + H_2O \rightarrow H_2SO_4 \tag{1.3}$$

Sulphuric acid either condenses on existing particles or nucleates at high relative humidity to form a sulphuric acid droplet. If abundant ammonia is available, depending on the ammonia concentration sulphuric acid is neutralised as bisulphate (reaction 1.4) or completely neutralised as ammonium sulphate (reaction 1.5):

$$H_2SO_4 + NH_3 \rightarrow (NH_4)HSO_4 \tag{1.4}$$

$$H_2SO_4 + 2NH_3 \rightarrow (NH_4)_2SO_4 \tag{1.5}$$

In Europe most areas exhibit sufficient ammonia to neutralise the available sulphuric acid and ammonium sulphate dominates. The gas-to-particle conversion of sulphur dioxide exhibits a diurnal, seasonal and latitudinal variability as it depends on the availability

of hydroxyl radicals which are formed by photochemistry depending on the the solar intensity.

Aqueous phase sulphate formation occurs when sulphur dioxide dissolves in cloud or fog droplets. It is the much faster pathway than the gas-phase pathway and dominates if clouds are abundant. The dissolved sulphur dioxide in the droplet is oxidised to sulphuric acid by ozone (O_3) or hydrogen peroxide (H_2O_2) (Hoffmann and Calvert, 1985). Figure 1.2 shows the rate (R) per (g m^{-3}) cloud liquid water content (L) of aqueous-phase oxidation of dissolved sulphur dioxide by ozone and hydrogen peroxide as a function of solution pH (Seinfeld and Pandis, 1998). Gas-aqueous equilibria are assumed for all reagents. While the rate of sulphate formation via the oxidation pathway by hydrogen peroxide shows a negligible dependency on droplet pH, the oxidation pathway by ozone strongly depends on the pH of the involved cloud/fog droplet. For an ozone gas-phase mixing ratio of 30 ppb (parts per billion) at 298 K (Kelvin), the reaction rate varies over 5 orders of magnitude between a droplet pH of 3 and a droplet pH of 6 which is a pH variation within the atmospheric range. The aqueous phase sulphate formation will be again addressed in Chapter 3.

Again, in the presence of ammonia, sulphuric acid will be neutralised as bisulphate or ammonium sulphate following reaction 1.4 or 1.5, respectively.

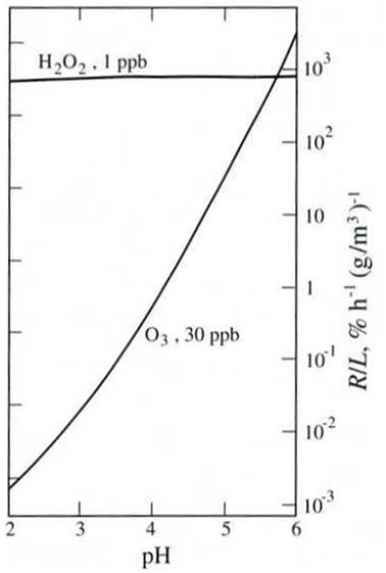

Figure 1.2 Rate of aqueous-phase oxidation of dissolved sulphur dioxide by ozone (30 ppb) and hydrogen peroxide (1 ppb) as a function of solution pH at 298 K. R/L represents the rate of reaction referred to gas-phase sulphur dioxide pressure per (g m^{-3}) of cloud liquid water content. Gas-aqueous equilibria are assumed for all reagents (Seinfeld and Pandis, 1998)

1.4.3 Nitrate formation

Atmospheric nitrate originates from the oxidation of nitrogen oxides (NO and NO_2 summerised by the term NO_x) to nitric acid (HNO_3). There are two pathways that account for the largest part of the formation of nitric acid.
During daytime the main pathway is the reaction of nitrogen dioxide (NO_2) with the hydroxyl radical:

$$OH \cdot + NO_2 \rightarrow HNO_3 \tag{1.6}$$

The oxidation of nitrogen dioxide by the hydroxyl radical (reaction 1.6) is much faster than reaction 1.1.
During nighttime hydroxyl radical concentrations are (almost) zero and the reaction of nitrogen dioxide with ozone dominates involving the following reactions:

$$O_3 + NO_2 \rightarrow NO_3 + O_2 \tag{1.7}$$

$$NO_3 + NO_2 \rightarrow N_2O_5 \tag{1.8}$$

$$N_2O_5 + H_2O \rightarrow 2HNO_3 \tag{1.9}$$

Hydrolysis of dinitrogen pentoxide (N_2O_5) takes place on the surface of aerosols and yields two equivalents of nitric acid.
The nitric acid resulting from reaction 1.6 or 1.9 may react reversibly with ammonia to from ammonium nitrate:

$$HNO_3 + NH_3 \longleftrightarrow NH_4NO_3 \tag{1.10}$$

Ammonium nitrate is a semi-volatile compound (Nenes et al., 1999) and may revert back into its gas-phase precursors under conditions of low ammonia concentrations or at high temperatures (e.g. Worobiec et al., 2003). Therefore, concentrations of ammonium nitrate exhibit a seasonal and diurnal variation with higher levels during colder periods of the year and night-time.

Furthermore, nitric acid is converted to sodium nitrate ($NaNO_3$) through the reaction with sea salt (NaCl), which results in the release of hydrochloric acid (HCl):

$$HNO_3 + NaCl \rightarrow NaNO_3 + HCl \tag{1.11}$$

Also, in the presence of mineral dust, nitric acid may be absorbed onto these particles forming e.g. calcium nitrate ($Ca(NO_3)_2$):

$$CaCO_3 + 2HNO_3 \rightarrow Ca(NO_3)_2 + CO_2 + H_2O \quad (1.12)$$

Other than ammonium nitrate, sodium nitrate and calcium nitrate are non-volatile and the reactions 1.11 and 1.12 are irreversible. Furthermore, while ammonium nitrate is predominantly found in the fine size fraction, sodium nitrate and calcium nitrate are predominantly found in the coarse size fraction as sea salt and mineral dust are also located in the coarse aerosol mode.

1.4.4 The NH_3-HNO_3-H_2SO_4 System

Ammonia preferentially neutralises sulphuric acid because sulphuric acid possesses an extremely low vapour pressure. Furthermore, ammonium sulphate is the preferred form of sulphate (Seinfeld and Pandis, 1998). The latter implicates that each mole of sulphate will remove two moles of ammonia from the gas-phase ($\rightarrow$ reaction 1.5). Ammonium nitrate will only be efficiently formed when the total ammonia (=[NH_3]+[NH_4]) exceeds the sulphate by a factor of two or more on a molar basis. Based on this an indicator referred to as 'Free ammonia' ([NH_3^F]) can be defined in molar units (e.g. Ansari and Pandis, 1998):

$$[NH_3^F] = [total\ ammonia] - 2 * [sulphate] \quad (1.13)$$

Whenever [NH_3^F] > 0 there is excess ammonia available to react with nitrate to form ammonium nitrate.

The thermodynamic equilibrium between gas and aqueous aerosol phase determining the concentrations of the involved species depends on temperature, relative humidity and the ambient concentrations of sulphate, total nitrate (=[HNO_3]+[NO_3]) and total ammonia (West et al., 1999).

In addition, the ambient concentrations of SIA and its precursors impact cloud/fog droplet pH, which regulates the oxidation pathway of sulphur dioxide by ozone and therewith the aqueous phase formation efficiency of sulphate (Fowler et al., 2007).

1.4.5 Sinks

SIA is removed from the atmosphere by wet and dry deposition processes. Dry deposition processes include the sedimentation of coarse particles or the adsorption or diffusion of gases or aerosols onto surfaces. The process of wet deposition includes the wet scavenging of gases and particles in the cloud (= rainout) and the wet scavenging below the cloud

(= washout).

With the exception of coarse mode nitrate (e.g. sodium nitrate) SIA is mainly present in the accumulation mode (Putaud et al., 2004). The removal of accumulation mode particles by dry deposition has been found to be inefficient compared to both lower and higher size ranges (e.g. Zhang et al., 2001) because neither brownian motion, nor sedimentation are effective pathways for accumulation mode particles. Also the removal by washout is inefficient in the accumulation size range. Figure 1.3 shows the collision efficiency for the capture of particles by rain drops below the cloud as a function of particle size (note that the x-axis indicates the particle radius and not diameter) resulting from various laboratory and model studies indicated on the right side of the figure. Also the radius of the involved rain droplet has been varied between 0.3 mm and 1.0 mm. Both laboratory and model results reveal a comparatively low collection efficiency for the accumulation mode size range while especially for particles in the coarse mode the removal is significantly more efficient. Therefore the main loss of SIA occurs through rainout processes.

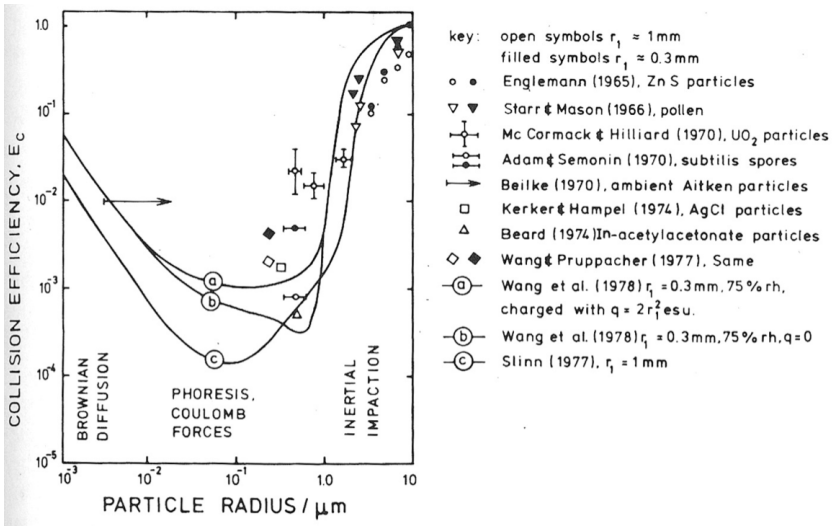

Figure 1.3 Collision efficiency for the capture of particles by rain drops below the cloud as a function of particle size. Solid lines indicate model studies, while the different markers indicate laboratory studies (Warneck, 1988).

1.5 Modelling SIA concentrations and deposition fluxes

Common tools to perform a combined modelling of the dynamical, physical and chemical processes of the atmosphere are eulerian CTMs. The three dimensional grid models require emissions, meteorological fields, land-use and boundary conditions as input data. The models solve the advection-diffusion partial differential equation based on emissions, transport (advection and diffusion), atmospheric physical and chemical transforma-

tions/destructions and removal processes. In general these models simulate gas-phase and aerosol phase. Other than observations which give us only a snapshot of species concentrations at a particular time and location CTMs deliver in space and time continuous concentration and deposition fields.

CTMs usually run on an hourly time resolution and can be applied on the global, regional (as applied within this thesis) or local scale with varying spatial grid resolution. In the vertical they may extend from 5-10km. The parameterizations of the different processes vary in complexity between different CTMs. Furthermore, CTMs can be on-line coupled or off-line coupled with their meteorological driver. Some of the most frequently applied CTMs on the regional scale over Europe are EMEP (Simpson et al., 2012), CHIMERE (Bessagnet et al., 2004), LOTOS-EUROS (Schaap et al., 2008), RCG (Beekmann et al., 2007), COSMO-MUSCAT (Wolke et al., 2004), EURAD (Memmesheimer et al., 2004), WRF/CHEM (Grell et al., 2005) and CMAQ (Mebust et al., 2003).

In the following a short summary of the modules most relevant for the simulation of SIA used in the CTMs is given. A photochemical mechanisms is used to simulate the relevant atmospheric gas-phase reactions including those involving SIA precursors resulting in sulphuric acid and nitric acid as described in the subsections 1.4.2 and 1.4.3. Frequently used photochemical mechanisms are e.g. the Carbon Bond Mechanism - IV (CBM-IV/V) (Gery et al., 1989), RADM2 (Stockwell et al., 1990), RACM (Stockwell et al., 1997) or SAPRC99 (Carter, 2000) or modifications of these mechanisms. Most models have an additional routine included to simulate the aqueous-phase transformation path for sulphate. Furthermore, a module to simulate the thermodynamic equilibrium between ammonia, gaseous nitric acid, particulate ammonium nitrate and ammonium sulphate and water as described in subsection 1.4.4 is applied. Commonly used modules are the ISORROPIA (Nenes et al., 1999) or ISORROPIA2 (Fountoukis and Nenes, 2007), which assume equilibrium between the gas and aerosol phase at all times. Finally, the removal processes dry and wet deposition need to be described. For the simulation of the dry deposition the so called resistance analogy approach (Erisman et al., 1994) is usually used with the canopy resistance treated analogous to the electric resistance in Ohm's law within electrical circuits. A frequently applied module is the DEPAC (Van Zanten et al., 2010) module. For the simulation of wet deposition processes simplified scavenging coefficients are applied that describe the loss of concentration per time step due to wet scavenging. The process descriptions within the different CTMs widely differ in complexity. Some models only account for the washout while others include comprehensive descriptions of the scavenging processes in and below the cloud.

When using CTMs someone should always be aware that the models remain limited tools exhibiting uncertainties and missing compounds, processes and dependencies. Moreover,

the model accuracy strongly depends on the accuracy of the input parameters. The involved uncertainties have to be assessed by means of continuous model evaluation and need to be considered when analysing the model results.

1.6 SIA mitigation in Europe

Already in the 1950s first studies demonstrated the interrelationship between sulphur emissions in continental Europe and the acidification of Scandinavian lakes (e.g. Barrett and Brodin, 1955; de Bary and Junge, 1963). To combat the adverse impacts on ecosystems a series of international conventions and agreements were implemented. Under the framework Convention on Long-range Transboundary Air Pollution (CLRTAP) established in 1979 within the United Nations Economic Commission for Europe (UN/ECE) several abatement protocols of acidifying and eutrophying emissions have been signed. In 1999, the protocol to abate acidification, eutrophication and ground-level ozone in Europe was signed in Gothenburg, Sweden (UN/ECE, 1999). The Gothenburg Protocol set emission ceilings for 2010 for the four pollutants: The SIA precursors sulphur dioxide, nitrogen oxides and ammonia and for VOCs. In 2012, the Protocol was amended to include national emission reduction commitments to be achieved in 2020 and beyond. In addition, the National Emissions Ceiling Directive (NECD 2001/81/EC) was introduced in 2001 (EC, 2001; EC, 2008) setting national emission ceilings for the EU countries for 2010 and 2020.

The implemented mitigation measures have led to significant emission reductions (Grennfelt and Hov, 2005). Figure 1.4 shows the past emission trends of nitrogen oxides, sulphur oxides and ammonia in the EU-27 (EU without Croatia) and EEA-32 (EU-27 plus Iceland, Liechtenstein, Norway, Switzerland and Turkey) group of countries and 2010 and 2020 emission ceilings for the respective pollutants. For the EEA-32 group of countries sulphur oxides emissions have decrease by 75%, nitrogen oxides emissions by 42% and ammonia emissions by 28% in the EEA-32 group of countries from 1990-2010. The EU-27 as a whole has met its overall target to reduce emissions of sulphur oxides and ammonia as specified by the EU's National Emissions Ceiling Directive for 2010 although 2 EU Member States have exceeded their ammonia 2010 emission ceilings (EEA, 2012). For nitrogen oxides the EU-27 as a whole is above their NECD 2010 emission ceilings as 12 EU Member States have exceeded their nitrogen oxides emission ceilings (EEA, 2012). Meeting the Gothenburg 2020 emission targets for nitrogen oxides and ammonia is an ongoing challenge for the EU.

As part of the conventions air pollution monitoring networks have been implemented over Europe providing a long-term observation capacity to be able to assess the effectiveness of

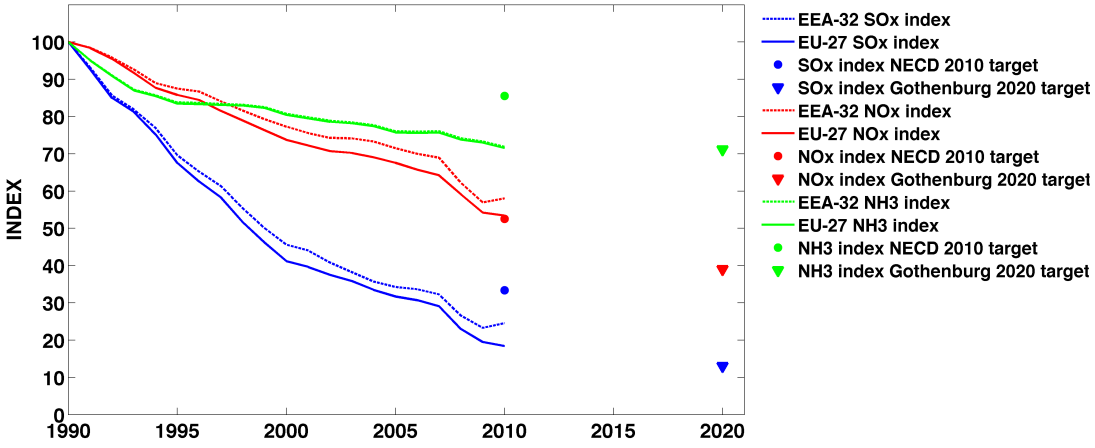

Figure 1.4 Past emission trends of nitrogen oxides (NO_x), sulphur oxides (SO_x) and ammonia (NH_3) in the EEA-32 and EU-27 group of countries. In addition - for the EU-27 - the aggregated Member State 2010 and 2020 emission ceilings for the respective pollutants are shown.
Data source: National emissions reported to the LRTAP Convention provided by the UN-ECE, provided by the European Environment Agency (EEA) in January 2014.

the implemented air quality management. Investigations based on these long-term observations have shown that the emission reductions of sulphur dioxide, nitrogen oxides and ammonia has led to decreasing concentrations of SIA and its precursors and wet deposition fluxes of sulphur (S) and nitrogen (N) (e.g. Løvblad et al., 2004). However, especially for some secondary species the implemented emission mitigation measures did not meet the expected concentration reduction (e.g. Tørseth et al., 2012). The latter non-linear response to the emission reduction will be discussed in detail within this thesis.

1.7 Research aims and outline of the thesis

1.7.1 Research aims

The previous introduction chapters have highlighted the role of SIA in the eutrophication of ecosystems, the formation of health relevant PM and the radiation balance of the earth. To effectively abate negative impacts a thorough understanding of the SIA budget is required. SIA has been studied over the last decades using both observations and model approaches. The studies revealed non-linear responses in the precursor emission-concentrations and the precursor emission-deposition relationships (Tarrasón et al., 2003; Fagerli and Aas, 2008).
At the start of this PhD study CTMs did not incorporate all processes leading to these non-linearities. Moreover, a few studies highlighted that the performance of these mod-

els show clear deficiencies in comparison to observed concentrations. Hence, the overall scientific scope of this thesis is to better understand the non-linear responses of SIA concentrations and sulphur and nitrogen deposition to precursor emission changes. The focus of this study is on the improvement of regional eulerian CTMs and the comprehensive evaluation of the models against observations with the focus on the non-linearity aspects. The outcome of this study will be highly relevant for policy makers with respect to the development of emission mitigation strategies that are effective for biodiversity, climate change and human health. This thesis is divided in three sequential studies for which we provide the research questions below.

Eulerian CTMs are used to simulate concentrations and wet and dry deposition fluxes of atmospheric chemical components including SIA and their precursors. The models are needed to investigate and understand the interactions between the different processes in the atmosphere. The complexity of the descriptions or parameterisations of these processes may vary from model to model and significantly determines the CPU demand required for the simulation.

Many CTMs still assume a constant droplet pH although cloud chemistry is highly dependent on cloud pH (Scire and Venkatram, 1985). Furthermore, the pH of atmospheric droplets constrains the uptake and subsequent removal of gases from the atmosphere through rain out (Seinfeld and Pandis, 1998). However, the description of wet scavenging processes within many CTMs is based on empirical approaches (e.g. Berge and Jakobsen, 1998) and is often rather crude. Model development and a comprehensive model evaluation concerning the description of aqueous phase chemistry as well as wet scavenging processes is needed to improve the simulation of the sulphur and nitrogen budget. Hence, the following research questions were addressed:

- Does the implementation of pH-dependent cloud chemistry and wet scavenging into a regional state-of-the-art CTM improve the model performance concerning air concentrations and wet deposition fluxes of sulphur and nitrogen compounds?
- How sensitive are the results of the improved model system to droplet pH variations?
- Can the improved model system including a modelled droplet pH be used to explain the origin, development and characteristics of observed PM_{10} episodes over Central Europe in spring 2009?

Furthermore, CTMs are used to analyse potential emission reduction strategies to quantify their effectiveness. The incorporation of pH-dependent cloud chemistry and wet scavenging adds non-linear responses to the model system and may modify the response of modelled SIA concentrations and deposition fluxes of S (sulphur) and N (nitrogen) to

changes in precursor emissions. The assessment of the change in deviation from linearity induced by the implementation of modelled droplet pH is an important information for the modeller community to account for when interpreting emission scenario simulations. The above is addressed by the following research questions:

- How sensitive are SIA levels to precursor emission changes during spring episodes?
- What is the impact of the improved cloud chemistry and wet scavenging descriptions on the modelled non-linear responses of SIA concentrations and deposition fluxes of S and N to precursor emission changes?
- For which precursor emissions are additional national measures in Germany (next to the European-wide measures) most effective in reducing SIA concentrations and deposition fluxes of S and N?

Capturing the non-linear responses of secondary species is still challenging for state-of-the-art CTMs. Within the first two studies of this thesis and in most other model evaluation studies, so called "operational evaluations" are performed comparing calculated concentrations to observations making use of standard statistical and graphical analysis to determine the model skill (Dennis et al., 2010). However, in order to provide robust policy support we also have to perform so called "dynamic evaluations" (Dennis et al., 2010) in which the ability of the model to simulate changes in air quality stemming from changes in source emissions and meteorological variability is assessed.
Emission mitigation measures have led to concentration reductions over Europe within the last decades (Tørseth et al., 2012) providing a good case for a dynamic model evaluation. Within the third study of this thesis an investigation of this 20 year period is presented addresing the following research questions:

- What are the observed trends in SIA and its precursors (SO_2, NO_x and NH_3) between 1990 and 2009 over Europe? Does the outcome change when considering the three different time periods 1990-2009, 1995-2009 and 2000-2009?
- How well does the LOTOS-EUROS model including pH-dependent cloud chemistry capture the observed trends and the non-linearity in the concentration responses?
- How does the SIA formation per unit precursor emission change between 1990 and 2009?

In total nine research questions will be addressed within this PhD study.

1.7.2 Outline of the thesis

The first two research questions are addressed in Chaper 3. The CTM REM-Calgrid (RCG) has been improved by implementing an enhanced description of aqueous-phase chemistry and wet deposition processes including droplet pH. A sensitivity study on cloud and rain droplet pH has been performed to investigate its impact on model aqueous-phase sulphate formation and gas wet scavenging. The improved model system is comprehensively evaluated concerning air concentrations of SIA and its precursors and wet deposition fluxes of S and N over Germany using surface observations.
The four subsequent research questions are approached by means of the study presented in Chapter 4. By means of an evaluation of the RCG model throughout high PM_{10} episodes over central Europe in spring 2009 using surface observations it is assessed if the model can be applied to explain the origin, development and characteristics of high PM_{10} episodes over Central Europe in spring 2009. Subsequently the episodes in spring 2009 are comprehensively analysed using RCG. Furthermore, the response of SIA concentrations to changes in precursor emissions over central Europe during spring 2009 is investigated applying the model. SIA concentrations are studied by means of several model runs for different emission scenarios using modelled and constant droplet pH. Sulphur dioxide, nitrogen oxides and ammonia emissions are varied within a domain covering Germany and within a domain covering Europe to assess the impact of national measures compared to European-wide measures.
Finally, the three last research questions are addressed in Chapter 5. In a first step, the pH dependent cloud chemistry that has been tested in RCG is implemented in the LOTOS-EUROS CTM. Subsequently, a model run of 20 years from 1990 to 2009 was performed over Europe using the LOTOS-EUROS model. By means of an operational and a dynamic evaluation using observations at European rural background sites we identify shortcomings and limitations of the model system and input data that need to be improved or considered when using the applied set up for future emission scenarios. In order to enable the analysis of trends in gas to particle conversion and atmospheric lifetime of the involved species a source apportionment module is used to trace the amount of SIA formed per unit emission of sulphur dioxide, nitrogen oxides and ammonia for four different regions over Europe from 1990 to 2009.

Chapter 2

Methods

Within this chapter the CTMs REM-Calgrid and LOTOS-EUROS used within this study are described in detail. Furthermore, the observations applied to evaluate the model simulations are introduced.

2.1 REM-Calgrid model description

The REM-Calgrid (RCG) model was developed at Freie Universität Berlin utilising the urban-scale photochemical model CALGRID (Yamartino et al., 1992) and the regional scale model REM3 (Hass et al., 1997; Römer et al., 2003) as the starting point. RCG is an off-line eulerian CTM (Beekmann et al., 2007; Stern et al., 2006) for the urban/regional scale.

The three-dimensional grid model simulates air pollution concentrations solving the advection - diffusion equation on a regular lat-lon-grid with variable resolution over Europe. Pollutant concentrations are calculated at the center of each grid cell volume, representing the average concentration over the entire cell (Cuvelier et al., 2013). Some of the default modelled species are ozone, nitrogen oxides, sulphur dioxide, ammonia, chemically unspecified primary particulate matter in the fine and coarse mode, elemental carbon, SIA and sea salt as well as species relevant as precursors or oxidants.

The horizontal master domain covers the area from 35° to 66.25° North and 10.5° West to 35.5° East, with a standard horizontal resolution of $0.5° \times 0.25°$ in latitude and longitude. Both, the use of a higher horizontal resolution and the choice of a smaller domain are possible. For the latter, RCG includes one-way grid nesting capabilities and pollutant concentration information calculated on a coarse grid can be used as boundary condition in the model run for the smaller model domain employing a higher grid resolution. In the vertical the coordinates are terrain following with the top of the modelling domain at a fixed height above the local terrain. One can either choose an arbitrary, fixed vertical grid

system of user-specified layer depths or dynamic vertical layers orientated at the mixing layer height to follow, in a simplified way, the vertical structure of the planetary boundary layer and the vertical mixing within. The latter implicates that the vertical layers vary in space and time.

The monotonic advection scheme used for the horizontal advection of pollutants was developed by Walcek (2000). Vertical diffusion parameters are derived using the Monin-Obukhov similarity theory for the description of the structure of the diabatic surface layer (K-theory). Gas-phase chemistry is simulated using an updated version of the CBM-IV photochemical reaction scheme (Gery et al., 1989), including Carter's 1-Product Isoprene scheme (Carter, 1996). RCG features the thermodynamic equilibrium module ISORROPIA to calculate the equilibrium between gaseous nitric acid, ammonia and particulate ammonium nitrate and ammonium sulphate and aerosol water (Nenes et al., 1999) to derive the concentrations of SIA. Production of secondary organic aerosol (SOA) is treated with a simplified version of the SORGAM module (Schell et al., 2001) which calculates the partitioning of semi-volatile organic compounds produced during VOC oxidation between the gas and the aerosol phase.

Dry Deposition fluxes are calculated following a resistance approach as proposed by Erisman et al. (1994). Turbulent and laminar resistance are calculated from surface roughness, Monin-Obukhov length, friction velocity and molecular diffusivity. Surface resistance is computed following Erisman and Van Pul (1994) for different surfaces taking into account species dependent (Henry constant, oxidation power), micro-meteorological and land-use information (Cuvelier et al., 2013). For particles, the surface resistance is considered to be zero.

Wet deposition fluxes are parameterised using scavenging coefficients λ to calculate the loss of concentration C per time step dt due to wet scavenging. Simplified the change in concentration is calculated by

$$\frac{dC}{dt} = -\lambda \cdot C \tag{2.1}$$

In the operational version of RCG the wet deposition module is based on simple scavenging coefficients considering below-cloud scavenging only. For gases the scavenging coefficients depend on the Henry constant and the precipitation rate assuming a constant droplet pH of 5. For particles identical scavenging coefficients are assumed for all particles. Furthermore, aqueous-phase sulphate formation in clouds is simulated via two pathways -oxidation by hydrogen peroxide and oxidation by dissolved ozone- applying reaction rates for a fixed cloud water content of 0.15 g m^{-3} and a constant droplet pH of 5.

Within this thesis a research version of RCG has been developed in which the model description concerning sulphate formation and wet deposition processes has been improved

and a modelled droplet pH has been implemented as described in Chapter 3.

As input data, RCG requires meteorological data at hourly intervals consisting of the three-dimensional fields of U- and V-wind components, temperature, water vapor and density and the two-dimensional fields Monin-Obukov-length, friction velocity, precipitation, cloud cover, mixing layer height, surface temperature, surface wind speed and snow cover. Within this study, two meteorological drivers have been used to force RCG.
(1) The diagnostic meteorological analysis system TRAMPER (Tropospheric Realtime Applied Meteorological Procedures for Environmental Research) which is based on an optimum interpolation procedure on isentropic surfaces and was developed at Freie Universität Berlin (Reimer, 1992; Gsella et al., 2014). The system incorporates a numerical statistical fine mesh analysis procedure for meteorological observations from weather services and all available local synoptic surface and upper air measurements.
(2) The COSMO-EU model which is the operational numerical weather prediction model of the German Weather Service (DWD) (Doms et al., 2011; Doms, 2011).
Furthermore, the model requires annual emissions of volatile organic compound, nitrogen oxides, carbon monoxide, sulphur dioxide, methane, ammonia, PM_{10}, and $PM_{2.5}$, split into point and gridded area sources. Using sector-dependent, monthly, day-of-week and hourly emission factors the hourly emissions are derived within the model run. Within this study, emissions for Germany were taken from a national inventory for the year 2005 (Builtjes et al., 2010) and combined with the European TNO-MACC (Monitoring Atmospheric Composition and Climate) data set for the same year (Denier van der Gon et al., 2010). Moreover, RCG includes modules to treat the emissions of sea salt aerosols (Gong et al., 1997) and wind-blown dust particles (Claiborn et al., 1998; Loosemore and Hunt, 2000). Biogenic VOC emissions are calculated based on land-use information including data for 115 forest trees (Koeble and Seufert, 2002). Land-use information is also needed for the dry deposition calculation. The land use data set used is based on CORINE/Smiatek (EEA, 2000), with a grid resolution of 0.0167° in longitude and latitude over Europe and 13 land use categories.
For the European domain model simulations boundary conditions were taken from climatological background concentrations for gases and aerosols while for the nested model simulations a RCG run covering Europe provided the boundary conditions.

2.2 LOTOS-EUROS model description

LOTOS-EUROS (LOng Term Ozone Simulation - EURopean Operational Smog) is a three dimensional CTM of similar complexity as the above described RCG. The off-line

Eulerian grid model simulates air pollution concentrations in the lower troposphere solving the advection-diffusion equation on a regular lat-lon-grid on the regional scale over Europe (Schaap et al., 2008; Wichink Kruit et al., 2012; Kranenburg et al., 2013). The current master domain of LOTOS-EUROS is 35°N-70°N and 30°W-60°E. The standard grid resolution is 0.50° longitude × 0.25° latitude, which is approximately 25×25 km^2. The use of a higher horizontal resolution and the choice of a smaller domain are possible. The vertical grid is based on terrain following vertical coordinates and extends to 3.5km above sea level. As optional in RCG, the model uses a dynamic mixing layer approach to determine the vertical structure, i.e. the vertical layers vary in space and time. The layer on top of a 25 m surface layer follows the mixing layer height, which is obtained from the meteorological input data that is used to force the model. The height of the two reservoir layers is determined by the difference between model top at 3.5 km and mixing layer height. Both layers are equally thick with a minimum of 50 m. In cases in which the mixing layer extends near or above 3.5km, the top of the model exceeds the 3.5km according to the above-mentioned description.
The horizontal advection of pollutants is is handled with the monotonic advection scheme developed by Walcek (2000). The vertical diffusion is simulated applying the standard local K-approach. Gas-phase chemistry is simulated using the TNO CBM-IV scheme, which is a modified version of the original scheme (Whitten et al., 1980). Hydrolysis of N_2O_5 is explicitly described following Schaap et al. (2004). The sulphate formation description developed within this thesis and described in Chapter 3 has also been implemented in LOTOS-EUROS. Hence, the model explicitly accounts for cloud chemistry computing sulphate formation as a function of cloud liquid water content and cloud droplet pH. For aerosol chemistry LOTOS-EUROS features the thermodynamic equilibrium module ISORROPIA2 (Fountoukis and Nenes, 2007) to model the gaseous nitric acid-ammonia-ammonium nitrate-ammonium sulphate-aerosol water equilibrium. SOA are not yet treated within LOTOS-EUROS.
Dry Deposition fluxes are parameterised following the resistance approach as described in Erisman et al. (1994). Furthermore, a compensation point approach for ammonia is included in the dry deposition module (Wichink Kruit et al., 2012). The wet deposition module is based on precipitation rates using simple scavenging coefficients for the below cloud scavenging of gases (Schaap et al., 2004) and particles (Simpson et al., 2003).
Furthermore, LOTOS-EUROS includes a source apportionment module, which enables tracking the origin of the modelled concentrations for different tracers (Kranenburg et al., 2013). Using a labelling technique the module calculates the contribution of specified sources for all model grid cells and time steps. The contributions per label are calculated as fractions of the total tracer concentration. Within this study the source apportion-

ment module has been used to analyse the amount of SIA formed per unit precursor gas emission to investigate changes in the gas-to-particle conversion over time.
For the investigation presented in Chapter 5 LOTOS-EUROS was forced with the regional climate model RACMO2 (Lenderink et al., 2003; van Meijgaard et al., 2008) of the Dutch weather service KNMI. At the boundaries the simulation was driven by meteorology from ERA-Interim reanalysis (Dee et al., 2011).
Annual emission totals applied in this study were provided by the International Institute for Applied Systems Analysis (IIASA). The data was generated using RAINS (Amann et al., 1999) and GAINS (Amann et al., 2011) model output. In LOTOS-EUROS, the temporal variation of the emissions is represented by monthly, day-of-the-week and hourly time factors that break down the annual totals for each source category. Furthermore, an included biogenic emission routine is based on detailed information on tree species over Europe (Koeble and Seufert, 2002). Sea salt emissions are described using Martensson et al. (2003) for the fine mode and Monahan et al. (1986) for the coarse mode.
As in RCG, the land use data set used in LOTOS-EUROS is based on CORINE/Smiatek (EEA, 2000), including 13 different land use categories and the boundary conditions for the master domain were taken from climatological background concentrations for gases and aerosols.

2.3 Observations

Along with the abatement conventions harmonized surface monitoring of atmospheric composition was initiated over Europe in the early 1970s (Tørseth et al., 2012). The monitoring networks are established on the European, national and local/urban scale and provide a means to assess the short-term and long-term effectiveness of implemented air quality management. In addition to the latter assessment the observed information on atmospheric composition is of key importance to validate and further develop models. Also within the here presented study surface observations of chemical constituents of various measurement networks have been used to evaluate the performed CTM simulations.
EMEP (European Monitoring and Evaluation Programme) is a European-wide network of observational sites. The main objective of EMEP is to provide governments with information of the deposition and concentration of air pollutants, as well as the quantity and significance of the long-range transmission of air pollutants and their fluxes across boundaries (Tørseth et al., 2012). Therefore, the measurement sites are located such that significant local influences, as e.g. local emission sources or topographic features, are minimised and the sites are representative for a larger region (Tørseth et al., 2012). Thus, EMEP solely includes sites in the rural background. The site criteria are defined within

the EMEP manual (EMEP/CCC, 2001) which also includes the EMEP data quality objectives to assure the consistency of the database. The data is publicly available and can be downloaded from the EMEP website (http://emep.int).
The measurements to which Germany has committed itself internationally are carried out and reported to EMEP by the Federal Environment Agency (Umweltbundesamt - UBA). In Germany, UBA serves as the national reference laboratory, together with the State Office for Nature, Environment and Consumer Affairs (Landesamt für Natur, Umwelt und Verbraucherschutz) of North-Rhine Westphalia, to set the benchmarks of air quality assessment. The UBA National EU Reference Laboratory coordinates quality assurance activities for the measurements (UBA, 2004) of the compounds regulated by EU Directive 2008/50/EC (EC, 2008) on ambient air quality and cleaner air for Europe.
Next to EMEP, the AirBase database contains European-wide surface observations of atmospheric chemical compounds. AirBase is the public air quality database of the European Environmental Agency (EEA) and includes air quality monitoring data and information submitted by presently, in 2014, 38 participating countries throughout Europe (http://acm.eionet.europa.eu/databases/airbase). Most EMEP sites are also included in the AirBase database. The AirBase system contains more than 40 pollutants and a larger number of stations than EMEP as the site criteria are less stringent and AirBase is not limited to rural background stations. The monitoring sites are classified into 'type of station' (traffic, industrial, background), the 'type of zone' (urban, suburban, rural) and the 'characterization of zone' (residential, commercial, industrial, agricultural, nature, unknown and combination of these). The national data suppliers are responsible for the quality of the data. Nevertheless, quality checks at the incoming data are performed (Mol and de Leeuw, 2005).

In Chapter 3 UBA monitoring sites are used for model evaluation purposes while in Chapter 4 additionally data from the AirBase database is applied to evaluate the used CTM. Finally, in Chapter 4 EMEP and AirBase data are used to compare to the results of the model simulation. In general, when applying measurements of concentrations and deposition fluxes of atmospheric chemical compounds for model evaluation purposes it should be kept in mind that the observations also exhibit uncertainties (e.g. Aas et al., 2007). Furthermore, predictions from three dimensional CTMs always represent volume-averaged concentrations or deposition fluxes reflecting volume-average weather, physical and chemical conditions, whereas observations are point measurements reflecting individual events (Dennis et al., 2010).

References

Aas, W. ; Hanssen, J. E. ; Schaug, J.: Field intercomparison of main components in air in EMEP. *Water Air Soil Poll. Focus* (2007), pp 1567–7230

Adams, P.J. ; Seinfeld, J.H. ; Koch, D.M. ; Mickley, L. ; Jacob, D.: General circulation model assessment of direct radiative forcing by the sulphate-nitrateammonium-water inorganic aerosol system. *J. Geophys. Res.* 102 (D1) (2001), pp 1097–1111

Amann, M. ; Bertok, I. ; Borken-Kleefeld, J. ; Cofala, J. ; Heyes, C. ; Höglund-Isaksson, L. ; Klimont, Z. ; Nguyen, B. ; Posch, M. ; Rafaj, P. ; Sandler, R. ; Schöpp, W. ; Wagner, F. ; Winiwarter, W.: Cost-effective control of air quality and greenhouse gases in Europe: Modelling and policy applications. *Environ. Modell. and Softw.* 26 (2011), pp 1489–1501

Amann, M. ; Cofala, J. ; Heyes, C. ; Klimont, Z. ; Schöpp, W.: *The RAINS Model: A Tool for Assessing Regional Emission Control Strategies in Europe.* Pollution Atmosphérique 4, Paris, France, 1999

Amann, M. ; Klimont, Z. ; Winiwarter, W.: *Emissions from agriculture and their control potentials.* TSAP Report No. 3, Version 1.0, DG-Environment of the European Commission, Belgium, 2012

Andreae, O.: Aerosols Before Pollution. *Science* 315 (2007), pp 50–51

Ansari, A. S. ; Pandis, S. N.: Responce of inorganic PM to precursor concentrations. *Environ. Sci. Technol.* 32 (1998), pp 2706–2714

Barrett, E. ; Brodin, G.: The acidity of Scandinavian precipitation. *Tellus* 7 (1955), pp 251–257

Bary, E. de ; Junge, C.: Distribution of sulfur and chloride over Europe. *Tellus* 15 (1963), pp 370–381

Bäumer, D. ; Vogel, B. ; Versick, S. ; Rinke, R. ; Möhler, O. ; Schnaiter, M.: Relationship of visibility, aerosol optical thickness and aerosol size distribution in an ageing air mass over South-West Germany. *Atmos. Environ.* 42 (2008), pp 989–998

Beekmann, M. ; Kerschbaumer, A ; Stern, R. ; Reimer, E. ; Möller, D.: PM measurement campaign HOVERT in the Greater Berlin area: model evaluation with chemically specified particulate matter observations for a one year period. *Atmos. Chem. Phys.* 7 (2007), pp 55–68

Berge, E. ; Jakobsen, H.A.: A regional scale multi-layer model for the calculation of long-term transport and deposition of air pollution in Europe. *Tellus* 50 (1998), pp 205–223

Bessagnet, B. ; Hodzic, A. ; Vautard, R. ; Beekmann, M. ; Cheinet, S. ; Honoré, C. ; Liousse, C. ; Rouil, L.: Aerosol modelling with CHIMERE - preliminary evaluation at the continental scale. *Atmos. Environ.* 38 (2004), pp 2803–2817

Bobbink, R. ; Hornung, M. ; Roelofs, J.M.: The effects of airborne pollutants on species diversity in natural and semi-natural European vegetation. *J. Ecol.* 86 (1998), pp 717–738

Bond, T.C. ; Doherty, S.J. ; Fahey, D.W. ; Forster, P.M. ; Berntsen, T. ; DeAngelo, B.J. ; Flanner, M.G. ; Ghan, S. ; Karcher, B. ; Koch, Kinne S. ; Kondo, Y. ; Quinn, P.K. ; Sarofim, M.C. ; Schultz, M.G. ; Schulz, M. ; Venkataraman, C. ; Zhang, H. ; Zhang, S. ; Bellouin, N. ; Guttikunda, S.K. ; Hopke, P.K. ; Jacobson, M.Z. ; Kaiser, J.W. ; Klimont, Z. ; Lohmann, U. ; Schwarz, J.P. ; Shindell, D. ; Storelvmo, T. ; Warren, S.G. ; Zender, C.S.: Bounding the role of black carbon in the climate system: a scientific assessment. *J. Geophys. Res., D* 118 (2013), pp 5380–5552

Boucher, O. ; Randall, D. ; Artaxo, P. ; Bretherton, C. ; Feingold, G. ; Forster, P. ; Kerminen, V.M. ; Kondo, Y. ; Liao, H. ; Lohmann, U. ; Rasch, P. ; Satheesh, S.K. ; Sherwood, S. ; Stevens, B. ; Zhang, X.Y.: *Clouds and Aerosols.* Climate Change 2013: The Physical Science Basis. Contribution of Working Group I to the Fifth Assessment Report of the Intergovernmental Panel on Climate Change [Stocker, T.F., D. Qin, G.-K. Plattner, M. Tignor, S.K. Allen, J. Boschung, A. Nauels, Y. Xia, V. Bex and P.M. Midgley (eds.)]. Cambridge University Press, Cambridge, United Kingdom and New York, NY, USA, 2013

Builtjes, P. ; Jörß, W. ; Stern, R. ; Theloke, J.: *Strategien zur Verminderung der Feinstaubbelastung. PAREST-Summary report, F&E 206 43 200/01.* UBA-Texte Nr. 09/2012, Umweltbundesamt, Dessau, Germany, 2010

Carter, W.: Condensed atmospheric photooxidation mechanisms for isoprene. *Atmos. Environ.* 30 (1996), pp 4275–4290

Carter, W.P.L.: *Implementation of the SAPRC-99 chemical mechanism into the Models-3 Framework.* Report to the US Environmental Agency, 2000

Charlson, Langner J. ; Rodhe, H. ; Leovy, C. B. ; Warren, S. G.: Perturbation of the Northern-Hemisphere radiative balance by backscattering from anthropogenic sulfate aerosols. *Tellus* 43 (1991), pp 152–163

Claiborn, C. ; Lamb, B. ; Miller, A. ; Beseda, J. ; Clode, B. ; Vaughan, J. ; Kang, L. ; Nevine, C.: Regional measurements and modelling of windblown agricultural dust: The Columbia Plateau PM_{10} Program. *J. Geophys. Res.* 103(D16) (1998), pp 19753–19767

Cuvelier, C. ; Thunis, P. ; Karam, D. ; Schaap, M. ; Hendriks, C. ; Kranenburg, R. ; Fagerli, H. ; Nyiri, Á. ; Simpson, D. ; Wind, P. ; Schulz, M. ; Bessagnet, B. ; Colette, A. ; Terrenoire, E. ; Rouil, L. ; Stern, R. ; Graff, A. ; Baldasano, J. M. ; Pay, M. T.: *ScaleDep: performance of European chemistry-transport models as function of horizontal spatial resolution.* EMEP Report 1/2013, 2013

Dee, D. P. ; Uppala, S. M. ; Simmons, A. J. ; Berrisford, P. ; Poli, P. ; Kobayashi, S. ; Andrae, U. ; Balmaseda, M. A. ; Balsamo, G. ; Bauer, P. ; Bechtold, P. ; Beljaars, A. C. M. ; Berg, L. van de ; Bidlot, J. ; Bormann, N. ; Delsol, C. ; Dragani, R. ; Fuentes, M. ; Geer, A. J. ; Haimberger, L. ; Healy,

S. B. ; Hersbach, H. ; Hólm, E. V. ; Isaksen, L. ; Kållberg, P. ; Köhler, M. ; Matricardi, M. ; McNally, A. P. ; Monge-Sanz, B. M. ; Morcrette, J.-J. ; Park, B.-K. ; Peubey, C. ; Rosnay, P. de ; Tavolato, C. ; Thépaut, J.-N. ; Vitart, F.: The ERA-Interim reanalysis: configuration and performance of the data assimilation system. *Q. J. R. Meteorol. Soc.* 137 (2011), pp 553–597

Dennis, R. ; Fox, T. ; Fuentes, M. ; Gilliland, A. ; Hanna, S. ; Hogrefe, C. ; Irwin, J. ; Rao, S.T. ; Scheffe, R. ; Schere, K. ; Steyn, D. ; Venkatram, A.: A framework for evaluating regional-scale numerical photochemical modeling systems. *Environ. Fluid Mech.* 10 (2010), pp 471–489

Doms, G.: *A Description of the Nonhydrostatic Regional COSMO-Model. Part I: Dynamics and Numerics.* Printed at Deutscher Wetterdienst, P.O. Box 100465, 63004 Offenbach, Germany, 2011

Doms, G. ; Förstner, J. ; Heise, E. ; Herzog, H.-J. ; Mironov, D. ; Raschendorfer, M. ; Reinhardt, T. ; Ritter, B. ; Schrodin, R. ; Schulz, J.-P. ; Vogel, G.: *A Description of the Nonhydrostatic Regional COSMO-Model. Part II: Physical Parameterization.* Printed at Deutscher Wetterdienst, P.O. Box 100465, 63004 Offenbach, Germany, 2011

EC: *Directive 2001/42/EC of the European Parliament and of the Council of 27 June 2001 on the assessment of the effects of certain plans and programmes on the environment.* European Commission, 2001

EC: *Directive 2008/50/EC of the European Parliament and of the Council on ambient air quality and cleaner air for Europe.* European Commission, 2008

EEA: *CORINE Land Cover 2000.* dataservice.eea.eu.int, 2000

EEA: *Air quality in Europe - 2012 report.* EEA report No. 4/2012, European Environment Agency, Copenhagen, 2012, 2012

Eeftens, M. ; Beelen, R. ; Hoogh, K. de ; Bellander, T. ; Cesaroni, G. ; Cirach, M. ; Declercq, C. ; Dedele, A. ; Dons, E. ; Nazelle, A. de ; Dimakopoulou, K. ; Eriksen, K. ; Falq, G. ; Fischer, P. ; Galassi, C. ; Grazuleviciene, R. ; Heinrich, J. ; Hoffmann, B. ; Jerrett, M. ; Keidel, D. ; Korek, M. ; Lanki, T. ; Lindley, S ; Madsen, C. ; Mölter, A. ; Nádor, G. ; Nieuwenhuijsen, M. ; Nonnemacher, M. ; Pedeli, X. ; Raaschou-Nielsen, O. ; Patelarou, E. ; Quass, U. ; Ranzi, A. ; Schindler, C. ; Stempfelet, M. ; Stephanou, E. ; Sugiri, D. ; Tsai, M.Y. ; Yli-Tuomi, T. ; Varro, M.J. ; Vienneau, D. ; Klot, S. ; Wolf, K. ; Brunekreef, B. ; Hoek, G.: Development of Land Use Regression Models for $PM_{2.5}$, $PM_{2.5}$ Absorbance, PM_{10} and PMcoarse in 20 European Study Areas; Results of the ESCAPE Project. *Environ. Sci. Technol.* 46 (20) (2012), pp 11195–11205

EMEP/CCC: *Manual for sampling and chemical analysis, EMEP/CCC Report 1/95 (Last rev. 2001).* Norwegian Institute for Air Research, Kjeller, 2001

Erisman, J. ; Van Pul, A.: Parameterization of surface resistance for the quantification of atmospheric deposition of acidifying pollutants and ozone. *Atmos. Environ.* 28 (1994), pp 2595–2607

Erisman, J.W. ; Pul A. van ; P., Wyers: Parametrization of surface-resistance for the quantification of atmospheric deposition of acidifying pollutants and ozone. *Atmos. Environ.* 28 (1994), pp 2595–2607

Fagerli, H. ; Aas, W.: Trends of nitrogen in air and precipitation: Model results and observations at EMEP sites in Europe, 1980-2003. *Environ. Pollut.* 154 (2008), pp 448–461

Forster, P. ; Ramaswamy, V. ; Artaxo, P. ; Berntsen, T. ; Betts, R. ; Fahey, D. W. ; Haywood, J. ; Lean, J. ; Lowe, D. C. ; Myhre, G. ; Nganga, J. ; Prinn, R. ; Raga, G. ; Schulz, M. ; ; Van Dorland, R.: *Changes in atmospheric constituents and in radiative forcing, in: Climate Change 2007: The Physical Science Basis.* Contribution of Working Group I to the Fourth Assessment Report of the Intergovernmental Panel on Climate Change, edited by: Solomon, S., Qin, D., Manning, M., Chen, Z., Marquis, M., Averyt, K. B., Tignor, M., and Miller, H. L., Cambridge University Press, Cambridge, UK, and New York, USA, 2007

Fountoukis, C. ; Nenes, A.: ISORROPIA II: A computationally efficient thermodynamic equilibrium model for Kalium - ÂCalcium - MagnesiumÂ - Ammonium - Sodium - Sulfate - Nitrate - Chloride - Water aerosols. *Atmos. Chem. Phys.* 7 (17) (2007), pp 4639–4659

Fowler, D. ; Smith, R. ; Müller, J. ; Cape, J. N. ; Sutton, M. ; Erisman, J. W. ; Fagerli, H.: Long-term trends in sulphur and nitrogen deposition in Europe and the cause of nonlinearities. *Water Air Soil Poll.* 7 (2007), pp 41–47

Gery, M.W. ; Whitten, G.Z. ; Killus, J.P. ; Dodge, M.C.: A photochemical kinetics mechanism for urban and regional scale computer modeling. *J. Geophys. Res.* 94 (D10) (1989), pp 12925–12956

Gon, H.A.C. Denier van der ; Visschedijk, A. ; Brugh, H. van den ; Dröge, R.: *F&E Vorhaben: Strategien zur Verminderung der Feinstaubbelastung - PAREST: A high resolution European emission data base for the year 2005.* TNO-Report, TNO-034-UT-2010-01895-RPT-ML, Utrecht, The Netherlands, 2010

Gong, S. L. ; Barrie, L. A. ; Blanchet, J.P.: Modelling sea-salt aerosols in the atmosphere. 1. Model development. *J. Geophys. Res.* 102 (1997), pp 3805–3818

Grell, G.A. ; Peckham, S.E. ; Schmitz, R. ; McKeen, S.A. ; Frost, G. ; Skamarock, W.C. ; Eder, B.: Fully coupled online chemistry within the WRF model. *Atmos. Environ.* 39 (2005), pp 6957–6975

Grennfelt, P. ; Hov, O.: Regional air pollution at a turning point. *Ambio* 34 (2005), pp 2–10

Gsella, A. ; Meij, A. de ; Kerschbaumer, A. ; Reimer, E. ; Thunis, P. ; Cuvelier, C.: Evaluation of MM5, WRF and TRAMPER meteorology over the complex terrain of the Po Valley, Italy. *Atmos. Environ.* 89 (2014), pp 797–806

Hass, H. ; Builtjes, P. J. H. ; Simpson, D. ; Stern, R.: Comparison of model results obtained with several European regional air quality models. *Atmos. Environ.* 31 (1997), pp 3259–3279

Haywood, J.M. ; Boucher, O.: Estimates of the direct and indirect radiative forcing due to tropospheric aerosols: A review. *Rev. Geophys.* 38 (2000), pp 513–543

Hoffmann, M.R. ; Calvert, J.G.: *Chemical Transformation Modules for Eulerian Acid Deposition Models.* The Aqueous-Phase Chemistry, EPA/600/3e85/017, Vol. 2. U.S. Environmental Protection Agency, Research Triangle Park, NC., USA, 1985

Kangas, L. ; Syri, S.: Regional nitrogen deposition model for integrated assessment of acidification and eutrophication. *Atmos. Environ.* 36 (2002), pp 1111–1122

Koeble, R. ; Seufert, G.: *Novel maps for forest trees in Europe.* Proceedings of the 8th European Symposium on the Physico-Chemical Behaviour of Atmospheric Pollutants, JRC Ispra, 2002

Kranenburg, R. ; Segers, A.J. ; Hendriks, C. ; Schaap, M.: Source apportionment using LOTOS EUROS: module description and evaluation. *Geosci. Model Dev.* 6 (2013), pp 721–733

Lenderink, G. ; Hurk, B. Van den ; Meijgaard, E. van ; Van Ulden, A. P. ; Cuijpers, J.: *Simulation of present-day climate in RACMO2: first results and model developments.* KNMI, Technical Report TR 252, De Bilt, The Netherlands, 2003

Liao, H. ; Seinfeld, J.H.: Global impacts of gas-phase chemistryaerosol interactions on direct radiative forcing by anthropogenic aerosols and ozone. *J. Geophys. Res.* 110 (2005), pp D18208

Loosemore, G. A. ; Hunt, J. R.: Dust resuspension without saltation. *J. Geophys. Res.* 105(D16) (2000), pp 20663–20671

Løvblad, G. ; Tarrasón, L. ; Tørseth, K. ; Dutchak, S.: *EMEP Assessment Part I: European Perspective.* Norwegian Meteorological Institute, Oslo, Norway, 2004

Martensson, E.M. ; Nilsson, E.D. ; Leeuw, G. de ; Cohen, L.H. ; Hansson, H.C.: Laboratory simulations and parameterization of the primary marine aerosol production. *J. Geophys. Res.* 108 (2003)

McFiggans, G. ; Artaxo, P. ; Baltensperger, U. ; Coe, H. ; Facchini, M. C. ; Feingold, G. ; Fuzzi, S. ; Gysel, M. ; Laaksonen, A. ; Lohmann, U. ; Mentel, T. F. ; Murphy, D. M. ; O'Dowd, C. D. ; Snider, J. R. ; Weingartner, E.: The effect of physical and chemical aerosol properties on warm cloud droplet activation. *Atmos. Chem. Phys.* 6 (2006), pp 2593–2649

McMurry, P.H. ; Shepherd, M.F. ; Vickery, J.S.: *Particulate Matter Science for Policy Makers: A NARSTO Assessment.* Cambridge University Press, 2004

Mebust, M. R. ; Eder, B. K. ; Binkowski, F. S. ; Roselle, S. J.: Models-3 Community Multiscale Air Quality (CMAQ) model aerosol component. *J. Geophys. Res.* 108(D6) (2003), pp 4184

Meijgaard, E. van ; Ulft, L. H. van ; Berg, W.J. van de ; Bosveld, F.C. ; Hurk, B.J.J.M. van den ; Lenderink, G. ; Siebesma, A.P.: *The KNMI regional atmospheric climate model RACMO version 2.1.* KNMI, Technical Report TR-302, De Bilt, The Netherlands, 2008

Memmesheimer, M. ; Friese, E. ; Ebel, A. ; Jakobs, H.J. ; Feldmann, H. ; Kessler, C. ; Piekorz, G.: Long-term simulations of particulate matter in Europe on different scales using sequential nesting of a regional model. *Int. J. Environ. Pollut.* 22 (2004), pp 108–132

Mol, W. ; Leeuw, F. de: *Making Air Quality Assessments with AIRBASE.* EnviroInfo 2005 (Brno) Informatics for Environmental Protection - Networking Environmental Information Copyright, Masaryk University Brno, Brno, Czech Republic, 2005

Monahan, E.C. ; Spiel, D.E. ; Davidson, K.L.: *A model of marine aerosol generation via whitecaps and wave disruption.* Oceanic Whitecaps and their role in air/sea exchange, edited by Monahan, E.C, Mac Niocaill, G., Reidel, D., Norwell, Mass., USA, 1986

Myhre, G. ; Myhre, C. E. ; Samset, B. H. ; Storelvmo, T.: Aerosols and their Relation to Global Climate and Climate Sensitivity. *Nature Education Knowledge* 4(5) (2013), pp 7

Nenes, A. ; Pilinis, C. ; Pandis, S.: Continued development and testing of a new thermodynamic aerosol module for urban and regional air quality models. *Atmos. Environ.* 33 (1999), pp 1553–1560

Pope, C. A. I. ; Ezzati, M. ; Dockery, D. W.: Fine-particulate air pollution and life expectancy in the United States. *N. Engl. J. Med.* 360 (2009), pp 376–386

Putaud, J.-P. ; Raesa, F. ; Van Dingenen, R. ; Bruggemann, E. ; Facchini, M. ; Decesari, S. ; Fuzzi, S. ; Gehrig, R. ; Hüglin, C. ; Laj, P. ; Lorbeer, G. ; Maenhaut, W. ; Mihalopoulos, N. ; Mueller, K. ; Querol, X. ; Rodriguez, S. ; Schneider, J. ; Spindler, G. ; Ten Brink, H. ; Tørseth, K. ; Wiedensohler, A.: A European aerosol phenomenology - 2: Chemical characteristics of particulate matter at kerbside, urban, rural and background locations in Europe. *Atmos. Environ.* 38 (2004), pp 2579–2595

Putaud, J.-P. ; Van Dingenen, R. ; Alastuey, A. ; Bauer, H. ; Birmili, W. ; Cyrys, J. ; Flentje, S. ; Gehrig, R. ; Hansson, H.C. ; Harrison, R.M. ; Herrmann, H. ; Hitzenberger, R. ; Hüglin, C. ; Jones, A. M. ; Kasper-Giebl, A. ; Kiss, G. ; Kousa, A. ; Kuhlbusch, Löschau G. ; Maenhaut, W. ; Molnar, A. ; Moreno, T. ; Pekkanen, J. ; Perrino, C. ; Pitz, M. ; Puxbaum, H. ; Querol, X. ; Rodriguez, S. ; Salma, I. ; Schwarz, J. ; Smolik, J. ; Schneider, G. ; Spindler, H. ; Ten Brink, H.M. ; Tursic, J. J. ; Viana, M. ; Wiedensohler, A. ; Raes, F.: A European aerosol phenomenology - 3: Physical and chemical characteristics of particulate matter from 60 rural, urban, and kerbside sites across Europe. *Atmos. Environ.* 44 (2010), pp 1308–1320

Ramanathan, V. ; Crutzen, P.J. ; Kiehl, J.T. ; Rosenfeld, D.: Atmosphere: aerosols, climate, and the hydrological cycle. *Science* 294 (2001), pp 2119–2124

Reimer, B.: *An operational meteorological diagnostic system for regional air pollution analysis and long term modelling.* Air Pollution Modelling and its Application IX, eds. H. v. Dop und G. Kallos, NATO Challenges of Modern Society, Kluwer Academic/Plenum Publisher, New York, 1992

Reiss, R. ; Anderson, E.L. ; Cross, C.E. ; Hidy, G. ; Hoel, D. ; McClellan, R. ; Moolgavkar, S.: Evidence of health impacts of sulfate- and nitrate-containing particles in ambient air. *Inhal. Toxicol.* 19 (2007), pp 419–449

Römer, M. ; Beekmann, M. ; Bergström, R. ; Boersen, G. ; Feldmann, H. ; Flatøy, F. ; Honore, C. ; Langner, J. ; Jonson, J. E. ; Matthijsen, J. ; Memmesheimer, M. ; Simpson, D. ; Smeets, P. ; Solberg, S. ; Stern, R. ; Stevenson, D. ; Zandveld, P. ; Zlatev, Z.: *Ozone trends according to ten dispersion models.* EUROTRAC-2 special report, GSF, Munich, Germany, 2003

Schaap, M.: *On the importance of aerosol nitrate over Europe Data analysis and modelling.* PhD Thesis, Instituut voor Marien en Atmosferisch Onderzoek, Universiteit Utrecht, 2003

Schaap, M. ; Loon, M. van ; Brink, H.M. ten ; Dentener, F.D. ; Builtjes, P.J.H.: Secondary inorganic aerosol simulations for Europe with special attention to nitrate. *Atmos. Chem. Phys.* 4 (2004), pp 857–874

Schaap, M. ; Sauter, F. ; Timmermans, R.M.A. ; Roemer, M. ; Velders, G. ; Beck, J. ; Builtjes, P.J.H.: The LOTOS-EUROS model: description, validation and latest developments. *Int. J. Environ. Pollut.* 32 (2) (2008), pp 270–290

Schaap, M. ; Weijers, E.P. ; Mooibroek, D. ; Nguyen, L. ; Hoogerbrugge, R.: *Composition and origin of Pariculate Matter in the Netherlands. Results from the Dutch Research Programme on Particulate.* Publication of the Netherlands Research Program on Particulate Matter, Report 5000099007/2010, ECN, PBL, TNO, RIVM, The Netherlands, 2010

Schell, B. ; Ackermann, I. J. ; Hass, H. ; Binkowski, F. ; Ebel, A.: Modelling the formation of secondary organic aerosol within a comprehensive air quality model system. *J. Geophys. Res.* 106(D22) (2001), pp 28275–28293

Schlesinger, R.B. ; Cassee, F.R.: Atmospheric secondary inorganic particulate matter: the toxicological perspective as a basis for health effects risk assessment. *Inhal. Toxicol.* 15 (2003), pp 197–235

Scire, J.S. ; Venkatram, A.: The contribution of in-cloud oxidation of SO_2 to wet scavenging of sulfur in convective clouds. *Atmos. Environ.* 19 (4) (1985), pp 637–650

Seinfeld, J.H. ; Pandis, N.: *Atmospheric Chemistry and Physics: From Air Pollution to Climate Change.* John Wiley and Sons, Inc., New York, 1998

Simpson, D. ; Benedictow, A. ; Berge, H. ; Bergström, R. ; Emberson, L. D. ; Fagerli, H. ; Flechard, C. ; Hayman, G. D. ; Gauss, M. ; Jonson, J. E. ; Jenkin, M. E. ; Nyiri, A. ; Richter, C. ; Semeena, V. S. ; Tsyro, S. ; Tuovinen, J.P. ; Valdebenito, A. ; Wind, P.: The EMEP MSC-W chemical transport model - technical description. *Atmos. Chem. Phys.* 12 (2012), pp 7825–7865

Simpson, D. ; Fagerli, H. ; Jonson, J. E. ; Tsyro, S. ; Wind, P. ; Tuovinen, J.-P.: *Transboundary Acidification, Eutrophication and Ground Level Ozone in Europe, Part 1: Unified EMEP Model Description.* EMEP Report 1/2003, Norwegian Meteorological Institute, Oslo, Norway, 2003

Simpson, D. ; Yttri, K. E. ; Klimont, Z. ; Kupiainen, K. ; Caseiro, A. ; Gelencser, A. ; Pio, C. A. ; Puxbaum, H. ; Legrand, M.: Modeling carbonaceous aerosol over Europe: Analysis of the CARBOSOL and EMEP EC/OC campaigns. *J. Geophys. Res.-Atmos.* 112 (2007), pp D23S14

Stern, R. ; Yamartino, R. ; Graff, A.: *Analyzing the response of a chemical transport model to emissions reductions utilizing various grid resolutions.* 28th ITM on Air Pollution Modelling and its Application. May 15-19, 2006, Leipzig, Germany, 2006

Stockwell, W.R. ; Kirchner, F. ; Kuhn, M. ; Seefeld, S.: A new mechanism for regional atmospheric chemistry modeling. *J. Geophys. Res.* 102 (D22) (1997), pp 25847–25879

Stockwell, W.R. ; Middleton, P. ; Chang, J.S. ; Tang, X.: The second generation regional acid deposition model chemical mechanism for regional air quality modeling. *J. Geophys. Res.* 95 (1990), pp 16343–16367

Tarrasón, L. ; Johnson, J.E. ; Fagerli, H. ; Benedictow, A. ; Wind, P. ; Simpson, D. ; Klein, H.: *EMEP Status Report 1-2003 - Part III: Source-Receptor Relationships, Transboundary acidification, eutrophication and ground level ozone in Europe.* Norwegian Meteorological Institute, Oslo, Norway, 2003

Tørseth, K. ; Aas, W. ; Breivik, K. ; Fjaeraa, A.M. ; Fiebig, M. ; Hjellbrekke, A.G. ; Myhre, C.L. ; Solberg, S. ; Yttri, K.E.: Introduction to the European Monitoring and Evaluation Programme (EMEP) and observed atmospheric composition change during 1972–2009. *Atmos. Chem. Phys.* 12 (2012), pp 5447–5481

UBA: *Manual for Quality Assurance (in German).* Texte 28/04, Fachgebiet II 5.6, Umweltbundesamt, Berlin, Germany, 2004

UN/ECE: *The 1999 Gothenburg Protocol to Abate Acidification, Eutrophication and Ground level Ozone.* UNECE Report, Gothenburg, Sweden, 1999

Van Zanten, M.C. ; Sauter, F.J. ; Wichink Kruit, R.J. ; Van Jaarsveld, J.A. ; Van Pul, W.A.J.: *Description of the DEPAC module: Dry deposition modelling with DEPAC-GCN2010.* RIVM report 680180001/2010, Bilthoven, the Netherlands, 2010

Vestreng, V. ; Ntziachristos, L. ; Semb, A. ; Reis, S. ; Isaksen, I.S.A. ; Tarrasón, L.: Evolution of NO_x emissions in Europe with focus on road transport control measures. *Atmos. Chem. Phys.* 9 (4) (2009), pp 1503–1520

Walcek, C. J.: Minor flux adjustment near mixing ratio extremes for simplified yet highly accurate monotonic calculation of tracer advection. *J. Geophys. Res.* 105(D7) (2000), pp 9335–9348

Warneck, P.: *Chemistry of the Natural Atmosphere.* International Geophysics Series, 41,Academic Press, San Diego, CA., 1988

Weijers, E. P. ; Sahan, E. ; Brink, H. M. ten ; Schaap, M. ; Matthijsen, J. ; Otjes, R. P. ; Arkel, F. van: *Contribution of secondary inorganic aerosols to PM_{10} and $PM_{2.5}$ in the Netherlands; measurement and modeling results.* PBL report 500099006, Bilthoven, The Netherlands, 2010

Weijers, E. P. ; Schaap, M. ; Nguyen, L. ; Matthijsen, J. ; Gon, H. A. C. Denier van der ; Brink, H. M. ten ; Hoogerbrugge, R.: Anthropogenic and natural constituents in particulate matter in the Netherlands. *Atmos. Chem. Phys.* 11 (2011), pp 2281–2294

West, J. J. ; Ansari, A. S. ; Pandis, S. N.: Marginal $PM_{2.5}$: Nonlinear Aerosol Mass Response to Sulphate Reductions in the Eastern United States. *J. Air Waste Manage.* 49 (1999), pp 1415–1424

Whitten, G. ; Hogo, H. ; Killus, J.: The Carbon Bond Mechanism for photochemical smog. *Environ. Sci. Technol.* 14 (1980), pp 14690–14700

WHO: *Health relevance of particulate matter from various sources.* Report on a World Health Organization Workshop, Bonn, Germany, 26-27 March 2007, Copenhagen, Denmark, 2007

Wichink Kruit, R. ; Schaap, M. ; Sauter, F. ; Swaluw, E. Van der ; Weijers, E.: *Improving the understanding of secondary inorganic aerosol distribution over the Netherlands.* TNO report TNO-060-UT-2012-00334, Utrecht, The Netherlands, 2012

Wolke, R. ; Knoth, O. ; Hellmuth, O. ; Schröder, W. ; Renner, E.: The parallel model system LM-MUSCAT for chemistry-transport simulations: coupling scheme, parallelization and applications. *Joubert, G.R., Nagel, W.E., Peters, F.J., Walter, W.V. (Eds.), Parallel Computing: Software Technology, Algorithms, Architectures, and Applications. Elsevier, Amsterdam* (2004), pp 363–370

Worobiec, A. ; De Hoog, J. ; Osan, J. ; Szaloki, I. ; Ro, C.U. ; Grieken, R. van: Thermal stability of beam sensitive atmospheric aerosol particles in electron probe microanalysis at liquid nitrogen temperature. *Spectrochim. Acta* B 58 (2003), pp 479–496

Yamartino, R.J. ; Scire, J. ; Carmichael, G.R. ; Chang, Y.S.: The CALGRID mesoscale photochemical grid model-I. Model formulation. *Atmos. Environ.* 26A (1992), pp 1493–1512

Zhang, L. ; Gong, S. ; Padro, J. ; Barrie, L.: A size-segregated particle dry deposition scheme for an atmospheric aerosol module. *Atmos. Environ.* 35 (2001), pp 549–560

Chapter 3

Paper I - Implementation and evaluation of pH-dependent cloud chemistry and wet deposition in the chemical transport model REM-Calgrid

S. Banzhaf (1), M. Schaap (2), A. Kerschbaumer (1), E. Reimer (1), R. Stern (1), E. van der Swaluw (3) and P.J.H. Builtjes (1,2)

(1) Institut für Meteorologie, Freie Universität Berlin, Carl-Heinrich-Becker Weg 6-10, 12165 Berlin, Germany
(2) TNO, Department Climate, Air Quality and sustainability, Princetonlaan 6, 3508 TA Utrecht, The Netherlands
(3) National Institute for Public Health and the Environment (RIVM), Antonie van Leeuwenhoeklaan 9, 3721 MA Bilthoven, The Netherlands

published in Atmospheric Environment, 49, 378-390, 2012
doi: http://dx.doi.org/10.1016/j.atmosenv.2011.10.069 [1]

[1]The paper has been reprinted with kind permission from the journal.

Abstract

The Chemistry Transport Model REM-Calgrid (RCG) has been improved by implementing an enhanced description of aqueous-phase chemistry and wet deposition processes including droplet pH. A sensitivity study on cloud and rain droplet pH has been performed to investigate its impact on model sulphate production and gas wet scavenging. Air concentrations and wet deposition fluxes of the model sensitivity runs have been analysed and compared to observations. It was found that droplet pH variation within atmospheric ranges affects modelled air concentrations and wet deposition fluxes significantly. Applying a droplet pH of 5.5 for July 2005, mean sulphate air concentrations increased by up to 10% compared to using a droplet pH of 5 while SO_2 domain wet deposition sum increased by 110%. Moreover, model results using modelled droplet pH for January and July 2005 have been compared to model results applying a constant pH of 5 and to observations. The comparison to observations has shown that using a variable droplet pH improves the model performance concerning air concentrations and wet deposition fluxes of the investigated sulphur and nitrogen compounds. For SO_x wet deposition fluxes the Root Mean Square Error (RMSE) decreased by 16% for July 2005 when using a variable droplet pH instead of a constant pH of 5. Concerning sulphate and SO_2 air concentrations the RMSE was reduced by 8% and 16% for July 2005, respectively. The results have revealed that applying a variable droplet pH is preferable to using a constant pH leading to better consistency concerning air concentrations and wet deposition fluxes.

3.1 Introduction

Enhanced deposition of sulphur and nitrogen compounds may damage ecosystems by eutrophying and acidifying soils and fresh water leading to a decrease in biodiversity in terrestrial and aquatic ecosystems (Wright et al., 1976; Bobbink et al, 1998; Rabalais, 2002). Based on this knowledge, international co-operations to reduce anthropogenic emissions of acidic precursors have been adopted since the 1980s. In 1999 the Protocol to Abate Acidification, Eutrophication and Ground-level Ozone was signed to the Convention on Long-range Transboundary Air Pollution (LRTAP) under the auspices of the United Nations Economic Commission for Europe (UNECE) (UNECE, 1999a). Within the convention each member state has to assess acid and nitrogen deposition across its territory. For this purpose the concept of Critical Loads, a quantitative estimate of the exposure below which significant harmful effects on specified sensitive elements of the environment do not occur according to present knowledge was introduced (ICP Modelling and Mapping, 2004). These Critical Loads are still exceeded over large parts of Europe

(Lorenz et al, 2008) indicating a continued need for further implementation of air pollution abatement strategies.

Chemical transport models (CTMs) are used to calculate sulphur and nitrogen dry and wet deposition fluxes. The description of wet deposition processes within many CTMs is based on empirical approaches (e.g. Berge et al., 1998) and often rather crude. A multi model evaluation on sulphur and nitrogen wet deposition fluxes (Dentener et al., 2006) including 23 models of different complexity in chemistry and physics showed that 60-70% of the calculated wet deposition rates for Europe and North America agreed to within ±50% with measurements. On the regional scale a model inter-comparison over Europe (Van Loon et al., 2004) showed that modelled wet deposition fluxes usually differ substantially from observations and also show a large scatter among the models. Model development concerning the description of wet scavenging processes as well as the sulphur and nitrogen budget in general is needed to improve modelling of wet deposition fluxes and thus the overall model performance.

Acidity or pH of atmospheric droplets depends on the balance of dissolved bases and acids. The major acidic components are sulphuric acid, nitric acid and carbon dioxide whereas ammonia is the dominant base. Organic acids may also lower pH while base-cations (e.g. from sea salt aerosol or mineral dust) neutralise atmospheric acids. The atmospheric range of long term mean pH values range between 4.7 and 5.2 in central Europe (Kvaalen et al., 2002; Fowler et al., 2005; Rogora et al., 2006). Lower values may be observed in areas with high anthropogenic (sulphur) emissions. On the other hand higher values around 6.2 may occur in dust rich areas in the Mediterranean (Calvo et al., 2010). Individual precipitation samples show high variability within 2 orders of magnitude in H+ around the mean value. Trend analysis has shown a decrease in the acidity of precipitation in the past 15-20 years over Europe following the reduced emission of S compounds (Rogora et al., 2006; Fowler et al., 2005). As cloud droplets are more concentrated than precipitation droplets, the range of pH is expected to be higher than in precipitation droplets (Collett et al., 1993).

The pH of atmospheric droplets constrains the uptake and subsequent removal of gases from the atmosphere through rain out (Seinfeld and Pandis, 1998). Moreover, cloud chemistry and sulphur chemistry in particular are highly dependent on pH regime (Scire and Venkatram, 1985). In contrast to the aqueous phase oxidation of sulphur dioxide to sulphate by hydrogen peroxide, the oxidation by ozone is pH dependent. Below pH= 4.5 the oxidation pathway via hydrogen peroxide is dominant, whereas the strongly increasing reaction rates of the ozone oxidation reaction with pH cause the ozone reaction to be dominant above pH= 5.5. Given the spatial and temporal variability observed in pH it is important to incorporate pH explicitly when modelling sulphate formation and wet

deposition fluxes. Moreover, accounting for pH dependent cloud chemistry is essential for investigating trends in sulphur concentrations and depositions (Fagerli and Aas, 2008). Redington et al. (2009) showed that aqueous-phase sulphate aerosol production is very sensitive to cloud pH in a model sensitivity study. However, many CTMs still assume a fixed pH value (Schaap et al., 2008 (LOTOS-EUROS); Beekmann et al., 2007 (RCG); Simpson et al., 2003 (EMEP); Redington et al., 2009 (NAME)). Other models incorporate pH dependent parameterisations (Bessagnet et al., 2004 (CHIMERE); Byun and Schere, 2006 (CMAQ); ENVIRON, 2010 (CAMx)) but only one study on the sensitivity of model results to droplet pH has been published (Redington et al., 2009). The aim of this study is to investigate the impact of pH-dependent parameterizations on the model performance for wet deposition and concentrations of sulphur and nitrogen components over Germany. In this study the CTM RCG was improved by implementing enhanced pH dependent physical and chemical descriptions of scavenging processes and sulphate production (section 3.2). Model sensitivity runs were carried out over Germany to investigate the sensitivity of sulphate formation and wet scavenging to pH (section 3.3). Next, simulations with a variable pH were performed. The overall model performance was evaluated by comparison of the wet deposition fluxes and air concentrations of sulphur and nitrogen compounds to observations. Finally, the results are discussed (section 3.4) and conclusions are presented in section 3.5.

3.2 Methods and Data

3.2.1 Model description

The off-line Eulerian grid model RCG simulates air pollution concentrations solving the advection-diffusion equation on a regular lat-lon-grid with variable resolution over Europe (Stern et al., 2006; Beekmann et al., 2007). The vertical transport and diffusion scheme accounts for atmospheric density variations in space and time and for all vertical flux components when employing either dynamic or fixed layers. The advection scheme was developed by Walcek (2000). Gasphase chemistry is simulated using the latest release of the CBM-IV photochemical reaction scheme (Byun and Ching 1999). RCG features a thermodynamic equilibrium module for secondary inorganic aerosols (ISORROPIA: Nenes et al., 1999). Dry Deposition fluxes are calculated following a resistance approach as proposed by Erisman et al. (1994). RCG has been evaluated within many urban and regional applications (e.g. Stern et al., 2006; Beekmann et al., 2007) and within the framework of European model inter-comparison studies (e.g. Van Loon et al. 2004; Stern et al. 2008; Vautard et al. 2007; Vautard et al. 2009).

In the operational version of RCG aqueous-phase sulphate formation is simulated via two pathways -oxidation by hydrogen peroxide (H_2O_2) and oxidation by dissolved ozone (O_3)- applying reaction rates for a fixed cloud water content of 0.15 g m^{-3} and a constant droplet pH of 5. Furthermore the wet deposition module is based on precipitation rates using simple scavenging coefficients assuming a constant droplet pH of 5 considering below-cloud scavenging only. In the present study a research version of RCG has been developed in which the model description concerning sulphate production and wet deposition processes was improved as described below.

3.2.1.1 Improved RCG sulphate production scheme

For the aqueous-phase conversion of dissolved SO_2 to sulphate in cloud water two pathways are considered in the model: oxidation by hydrogen peroxide and oxidation by ozone. The concentrations of the reactants in cloud water are calculated using their Henry's law coefficients. Reaction rates are taken from Hoffmann and Calvert (1985) and McArdle and Hoffmann (1983). The effective reaction rates are functions of variable cloud liquid water content and droplet pH. Before the system is solved the cloud pH is estimated using the concentrations of the (strong) acids and bases including the buffering by bi-carbonate (through CO_2).

$$[H^+] = 2[SO_4^{2-}] + 2[SO_3^{2-}] + [HSO_3^-] + [NO_3^-] + [HCO_3^-] - [NH_4^+]$$

The reaction rate of the oxidation by ozone varies strongly over the range of pH values in cloud water while the oxidation rate by hydrogen peroxide shows negligible variability as function of pH (Seinfeld and Pandis, 1998). For pH values below 4.5 the ozone oxidation rate is several magnitudes lower than that of hydrogen peroxide. As pH increases the ozone oxidation rate increases fast to the same magnitude around pH $\sim$ 4.5 - 5 and increases further for pH $>$ 5.

3.2.1.2 Improved RCG wet deposition scheme

The improved RCG wet deposition scheme distinguishes between in-cloud and below-cloud scavenging for gases and particles. Moreover the advanced scheme integrates wet deposition throughout the column. Moving layer by layer downwards, from the layer of cloud top to ground level the loss of material (i.e. the scavenged material) of each layer is transported by the droplet to the layer below. The local equations given below are applied for each model level. In-cloud scavenging is dependent on the cloud liquid water content and cloud water pH. The gas in-cloud scavenging coefficient $\lambda_{icg} = \lambda_{aq} + \lambda_g$ consists of a

factor for the aqueous phase scavenging λ_{aq} [1/s] (equation 3.1) and a factor for scavenging of ambient gases λ_g [1/s] (equation 3.4) (Seinfeld and Pandis, 1998; ENVIRON, 2010).

$$\lambda_{aq} = \frac{4.2 \times 10^{-7} \cdot E_c \cdot P}{d_d} \frac{H^*(T, pH) \cdot c_g \cdot L_c}{c \cdot \rho_w} \tag{3.1}$$

with

$$c = c_g + c_{aq} \cdot \frac{L_c}{\rho_w} \tag{3.2}$$

and

$$H^*(T, pH) = \frac{c_{aq}}{c_g} \tag{3.3}$$

$$\lambda_g = 1.67 \times 10^{-6} \frac{K_c \cdot P}{d_d \cdot v_d} \tag{3.4}$$

E_c is the collection efficiency for precipitation collecting cloud droplets, P [mm/h] the precipitation rate at ground level, H^*(T,pH) the effective Henry's law coefficient, c_g [μmol m^{-3} air] the gas concentration, c_{aq} [μmol m^{-3} water] the aqueous concentration, c [μmol m^{-3} air] the total grid cell concentration, L_c [g m^{-3}] the cloud water content, d_d [m] the drop diameter, ρ_w [g m^{-3}] the water density, K_c [m/s] the mass transfer coefficient and v_d [m/s] the mean drop fall speed.
Since below the cloud the ambient gas is subject to scavenging the below-cloud scavenging coefficient λ_{bcg} is equal to λ_g (equation 3.4). This equation accounts for the mass transfer of ambient gases to the droplet surface and can be used to calculate the scavenging of very soluble gases for which the scavenging is irreversible. To consider gases with low solubility and reversible scavenging, droplet saturation is incorporated for gas wet scavenging by calculating the maximum possible gas in solution c_{eq} as a function of pH. Rainwater pH is calculated on each model level as described above. The change in gas concentration $\triangle$c is relaxed towards the difference between the maximum possible gas in solution for the given conditions and the amount of pre-existing gas in solution from layers above c_0 (ENVIRON, 2010) (equation 3.5):

$$\triangle c = (c_{eq} - c_0) \cdot (1 - exp(-\lambda_{icg/bcg} \cdot \triangle t)) \tag{3.5}$$

where c_{eq} [μmol m^{-3} air] is the equilibrium gas concentration calculated by means of the effective Henry's law coefficient H^*(T,pH), c_0 [μmol m^{-3} air] is the pre-existing gas in the droplet solution and $\triangle$t [s] the applied timestep. Following equation 3.5 the change in gas

concentration $\triangle$c [μmol m^{-3} air] can be either positive or negative. In this way, aqueous equilibrium between ambient gas and precipitation is not assumed as a consequence of the relatively short residence times of falling precipitation through a given grid cell.
A model calculation using a simple single column model version of the RCG wet deposition scheme illustrates the behaviour of RCG gas wet scavenging for variable droplet pH. For the model run initial concentrations of SO_2, SO_4, NO_3, HNO_3, NH_3 and NH_4 were fixed to 0.2 ppb on all 20 vertical layers (up to 5000 m). Layers 4 to 6 (1000 m - 1500 m) were cloud layers assuming cloud water content of 0.3 g m^{-3}. The precipitation rate was set to 20 mm h^{-1}. Temperature, density and pressure were set to 284 K, 1 kg $^{-3}$ and respectively 1000 hPa on all vertical layers for this simple experiment. Hence, no gas-phase chemistry or vertical mixing was included. Figure 3.1 shows the SO_2 and NH_3 wet deposition flux for pH values from 3 to 10. As droplet pH increases SO_2 wet deposition flux increases due to an increase of in-cloud scavenging with increasing droplet pH. SO_2 wet deposition flux converges to a maximum value of about 3x10^{-4} mg m^{-2} for the given conditions.

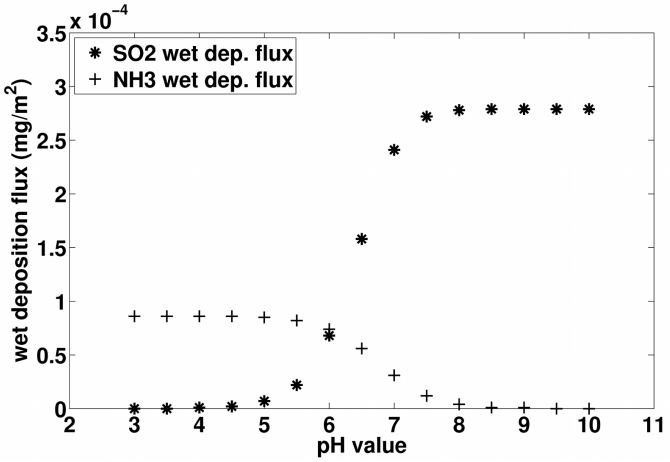

Figure 3.1 Influence of pH variation on model wet deposition flux for SO_2 ($*$) and NH_3 ($+$).

Using equation 3.2 and 3.3, equation 3.1 can be written as

$$\lambda_{aq} = \frac{4.2 \times 10^{-7} \cdot E_c \cdot P}{d_d} \frac{(c - c_g)}{c} \tag{3.6}$$

For high pH the effective Henry's law coefficient H*(T,pH) for SO_2 is very high (Seinfeld and Pandis, 1998). Hence, most available SO_2 dissolves into cloud water, SO_2 gas concentration moves towards zero and the gas in-cloud scavenging coefficient stops increasing with increasing cloud water pH and so does the SO_2 wet deposition flux. The opposite behaviour can be observed for NH_3 since the effective Henry's law coefficient H*(T,pH) for NH_3 decreases with increasing pH. Thus, NH_3 wet deposition increases with decreasing

droplet pH and converges to a maximum of about 0.9×10^{-4} mg m^{-2} for the applied set up.

For the scavenging of particles it is assumed that within cloud layers all aerosols exist within the cloud water. Thus the particle in-cloud scavenging coefficient λ_{icp} [1/s] is:

$$\lambda_{aq} = \frac{4.2 \times 10^{-7} \cdot E_c \cdot P}{d_d} \tag{3.7}$$

with E_c the collection efficiency for precipitation collecting cloud droplets. The particle below-cloud scavenging coefficient λ_{bcp}[1/s] is expressed by:

$$\lambda_{aq} = \frac{4.2 \times 10^{-7} \cdot E_p \cdot P}{d_d} \tag{3.8}$$

with E_p the collection efficiency for particles. E_p is a function of the particle diameter (Seinfeld and Pandis, 1998; ENVIRON, 2010).

3.2.2 Summary of model runs

All model runs were performed on a domain covering Germany (47.2N-55.1N; 5.4E-15.7E) with a horizontal resolution of approximately 7×7 km^2 and 20 vertical layers up to 5000 m. A RCG run covering Europe provided the Boundary Conditions. Emissions for Germany were taken from a national inventory (Jörß et al., 2010; Thiruchittampalam et al., 2010), while high resolution European emissions are obtained from TNO (Denier van der Gon et al., 2010). The model sensitivity study was performed over 4 weeks in summer 2005 (5th July- 2nd August 2005). The base run was carried out forcing droplet pH to a constant value of 5. Sensitivity runs were performed applying a constant droplet pH of 4.5, 5.5, 6 and 6.5 for

Case 1: sulphate production while retaining a constant pH of 5 for gas wet scavenging
Case 2: gas wet scavenging while retaining a constant pH of 5 for sulphate production
Case 3: sulphate production and gas wet scavenging

The pH range has been chosen to represent the observed range in pH in central Europe. The minimum value of pH= 4.5 is chosen because the pH dependent oxidation by ozone is very limited at and below this level.
Furthermore, a run using modelled droplet pH was carried out for the mentioned summer period and 4 weeks in winter 2005 (4th January- 1st February 2005) since measured pH in precipitation varies over the year with higher values in summer and lower values in winter:

Case 4: variable droplet pH for sulphate production and gas wet scavenging

3.2.3 Meteorological Data

Considering the importance to use accurate precipitation data, the diagnostic analysis system TRAMPER (TRopospheric Realtime Applied Meteorological Procedures for Environmental Research) was employed to derive the meteorological fields for the current investigation. TRAMPER incorporates a numerical statistical fine mesh analysis procedure for meteorological observations from weather services and all available local measurements (Reimer and Scherer 1992; Flemming et al. 2000). The first guess given by ECMWF meteorological forecast fields is shifted towards the observations using optimal interpolation. The basic variables Montgomery potential, pressure, local stability, wind vector components, vertical shear of components and relative humidity are analysed for central Europe (45N-55N; 3E-18E) on the surface and 24 isentropic levels up to 560 K in the stratosphere. The analysis of precipitation is solely based on observations. The precipitation measurements are processed applying an interpolation scheme, which considers cloud type information from surface and satellite observations. The observation of cloud cover, cloud type and cloud height are interpolated and adjusted to the model by use of the models' basic variables. 3D clouds are then generated using cloud cover, cloud type and cloud base and top combined with cloud parameter statistics on the liquid water content of the different cloud types (Simmer 1994, Stephens 1994) and its vertical distribution (Rogers and Yau 1989, Albrecht et al. 1990). TRAMPER precipitation fields show good agreement with independent measurements concerning spatial distribution and magnitude (Builtjes et al., 2011). Comparison to cloud radar measurements has shown that TRAMPER is able to reproduce well cloud height and cloud liquid water content values (Builtjes et al., 2011).

3.2.4 Observational Data

For evaluation of TRAMPER precipitation, RCG wet deposition fluxes and RCG air concentrations data from the national German monitoring network (UBA, 2004) were used (See Figure 3.2 and Table 3.1). For January 2005 and July 2005 observations of 15, respectively 17 stations were used for evaluation purposes. At all sites precipitation sampling is performed by using wet-only collectors (Firma Eigenbrodt, Germany). The funnel of the wet-only collector is closed with a lid when there is no precipitation, insuring that no contribution from dry deposition enters the collector. From the collected week samples the amount of precipitation is derived, pH and electrolytic conductivity are determined and a chemical analysis identifying the content of major ions is performed. At all stations

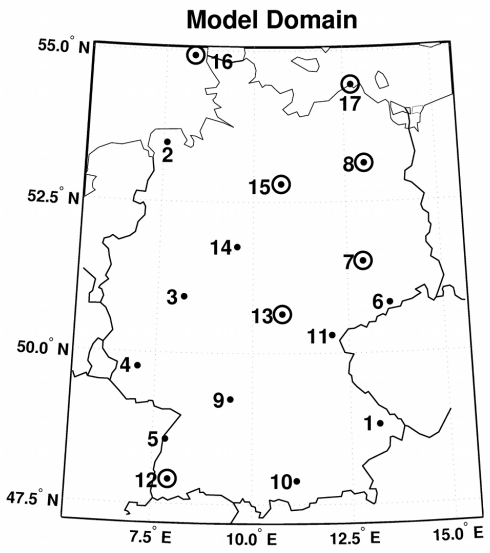

Figure 3.2 Model Domain and locations of all used UBA wet deposition flux measurement sites (.) and UBA air concentration measurement sites (o) listed in Table 1.

an additional meteorological rain gauge (Joss Tognini or Hellmann) is used for the observations of precipitation amounts. Air concentrations of sulphur dioxide, sulphate and ammonia are sampled using the filter pack method (EMEP, 1996). Out of an air stream airborne particles containing sulphate are collected on an aerosol filter while SO_2 and NH_3 are collected on impregnated filters. In contrast to the weekly wet deposition fluxes, air concentrations are available as daily means.
Note, that whenever we refer to 'mean pH' the pH of the mean acid concentration is meant.

3.3 Results

3.3.1 Evaluation of precipitation

Precipitation varies significantly in space and time, which is difficult to capture by the meteorological model. High quality precipitation fields are required by the CTM to simulate wet deposition fluxes correctly. Hence, precipitation fields need to be evaluated and the outcome must be considered when analysing the models wet deposition fluxes. Figure 3.3 shows TRAMPER monthly precipitation sums for July 2005 (a) and January 2005 (b) compared to observations. For most stations the measured precipitation sums are reproduced well. However, TRAMPER tends to overestimate at stations with low precipitation sums and to underestimate at stations with high precipitation sums. For both

Table 3.1 List of UBA stations and used site observations

No. in Fig. 3.2	Station name	Wet deposition flux obs.	Air conc. obs.
1	Brotjacklriegel	SO_x, NH_x	-
2	Dunum	SO_x, NH_x	-
3	Hilchenbach	SO_x, NH_x	-
4	Deuselbach	SO_x, NH_x	-
5	Kehl	SO_x, NH_x	-
6	Lehnmühle	SO_x, NH_x	-
7	Melpitz	SO_x, NH_x	SO_4
8	Neuglobsow	SO_x, NH_x	SO_4, SO_2, NH_3
9	Oehringen	SO_x, NH_x	-
10	Raisting	SO_x, NH_x	-
11	Regnitzlosau	SO_x, NH_x	-
12	Schauinsland	SO_x, NH_x	SO_4, SO_2, NH_3
13	Schmücke	SO_x, NH_x	SO_4, SO_2
14	Solling	SO_x, NH_x	-
15	Waldhof	SO_x, NH_x	SO_4, SO_2, NH_3
16	Westerland	SO_x, NH_x	SO_4, SO_2, NH_3
17	Zingst	SO_x, NH_x	SO_4, SO_2, NH_3

months the Root Mean Square Error amounts to 24 mm (observed mean: July=100.2 mm; January=56.8 mm) and spatial correlations are high with 0.80 for July and 0.85 for January.

3.3.2 Sensitivity Study for July 2005

Here we discuss the results of the model sensitivity study on droplet pH variations, which was performed for July 2005. The base run was carried out using a constant model droplet pH of 5.

3.3.2.1 Model cloud chemistry and gas wet scavenging sensitivity to droplet pH

Figure 3.4(a) illustrates the sensitivity of model sulphate formation to droplet pH (= Case 1). The figure shows the vertical distribution of the domain average sulphate air concentration of the different droplet pH runs. Sulphate concentrations increase with increasing model droplet pH due to a higher sulphate production rate via the O_3 oxidation pathway. Applying a droplet pH of 6.5 average domain sulphate concentrations increase by up to 46% compared to the base run. The enhancement is significant for model runs with droplet pH greater 5 as for pH lower than 5 the reaction rate of oxidation via

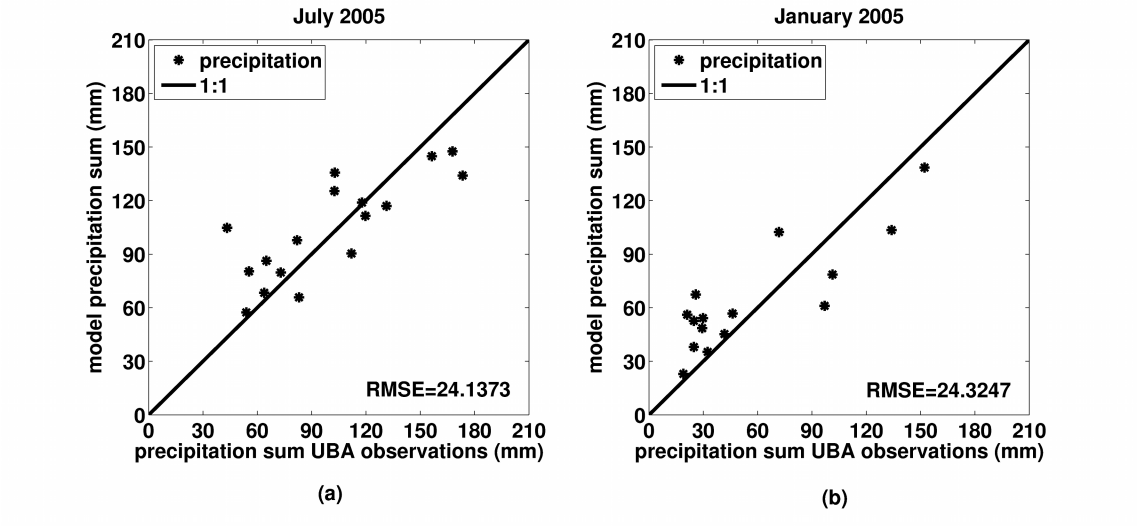

Figure 3.3 TRAMPER monthly precipitation sums for July 2005 (a) and January 2005 (b) compared to observations at 17 (July) respectively 15 (January) UBA stations.

H_2O_2 is several magnitudes higher than that of the O_3 oxidation pathway. Since sulphate production is a SO_2 sink the domain average SO_2 (not shown here) concentration decreases with increasing pH.

Figure 3.4b displays the sensitivity of wet scavenging to droplet pH (= Case 2). The deviation of the domain wet deposition sum from the base run is presented for different droplet pH runs. Most significant is the increase of the SO_2 wet deposition flux with increasing model droplet pH (enhancement by a factor of approximately 20 for the pH 6.5 run). This is because more SO_2 can be dissolved in the droplets as the pH of the latter increases. Similarly, NH_3 wet deposition fluxes decrease with increasing model droplet pH. The decrease is less significant than for SO_2 due to the high solubility of NH_3. The decline of the NH_3 wet deposition flux leads to higher NH_3 air concentrations resulting in an enhanced formation of ammonium nitrate, and hence to an increase of NO_3 wet deposition fluxes. Figure 3.4 (c,d) shows the results of Case 3. Model droplet pH was varied within both, sulphate production and gas wet scavenging. Comparing results of Case 3 to results of Case 1 and 2 displays the coupling between sulphate formation and gas wet scavenging processes. In Case 3 the increase of domain average sulphate concentration with increasing pH is slightly damped due to less SO_2 availability with increasing droplet pH caused by a higher SO_2 gas wet scavenging rate. Applying a droplet pH of 6.5 average domain sulphate concentrations now increase by up to 43% compared to the base run instead of by 46% as in Case 1. The increase of domain SO_2 wet deposition sum with increasing pH is much smaller than in Case 2. Hence, the more effective sulphate formation in between precipitation events and prior to rain out in clouds dominates the impact of

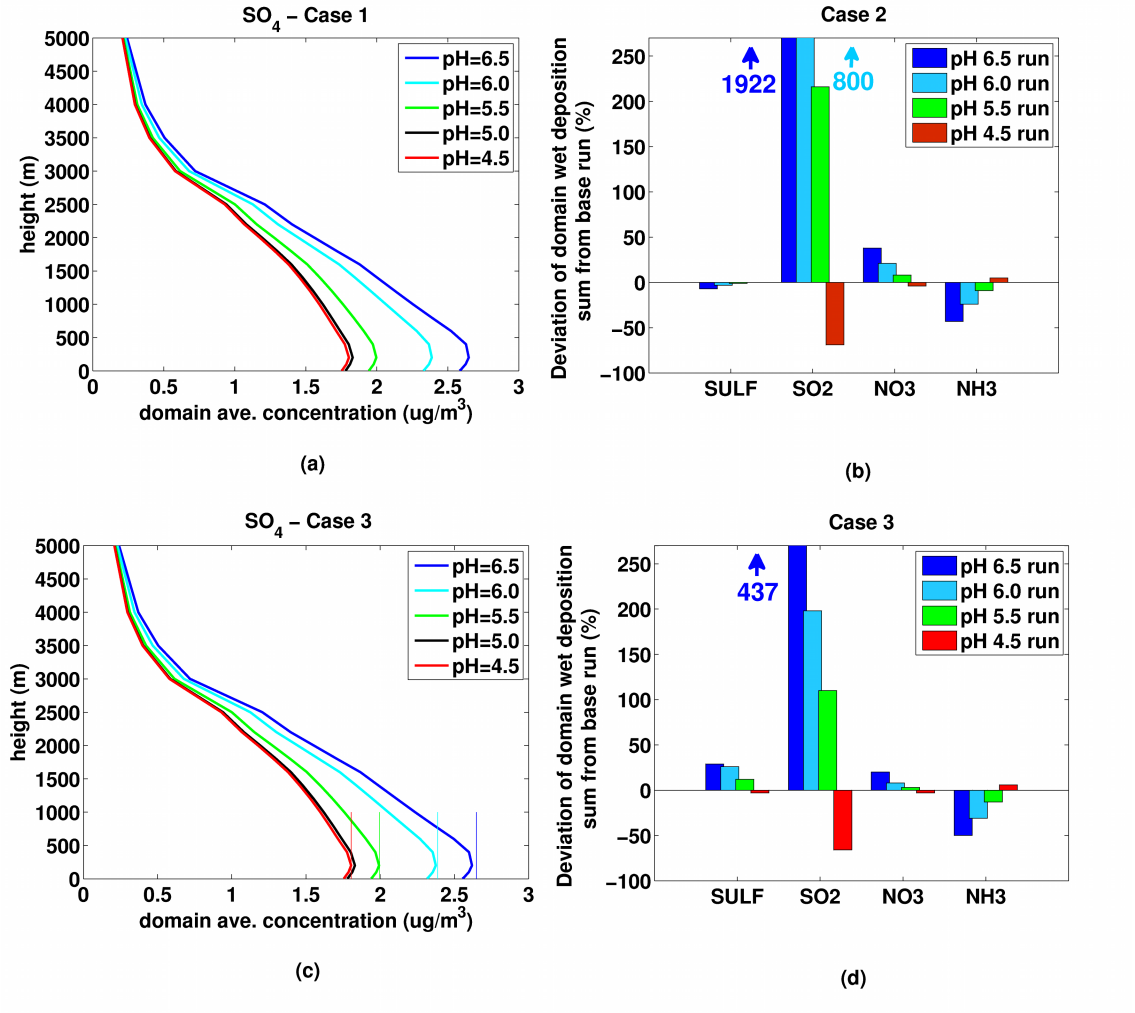

Figure 3.4 Vertical distribution of domain average sulphate air concentration for (a) Case 1 and (c) Case 3 (vertical lines show maximum values of Case 1) and deviation of the domain wet deposition sum from the base run for (b) Case 2 and (d) Case 3 of the different droplet pH runs for the investigation period.

variable pH. Consequently, also the sulphate wet deposition flux increases with increasing pH. Finally, due to a higher rate of ammonium sulphate formation with increasing pH in Case 3 less NH_3 is available for ammonium nitrate formation and hence, the increase of NO_3 wet deposition fluxes is lower for Case 3 than for Case 2. Note, that the changes in wet deposition fluxes are balanced by those in dry deposition, illustrating a shifting balance between the formation, lifetime and removal processes.

3.3.2.2 Model sensitivity to pH and comparison to observations

Figure 3.5a presents the daily mean surface sulphate air concentrations of the different model runs of Case 3 compared to observations at the UBA station Melpitz. The impact of model droplet pH variation on sulphate concentrations is significant. RCG reproduces

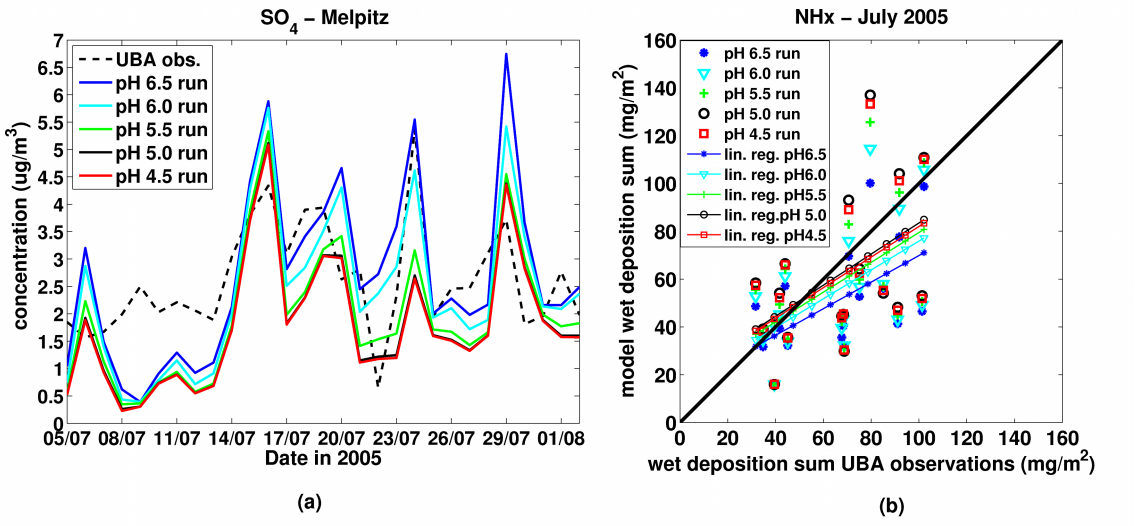

Figure 3.5 (a) Modelled and observed daily mean surface sulphate air concentrations at UBA station Melpitz and (b) modelled versus observed NH_x wet deposition sums at 17 UBA stations spread over Germany.

well the temporal evolution of the observed concentrations and the absolute values are within the right range for all droplet pH runs. Since the pH value of atmospheric droplets varies throughout the investigation period and other model uncertainties are present, there is not one particular droplet pH run that compares best to the observations. Weekly measured rainwater pH at Melpitz ranged from 4.7 to 5.8 in July 2005. Figure 3.5b shows the modelled NH_x wet deposition fluxes of the model sensitivity runs compared to observations at 17 UBA stations spread over Germany. TRAMPER precipitation (shown in section 3.3.1) compared well to the precipitation measurements. RCG simulates the wet fluxes within the right range. However, the analysis of the modelled fluxes demonstrates their significant dependency on droplet pH variation.

3.3.3 Variable droplet pH

Here results using a modelled droplet pH are shown. Model droplet pH, air concentrations of sulphate, SO_2 and NH_3 and wet deposition fluxes of sulphate and reduced nitrogen are analysed and compared to a model run applying a constant droplet pH of 5 and to observations.

3.3.3.1 Air concentrations

Figure 3.6 shows daily model mean surface sulphate concentrations compared to observations at Melpitz as in Figure 3.5(a) but now using modelled droplet pH. For comparison the results of the run using a constant droplet pH of 5 are also included. RCG is able

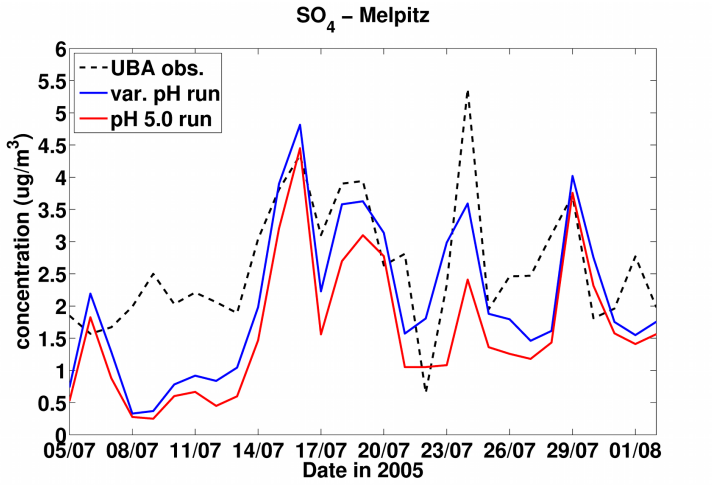

Figure 3.6 RCG daily mean surface sulphate air concentrations applying modelled droplet pH and a constant pH of 5 compared to observations at Melpitz for July 2005.

to capture the temporal trend of the observed concentrations. A systematic difference concerning the absolute values can be observed between the variable droplet pH run and the fixed droplet pH of 5 run. Periods during which both runs show similar results are either periods in which either droplet pH was close to 5 or periods with minor cloudiness and low precipitation amounts. In case of larger deviations between the two runs the variable droplet pH run performs better in capturing the observed peaks.

Figure 3.7 shows modelled daily mean surface sulphate, SO_2 and NH_3 air concentrations applying modelled droplet pH (crosses) and a constant pH of 5 (dots) for July (left panels) and January (right panels) compared to observations at 6, 5 and respectively 4 sites spread over Germany. Table 3.2 summarizes the observed mean, RMSE and BIAS with a positive BIAS indicating an overestimation and a negative BIAS indicating an underestimation by the model. RCG is able to simulate observed daily mean sulphate concentrations but tends to underestimate the concentrations in July 2005 within both runs (see Figure 3.7(a)). Applying a variable droplet pH the corresponding RMSE decreases by 8% and the corresponding BIAS decreases by 43% compared to using a constant pH of 5. For SO_2 (see Figure 3.7(c)) the RMSE for July decreases by 16% when using a variable droplet pH. The correspondent BIAS decreases considerably from 1.17 μg m^{-3} to -0.14 μg m^{-3} showing that the constant droplet pH of 5 run overestimates daily mean SO_2 air concentrations while the variable droplet pH run has a slight tendency to underestimate SO_2 air concentrations. For NH_3 daily mean surface concentrations in July (see Figure 3.7(e)) the difference between the RMSE of the two runs is negligible while the BIAS indicates that the variable droplet pH run tends to overestimate NH_3 concentrations (+4% when comparing modelled mean to observed mean) while the fixed pH of 5 run

Table 3.2 Observed mean (a), RMSE and BIAS of modelled daily mean surface air concentrations of sulphate, SO_2 and NH_3 at 6, 5 and respectively 4 UBA stations for (b) July and (c) January including results for sensitivity runs inducing ±25% NH_3 emissions

(a)			
Observed Mean	SO_2 (μg m^{-3})	SO_4 (μg m^{-3})	NH_3 (μg m^{-3})
July	0.72	2.29	1.56
January	0.94	1.76	0.3

(b)						
JULY Air Concentration	SO_2 RMSE (μg m^{-3})	SO_2 BIAS (μg m^{-3})	SO_4 RMSE (μg m^{-3})	SO_4 BIAS (μg m^{-3})	NH_3 RMSE (μg m^{-3})	NH_3 BIAS (μg m^{-3})
Variable droplet pH	0.56	-0.14	1.15	-0.44	0.93	0.06
Fixed droplet pH=5	0.67	1.17	1.25	-0.77	0.92	-0.14

(c)						
JANUARY Air Concentration	SO_2 RMSE (μg m^{-3})	SO_2 BIAS (μg m^{-3})	SO_4 RMSE (μg m^{-3})	SO_4 BIAS (μg m^{-3})	NH_3 RMSE (μg m^{-3})	NH_3 BIAS (μg m^{-3})
Variable droplet pH	3.14	2.52	0.93	-0.03	1.64	1.25
Fixed droplet pH=5	3.74	3.19	1.01	-0.69	1.55	1.16
Variable droplet pH/ +25% NH_3 emission	3.04	2.39	1	0.11	2.24	1.78
Fixed droplet pH=5/ +25% NH_3 emission	3.74	3.19	1	-0.69	2.09	1.62
Variable droplet pH/ -25% NH_3 emission	3.27	2.68	0.9	-0.2	1.14	0.87
Fixed droplet pH=5/ -25% NH_3 emission	3.74	3.2	1.02	-0.7	1.14	0.82

underestimates NH_3 concentrations (-9% when comparing modelled mean to observed mean).

For January (Figure 3.7 right panels) the comparison to observations shows that sulphate concentrations (Figure 3.7(b)) are captured well by RCG. Again the performance of the variable droplet pH run is better than the performance of the fixed pH of 5 run. The RMSE decreases by 8%. The BIAS is considerably lower for the variable droplet pH run with an underestimation of modelled mean to observed mean by 2% while using a fixed droplet pH of 5 resulted in an underestimation by 39%. SO_2 and NH_3 daily mean surface concentrations for January (see Figure 3.7(d,f)) are substantially overestimated by both model runs due to an overestimation of the occurrence of stable atmospheric conditions.

3.3.3.2 Wet Deposition Fluxes

Figure 3.8 shows modelled wet deposition fluxes of SO_x and NH_x for July and January using modelled droplet pH (crosses) and using a constant droplet pH of 5 (dots) compared to observations. Table 3.3 summarizes the corresponding RMSE and BIAS. Wet deposition fluxes of nitrate have also been investigated within this study but results are not shown

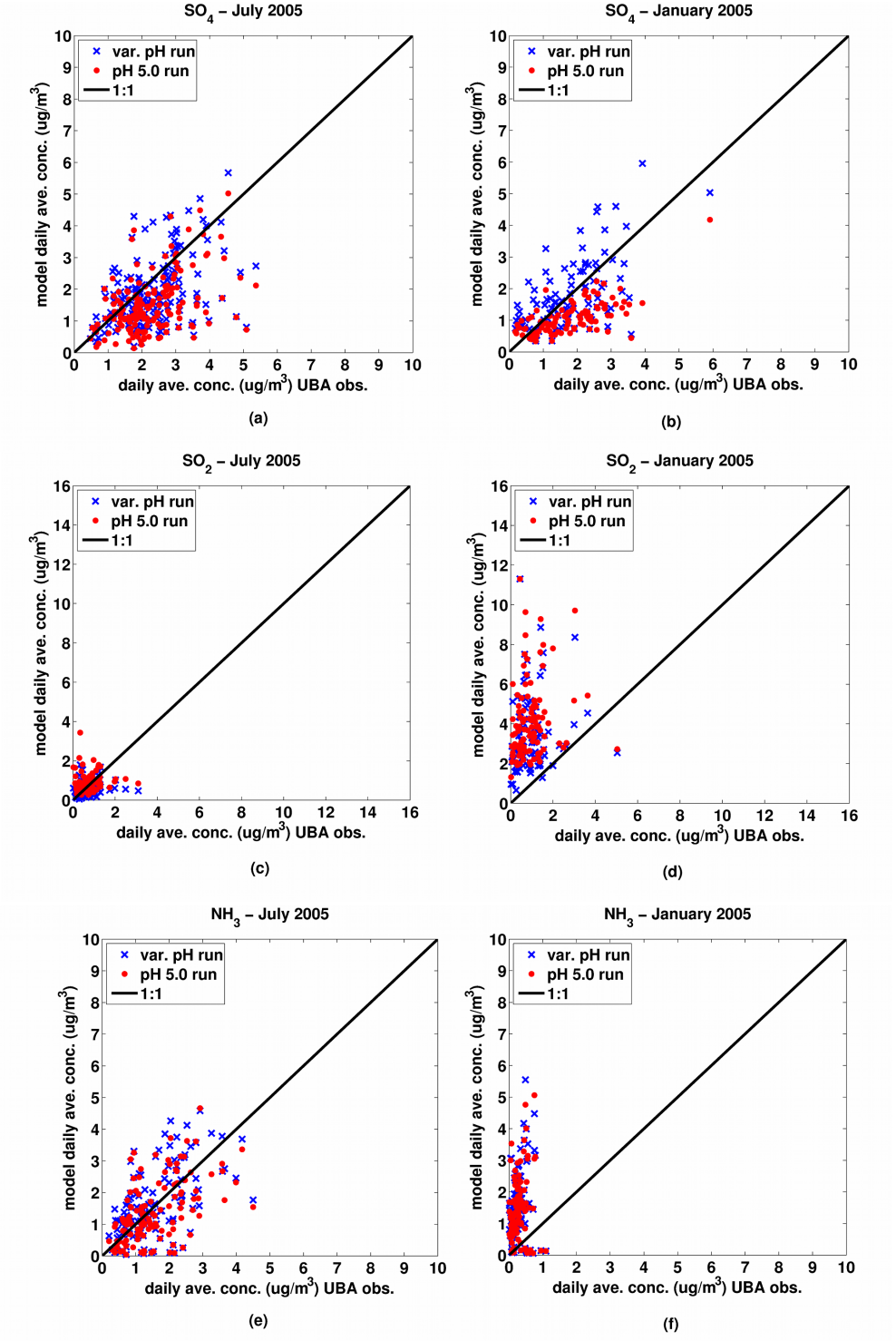

Figure 3.7 RCG daily mean surface concentration of sulphate (a,b), SO_2 (c,d) and NH_3 (e,f) versus observations at 6, 5 and respectively 4 UBA sites spread over Germany applying modelled droplet pH (crosses) and a constant pH of 5 (dots) for July 2005 (left panels) and January 2005 (right panels).

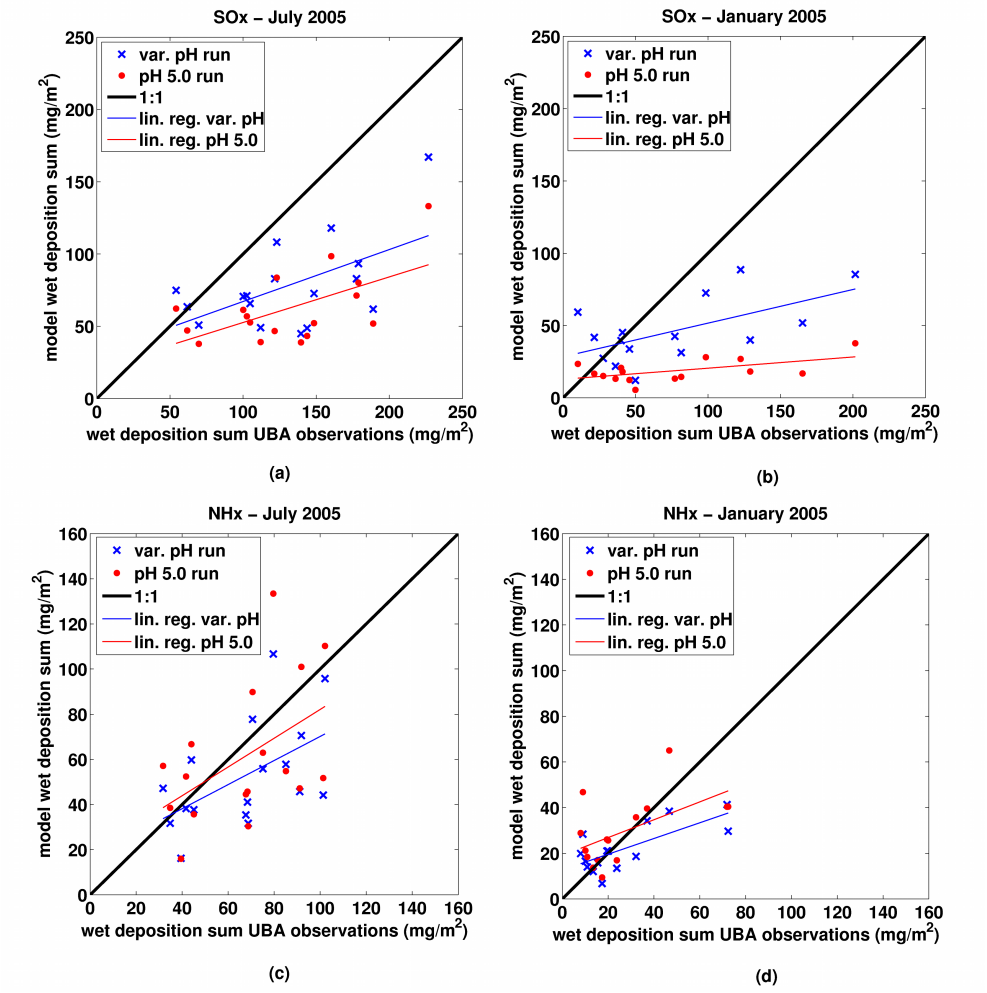

Figure 3.8 RCG wet deposition sums of SO_x (a,b) and NH_x (c,d) versus observations at 17 (July) respectively 15 (January) UBA stations applying modelled droplet pH (crosses) and a constant pH of 5 (dots) for July (left panels) and January (right panels).

here since nitrate wet fluxes showed only very little sensitivity to droplet pH variations. RCG underestimates SO_x wet deposition fluxes for January and July 2005 (see Figures 3.8(a,c)). However, using a variable droplet pH improves the models' RMSE concerning SO_x wet deposition flux by 16% in July and 29% in January. NH_x wet deposition fluxes are reproduced well by RCG. RMSE and BIAS are considerably lower in January than in July, as are the absolute amounts of wet deposition flux at all stations since precipitation sums are lower in January than in July and there is much less agricultural action involving NH_3 emissions during wintertime. Furthermore, using a variable droplet pH the RMSE concerning NH_x wet deposition fluxes is reduced by 5% for July and by 9% for January compared to using a constant droplet pH of 5.

The results shown in Figure 3.8(b,d) indicate that RCG tends to overestimate the observed values at stations with low NH_x wet deposition flux and to underestimate at stations with

Table 3.3 Observed mean (a), RMSE and BIAS of modelled wet deposition fluxes of SO_x and NH_x at 17 (July) respectively 15 (January) UBA stations for (b) July and (c) January including results for sensitivity runs inducing ±25% NH_3 emissions

(a)		
Observed Mean	SO_x (mg m^{-2})	NH_x (mg m^{-2})
July	130.3	66.9
January	76.5	27.2

(b)				
JULY Wet Deposition	SO_x RMSE (mg m^{-2})	SO_x BIAS (mg m^{-2})	NH_x RMSE (mg m^{-2})	NH_x BIAS (mg m^{-2})
Variable droplet pH	64.8	-52.2	26.5	-14.4
Fixed droplet pH=5	77.5	-68.1	28	-5.9
(c)				
JANUARY Wet Deposition	SO_x RMSE (mg m^{-2})	SO_x BIAS (mg m^{-2})	NH_x RMSE (mg m^{-2})	NH_x BIAS (mg m^{-2})
Variable droplet pH	54.5	-30.4	15.9	-5.1
Fixed droplet pH=5	76.9	-57.9	17.5	2.4
Variable droplet pH/ +25% NH_3 emission	51.1	-24.8	14.9	-2
Fixed droplet pH=5/ +25% NH_3 emission	77.7	-58.6	20.8	9.3
Variable droplet pH/ -25% NH_3 emission	59.8	-37.9	17.9	-8.6
Fixed droplet pH=5/ -25% NH_3 emission	76.9	-57.9	17.3	-4.3

high NH_x wet deposition flux. Similar behaviour was observed when comparing TRAMPER precipitation to observations (section 3.3.1). Figure 3.9(a,b) shows the TRAMPER rain deviation from observations and the RCG NH_x wet deposition flux deviation from observations in percent for July 2005 (a) and for January 2005 (b) for the variable droplet pH run. In July three UBA stations exhibited high monthly precipitation sums of 156 mm, 168 mm and 173 mm, which were underestimated by TRAMPER by up to 20%. Hence, using TRAMPER precipitation RCG underestimated NH_x wet deposition fluxes at these stations. Two stations observed rather low monthly precipitation sums of 63mm and 43mm, which were overestimated by TRAMPER leading to an overestimation of NH_x wet deposition fluxes by RCG at these stations. Similar behaviour can be observed in January for three stations with rather high and two stations with rather low monthly precipitation sums. Model precipitation error and CTM wet deposition flux error are in line and correlated.

When using a constant pH of 5 (see Figure 3.9(c,d)) on the other hand model precipitation and model wet deposition error are not in line. Although TRAMPER underestimated precipitation, RCG overestimated the corresponding NH_x wet deposition flux at several stations. Hence, applying a constant droplet pH of 5 leads to physical inconsistencies

within the model.

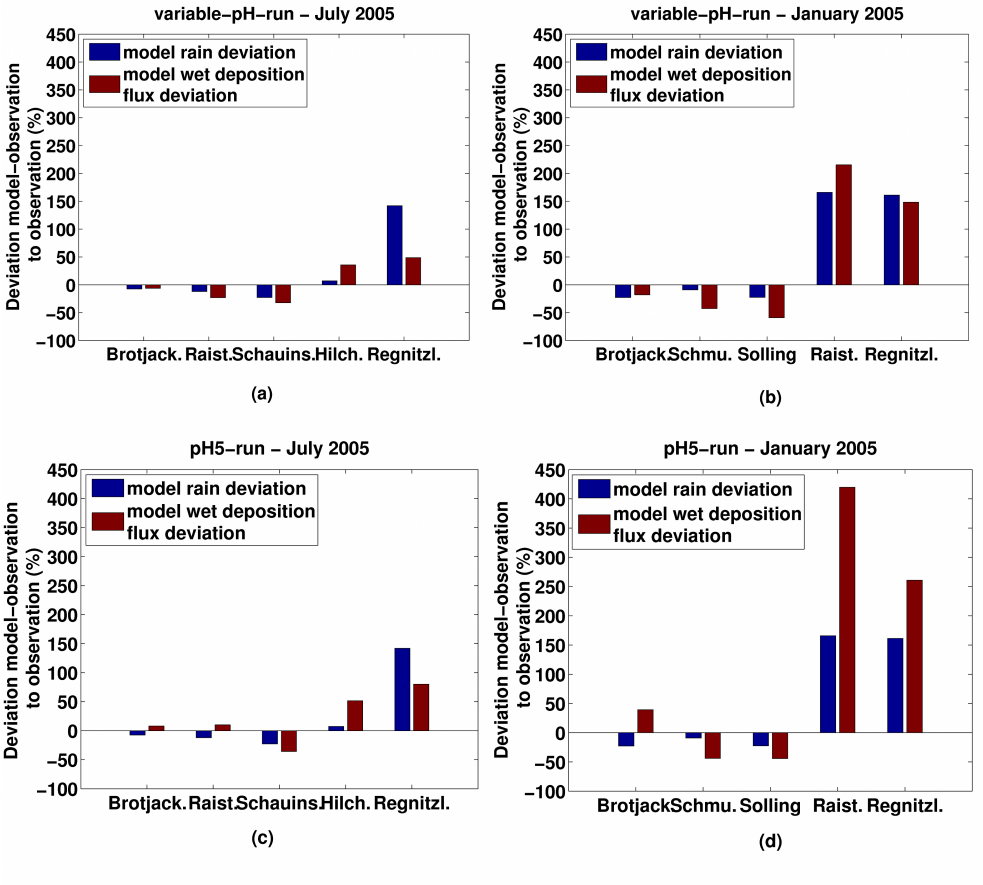

Figure 3.9 TRAMPER precipitation deviation from observations and RCG NH_x wet deposition flux deviation from observations for (a,b) the variable droplet pH run and (c,d) the fixed droplet pH of 5 run at selected UBA stations for July 2005 (left panels) and January 2005 (right panels).

3.3.3.3 Modelled droplet pH

There are no measurements of the vertical distribution of droplet pH that can be used for evaluation purposes. However, precipitation pH observations at ground level are available to verify if droplet pH is modelled within the right range. Figure 3.10 shows the modelled monthly mean droplet pH (= pH of the mean acid concentration) for July 2005 (cycles) and January 2005 (crosses) compared to monthly mean measured precipitation pH at the available UBA stations. The comparison is given for modelled droplet pH at 1000 m (see Figure 3.10(a)) and ground level (see Figure 3.10(b)). UBA observations show higher pH values in precipitation in July than in January.

Comparing modelled droplet pH of model level 9 (= 1000 m height) to ground level

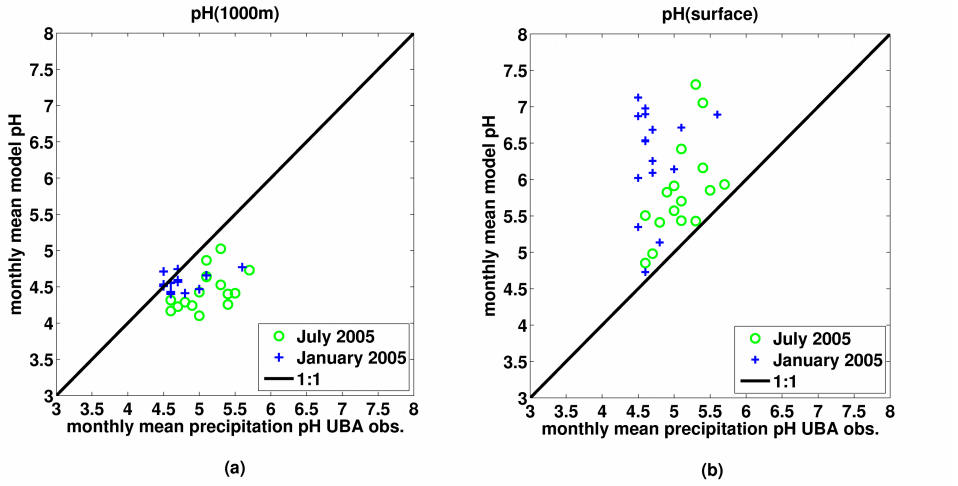

Figure 3.10 RCG monthly mean droplet pH (a) in 1000 m height and (b) on ground level versus monthly mean precipitation pH at 16 UBA stations for July 2005 (cycles) and January 2005 (crosses).

observations shows that the model compares well to the observed mean pH values for January at most stations. The RMSE for the comparison to all stations shown in Table 3.4 is with 0.31 low for January (observed mean= 4.80). However, the model simulates pH values in 1000 m lower than observed precipitation pH at 4 stations for January (BIAS= -0.17) and at most stations for July (BIAS= -0.64). The average vertical distribution of ammonia shows highest concentrations near ground and a fast decrease with height. Hence this outcome is reasonable since ammonia uptake will increase the droplet pH during its fall to the surface. Due to higher ammonia emissions leading to higher ammonia concentrations in July compared to January the difference between precipitation pH and droplet pH in 1000 m is higher for July. Comparing modelled ground level droplet pH to precipitation observations shows that RCG severely overestimates ground level pH at several sites for July (BIAS= 0.74) and at most sites for January (BIAS= 1.58). While for July droplet pH is simulated satisfying at a few stations (RMSE= 0.9) the RMSE is with 1.73 unsatisfactory high for January. The potential reasons for the overestimation are discussed below.

3.4 Discussion

Figure 3.11 shows daily precipitation pH measurements at 3 UBA stations for 2008 (UBA, 2004). A well-defined seasonal cycle can be observed with maximum pH values in summer and lower values during wintertime. pH values of precipitation increase in springtime,

Table 3.4 Observed mean precipitation pH and RMSE and BIAS of modelled droplet pH at ground level and 1000 m height at 16 UBA stations

Droplet pH	Observed mean pH	RMSE 1000 m height	BIAS 1000 m height	RMSE Ground level	BIAS Ground level
July	5.27	0.7	-0.64	0.9	0.74
January	4.8	0.31	-0.17	1.73	1.58

which may be due to agricultural practises that lead to an increase of atmospheric ammonia. Furthermore, burdens of alkaline components such as mineral matter peak in summer. In fall, pH decreases again as biological and therewith agriculture activity deceases coinciding with an increase of sulphur emissions following domestic heating starting in fall. Assuming that precipitation pH reflects cloud water pH a range of 4.0-6.5 seems to incorporate most of the variability. On average, this corresponds to a pH slightly lower than pH= 5. However, such a fixed pH does not represent the two orders of magnitude variability in acid concentration. Moreover, considering the pH dependent chemistry results have shown that a constant droplet pH of 5 represents low droplet pH cases adequately while cases with pH values greater 5 are not well represented. Hence, a fixed pH of 5 is not suited as effective pH in aqueous phase chemistry.

Model simulations with a variable pH showed an improvement of the model performance for sulphate, sulphur dioxide concentrations and SO_x wet deposition fluxes. The RMSE decreased for these components for January and July. Sulphate concentrations bias was reduced to a larger extend in winter than in summer, explained by the lack of hydrogen peroxide and therefore higher dependency on ozone oxidation in winter. Although the model skill increases by introducing pH dependent processes, we have identified a number of shortcomings to the model. For example, for January a deficiency of vertical mixing was found to be the reason for strong overestimations of SO_2 and NH_3 surface air concentrations. The meteorological driver TRAMPER overestimated the number of stable condition occurrences resulting in too little mixing. An RCG simulation applying meteorological data provided by COSMO-EU (not shown here) showed considerably lower SO_2 and NH_3 surface concentrations. Also, a systematic bias in sulphate air concentrations remains. This underestimation might also link to a lack of vertical mixing and therefore a lack of SO_2 availability within cloud layer heights leading to lower aqueous phase sulphate formation combined with a reduced occurrence of sulphate downward mixing. Although this hypothesis may also partly explain the systematic underestimation of the wet deposition fluxes, we feel that it is one of many uncertainties to be reduced in current CTMs. Important uncertainties in sulphate and other aerosol budgets also arise from the uncertainty in the dry deposition flux (Pryor et al., 2008; Petroff et al., 2008). A

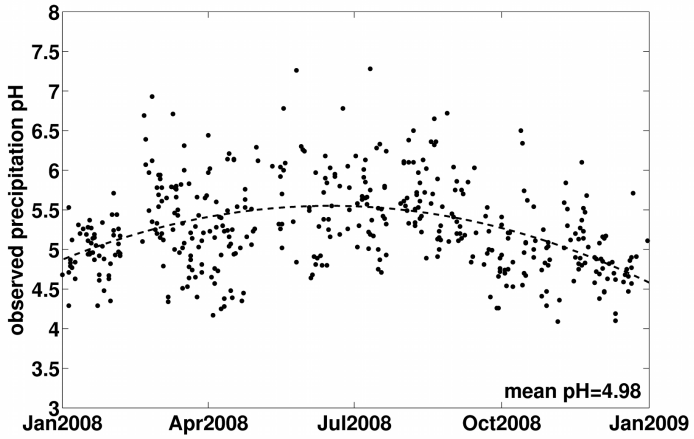

Figure 3.11 Daily precipitation pH observations at UBA stations Schauinsland, Neuglobsow and Waldhof for year 2008.

too low concentration and wet deposition flux can also be explained by a too effective dry deposition process. The currently used dry deposition scheme (Erisman et al., 1994) is more efficient than that of e.g. Zhang et al. (2001). A lack of dry deposition measurements hampers the model description and evaluation of this aspect. Another major area for improvement concerns ammonia and its emission estimates, including its seasonal variation. Given the uncertainties in ammonia, sensitivity simulations were carried out by varying ammonia emissions by ±25% for both a variable droplet pH and a fixed pH of 5. The model evaluation (see Table 2 and 3) shows that the model performance for ammonia concentrations and NH_x wet deposition fluxes vary in line with the induced emission changes. More importantly, the results show that the improvement of the model performance by using variable pH for sulphate and sulphur dioxide concentrations as well as SO_x wet deposition fluxes is robust.

The model performance for ammonia itself is not so much affected by the inclusion of a variable pH in cloud and rainwater. This can be explained by the importance of dry deposition in the ammonia budget (Sutton et al., 1995; Sutton et al., 1998). Model performance concerning wet deposition fluxes of reduced ammonia on the other hand has improved as illustrated by the lower RMS error. Comparing TRAMPER precipitation performance to RCG NH_x wet deposition flux performance pointed out that for the variable droplet pH run precipitation error and wet deposition flux error were correlated and in line. An overestimation of precipitation led to an overestimation of the NH_x wet deposition flux and vice versa. In contrast, precipitation and wet deposition flux error were not in line using a constant pH of 5 indicating physical inconsistencies within the model when applying a fixed pH. Hence, in the budget of reduced nitrogen improvements were

found when using variable pH.

Comparing modelled ground level droplet pH to measured precipitation pH at 16 UBA stations has shown that RCG severely overestimated ground level droplet pH at most sites. The ammonia emission sensitivity runs described above have indicated that model droplet pH is very sensitive to ammonia air concentrations (not shown here). A similar overestimation of pH was found in a study by Redington et al. (2009) using an aqueous phase chemistry of comparable complexity as used in this study. The authors showed that modelled pH was found to be very sensitive to relatively small changes in the ammonia emissions and linked the pH overestimation to an overestimation of ammonia air concentrations. Also, RCG tends to overestimate surface ammonia air concentrations in July and especially in January. Hence, the overestimation of ammonia concentrations, potentially amplified by the underestimation of sulphate concentrations, contributes to the overestimation of droplet pH in the lower model levels. The modelled droplet pH strongly increases due to efficient uptake of ammonia within lower model layers. Note that the modelled uptake may be impacted by artificial dilution of the short-lived ammonia within a grid cell due to inhomogeneous landscape and associated concentration patterns, locations of measurement stations away from local sources. Also, the effects of other buffering systems such as sea salt, mineral dust and organic components are not accounted for. Moreover, also organic compounds can be oxidised to organic acids, lowering cloud (and subsequently rain) water pH (Deguillaume et al., 2009). However, we feel that for the investigation area these effects are of secondary importance compared to the impact of ammonia concentrations on modelled pH.

In the atmosphere cloud pH can differ from precipitation pH (Collett et al., 1993; Kalina and Puxbaum, 1994; Brantner et al., 1994). Species concentrations in cloud water are mostly higher than simultaneously observed precipitation concentrations. Depending on the balance between acidic and basic inputs to the aqueous phase cloud pH is either higher or lower than that of precipitation. This results partly from the relatively clean growth of ice-phase precipitation particles through vapour deposition to an ice crystal nucleus and from the fact that soluble gases have more time to equilibrate with cloud drops than they do with rapidly falling precipitation particles (Collett et al., 1993). Hence, rainwater measurements are not a good substitute for cloud chemistry measurements (Aleksic et al., 2009) and thus, the comparison above must be interpreted with care. RCG does not distinguish between cloud droplet and precipitating droplet when estimating pH. A distinction might be necessary and assumptions within the model code concerning the interaction of precipitating (= falling) droplets with their surrounding might need to be further detailed.

State of the art aqueous phase chemistry models that are currently developed are char-

acterised by increasing complexity. Advanced aqueous phase chemical mechanisms have been introduced and developed in the past years. For example, the Chemical Aqueous Phase Radical Mechanism (CAPRAM) includes hundreds of aqueous-phase chemical reactions and species to model the fate of inorganic as well as organic compounds (Herrmann et al., 2000; Herrmann et al., 2005). Although the number of CAPRAM aqueous-phase chemical reactions has been reduced by a factor of 4 (Deguillaume et al., 2009), the computational burden is too large to apply it in a CTM. Fahey and Pandis (2003) emphasised the importance of incorporating a size-resolved aqueous phase chemistry scheme in 3D CTMs instead of using bulk models. However, the applied size-resolved aqueous phase scheme introduced a significant increase of computational cost. Additionally, compared to applying more simple bulk schemes the impact of uncertainties within microphysical model inputs, like liquid water content, on model results increased when applying the size-resolved aqueous phase scheme. Although the above mentioned studies with more detailed descriptions of aqueous phase chemistry than ours exhibit encouraging results, the required detailed microphysical input as well as the large computational effort for the treatment of explicit chemistry prohibits their use in operational regional scale CTMs.

3.5 Conclusions

The chemical transport model RCG has been improved by implementing an upgraded description of aqueous-phase chemistry. Furthermore, a new wet deposition scheme including cloud liquid water content dependent in-cloud scavenging and pH dependent droplet saturation was incorporated. A sensitivity study varying cloud and rain droplet pH from 4.5 to 6.5 has been performed and it was found that modelled air concentrations and wet deposition fluxes of sulphur and reduced nitrogen species are significantly affected by droplet pH variation within atmospheric ranges. Applying a droplet pH of 5.5 within the aqueous-phase chemistry and the gas wet scavenging scheme modelled mean sulphate air concentrations increase by up to 10% compared to the base run (pH= 5) while the SO_2 domain wet deposition sum increases by 110%. Although the effects of pH variations on cloud chemistry and wet scavenging processes are connected, the effect on sulphate formation in clouds in between precipitation events and prior to rain out dominates the impact of pH variations. Oxidised nitrogen species were not found to be very sensitive to droplet pH variations. A model run using modelled droplet pH has been performed and compared to a model run applying a constant pH of 5 and to observations. The results have shown that using a variable droplet pH improves the model performance concerning air concentrations and wet deposition fluxes of the investigated sulphur and nitrogen compounds. For sulphate and SO_2 air concentrations the RMSE was reduced by 8% and

16%, respectively, for the investigation period in summer 2005. For the same time period the RMSE concerning SO_x wet deposition fluxes decreased by 16% when using modelled droplet pH. Explicit description of droplet pH has a significant impact on resultant model air concentrations and wet deposition fluxes. The pH dependency is only one part of the complex interaction of the sulphur and nitrogen cycle. Moreover, many other uncertain processes affect the model outcome. This complexity complicates the process of identifying the origin of occurring model errors. Despite the considerations discussed in section 3.4 and other model shortcomings our results indicate that modelling droplet pH is preferable to using a constant pH leading to better model consistency concerning air concentrations and wet deposition fluxes.

Acknowledgements

This work was funded by TNO within the framework of the R&D Project 370764200 -"MAPESI" (Modelling of Air Pollutants and EcoSystem Impact)- funded by the Federal Environment Agency (Umweltbundesamt, Germany).We thank the Federal Environment Agency also for providing the comprehensive measurement data. Further support was provided by Freie Universität Berlin.

References

Albrecht, B. A., Fairall, C. W., Thomson, D. W., White, A. B., Snider, J. B., and Schubert, W. H., 1990. Surface-based remote sensing of the observed and the adiabatic liquid water content of stratocumulus clouds, Geophysical Research Letters, 17, 89-92.

Aleksic, N., Roy, K., Sistla, G., Dukett, J., Houck, N., Casson, P., 2009. Analysis of cloud and precipitation chemistry at Whiteface Mountain, NY. Atmospheric Environment, Volume 43 , Issue: 17.

Beekmann, M., Kerschbaumer A., Reimer E., Stern R., Möller D., 2007. PM measurement campaign HOVERT in the Greater Berlin area: model evaluation with chemically specified particulate matter observations for a one year period. Atmospheric Chemistry and Physics, 7, 55-68.

Berge, E. and Jakobsen, H. A., 1998. A regional scale multi-layer model for the calculation of long-term transport and deposition of air pollution in Europe. Tellus 50, 205-223.

Bessagnet, B., Hodzic, A., Vautard, R., Beekmann, M., Cheinet, S., Honoré, C., Lious, C. and Rouil, C., 2004. Aerosol modeling with CHIMERE-preliminary evaluation at the continental scale, Atmospheric Environment 38, pp. 2803-2817.

Bobbink, R., Hornung, M., and Roelofs, J. M., 1998. The effects of airborne pollutants on species diversity in natural and semi-natural European vegetation, Journal of Ecology, 86, 717- 738.

Brantner B., Fierlinger, H., Puxbaum, H. and Berner, A., 1994. Cloudwater chemistry in the subcooled droplet regime at Mount Sonnblick (Salzburg, Austria). Water, Air & Soil Pollution 74, 363-384.

Builtjes, P.J.H., Hendriks, E., Koenen, M., Schaap, M., Banzhaf, S., Kerschbaumer, A., Gauger, T., Nagel, H.-D., Scheuschner, T., Schlutow, A., 2011. Erfassung, Prognose und Bewertung von Stoffeintraegen und ihren Wirkungen in Deutschland (in German). MAPESI-Project: Modelling of Air Pollutants and Ecosystem Impact. UBA report to BMU/UBA FE-Nr. 3707 64 200; Texte 38/201; ISSN 1862-4804; Umweltbundesamt, Dessau-Roßlau, 2011.

Byun, D., Ching, J., 1999. Science Algorithms of the EPA Models-3 Community Multiscale Air Quality (CMAQ) Modeling System. EPA/600/R-99/030. US EPA.

Byun, D., and Schere, K. L., 2006. Review of the governing equations, computational algorithms, and other components of the Models-3 Community Multiscale Air Quality (CMAQ) modeling system. Applied Mechanics Reviews 59, 51-77.

Calvo, A.I., Olmo, F.J., Lyamani, H., Alados-Arboledas, L.,Castro, A., Fernández-Raga, M., Fraile, R., 2010. Chemical composition of wet precipitation at the background EMEP station in VÃznar Granada, Spain) (2002-2006). Atmospheric Research, 96, 408-420.

Collett Jr., J., Oberholzer, B., Staehelin, J., 1993. Cloud chemistry at MT Rigi, Switzerland: dependence on drop size and relationship to precipitation chemistry. Atmospheric Environment 27A, 37-42.

Deguillaume, L. , Tilgner, A. , Schrödner, R. , Wolke, R. , Chaumerliac, N. , Herrmann, H., 2009. Towards an operational aqueous phase chemistry mechanism for regiona chemistry-transport models: CAPRAM-RED and its application to the COSMO-MUSCAT model. Journal of Atmospheric Chemistry, Vol. 64 , No. 1 , p. 1-35 DOI 10.1007/s10874-010-9168-8 (Springer-Verlag).

Denier van der Gon, H.A.C., Visschedijk, A., van der Brughand, H., Dröge, R., 2010. A high resolution European emission data base for the year 2005. A contribution to UBA-Projekt PAREST: Particle Reduction Strategies, TNO report TNO-034-UT-2010-01895-RPT-ML, Utrecht, 2010.

Dentener, F. , Drevet, J., Lamarque, J. F., et al., 2006. Nitrogen and sulfur deposition on regional and global scales: A multimodel evaluation. Global Biogeochemical Cycles 20, GB4003.

EMEP Co-operative Programme for Monitoring and Evaluation of the Long-range Transmission of Air Pollutants in Europe, 1996: EMEP manual for sampling and chemical analysis. EMEP/CCC-Report 1/95. Norwegian Institute for Air Research.

ENVIRON, 2010. CAMx User's Guide, Comprehensive air quality model with extensions, Version 5.20, ENVIRON International Corporation, 279 pp.

Erisman, J.W., van Pul, A. and Wyers, P., 1994. Parametrization of surface-resistance for the quantification of atmospheric deposition of acidifying pollutants and ozone, Atmospheric Environment 28, 2595-2607.

Fagerli H. and Aas, W., 2008. Trends of nitrogen in air and precipitation: Model results and observations at EMEP sites in Europe, 1980-2003. Environmental Pollution 154, 3, 448-461. doi:10.1016/j.envpol.2008.-01.024.

Fahey, K.M. and Pandis, S.N., 2003. Size-resolved aqueous-phase atmospheric chemistry in a three-dimensional chemical transport model. Journal of Geophysical Research-Atmospheres 108, D13204.

Flemming, J. and Reimer, E., 2000. The impact of special features of numerically predicted and analysed meteorological data on the results of ozone forecast by a PBL- chemical transport model, in ITM Air pollution modelling and its applications XXIII , eds. S. Gryning und E. Batchvarova, NATO CMS, Kluwer Academic / Plenum Publishers, New York.

Fowler, D., Smith, R. I., Muller, J. B. A., Hayman, G., and Vincent, K. J., 2005. Changes in the atmospheric deposition of acidifying compounds in the UK between 1986 and 2001. Environmental Pollution 137, pp. 15-25.

Herrmann, H., Ervens, B., Jacobi, H.-W., Wolke, R., Nowacki P., Zellner, R., 2000. CAPRAM 2.3: A chemical aqueous phase radical mechanism for tropospheric chemistry. Journal of Atmospheric Chemistry 36, 231-284.

Herrmann, H., Tilgner, A., Barzaghi, P., Majdik, Z., Gligorovski, S., Poulain, L., Monod, A., 2005.

Towards a more detailed description of tropospheric aqueous phase organic chemistry: CAPRAM 3.0. Atmospheric Environment 39, 4351-4363.

Hoffmann, M.R. and Calvert, J.G., 1985. Chemical Transformation Modules for Eulerian Acid Deposition Models, Vol. 2, The Aqueous-Phase Chemistry, EPA/600/3-85/017, U.S. Environmental Protection Agency, Research Triangle Park, NC.

ICP Modelling and Mapping, 2004. Manual on Methodologies and Criteria for Modelling and Mapping Critical Loads and Levels and Air Pollution Effects, Risks and Trends. Federal Environmental Agency (Umweltbundesamt), Berlin, www.icpmapping.org, UBA Texte 52/04.

Jörß, W., Kugler, U., Theloke, J., 2010. "Emissionen im PAREST Referenzszenario 2005-2020", Parest-Bericht Mai 2010.

Kalina, M. F. and Puxbaum, H., 1994. A study of the influence of riming of ice crystals on snow chemistry during different seasons in precipitating continental clouds. Atmospheric Environment 28, pp. 3311-3328.

Kvaalen H., Solberg S., Clarke N., Torp T., Aamlid D., 2002. Time series study of concentrations of SO42- and H+ in precipitation and soil waters in Norway. Environmental Pollution, 117 (2), pp. 215-224.

Lorenz M., Nagel, H.-D. , Granke, O., Kraft, P., 2008. Critical loads and their exceedances at intensive forest monitoring sites in Europe. Environmental Pollution 155: 426-435.

McArdle, J.V. and Hoffmann, M.R., 1983. Kinetics and Mechanism of the oxidation of aquated sulfur dioxid by hydrogen peroxide at low pH, Journal of Physical Chemistry 87, 5425-5429.

Nenes A., Pilinis, C. and Pandis, S., 1999. Continued development and testing of a new thermodynamic aerosol module for urban and regional air quality models, Atmospheric Environment 33, pp. 1553-1560.

Petroff, A., Mailliat, A., Amielh, M., Anselmet, F., 2008. Aerosol dry deposition on vegetative canopies. PartI: Review of present knowledge. Atmospheric Environment, 42, 3625-3653.

Pryor, S., Gallagher, M., Sievering, H., Larsen, S., Barthelmie, R., Birsan, F., 2008. A review of measurement and modeling results of particle atmosphere-surface exchange. Tellus B, 60, 42-75.

Rabalais, N. N. , 2002. Nitrogen in aquatic ecosystems, Ambio, 31(2), 102-112.

Redington A.L., Derwent, R.G., Witham, C.S., Manning, A.J., 2009. Sensitivity of modelled sulphate and nitrate aerosol to cloud, pH and ammonia emissions. Atmospheric Environment, Volume 43, Issue 20, pp. 3227-3234.

Reimer, E. and Scherer, B., 1992. An operational meteorological diagnostic system for regional air pollution analysis and long term modeling. Air Pollution Modelling and its Application IX, Kluwer Academic/Plenum Publisher, New York.

Rogers, R.R. and Yau, M.K., 1989. A Short Course in Cloud Physics, International Series in Natural Philosophy, Volume 113, Pergamon, Great Britain, 293pp.

Rogora, M., Mosello, R., Arisci, S., Brizzio, M.C., Barbieri, A., Balestrini, R., Waldner, P., Schmitt, M., Stähli, M., Thimonier, et al., 2006. An overview of atmospheric deposition chemistry over the Alps: Present status and long-term trends. Hydrobiologia, Volume 562 (1), pp. 17-40.

Schaap, M., Sauter, F., Timmermans, R., Roemer, M., Velders, G., Beck, J., Builtjes, P., 2008. The LOTOS-EUROS model: description, validation and latest developments. International Journal of Environmental Pollution 32 (2), 270-290.

Scire, J.S. and Venkatram, A., 1985. The contribution of in-cloud oxidation of SO_2 to wet scavenging of sulfur in convective clouds. Atmospheric Environment, Volume 19, Issue 4, pp. 637-650.

Seinfeld, J.H. and Pandis, N., 1998. Atmospheric Chemistry and Physics: From Air Pollution to Climate Change. From Air Pollution to Climate Change, John Wiley and Sons, Inc., New York, 1326 pp.

Simmer, C., 1994. Satellitenfernerkundung hydrologischer Parameter der Atmosphäre mit Mikrowellen. Verlag Dr. Kovac, 1994. 313p.

Simpson, D., Fagerli, H., Jonson, J., Tsyro, S., Wind, P., Tuovinen, J.-P., 2003. The EMEP Unified Eulerian Model. Model Description. EMEP/MSC-W Report 1/2003. The Norwegian Meteorological Institute, Oslo, Norway.

Stephens G.L., 1994. Remote Sensing of the Lower Atmosphere: An Introduction, published by Oxford University Press. Inc.

Stern, R., Yamartino, R., Graff, A., 2006. Analyzing the response of a chemical transport model to emissions reductions utilizing various grid resolutions. In: Twenty-eighth ITM on Air Pollution Modelling and its Application, Leipzig, Germany, 15-19 May 2006.

Stern R., Builtjes, P., Schaap, M., Timmermans, R., Vautard, R., Hodzic, A., Memmesheimer, M., Feldmann, H., Renner, E., Wolke, R., Kerschbaumer, A., 2008. A model inter-comparison study focussing on episodes with elevated PM_{10} concentrations. Atmospheric Environment 42, 4567-4588.

Sutton, M.A., Schjorring, J.K., Wyers, G.P., 1995. Plant-atmosphere exchange of ammonia. Philosophical Transactions of the Royal Society of London Series A 351, 261-278.

Sutton, M.A., Lee, D.S., Dollard, G.J., Fowler, D., 1998. Introduction atmospheric ammonia: emission, deposition, and environmental impacts. Atmospheric Environment 32, 269-271.

Thiruchittampalam, B., Köble, R., Theloke, J., Kugler, U., Uzbasich, M., Geftler, T., 2010. "Dokumentation des PAREST Emissionsverteilungsmodells für Deutschland"
PAREST-Bericht Juli 2010.

UBA, 2004. Manual for Quality Assurance (in German), Texte 28/04, ISSN 0722-186X, Umweltbundesamt - Berlin, Fachgebiet II 5.6, 536 pp.

UNECE, 1999. Protocol to the 1979 Convention on Long-Range Transboundary Air Pollution to Abate Acidification, Eutrophication and Ground-Level Ozone. United Nations Economic Commission for Europe.

Van Loon M., Roemer, M.G.M., Builtjes, P.J.H., 2004. Model intercomparison in the framework of the review of the Unified EMEP model, TNO Report R2004/282, TNO, Utrecht, The Netherlands, www.tno.nl.

Vautard R., Builtjes, P., Thunis, P., et al., 2007. Evaluation and intercomparison of Ozone and PM_{10} simulations by several chemistry-transport models over 4 European cities within the City-Delta project, 2007, Atmospheric Environment 41, pp. 173-188.

Vautard, R., Schaap, M., Bergström, R., et al., 2009. Skill and uncertainty of a regional air quality model ensemble. Atmospheric Environment 43, 4822-4832.

Walcek, C.J., 2000. Minor flux adjustment near mixing ratio extremes for simplified yet highly accurate monotonic calculation of tracer advection, Journal of Geophysical Research, 105, D7, 9335-9348.

Wright, R.F., Dale, T., Gjessing, E.T., Hendrey, G.R., Henriksen, A., Johannessen, M., and Muniz, I.P., 1976. Impact Of Acid Precipitation On Freshwater Ecosystems In Norway. Water, Air & Soil Pollution. 6 (2-4): p. 483-499.

Zhang, L., Gong, S., Padro, J., Barrie, L., 2001. A size-segregated particle dry deposition scheme for an atmospheric aerosol module. Atmospheric Environment 35, pp. 549-560.

Chapter 4

Paper II - Impact of emission changes on secondary inorganic aerosol episodes across Germany

S. Banzhaf (1), M. Schaap (2), R.J. Wichink Kruit (2), H.A.C. Denier van der Gon (2), R. Stern (1) and P.J.H. Builtjes (1,2)

(1) Institut für Meteorologie, Freie Universität Berlin, Carl-Heinrich-Becker Weg 6-10, 12165 Berlin, Germany
(2) TNO, Department Climate, Air Quality and sustainability, Princetonlaan 6, 3508 TA Utrecht, The Netherlands

published in Atmospheric Chemistry and Physics, 13, 11675-11693, 2013
doi: http://dx.doi.org/10.5194/acp-13-11675-2013 [2]

[2]The paper has been reprinted with kind permission from the journal.

Abstract

In this study, the response of secondary inorganic aerosol (SIA) concentrations to changes in precursor emissions during high PM_{10} episodes over central Europe in spring 2009 was investigated with the Eulerian Chemistry Transport Model (CTM) REM-Calgrid (RCG). The model performed well in capturing the temporal variation of PM_{10} and SIA concentrations and was used to analyse the different origin, development and characteristics of the selected high PM_{10} episodes. SIA concentrations, which contribute to about 50 % of the PM_{10} concentration in northwestern Europe, have been studied by means of several model runs for different emission scenarios. SO_2, NO_x and NH_3 emissions have been varied within a domain covering Germany and within a domain covering Europe. It was confirmed that the response of sulfate, nitrate and ammonium concentrations and deposition fluxes of S and N to SO_2, NO_x and NH_3 emission changes is non-linear. The deviation from linearity was found to be lower for total deposition fluxes of S and N than for SIA concentrations. Furthermore, the study has shown that incorporating explicit cloud chemistry in the model adds non-linear responses to the system. It significantly modifies the response of modelled SIA concentrations and S and N deposition fluxes to changes in precursor emissions. The analysis of emission reduction scenario runs demonstrates that next to European-wide emission reductions additional national NH_3 measures in Germany are more effective in reducing SIA concentrations and deposition fluxes than additional national measures on SO_2 and NO_x.

4.1 Introduction

Particulate matter has adverse impact on public health (Pope et al., 2007, 2008). The European Commission established directives regarding PM_{10} concentration level to avoid, prevent or reduce harmful effects on human health (European Commission, 2008). The analysis of observations reveals that the current EU limit values for PM_{10} are still exceeded over large parts of Europe (EEA, 2012) indicating a continued need for further implementation of abatement strategies. Secondary inorganic aerosol (= SIA: SO_4^{2-}, NO_3^- and NH_4^+) originating from gaseous precursors such as SO_2, NO_x and NH_3 (Fountoukis and Nenes, 2007) comprises an important fraction of PM_{10}. Experimental studies have shown that in the rural background the average PM_{10} is dominated by SIA contribution (Van Dingenen et al., 2004; Putaud et al., 2004). Moreover, during PM episodes the fraction of SIA is higher than on average (Weijers et al., 2011). After removal of SIA and its precursors from the atmosphere they contribute to eutrophication and acidification of soils and water bodies with harmful effects to vulnerable ecosystems (Bobbink et al.,

1998).

SIA is dominated by ammonium-sulfate and ammonium-nitrate salts (Putaud et al., 2010). The precursor gases NO_x and SO_2 are oxidised to form HNO_3 and H_2SO_4, respectively. Ammonium-sulfate and ammonium-nitrate are then formed when nitric acid and sulfuric acid are neutralised by NH_3. In contrast to ammonium-sulfate, ammonium-nitrate is a semi-volatile component (Nenes et al., 1999). NH_3 preferentially neutralizes sulfuric acid due to its low saturation vapour pressure. If abundant NH_3 is available, ammonium-nitrate may form. The thermodynamic equilibrium between gas and aqueous aerosol phase is determined by temperature, relative humidity and the ambient concentrations of sulfate, total nitrate and total ammonia (West et al., 1999). In addition, NH_3 constrains cloud droplet pH, which regulates the oxidation pathway of SO_2 and therewith the formation efficiency of sulfate (Fowler et al., 2007). Furthermore, the dry deposition velocities of NH_3 and SO_2 are connected (Fowler et al., 2001). Hence, emission reductions of gaseous SIA precursors lead to shifts in the equilibrium and affect the formation, residence time and removal of sulfur and nitrogen compounds and result in a non-linear response of the SIA concentrations (Fagerli and Aas, 2008). The impact of the complex interactions varies seasonally and regionally over Europe with changing emission regime. Among emission changes of SO_2, NO_x and NH_3, responses to NH_3 emission changes show the largest non-linear behaviour (Tarrasón et al., 2003). Former studies over Europe regarding responses of ambient PM levels to emission reductions indicate that a decrease of NH_3 emissions may entail a high reduction potential for SIA (and therewith PM) concentrations and deposition fluxes of S and N (e.g. Erisman and Schaap, 2004; Derwent et al., 2009; Redington et al., 2009; Matejko et al., 2009). Pinder et al. (2007) found that reducing NH_3 emissions may offer significant cost savings compared to further controls on SO_2 and NO_x (in the US). In contrast, other studies indicated that for regions, in which SIA formation is SO_2– and HNO_3–limited due to high NH_3 concentrations, a decrease in SO_2 and NO_x emissions may result in a large reduction of SIA concentrations (Pay et al., 2012; de Meij et al., 2009). Further research is needed to consider and include the impact of the non-linear system described above in current PM_{10} mitigation strategies.

So far, investigations on the impact of emission reductions of precursors SO_2, NO_x and NH_3 on SIA or PM concentrations focussed on long-term trends (Fagerli and Aas, 2008; Fowler et al., 2005; Lövblad et al., 2004; Erisman et al., 2003), on the analysis of one specific year (Tarrasón et al., 2003; Derwent et al., 2009) or on separate months (Erisman and Schaap, 2003; Renner and Wolke, 2010; de Meij et al., 2009), but not on specific periods with elevated PM_{10} levels. During the last decade, springtime high PM_{10} episodes were repeatedly reported in large areas over Europe with PM_{10} concentrations above 100 μg m^{-3} (e.g. 2006, 2007, 2009 and 2011). Springtime is marked by periods of fair weather

with medium temperatures combined with high NH_3 emission due to incipient agricultural activity. The latter leads to high NH_3 availability, which enhances SIA formation.
In this study, the development and characteristics of two high PM_{10} episodes over central Europe in spring 2009 are studied. Furthermore, the response of modelled SIA concentrations to changes in the precursor emission is investigated for this time period. With respect to the latter, the sensitivity of modelled SIA concentrations to changes in NH_3 emissions is investigated. Furthermore, SIA concentrations are calculated for different scenario runs with simultaneously varying SO_2, NO_x and NH_3 emissions. A critical question for national policy makers is how much reduction in population exposure can be achieved by national measures versus generic European measures. We define measures in the German national domain and compare the impact with European-wide measures. Therefore, for each scenario run, two cases were simulated: in the first case the emission scenario runs were only applied to the model domain covering Germany, and in the second case, the emission scenario runs were also applied to the European model domain, which provides the boundary conditions for the national domain. Besides SIA concentrations, deposition fluxes of S and N are also included in the analysis. Deposition fluxes are important sinks for SIA and the air concentrations of its precursor gases.
In the following section, the model and observations are described. A detailed overview of the model set up and the performed emission scenario runs is given. In Sect. 4.3, the investigation period is described. In the subsequent section (Sect. 4.4) the characteristics of the PM episodes in spring 2009 and results of the model evaluation and the emission scenario runs are presented. The results are discussed and conclusions are drawn in Sect. 4.5.

4.2 Methods and Data

4.2.1 Model description and set-up

The Eulerian grid model REM-Calgrid (RCG) simulates air pollution concentrations solving the advection-diffusion equation on a regular latitude-longitude-grid with variable resolution over Europe (Beekmann et al., 2007; Stern, 2006). RCG is offline-coupled to the German Weather Service operational NWP model COSMO-EU (Schättler et al., 2008). The vertical transport and diffusion scheme accounts for atmospheric density variations in space and time and for all vertical flux components. For the horizontal advection of pollutants the advection scheme developed by Walcek (2000) is used. Gas-phase chemistry is simulated using an updated version of the photochemical reaction scheme CBM-IV (Gery et al., 1989), including Carter's 1-product isoprene scheme (Carter, 1996), as described

in Gipson and Young (1999). Furthermore, RCG features thermodynamic equilibrium modules for secondary inorganic aerosols (ISORROPIA: Nenes et al., 1999) and organic aerosols (SORGAM: Schell et al., 2001). RCG includes modules to treat the emissions of sea salt aerosols (Gong et al., 1997) and wind-blown dust particles (Claiborn et al., 1998; Loosemore und Hunt, 2000). Dry deposition fluxes are calculated following a resistance approach as proposed by Erisman et al. (1994).

RCG is used within Germany to evaluate emission reduction strategies for the German government (PAREST; Builtjes et al., 2010). Moreover, RCG is one of the models that are used to benchmark the EMEP model against within the Task Force on Measurements and Modelling (TFMM) EURODELTA (Vautard et al., 2009) studies.

For this study, a research version of RCG was used as described in Banzhaf et al. (2012). It includes enhanced physical and chemical descriptions of scavenging processes and sulfate production as a function of cloud liquid water content and cloud/rain droplet pH. Cloud droplet pH is estimated using the concentrations of the (strong) acids and bases, including the buffering by bi-carbonate (through CO_2). For the formation of sulfate in cloud water the oxidation of dissolved SO_2 by hydrogen peroxide and ozone are simulated. Sulfate formation and wet scavenging can either be calculated using modelled droplet pH or using a constant droplet pH. Banzhaf et al. (2012) showed that a modelled droplet pH gives a better model performance and better model consistency concerning air concentrations and wet deposition fluxes than a constant pH. The RCG wet deposition scheme distinguishes between in-cloud and below-cloud scavenging of gases and particles. The applied scheme integrates wet deposition throughout the column.

The model runs for spring 2009 were performed on a domain covering Germany (47.2° N–55.1° N; 5.4° E–15.7° E), in the following referred to as the German domain (GD), with a horizontal resolution of approximately $7 \times 7\,\mathrm{km}^2$ and 20 vertical layers up to 5000 m. An RCG run covering Europe (35.1° N–66.3° N; 10.2° W–30.8° E), in the following referred to as the European domain (ED), provided the boundary conditions. Emissions for Germany were taken from a national inventory for the year 2005 (Appelhans et al., 2012, Builtjes et al., 2010) and combined with the European TNO-MACC (Monitoring Atmospheric Composition and Climate) data set for the same year (Denier van der Gon et al., 2010; Kuenen et al., 2011). The spatial distributions of the total annual NH_3, SO_x and NO_x emissions of the German domain are presented in Fig. 4.1. The distributions illustrate that emission regimes vary significantly. Agricultural ammonia-rich areas are situated in the northwest and southeast of the domain. The SO_x emissions are located in the industrial areas whereas NO_x emissions are highest in urbanised regions and transport corridors. The temporal variation of the emissions is represented by monthly, day-of-the-week and hourly time factors for each source category. These factors were taken from

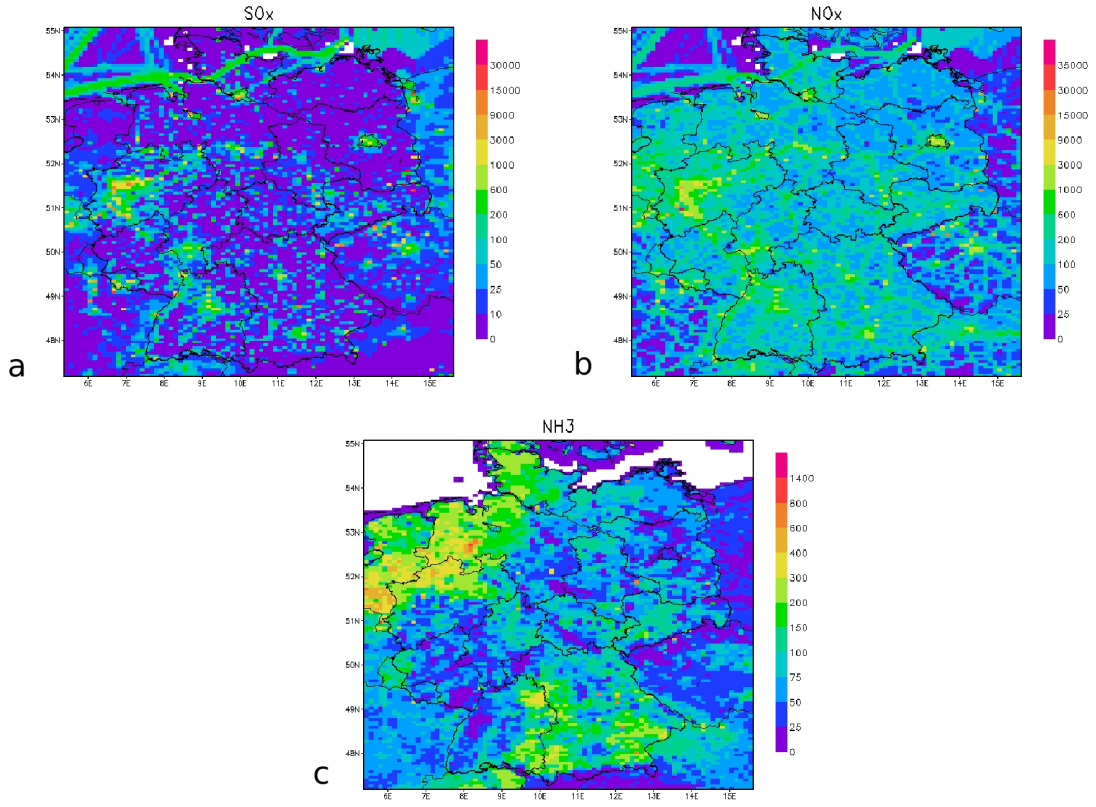

Figure 4.1 Spatial distribution of the total annual (a) SO_x, (b) NO_x and (c) NH_3 emissions in t a^{-1} $cell^{-1}$.

the EURODELTA database (Thunis et al., 2008). The applied monthly and hourly time factors for ammonia are shown in Fig. 4.2. The seasonal variation in ammonia emissions is uncertain and may differ regionally as a function of farming procedures and climatic conditions (Geels et al., 2012). The seasonal variation for Germany shows a distinct maximum in March/April due to the application of manure. The diurnal cycle in the emission follows the empirically derived distribution by Asman (2001) with half the average value at midnight and twice the average at noon.

4.2.2 Model runs

To investigate the mitigation potential of emission reductions of the precursor gases SO_2, NO_x and NH_3 on SIA concentrations and S and N deposition fluxes, a base case simulation and model runs for three reduction scenarios have been performed:

1. reducing NH_3 emissions only,

2. reducing SO_2 and NO_x emissions simultaneously, and

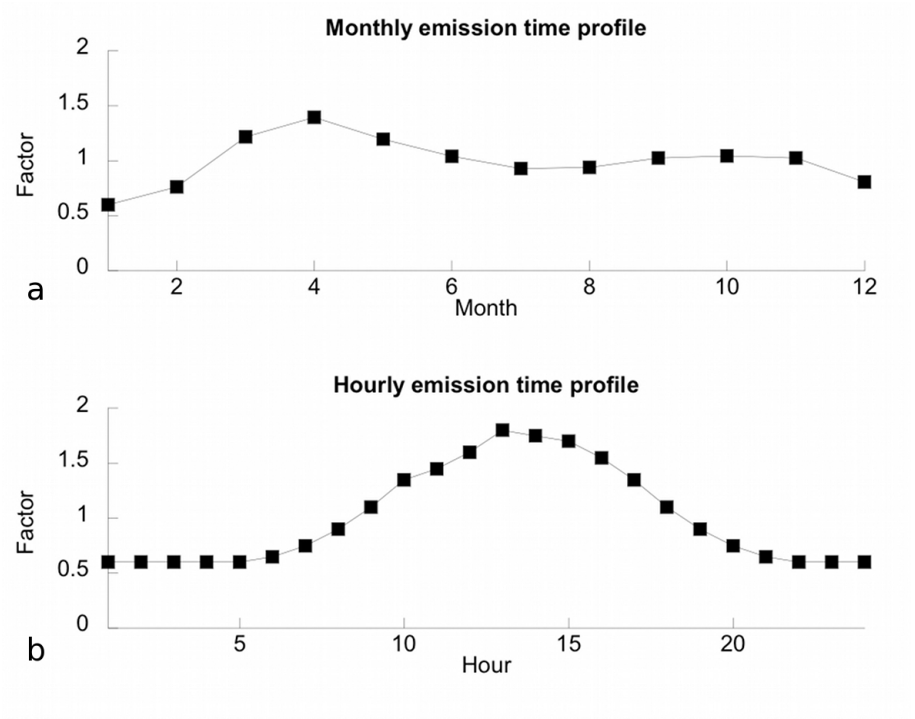

Figure 4.2 Profiles of (a) monthly and (b) hourly ammonia emission factors applied in RCG.

3. reducing SO_2, NO_x and NH_3 simultaneously.

The emission reduction scenario runs are listed and labelled in Table 4.1. All model runs have been performed using modelled droplet pH. To study the impact of national measures compared to European-wide mitigation efforts, all reduction scenario runs have been performed twice:

1. emissions have been reduced within the German domain only (scenario runs denoted by GD) and

2. emissions have been reduced within the German domain and within the European domain lowering the boundary conditions (scenario runs denoted by ED).

Table 4.1 Overview of performed emission reduction scenario runs and their set-up.

Scenario runs	pH modelled	pH constant	German domain (GD)	European domain (ED)
base run	x	–	x	x
$-40\,\%NH_3$	x	–	x	x
$-20\,\%NO_x$ $-50\,\%SO_2$	x	–	x	x
$-40\,\%NH_3$ $-20\,\%NO_x$ $-50\,\%SO_2$	x	–	x	x

For simplicity, the emission reductions to assess national or regional measures were applied to the whole German zoom domain. Inevitably, this domain comprises parts of neighbouring countries and seas. As for the land area, around two thirds of the emissions in the GD domain are from Germany itself (see Table 4.2).

Table 4.2 Total annual German and German domain SO_x, NO_x and NH_3 emissions and the ratio of German emissions to German domain emissions.

Emissions	SO_x ($t\,a^{-1}$)	NO_x ($t\,a^{-1}$)	NH_3 ($t\,a^{-1}$)
German domain emissions	979 800	2 402 052	876 200
German emissions	561 580	1 543 970	606 880
German emissions/ German domain emissions	0.57	0.64	0.69

To study the model sensitivity to ammonia emission changes in more detail, additional model runs have been performed in which ammonia emissions have been varied on the German domain 20 %-stepwise from −60 % to +40 %. The emission scenario runs are listed and labelled in Table 4.3. To study the sensitivity of the model results to the variable pH in cloud water, which has often been neglected in previous studies, the sensitivity runs have been performed twice:

1. applying modelled droplet pH and
2. applying a constant pH of 5.5.

Finally, to study the impact of long-range transport, the −40 % NH_3 emission scenario run has been performed on the German domain (scenario runs denoted by GD) and on the European domain implying emission reduction within the German and the boundary conditions (scenario runs denoted by ED).

Table 4.3 Overview of performed ammonia emission sensitivity scenario runs and their set-up.

Scenario runs	pH modelled	pH constant	German domain (GD)	European domain (ED)
−60 % NH_3	x	x	x	–
−40 % NH_3	x	x	x	x
−20 % NH_3	x	x	x	–
base run	x	x	x	–
+20 % NH_3	x	x	x	–
+40% NH_3	x	x	x	–

4.2.3 Observations

AirBase (European AIR quality database, http://airbase.eionet.europa.eu/) provides PM_{10} air concentrations for a large number of European measurement stations. For the evaluation of RCG, PM_{10} model results have been compared to daily averages of PM_{10} at 42 rural background stations in AirBase within Germany. A comparison to 63 suburban background stations in AirBase over Germany has also been included.
Data from the national German monitoring network (UBA, 2004) are used for evaluation of COSMO-EU precipitation and RCG wet deposition fluxes. Precipitation sampling is performed by using wet-only collectors (Firma Eigenbrodt, Germany). Weekly total precipitation and wet deposition fluxes for 11 stations within Germany were available. At the time of writing no quality-controlled SIA measurement data for Germany were available. Measurement data of sulfate, nitrate and ammonium for three observational sites (Vredepeel, Kollumerwaard, Valthermond) close to the German border were supplied by the Dutch National Institute for Public Health and the Environment (www.rivm.nl). The locations of all stations are shown in Fig. 4.3.

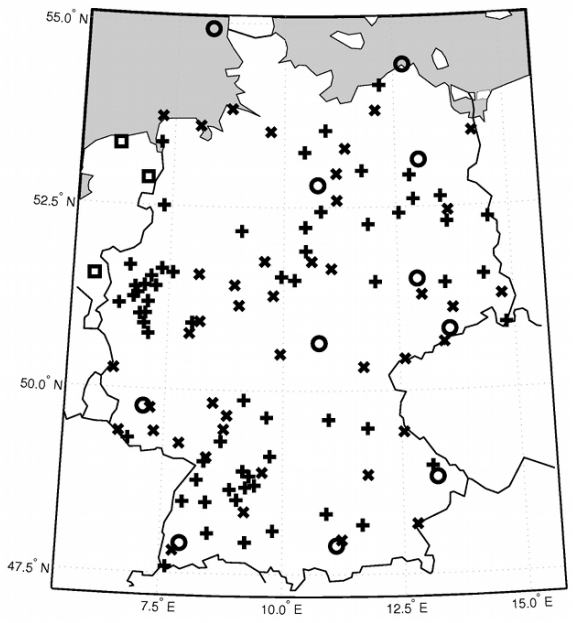

Figure 4.3 Map of observational station locations: PM_{10} concentrations (rural background) (x), PM_{10} concentrations (suburban background) (+), SIA concentrations ([]), wet deposition fluxes (o).

4.3 Investigation period

4.3.1 Meteorological conditions

The investigation period was 24 March to 28 April in spring 2009. According to the German Weather Service, the mean temperature over central Europe in spring 2009 was up to 3 K higher than the mean of the reference period of 30 years (1961–1990). In April this temperature anomaly was even more than 4 K. This extremely warm, dry and sunny weather in April 2009 was related to high-pressure systems with rather stable air conditions and little atmospheric mixing. In Germany, in April 2009 the mean temperature of 11.9 °C was 4.5 K higher than the mean of the reference period. April 2009 was announced as the warmest April since the beginning of comprehensive weather observations 120 years ago. Sunshine duration was 62 % above average while, regionally, precipitation amounts were far below average. For example, at station Berlin-Buch only 1 mm of precipitation was observed in April. The weather conditions were especially dry and sunny for north eastern Germany, north western Poland and the northern part of the Czech Republic, with monthly mean cloud fractions of 20–40 %, whereas the climatological mean (1971–2000) of cloud fraction over central Europe amounts to 60–75 % for April. Mean cloud fraction in central and eastern Germany and western Czech Republic was, with 40–50 %, also below the climatological mean while in western and southwestern Germany, the Netherlands, Belgium, France and Great Britain the mean cloud fraction was above 60%.

4.3.2 PM_{10} concentrations

Stable air conditions lead to high PM_{10} levels (Mues et al., 2012; Demuzere et al., 2009). For April 2009 the average PM_{10} concentration over German rural background stations operated by UBA was 25 % higher than the average over the previous 9 years (2000–2008) (UBA, 2010). The EU limit for daily mean PM_{10} (24 h average above 50 μg m^{-3}) was exceeded between 9 and 12 days in this month at most stations in Belgium and the Netherlands and at several stations in Germany. There were two main high PM_{10} episodes within the investigation period: one from about 2 to 7 April and one from about 11 to 16 April. Figure 4.4 shows the daily mean PM_{10} concentration distribution over Germany derived by Optimal Interpolation of observations for the peak days of each episode. PM_{10} daily mean concentrations above 100 μg m^{-3} were measured at several stations in central Europe within both episodes. On 13 April, daily mean PM_{10} concentrations of around 150 μg m^{-3} were measured at rural background stations in North Rhine-Westphalia in the west of Germany. In both episodes the fraction of SIA was very high, with measured daily mean SIA concentrations of up to above 70 μg m^{-3}. In this study, the extremely

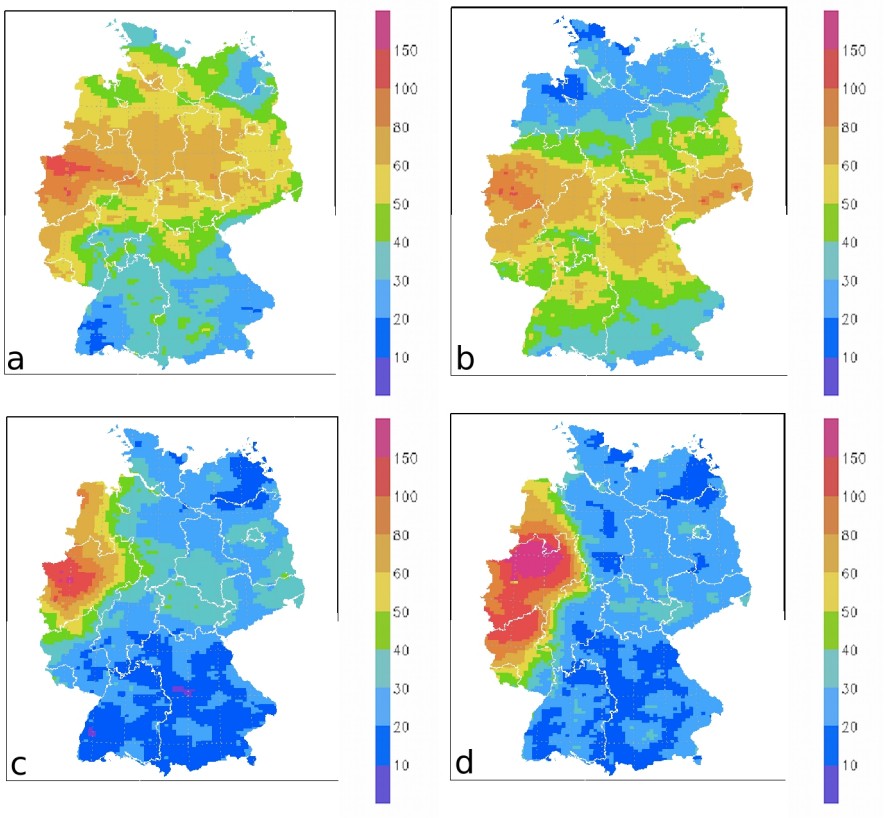

Figure 4.4 Daily mean PM_{10} concentrations in μg m^{-3} on (a) 4 and (b) 5 April 2009 and (c) 12 and (d) 13 April 2009 derived by Optimal Interpolation of observations.

high concentration levels and their origin during these episodes are investigated, which is highly relevant for mitigation purposes.

4.4 Results

4.4.1 Model performance

Figure 4.5a shows a scatter plot of the modelled daily mean PM_{10} concentrations of the base run compared to observations at 42 rural background stations within Germany. The corresponding statistics are given in Table 4.4. The model performs well with a correlation of 0.75. The model tends to overestimate low PM_{10} values and underestimate the high peaks. The bias of +2.95 μg m^{-3} (observed mean 22.56 μg m^{-3}) indicates a slight overall overestimation by the model. A comparison of modelled PM_{10} concentrations to 63 suburban background stations (not shown here) reveals a similar correlation coefficient of 0.71. The observed daily mean PM_{10} concentrations are with 27.01 μg m^{-3} higher than for the rural background stations. Also the RMSE is higher than for rural background

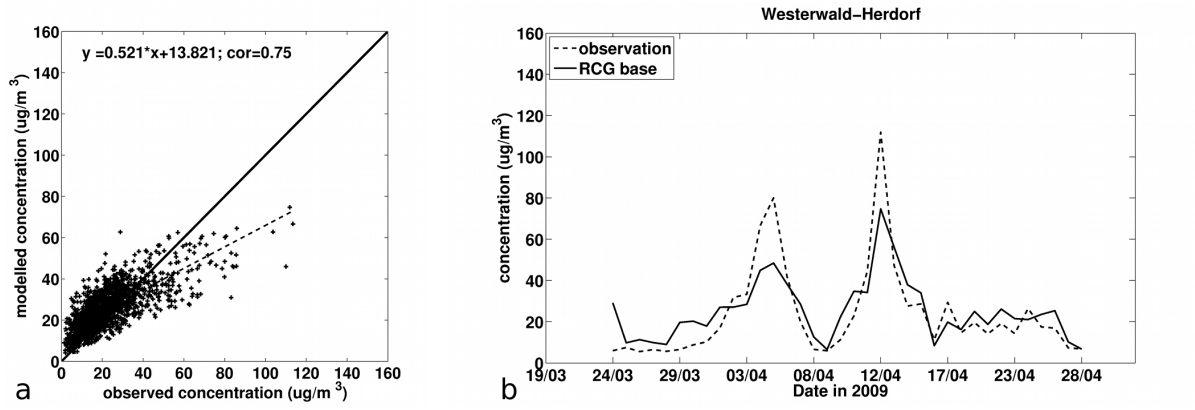

Figure 4.5 Daily mean modelled PM_{10} concentrations (a) versus observations at 42 AirBase sites and (b) versus observations at AirBase site Westerwald-Herdorf.

stations, which is partly related to a higher frequency of peak values. Figure 4.5b shows the time series of PM_{10} daily means at station Westerwald-Herdorf. The model nicely reproduces the temporal variation of PM_{10} concentrations throughout the investigation period. However, as already recognised in the scatter plot, the model tends to underestimate peak values and overestimate low values.

Figure 4.6a shows modelled daily mean SIA concentrations compared to measurements at 3 Dutch observational sites. The model performs well with a correlation coefficient of 0.76. The bias of -2.10 μg m^{-3} indicates a slight overall underestimation of SIA concentrations by the model. Similar to the PM_{10} concentrations, the SIA concentrations in the high concentration range are underestimated by the model.

In Fig. 4.6b, time series of the SIA components SO_4^{2-}, NO_3^- and NH_4^+ at station Kollumerwaard (NL) are presented. The high correlation coefficients for SO_4^{2-}, NO_3^- and NH_4^+ in Table 4.4 indicate that the model captures the temporal variability of SIA concentrations well. The model tends to overestimate SO_4^{2-} concentrations and underestimate NO_3^- concentrations while NH_4^+ concentrations are simulated well for the considered period. The correlations for the precursor gases SO_2 and NO_2 (NH_3 concentration measurements were unfortunately not available for Germany in 2009) show that RCG is able to capture the temporal variability of the analysed species concentrations. Surface SO_2 concentrations tend to be overestimated by RCG, while NO_2 concentrations tend to be underestimated. Total wet deposition fluxes of SO_x, NO_y and NH_x for the investigation period are compared to observations at 11 UBA sites within Germany. The model performance concerning wet deposition fluxes is summarised in Fig. 4.7. The corresponding statistics are given in Table 4.4. The spatial correlations between model results and observations are high, with values of 0.82, 0.80 and 0.74 for SO_x, NO_y and NH_x, respectively. The bias indicates

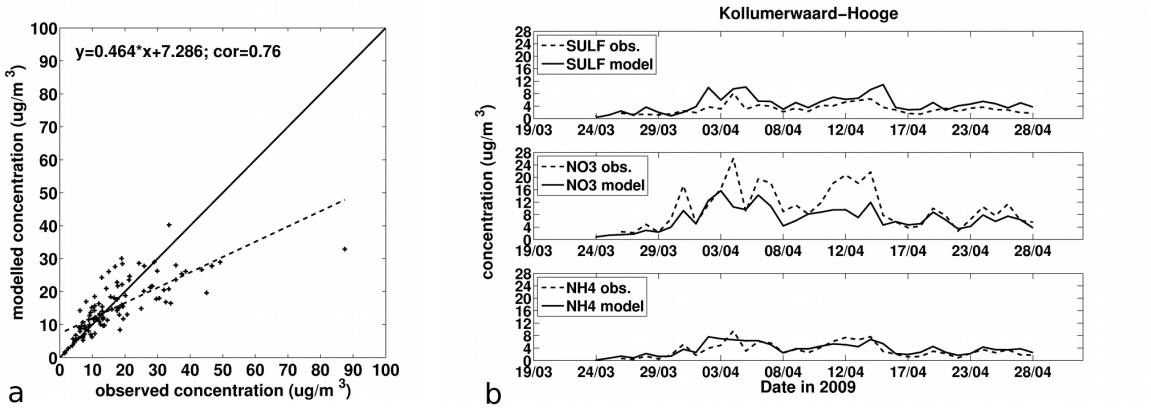

Figure 4.6 Daily mean modelled SIA concentrations (a) versus observations at 3 RIVM sites and (b) versus observations at station Kollumerwaard.

that SO_x and NH_x wet deposition fluxes are underestimated by the model while NO_y is slightly overestimated. Figure 4.7d shows the comparison of COSMO-EU precipitation to observations at the 11 wet deposition measurement sites. The spatial correlation is 0.57. Although some shortcomings can be identified, the overall performance is satisfactory and in line with or better than in previous studies (e.g. Stern et al., 2008; Solazzo et al., 2012). The model is able to capture the main variability of the components' concentrations and deposition fluxes in space and time.

4.4.2 Origin and characteristics of the PM_{10} episodes in spring 2009

The model evaluation in Sect. 4.4.1 has shown that RCG performs well in simulating the temporal and spatial variation of SIA and PM_{10} concentrations within the investigation period. Thus, RCG is used to investigate origin and characteristics of the high PM_{10} episodes in spring 2009.

4.4.2.1 First episode (2 April 2009–7 April 2009)

From the end of March, a high-pressure system over northern central Europe determined the weather pattern over the investigation area. In northern France and northern Netherlands the stagnant air conditions led to the accumulation of SIA precursor gases, enhancing local SIA formation in the beginning of April. SIA was dominated by ammonium-nitrate due to elevated NO_x levels originating from road transport and shipping activities, combined with high NH_3 emission levels originating from local agricultural activity. On 3

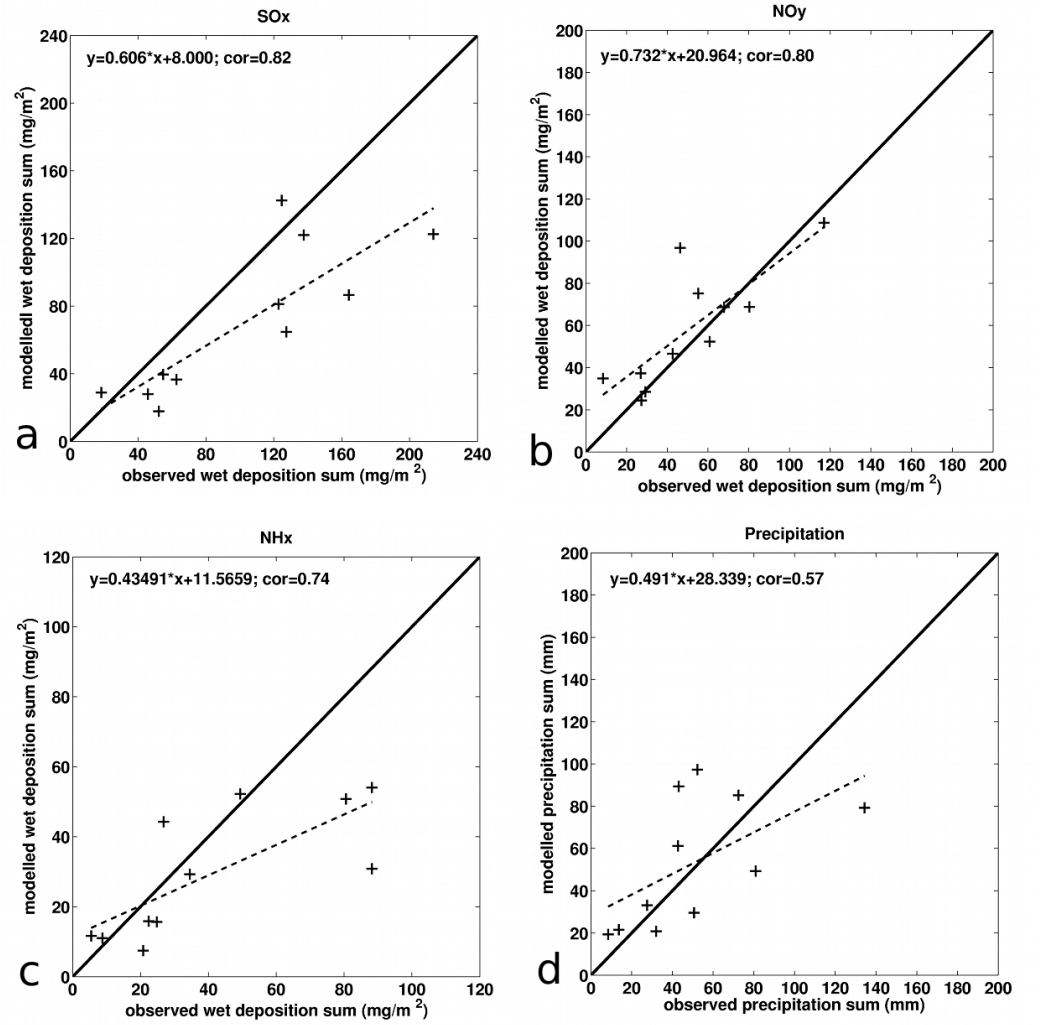

Figure 4.7 Modelled wet deposition sum of (a) SO_x, (b) NO_y, (c) NH_x and (d) total precipitation for the investigation period versus observations at 11 UBA sites.

April a ridge over the Atlantic sea west of France induced clouds over northern and central France. The cloud cover was 50–100 %. On 4 April, a trough passed the British Islands and moved westwards transporting the polluted air masses, containing high SIA and high NO_x concentrations, towards Germany. Passing ammonia-rich areas, further ammonium-nitrate formation occurred within the humid air mass. The polluted air mass reached Germany in the late morning hours of 4 April and spread out over the country in the following hours. On 4 April, by the time of the arrival of the polluted air mass, the cloud cover across Germany was largely between 70–100 %. Figure 4.8a shows modelled average SIA concentrations of the base run for 4 April. Average SIA concentrations exceeded 45 μg m^{-3} that day. We would like to stress that the spatial distribution of modelled SIA concentrations in Fig. 4.8a compares well to the spatial distribution of observed PM_{10} concentrations on 4 April shown in Fig. 4.4a. On 5 April a high-pressure

Table 4.4 Statistical comparison between measured and modelled concentrations and wet deposition fluxes at different stations (see Fig. 4.3) for the investigation period. Observed mean, as well as BIAS, RMSE and correlation are given.

Concentrations and wet deposition fluxes	Observed mean	RMSE	BIAS	Correlation
PM_{10} concentration (rural background)	22.56 μg m^{-3}	10.36 μg m^{-3}	2.95 μg m^{-3}	0.75
PM_{10} concentration (suburban background)	27.01 μg m^{-3}	12.61 μg m^{-3}	1.28 μg m^{-3}	0.71
SIA concentration (rural background)	17.55 μg m^{-3}	8.88 μg m^{-3}	-2.10 μg m^{-3}	0.76
SO_4^{2-} concentration (rural background)	3.4 μg m^{-3}	2.6 μg m^{-3}	1.3 μg m^{-3}	0.63
NO_3^- concentration (rural background)	11.7 μg m^{-3}	6.3 μg m^{-3}	-3.5 μg m^{-3}	0.76
NH_4^+ concentration (rural background)	4.1 μg m^{-3}	2.16 μg m^{-3}	0.17 μg m^{-3}	0.73
SO_2 concentration (rural/suburban background)	3.9 μg m^{-3}	5.4 μg m^{-3}	2.9 μg m^{-3}	0.62
NO_2 concentration (rural/suburban background)	15.0 μg m^{-3}	8.8 μg m^{-3}	-4.5 μg m^{-3}	0.65
SO_x wet deposition	102.27 mg m^{-2}	45.9 mg m^{-2}	-32.2 mg m^{-2}	0.82
NO_y wet deposition	50.10 mg m^{-2}	19.2 mg m^{-2}	7.3 mg m^{-2}	0.80
NH_x wet deposition	40.91 mg m^{-2}	23.4 mg m^{-2}	-11.6 mg m^{-2}	0.74
Precipitation	50.75 mm	29.4 mm	2.5 mm	0.57

system built up over northern Germany. The stagnant air conditions led to the accumulation of pollutants that had been transported to Germany (mainly SIA and precursor NO_x) during 4 April and local emitted pollutants. As a result, the SIA originating from local formation in Germany on 5 April added up to the SIA originating from long-range transport. Modelled hourly SIA concentrations exceeded 70 μg m^{-3} on 5 April.

4.4.2.2 Second episode (11–16 April 2009)

From 11 to 16 April a ridge over central Europe led to warm weather and stagnant air conditions over Germany. The latter resulted in pollutant accumulation and enhanced local SIA formation over western Germany due to high precursor emissions in the Ruhr area and its surrounding. On 13 and 14 April western Germany was situated on the very western border of the ridge with very stagnant conditions favouring the build-up and local formation of SIA and precursor levels. While large parts of northeastern and southeastern Germany were cloud-free, in the west and southwestern Germany the cloud cover was 40–100 %. The latter was also the case for large parts of Belgium and northern France. Different from the first episode, ammonium-sulfate and ammonium-nitrate levels were equally high. The model simulations show that ammonium-sulfate was mainly formed during the daytime when temperatures were high (above 25 °C) while ammonium-nitrate

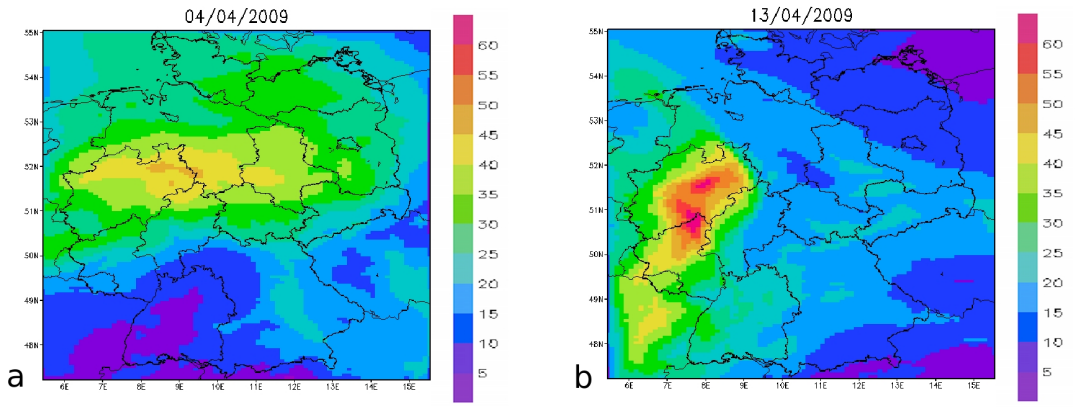

Figure 4.8 Modelled mean SIA concentration of the base run for (a) 4 April 2009 and (b) 13 April 2009.

was mainly formed during the nighttime and early morning hours at moderate temperatures (10–15 °C) and high relative humidity (80–90 %). Figure 4.8b shows modelled average SIA concentrations for 13 April. In North Rhine-Westphalia, in the west of Germany, average SIA concentrations exceeded a daily average of 60 μg m^{-3}. Again, the spatial distribution of modelled SIA concentrations in Fig. 4.8b compares well to the spatial distribution of observed PM_{10} concentrations on 13 April shown in Fig. 4.4d.
The analysis using RCG shows that the high SIA concentrations are of different origin for the two episodes. Within the first episode, SIA was mainly formed outside of Germany while within the second episode, SIA mainly originated from local sources within Germany. This will be further discussed in Sect. 4.5.

4.4.3 Emission scenarios

4.4.3.1 Sensitivity of SIA concentrations to ammonia emission changes

Figure 4.9 presents a time series of daily mean sulfate, nitrate and ammonium concentrations at station Westerwald-Herdorf. The station location is marked (x) on the map on the upper right-hand side. The station is located in the western part of Germany and was affected by both episodes. Figure 4.9 includes 3 different runs: base run, -40% $NH_{3\,GD}$ run and $+40\%$ $NH_{3\,GD}$ run. The figure again illustrates that the first episode around 4 April was dominated by ammonium-nitrate while during the second episode around 12 April ammonium-sulfate and ammonium-nitrate levels were equally high.
All SIA components clearly show a dependency on ammonia emission changes: mean concentrations increase compared to the base run when ammonia emissions are increased and vice versa. Sulfate concentrations are sensitive to changes in ammonia emission as

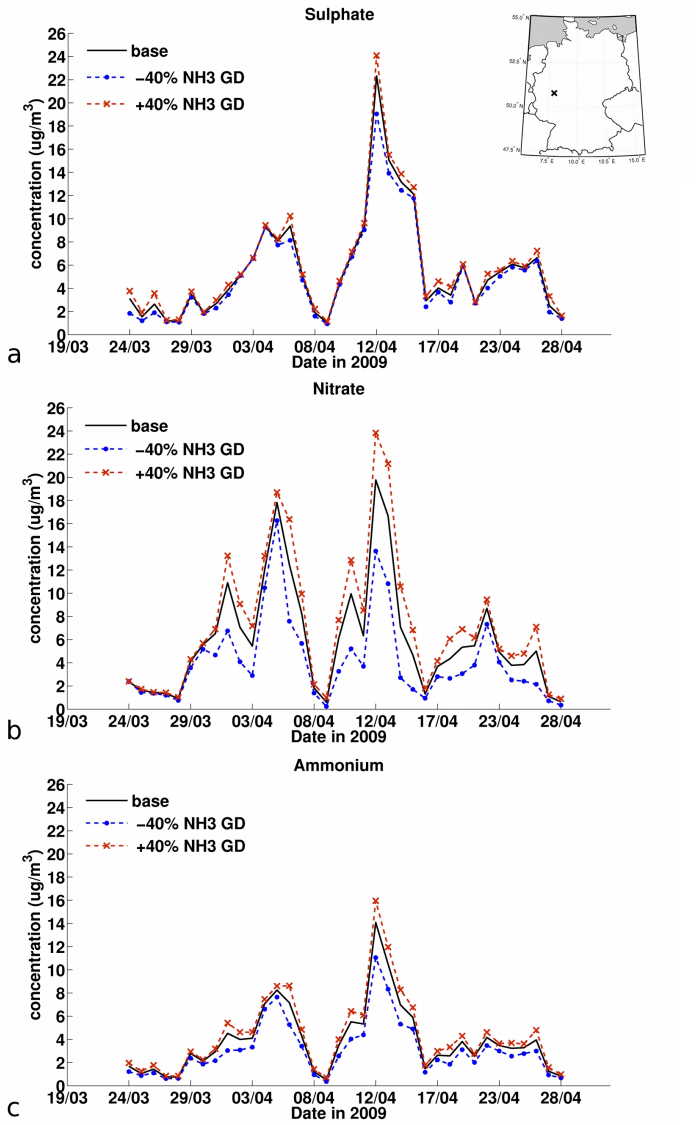

Figure 4.9 Daily mean (a) sulfate, (b) nitrate and (c) ammonium concentration at station Westerwald-Herdorf for different ammonia emission scenario runs.

ammonia affects droplet pH and consequently the rate of sulfate formation. Also, changes in ammonia emissions affect the availability of "free ammonia" and therewith affect the amount of ammonium-nitrate formation. The comparison of Fig. 4.9a and b shows that changes in ammonia emissions affect nitrate concentrations to a higher extent than sulfate concentrations. Relative to the base run, nitrate concentrations increase by up to 42% for the +40% $NH_{3\,GD}$ run and decrease by up to 60 % for the −40% $NH_{3\,GD}$ run during the PM_{10} episodes.

The sensitivity of SIA concentrations to ammonia emission changes for the German domain (GD) scenario runs is small on 4 and 5 April, but much larger on 12 and 13 April. These different sensitivities illustrate the importance of transport for the first episode and

the local built up for the second episode. The non-linearity observed in the responses is further addressed below.

4.4.3.2 Reduction scenarios

The impact of 3 different emission reduction scenarios for 2 domains (GD and ED) on the mean modelled SIA concentration and total deposition flux in the German domain is presented in Fig. 4.10. Concentrations and deposition fluxes are averaged over the investigation period from 24 March to 28 April. The change in average SIA concentration and deposition fluxes compared to the base run refers to averages over the German domain. The corresponding relative changes in concentration and deposition flux are presented in Tables 4.5 and 4.6, respectively. Figure 4.10a and b shows the results for emission reductions in the German domain and Fig. 4.10c and d shows the results for emission reductions in the European domain. The plots on the left-hand side show the SIA concentrations and the plots on the right-hand side the total deposition fluxes.

GD emission reduction impact on SIA concentrations and total deposition fluxes

Figure 4.10a shows that the air concentrations of particulate sulfate, nitrate and ammonium decrease for all performed emission reduction scenario runs compared to the base run. The mean SIA concentrations are reduced by $-4.6\,\%$, $-12.6\,\%$ and $-15.8\,\%$ within the -NO_x-$SO_{2\,GD}$, -$NH_{3\,GD}$ and -NH_3-NO_x-$SO_{2\,GD}$ scenario run, respectively. This indicates a non-linear behaviour considering the corresponding precursor reductions. Sulfate concentrations are reduced by $-0.26\ \mu g\ m^{-3}$ ($-5.7\,\%$) and $-0.27\ \mu g\ m^{-3}$ ($-5.9\,\%$), within the -NO_x-$SO_{2\,GD}$ and the -$NH_{3\,GD}$ scenario run, respectively. The -NH_3-NO_x-$SO_{2\,GD}$ scenario run leads to a reduction of $-0.48\ \mu g\ m^{-3}$ ($-10.5\,\%$) in sulfate concentrations. This is less reduction in sulfate concentrations than the sum of sulfate concentration reductions of the scenario runs -NO_x-$SO_{2\,GD}$ and -$NH_{3\,GD}$. Nitrate is only slightly reduced within the –NO_x-$SO_{2\,GD}$ scenario run ($-0.19\ \mu g\ m^{-3}$) but is significantly reduced within the -$NH_{3\,GD}$ scenario run ($-0.91\ \mu g\ m^{-3}$). With a reduction of $-1.0\ \mu g\ m^{-3}$ the reduction in nitrate concentrations within the -NH_3-NO_x-$SO_{2\,GD}$ scenario run is also less than the sum of nitrate concentration reductions of the scenario runs -NO_x-$SO_{2\,GD}$ and -$NH_{3\,GD}$. The latter non-linearity can also be observed for ammonium concentrations, with reductions of $-0.14\ \mu g\ m^{-3}$, $-0.41\ \mu g\ m^{-3}$ and $0.50\ \mu g\ m^{-3}$ for the -NO_x-$SO_{2\,GD}$, -$NH_{3\,GD}$ and -NH_3-NO_x-$SO_{2\,GD}$, respectively.

Figure 4.10b shows that other than for SIA concentrations, the reduction scenario runs do not only result in reductions in deposition fluxes. Reduced nitrogen dry deposition fluxes

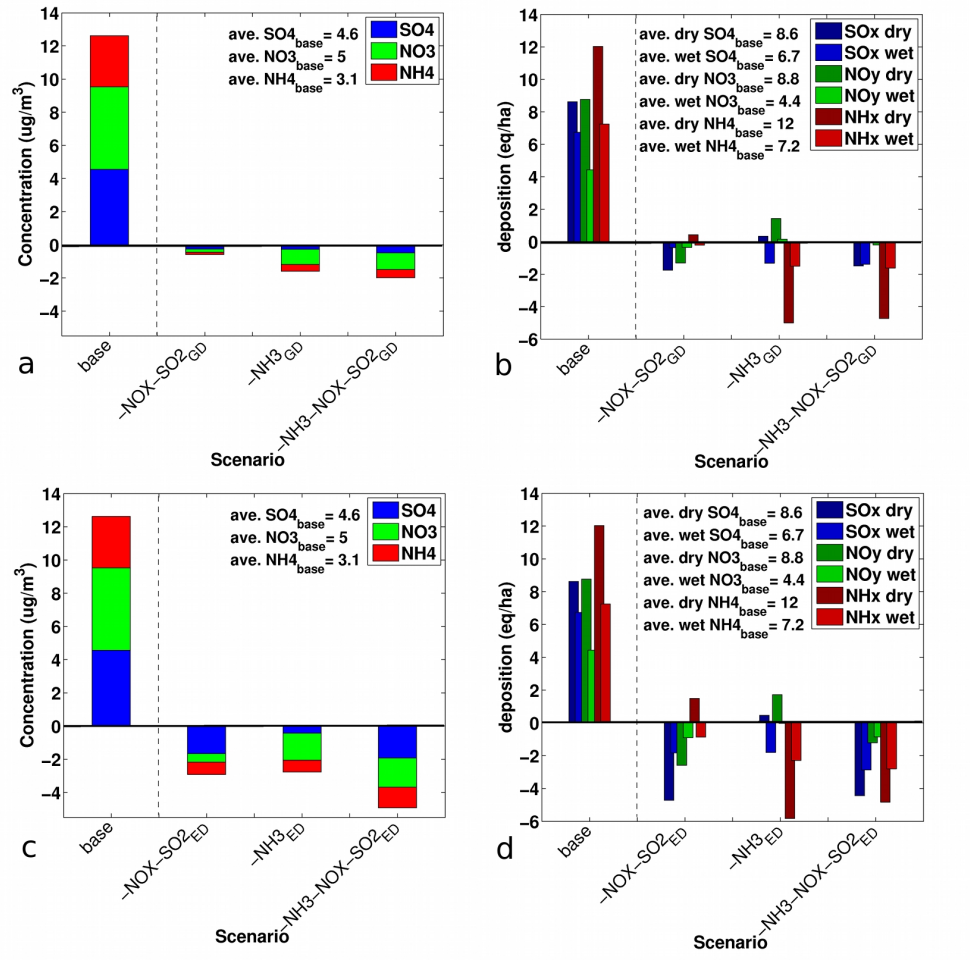

Figure 4.10 Mean modelled (a) SIA concentration and (b) total deposition flux of the base run to the left of the dashed line and mean change in (a) SIA concentration and (b) total deposition flux for different emission scenario runs to the right of the dashed line. (a, b) show results for scenario runs on the German domain excluding the boundary conditions and (c, d) those on the German domain including the boundary conditions. The mean refers to the average over the investigation period from 24 March to 28 April.

are slightly increased compared to the base run when NO_x and SO_2 emissions are reduced. Due to the reduction of SO_2 and NO_x, less ammonia is consumed for the neutralisation of nitrate and sulfate leading to a higher concentration, lower transport distances and thus higher deposition within the country. A similar effect is observed for oxidised nitrogen deposition when ammonia emissions are reduced. Within the -$NH_{3\,GD}$ scenario run the total deposition of oxidised nitrogen is increased by 11.9 %.

For the same scenario run, the reduced nitrogen total deposition is decreased by −33.8 %. The NH_3 emission reductions cause a decrease in ammonium nitrate formation, which leads to higher HNO_3 air concentrations and therewith to higher total deposition fluxes of oxidised nitrogen. As the deposition velocity of HNO_3 is high, HNO_3 dry deposition

Table 4.5 Relative change in concentration compared to the base run for total SIA, SO_4^{2-}, NO_3^- and NH_4^+ for the German domain emission scenario runs and the European domain emission scenario runs.

Scenario run	Change in concentration on GD (%)				Change in concentration on ED (%)			
	SIA	SO_4	NO_3	NH_4	SIA	SO_4	NO_3	NH_4
-NO_x-SO_2	−4.6	−5.7	−3.8	−4.5	−23.1	−36.4	−10.2	−22.5
−NH_3	−12.6	−5.9	−18.3	−13.2	−21.9	−9.4	−32.7	−22.9
-NH_3-NO_x-SO_2	−15.8	−10.5	−20.2	−16.1	−39.1	−42.2	−35.3	−40.0

fluxes increase. As the decrease in reduced nitrogen is larger than the increase in oxidised nitrogen, the total N deposition is still reduced for the –$NH_{3\,GD}$ scenario run by −15.2 % while total deposition of S is reduced by −6.5 %. For the –NH_3-NO_x-$SO_{2\,GD}$ scenario run all components' wet and dry deposition fluxes are reduced (total deposition of S by −18.9 % and N by −20.3 %). For the -NO_x-$SO_{2\,GD}$ scenario run the reduction of total S deposition amounts to −13.9 % and that of total N deposition to −4.4 %. Comparing the resultant deposition fluxes of the scenario runs -NO_x-$SO_{2\,GD}$ and -$NH_{3\,GD}$ to those of scenario run –NH_3-NO_x-$SO_{2\,GD}$ shows that S and N deposition fluxes react more linearly on the emission changes than the SIA concentrations.

Table 4.6 Relative change in deposition of S and N compared to the base run for the German domain scenario runs and the European domain scenario runs.

Scenario run	Change in deposition on GD (%)		Change in deposition on ED (%)	
	S	N	S	N
-NO_x-SO_2	−13.9	−4.4	−42.6	−8.8
-NH_3	−6.5	−15.2	−8.7	−19.8
-NH_3-NO_x-SO_2	−18.9	−20.3	−47.5	−29.9

German domain vs. European domain emission reductions

Figure 4.10c and d shows the change in average German domain SIA concentrations and deposition fluxes resulting from the model runs for the different emission scenarios on the European domain. Concentrations of SIA are reduced by −23.1 %, −21.9 % and −39.1 % for the -NO_x-$SO_{2\,ED}$, -$NH_{3\,ED}$ and -NH_3-NO_x-$SO_{2\,ED}$ scenario run, respectively. The reduction in sulfate concentrations within the German domain changes significantly from GD to ED scenario run. The -NH_3-NO_x-$SO_{2\,ED}$ scenario run is less effective in reducing SIA concentrations than the results of the scenario runs -NO_x-$SO_{2\,ED}$ and -$NH_{3\,ED}$ would suggest if linearity were assumed. The deviation from linearity is larger for the ED runs than for the GD runs in Fig. 4.10a. Among all reduction scenario runs the -$NH_{3\,GD/ED}$ scenario runs show the least relative and absolute differences between GD and ED simulations.

The latter is also valid for the deposition fluxes. The -$NH_{3\,GD/ED}$ scenario runs show the least differences between the GD and ED runs. The deviation from linearity is larger for the ED runs than for the GD runs. For the deposition fluxes the change in S compounds is most significant between GD and ED scenario runs. The total S deposition is reduced by $-42.6\,\%$, $-8.7\,\%$ and $-47.5\,\%$ and the total N deposition by $-8.8\,\%$, $-19.8\,\%$ and $-29.9\,\%$ for the -NO_x-$SO_{2\,ED}$, -$NH_{3\,ED}$ and -NH_3-NO_x-$SO_{2\,ED}$ scenario runs, respectively.

4.4.3.3 Response to ammonia emission changes

Following the findings of Sect. 4.4.3.2 the response of SIA concentrations and S and N deposition fluxes to ammonia emission changes has been further investigated. The applied emission scenarios are summarised in Table 4.3.

Figure 4.11a shows base case average SIA concentration of the investigation period. Average SIA concentrations were highest in and around the Ruhr area. Figure 4.11b and c shows the absolute and relative SIA reduction compared to the base case when reducing NH_3 by $40\,\%$ on the German domain. The highest absolute reduction of average SIA concentrations of more than 3 μg m^{-3} is achieved south of the Ruhr area where average SIA concentrations were high. The highest relative reduction amounts up to $22\,\%$ in the southwestern part of the domain. The comparison of absolute and relative SIA reduction to the NH_3 emission map in Fig. 4.1c clearly shows that the NH_3 measure leads to highest SIA reduction in areas with moderate and low NH_3 emission densities. In ammonia-rich areas in northwestern and southeastern Germany the reduction is less distinct, however, it still amounts to more than $10\,\%$.

In Fig. 4.12a, the change in average modelled SIA concentration within the German domain is plotted against the stepwise change in the NH_3 emissions using modelled droplet pH (solid line) and a constant pH of 5.5 (dashed line). A polynomial curve was fitted through the data. The response of SIA concentrations on NH_3 emission changes is non-linear. The larger the reduction of the NH_3 emissions gets, the more effective the reductions in the SIA concentrations are. Compared to the base run, the change in average modelled SIA concentration amounts -2.7 μg m^{-3} for the $-60\,\%$ NH_3 run when applying a modelled droplet pH. When a constant pH of 5.5 is used, a decrease in the mean modelled SIA concentration of -2.3 μg m^{-3} is obtained. Hence, using a modelled droplet pH, the model simulates NH_3 emission reductions to be about $20\,\%$ more effective in reducing SIA concentrations than when using a constant pH. A reduction of NH_3 emissions leads to reduced neutralisation of cloud acidity and consequently to less sulfate production, which is not accounted for using a constant droplet pH. The impact of the consideration of droplet pH on model results has been extensively described in an earlier publication (Banzhaf et al., 2012). It was found that modelled droplet pH ranges between 3 and 8.

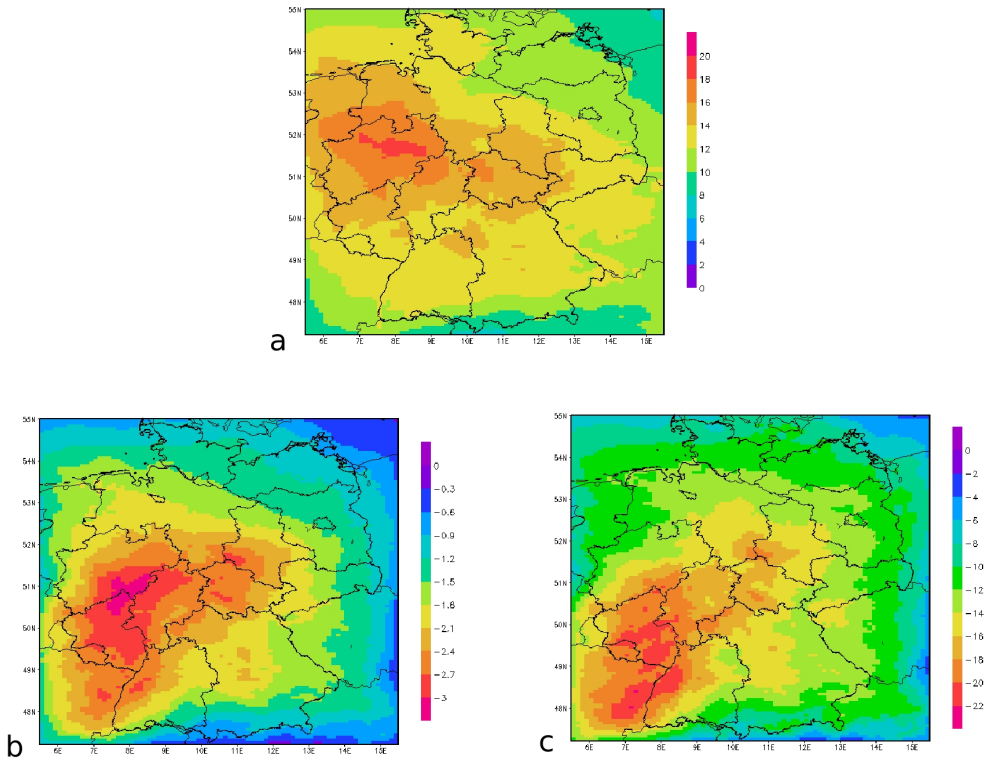

Figure 4.11 (a) Base case mean SIA concentration(μg m^{-3}) of the investigation period and (b) absolute and (c) relative SIA reduction by means of the $-40\,\%NH_3$ GD scenario run compared to the base case.

While the oxidation of dissolved SO_2 by H_2O_2 is independent of pH, the oxidation pathway via ozone is highly dependent on droplet pH (Seinfeld and Pandis, 1998). For pH values higher than 5 the reaction rate of the ozone oxidation pathway reaches the same order as that of the H_2O_2 oxidation pathway and exceeds the latter for pH values higher than ∼5.7. Hence, for pH values higher than 5 sulfate formation increases considerably with increasing droplet pH. Hence, the assumed constant droplet pH described only the low pH cases correctly.

Figure 4.12b shows the average total SO_x, NO_y and NH_x deposition within the German domain. The response of SO_x, NO_y and NH_x total deposition fluxes on ammonia emission changes is non-linear, similar as with the SIA concentrations. Only marginal changes in total SO_x deposition occur when ammonia emissions are varied and a constant droplet pH is used. Applying a modelled droplet pH, total SO_x deposition varies with varying ammonia emissions. As for the sulfate concentrations, the reason is the missing feedback between ammonia concentrations and droplet pH. NO_y total deposition shows no dependency on droplet pH. However, ammonia emission reductions result in an increase of the total NO_y deposition. Ammonia emission reduction leads to less ammonium–nitrate

formation and hence to higher HNO_3 concentrations. The latter results in a significant increase of HNO_3 dry deposition, which increases NO_y deposition fluxes. Reducing ammonia emissions leads to a decrease of the total NH_x deposition flux and vice versa for increased ammonia emissions. Reductions of the total NH_x deposition flux are larger for the model runs using a constant pH than for the model runs using a modelled droplet pH. This is because a decrease in ammonia emissions leads to a decrease of the droplet pH. Hence, ammonia is wet scavenged more effectively and the decrease in NH_x deposition is less effective.

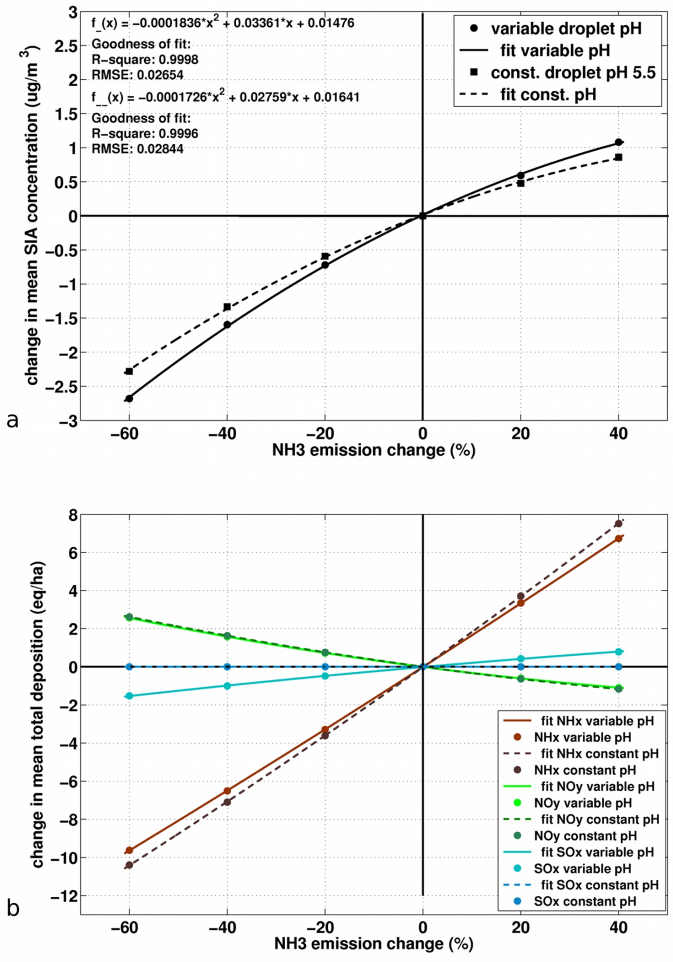

Figure 4.12 Response of (a) the mean modelled SIA concentration and (b) the mean modelled SO_x, NO_y and NH_x total deposition in the German domain to ammonia emission changes using a variable (solid line) or constant (dashed line) droplet pH.

4.5 Discussion and conclusions

In this study the response of modelled SIA concentrations to changes in precursor gas emissions during two high PM episodes over central Europe in spring 2009 has been investigated. The applied CTM, i.e. RCG, performed well in capturing the temporal variation of the PM_{10} and SIA concentrations. The model was successfully used to analyse the origin, development and characteristics of the investigated episodes.

The two SIA episodes were of different origin. For the first episode SIA was mainly formed outside the German domain. Hence, changes in ammonia emissions within the German domain did not impact SIA concentrations in Germany as severely as changes on the European domain. Within the second episode the sensitivity of SIA concentrations to changes in ammonia emissions in the German domain indicated that the high SIA concentrations originated from local sources within the German domain. The response of modelled SIA concentrations and connected deposition fluxes to precursor emission changes was non-linear. The response was found to be more linear for total deposition fluxes of sulfur and nitrogen than for SIA concentrations. Our knowledge on the constituents' non-linear relationships and interactions needs to be further improved and ideally implemented in our models. The latter is fundamental in order to be able to assist policy-makers to develop sustainable mitigation strategies and adapt the latter to seasonal and spatial variations in the emission pattern (West et al., 1999; Tsimpidi et al., 2007). Hence, models with linearised chemistry (e.g. OPS (Operational Priority Substances) model; Van Jaarsveld, 2004) are not suitable for this purpose.

The impact of national measures compared to European-wide mitigation efforts has been studied by means of several reduction scenarios with decreased emissions within the German domain only or within the European domain. Important source areas are located upwind of Germany and long range transport adds a significant fraction to the locally formed SIA. Therefore, decreasing emissions on the European domain (ED scenario runs) is more effective for all performed emission scenarios in reducing SIA concentration and total deposition fluxes than reducing emissions on the German domain (GD scenario runs). The difference between GD and ED scenario runs is more severe for pollutants that are affected to a large extent by long-range transport as e.g. SO_2. This outcome confirms that a European-wide mitigation strategy is essential to achieve substantial pollutant concentration reductions.

As NH_3 is more local than SO_2 and NO_x the effectiveness of NH_3 emission reduction shows the least difference between GD and ED scenario runs. Sulfate and nitrate concentrations are only slightly reduced when reducing emissions of SO_2 and NO_x simultaneously on the German domain. Although SO_2 German domain emissions are reduced by 50 % the

resultant sulfate reduction is slightly less than the reduction in sulfate when NH_3 emissions are reduced by 40 %. The latter reduction in sulfate concentrations results solely from a reduced neutralisation of cloud acidity. Moreover, the simultaneous NO_x and SO_2 emission reductions lead to increased OH levels, which counteract the sulfate reduction as the rate of homogeneous oxidation of SO_2 is increased (Tarrasón et al., 2003; Derwent et al., 2009). On average aqueous-phase formation is responsible for more than half of ambient atmospheric sulfate (Karamachandani and Venkatram, 1992; McHenry and Dennis, 1994). Locally, in the presence of clouds aqueous-phase sulfate production dominates over gas-phase sulfate formation while for sunny cloud-free conditions gas-phase sulfate formation is the dominant sulfate formation pathway. Additionally, the NO_x reduction is partly compensated by an increase in ammonium-nitrate due to the SO_2 emission reduction. Furthermore, the increase in OH levels also reduces the nitrate response as it leads to an increased conversion of NO_x to HNO_3 counteracting for the decrease in NO_x (Fagerli and Aas, 2008). In contrast, nitrate is significantly reduced as soon as NH_3 emissions are reduced. The results demonstrate that national NH_3 measures in addition to EU-wide efforts in Germany are more effective to reduce SIA concentrations and deposition fluxes than additional national measures on SO_2 and NO_x.

The potential of control strategies concerning SIA and PM reduction is strongly connected to the specific emission regime of the investigated region. We have found that NH_3 measures lead to highest SIA reduction in areas with moderate and low NH_3 emission densities. In these regions SIA formation is limited by the availability of NH_3 while in ammonia-rich areas SIA formation is limited by HNO_3. Following a reduction of NH_3 in these HNO_3-limited regimes a sufficient amount of NH_3 remains to neutralize the available HNO_3.

The non-linear response in the emission-concentrations and the emission-deposition relationship has been subject of several investigations over Europe in the past two decades. Pay et al. (2012) suggested that control strategies concerning SIA in northwestern Europe should focus on reductions of SO_2 and NO_x emissions. However, the conclusion was drawn based on the analysis of the indicators "free ammonia" (TNH_3 - $2SO_4^{2-}$; with TNH_3 and SO_4^{2-} as concentrations in μg m^{-3}), "S-ratio" ($SO_2/(SO_2+SO_4^{2-})$; with SO_2 and SO_4^{2-} as concentrations in μg m^{-3}) (Hass et al., 2003) and "G-ratio" ((TNH_3 - $2\,SO_4^{2-}$)/TNO_3; with TNH_3, SO_4^{2-} and TNO_3 as concentrations in μg m^{-3}) (Ansari and Pandis, 1998). These indicators do not include all sensitivities, e.g. OH interactions, which contribute to non-linearities in the sulfur and oxidised nitrogen budget (Tarrasón et al., 2003; Derwent et al., 2009). However, our findings are in line with earlier studies for different European regions (e.g. Tarrasón et al., 2003; Derwent et al., 2009; Erisman and Schaap, 2004; Builtjes et al., 2010) showing that NH_3 emission reduction measures maintain a high reduction

potential for SIA and therewith PM_{10} concentrations. The response of SIA concentrations on NH_3 emission changes was found to be non-linear with an increasing SIA reduction effectiveness with increasing reduction of NH_3 emissions. The latter was also found in the German PAREST project in which model runs for different scenarios were performed on an annual basis for the year 2005 (Builtjes et al., 2010). Tarrasón et al. (2003) performed model runs for emission scenarios reducing German emissions of NO_x ($-25\,\%$) and NH_3 ($-25\,\%$) separately for the year 2000 using the EMEP model. The maximum reduction in annual mean SIA concentration following the $-25\,\%$ NH_3 emission reduction was about 1 μg m^{-3}. Considering that SIA concentrations peak in springtime, this is in good agreement with the maximum reduction in mean SIA concentrations (not shown here) of 1.3 μg m^{-3} for the $-20\,\%$ NH_3 emission scenario run in the investigation presented here. In addition to the SIA reduction stated by former studies, this study accounted for an additional sulfate reduction. When NH_3 emissions are decreased, sulfate is reduced due to a reduced neutralisation of cloud acidity through the variable droplet pH approach (Banzhaf et al., 2012) as suggested by Redington et al. (2009). The incorporation of the explicit cloud chemistry adds more non-linearity to the system. All SIA components are sensitive to ammonia emission changes when using a modelled droplet pH, while the change in SIA concentrations results solely from changes in nitrate and ammonium concentrations when assuming a constant droplet pH.

Although RCG simulates the temporal development of the PM episodes well, some shortcomings of the model have been identified. The model was not able to capture the PM_{10} peaks, which is partly due to missing components in the modelled PM budget. In contrast, low PM_{10} levels are simulated too high. As the latter is not the case for the overall SIA concentrations, the reason for overestimation likely originates from the primary fraction. It was found that this overestimation is connected to high levels of wind blown dust for high wind speed conditions. As high PM levels during the investigation period occur at low wind speeds, high concentrations of wind blown dust do not occur during these episodes. The slight overestimation of sulfate concentrations can be partly attributed to an overestimation of modelled droplet pH leading to a too high rate of sulfate formation. Next to the buffering by carbon dioxide the effects of other buffering systems such as sea salt, mineral dust and organic components (Deguillaume et al., 2009) are not accounted for when modelling droplet pH (Banzhaf et al., 2012). In contrast to the sulfate concentrations, the nitrate concentrations are underestimated by RCG. This is partly connected to the overestimation of sulfate, which leads to a lower rate of ammonium-nitrate formation. Furthermore, evaluations of the applied equilibrium module ISORROPIA (Nenes et al., 1999) have indicated diverse shortcomings within the approach concerning the equilibrium between nitric acid and particulate ammonium nitrate (e.g. Schaap et al., 2011; Morino

et al., 2006; Fisseha et al., 2006). The uncertainty in ammonia emission inventories in space and time (Geels et al., 2012) leads to an additional uncertainty in the modelled nitric acid-ammonium nitrate-equilibrium and the overall modelled SIA formation. Next to the uncertainty in space and time according to EMEP (2009) the uncertainty in magnitude of absolute annual ammonia emission values amounts about $\pm 30\,\%$ in Europe. As non-linearities are to a large extent controlled by ammonia, the uncertainty in ammonia emissions severely impacts the modelled SIA budget. Also the correlations for the precursor gases SO_2 and NO_2 in air are encouraging as they show the ability of the model to capture the temporal variability of the analysed species concentrations. However, RCG tends to overestimate SO_2 concentrations, while NO_2 concentrations tend to be underestimated. As former studies have shown primary pollutants – like SO_2 and NO_2 (which can be considered as almost primary pollutant as it is formed rapidly from emitted NO) – are more difficult to model (Vautard et al., 2009). The evaluation of modelled SO_x, NO_y and NH_x wet deposition fluxes indicated a good model performance with correlation coefficients between 0.74 and 0.82. The improvement of the spatial representation of precipitation of the meteorological driver may lead to a better representation of modelled wet deposition fluxes.

To further improve the performance of RCG, several options are identified: (1) inclusion of coarse nitrate from the reaction of HNO_3 with soil and sea-salt particles (Pakkanen, 1996), (2) accounting for the co-deposition of SO_2 and NH_3 (Flechard et al., 1999) within the deposition routine, and (3) incorporation of the compensation point in the RCG dry deposition scheme (Wichink Kruit et al., 2010). The implementation of these processes may add further interdependencies and non-linear responses. The resultant variations in the response to emission changes need to be identified and understood. Therefore, a future study should expand the investigation period to several years/springs to better differentiate between episodes and non-episodes. In addition, a dynamic evaluation should be performed to investigate the ability of the model to correctly respond to emission changes. We are currently investigating the model performance for the 20 year period from 1990 to 2009 for this purpose.

This study confirmed the important role of NH_3 when considering reductions of SIA concentrations and deposition fluxes of sulfur and nitrogen compounds. The NEC Directive and the Gothenburg protocol provide national emission ceilings for SO_2, NO_x, NH_3 and VOC. Following the latest current legislation baseline, according to Amann et al. (2012), SO_2 and NO_x emissions will decrease significantly from 2010–2030 in the EU-27 (SO_2: $\sim$ -70 %; NO_x: $\sim$ -65 %) and Germany (SO_2: $\sim$ -45 %; NO_x: $\sim$ -65 %) compared to 2005 emissions. NH_3 emissions are expected to increase for the EU-27 ($\sim$ +2 %) and for Germany ($\sim$ +11 %). However, results of a "maximum technically feasible reduction"

(MTFR) scenario show that available measures could reduce NH_3 emissions significantly for the EU-27 ($\sim$ -30 %) and Germany ($\sim$ -35 %) compared to the current legislation baseline. The latter reveals that the NH_3 reduction potential is not fully utilised yet. EU ammonia emission targets for 2010 and 2020 given by the NEC Directive and the Gothenburg protocol are not stringent enough and do not force the European member states policy to act on ammonia emission reduction. Next to the reduction potential the cost-effectiveness of measures needs to be considered. In Europe, costs for air pollution control including the costs for the current legislation baseline are significantly lower in the agricultural sector (which includes $\sim$95 % of the total NH_3 emissions) than in other sectors, where stringent emission control is already in force (Amann et al., 2011, 2012; Appelhans et al., 2012; Builtjes et al., 2010). Future negotiations for further emission reductions over Europe should focus on further implementation of sustainable and cost-effective NH_3 measures.

Acknowledgements

This work was funded by TNO within the framework of the R&D Project 3710 63 246 –"PINETI" (Pollutant Input and Ecosystem Impact) – funded by the Federal Environment Agency (Umweltbundesamt, Germany). We thank the Federal Environment Agency (Germany), the RIVM (The Netherlands) and the EEA for providing the comprehensive measurement data and the German Weather Service (DWD) for providing COSMO-EU data. Further support was provided by Freie Universität Berlin.

Edited by: B. Ervens

References

Amann, M., Bertok, I., Borken-Kleefeld, J., Cofala, J., Heyes, C., Höglund-Isaksson, L., Klimont, Z., Rafaj, P., Schöpp, W., and Wagner, F.: Cost-effective Emission Reductions to Improve Air Quality in Europe in 2020. Analysis of Policy Options for the EU for the Revision of the Gothenburg Protocol. NEC Scenario Analysis Report #8. International Institute for Applied Systems Analysis (IIASA), Laxenburg, Austria, 2011.

Amann, M., Borken-Kleefeld, J., Cofala, J., Heyes, C., Klimont, Z., Rafaj, P., Purohit, P., Schöpp, W., and Winiwarter, W.: Future Emissions of Air Pollutants in Europe – Current Legislation Baseline and the Scope for Further Reductions. TSAP Report No 1. International Institute for Applied Systems Analysis (IIASA), Laxenburg, Austria, 2012.

Ansari, A. S. and Pandis, S. N.: Responce of inorganic PM to precursor concentrations, Environ. Sci. Technol., 32, 2706–2714, 1998.

Appelhans, J., Builtjes, P., Jörß, W., Stern, R., and Theloke, J.: Exploring strategies to reduce particle concentrations- Results of the research project PAREST, Immissionsschutz 1–12, Erich Schmitt-Verlag Berlin, ISSN1430-9262, 2012.

Asman, W. A. H.: Modelling the atmospheric transport and deposition of ammonia and ammonium: an overview with special reference to Denmark, Atmos. Environ., 35, 1969-1983, 2001.

Banzhaf, S., Schaap, M., Kerschbaumer, A., Reimer, E., Stern, R., van der Swaluw, E., and Builtjes, P.: Implementation and evaluation of pH-dependent cloud chemistry and wet deposition in the chemical transport model REM-Calgrid, Atmos. Environ., 49, 378–390, 2012.

Beekmann, M., Kerschbaumer, A., Reimer, E., Stern, R., and Möller, D.: PM measurement campaign HOVERT in the Greater Berlin area: model evaluation with chemically specified particulate matter observations for a one year period, Atmos. Chem. Phys., 7, 55–68, doi10.5194/acp-7-55-2007, 2007.

Bobbink, R., Hornung, M., and Roelofs, J. M.: The effects of airborne pollutants on species diversity in natural and semi-natural European vegetation, J. Ecol., 86, 717–738, doi10.1046/j.1365-2745.1998.8650717.x, 1998.

Builtjes, P., Jörß, W., Stern, R., and Theloke, J.: Strategien zur Verminderung der Feinstaubbelastung. PAREST-Summary report, FKZ 206 43 200/01. UBA-Texte Nr. 09/2012. 2012 Umweltbundesamt, www.umweltbundesamt.de (last access: May 2013), 2010.

Carter, W. P. L.: Condensed atmospheric photooxidation mechanisms for isoprene. Atmos. Environ., 24, 4275–4290, 1996.

Claiborn, C., Lamb, B., Miller, A., Beseda, J., Clode, B., Vaughan, J., Kang, L., amd Newvine, C.: Regional measurements and modeling of windblown agricultural dust: The Columbia Plateau PM_{10} Program, J. Geophys. Res., 103, 19753–19767, 1998.

Deguillaume, L., Tilgner, A., Schrödner, R., Wolke, R., Chaumerliac, N., and Herrmann, H.: Towards an operational aqueous phase chemistry mechanism for regional chemistry-transport models: CAPRAM-RED and its application to the COSMO-MUSCAT model. J. Atmos. Chem., 64, 1–35, 2009.

de Meij, A., Thunis, P., Bessagnet, B., and Cuvelier, C.: The sensitivity of the CHIMERE model to emissions reduction scenarios on air quality in Northern Italy, Atmos. Environ., 43, 1897–1907, 2009.

Demuzere, M., Trigo, R. M., Vila-Guerau de Arellano, J., and van Lipzig, N. P. M.: The impact of weather and atmospheric circulation on O_3 and PM_{10} levels at a rural mid-latitude site, Atmos. Chem. Phys., 9, 2695–2714, doi10.5194/acp-9-2695-2009, 2009.

Denier van der Gon, H. A. C., Visschedijk, A., van den Brugh, H., and Dröge, R.: F&E Vorhaben: Strategien zur Verminderung der Feinstaubbelastung – PAREST: A high resolution European emission data base for the year 2005, TNO-Report, TNO-034-UT-2010-01895_RPT-ML, Utrecht, 2010.

Derwent, R. G., Witham, C. J., Redington, A. L., Jenkin, M., Stedman, J, Yardley, R., and Hayman, G.: Particulate matter at a rural location in southern England during 2006: model sensitivities to precursor emissions. Atmos. Environ., 43, 689–696, 2009.

EEA: Air quality in Europe – 2012 report. EEA Report No 4/2012. ISBN:978-92-9213-328-3. European Environment Agency (EEA), Copenhagen, Denmark, 2012.

EMEP: Transboundary, acidification, eutrophication and ground level ozone in Europe in 2007 EMEP August 2009, ISSN 1504-6192, 2009.

Erisman, J. W. and Schaap, M.: The need for ammonia abatement with respect to secondary PM reductions in Europe. Environ. Pollut., 129, 159–163, 2004.

Erisman, J. W., van Pul, A., and Wyers, P.: Parametrization of surface-resistance for the quantification of atmospheric deposition of acidifying pollutants and ozone. Atmos. Environ., 28, 2595–2607, 1994.

Erisman, J. W., Grennfelt, P., and Sutton, M.: The European perspective on nitrogen emission and deposition. Environ. Int., 29, 311–325, 2003.

European Commission: European Commission. Directive 2008/50/EC of the European Parliament and of the Council of 21 May 2008 on ambient air quality and cleaner air for Europe. Technical Report 2008/50/EC, L152, Off. J. Eur. Commun, 2008.

Fagerli, H. and Aas, W.: Trends of nitrogen in air and precipitation: Model results and observations at EMEP sites in Europe, 1980–2003, Environ. Pollut., 154, 448–461, 2008.

Fisseha, R., Dommen, J., Gutzwiller, L., Weingartner, E., Gysel, M., Emmenegger, C., Kalberer, M., and Baltensperger, U.: Seasonal and diurnal characteristics of water soluble inorganic compounds in the gas and aerosol phase in the Zurich area, Atmos. Chem. Phys., 6, 1895–1904, doi10.5194/acp-6-1895-2006,

2006.

Flechard, C. R., Fowler, D., Sutton, M. A., and Cape, J. N.: A dynamic chemical model of bi-directional ammonia exchange between semi-natural vegetation and the atmosphere, Q. J. Roy. Meteor. Soc., 125, 2611–2641, 1999.

Fountoukis, C. and Nenes, A.: ISORROPIA II: a computationally efficient thermodynamic equilibrium model for K^+,Ca^{2+},Mg^{2+},NH_4^+,Na^+,SO_4^{2-},NO_3^-,Cl^-, H_2O aerosols, Atmos. Chem. Phys., 7, 4639–4659, doi10.5194/acp-7-4639-2007, 2007.

Fowler, D., Sutton, M., Flechard, C., Cape, J. N., Storeton-West, R. L., Coyle, M., and Smith, R. I.: The Control of SO_2 Dry Deposition on to Natural Surfaces by NH_3 and its Effects on Regional Deposition, Water Air Soil Poll., Focus, 1, 39–48, 2001.

Fowler, D., Müller, J., Smith, R. I., Cape, J. N., and Erisman, J. W.: Nonlinearities in source-receptor relationships for sulfur and nitrogen compounds, Ambio., 34, 41–46, 2005.

Fowler, D., Smith, R., Müller, J., Cape, J. N., Sutton, M., Erisman, J. W., and Fagerli, H.: Long-term trends in sulphur and nitrogen deposition in Europe and the cause of nonlinearities, Water Air Soil Poll., 7, 41–47, 2007.

Geels, C., Andersen, H. V., Ambelas Skjøth, C., Christensen, J. H., Ellermann, T., Løfstrøm, P., Gyldenkærne, S., Brandt, J., Hansen, K. M., Frohn, L. M., and Hertel, O.: Improved modelling of atmospheric ammonia over Denmark using the coupled modelling system DAMOS, Biogeosciences, 9, 2625–2647, doi10.5194/bg-9-2625-2012, 2012.

Gery, M. W., Whitten, G. Z., Killus, J. P., and Dodge, M. C.: A photochemical kinetics mechanism for urban and regional scale computer modeling, J. Geophys. Res., 94, 12925–12956, 1989.

Gipson, G. and Young, J.: Gas phase chemistry, Chapter 8 in: Science algorithms of the EPA models-3 community multiscale air quality (CMAQ) modeling system, Edited by: Byun, D. W. and Ching, J. K. S., Atmospheric Modeling Division National Exposure Research Laboratory US Environmental Protection Agency Research Triangle Park, NC 27711, EPA/600/R-99/030, 1999.

Gong, S. L., Barrie, L. A., and Blanchet, J.-P.: Modelling sea-salt aerosols in the atmosphere. 1. Model development. J. Geophys. Res., 102, 3805–3818, 1997.

Hass, H., van Loon, M., Kessler, C., Stern, R., Matthijsen, J., Sauter, F., Zlatev, Z., Langner, J., Foltescu, V., and Schaap, M.: Aerosol Modelling: Results and Intercomparison from 15 European Regional-scale Modelling Systems, EUROTRAC-2 Special report, Eurotrac-ISS, Garmisch Partenkirchen, Germany, 2003.

Karamachandani, P., and Venkatram, A.: The role of non-precipitating clouds in producing ambient sulfate during summer: results from simulations with the Acid Deposition and Oxidant Model (ADOM), Atmos. Environ. 26A, 1041–1052, 1992.

Kuenen, J., Denier van der Gon, H., Visschedijk, A., van der Brugh, H., and van Gijlswijk, R.: MACC European emission inventory for the years 2003–2007. TNO report, TNO-060-UT-2011-00588, Utrecht, 2011.

Lövblad, G., Tarrasón, L., Tørseth, K., and Dutchak, S.: EMEP Assessment Part I: European Perspective. Norwegian Meteorological Institute, P.O. Box 43, N-313 Oslo, Norway, 2004.

Loosmore, G. A. and Hunt, J. R.: Dust resuspension without saltation. J. Geophys. Res., 105, 20663–20671, doi10.1029/2000JD900271, 2000.

Matejko, M., Dore, A. J. Hall, J., Dore, C. J., Blas, M., Kryza, M., Smith, R., and Fowler, D.: The influence of long term trends in pollutant emissions on deposition of sulphur and nitrogen and exceedance of critical loads in the United Kingdom, Environ. Sci. Policy, 12, 882–896, 2009.

McHenry, J. N. and Dennis, R. L.: The relative importance of oxidation pathways and clouds to atmospheric ambient sulfate production as predicted by Regional Acid Deposition Model, J. Appl. Meteorol., 33, 890–905, 1994.

Morino, Y., Kondo, Y., Takegawa, N., Miyazaki, Y., Kita, K., Komazaki, Y., Fukuda, M., Miyakawa, T., Moteki, N., and Worsnop, D. R.: Partitioning of HNO_3 and particulate nitrate over Tokyo: Effect of vertical mixing, J. Geophys. Res. Atmos., 111, D15215, doi10.1029/2005JD006887, 2006.

Mues, A., Manders, A., Schaap, M., Kerschbaumer, A., Stern, R., and Builtjes, P.: Impact of the extreme meteorological conditions during the summer 2003 in Europe on particle matter concentrations – an observation and model study, Atmos. Environ., 55, 377–391, 2012.

Nenes, A., Pilinis, C., and Pandis, S.: Continued development and testing of a new thermodynamic aerosol module for urban and regional air quality models, Atmos. Environ., 33, 1553–1560, 1999.

Pakkanen, T. A.: Study of formation of coarse particle nitrate aerosol, Atmos. Environ., 30, 2475–2482, 1996.

Pay, M. T., Jiménez, P., and Baldasano, J.: Assessing sensitivity regimes of secondary inorganic aerosol formation in Europe with the CALIOPE-EU modeling system, Atmos. Environ., 51, 146–164, 2012.

Pinder, R. W., Adams, P. J., and Pandis, S. N.: Ammonia emission controls as a costeffective strategy for reducing atmospheric particulate matter in the eastern United States, Environ. Sci. Technol., 41, 380–386, 2007.

Pope, C. A.: Mortality effects of longer term exposures to fine particulate air pollution: review of recent epidemiological evidence, Inhal. Toxicol., 19 (Suppl. 1), 33–38, 2007.

Pope, C. A., Renlund, D. G., Kfoury, A. G., May, H. T., and Horne, B. D.: Relation of heart failure hospitalization to exposure to fine particulate air pollution, Am. J. Cardiol. 102, 1230–1234, 2008.

Putaud, J.-P., Raesa, F., Van Dingenen, R., Bruggemann, E., Facchini, M., Decesari, S., Fuzzi, S., Gehrig, R., Hueglin, C., Laj, P., Lorbeer, G., Maenhaut, W., Mihalopoulos, N., Mueller, K., Querol, X., Rodriguez, S., Schneider, J., Spindler, G., ten Brink, H., Tørseth, K., and Wiedensohler, A.: A European aerosol phenomenology—2:chemical characteristics of particulate matter at kerbside, urban, rural and background sites in Europe, Atmos. Environ., 38, 2579–2595, 2004.

Putaud, J.-P., Van Dingenen, R., Alastuey, A., Bauer, H., Birmili, W., Cyrys, J., Flentje, H., Fuzzi, S., Gehrig, R., Hansson, H. C., Harrison, R. M., Herrmann, H., Hitzenberger, R., Huglin, C., Jones, A. M., Kasper-Giebl, A., Kiss, G., Kousa, A., Kuhlbusch, T. A. J., Löschau, G., Maenhaut, W., Molnar, A., Moreno, T., Pekkanen, J., Perrino, C., Pitz, M., Puxbaum, H., Querol, X., Rodriguez, S., Salma, I., Schwarz, J., Smolik, J., Schneider, J., Spindler, G., ten Brink, H., Tursic, J., Viana, M., Wiedensohler, A., and Raes, F.: A European aerosol phenomenology e 3: Physical and chemical characteristics of particulate matter from 60 rural, urban, and kerbside sites across Europe, Atmos. Environ., 44, 1308–1320, 2010.

Redington, A. L., Derwent, R. G., Witham, C. S., and Manning, A. J.: Sensitivity of modelled sulphate and nitrate aerosol to cloud, pH and ammonia emissions, Atmos. Environ., 43, 20, 3227–3234, 2009.

Renner, E. and Wolke, R.: Modelling the formation and atmospheric transport of secondary inorganic aerosols with special attention to regions with high ammonia emissions. Atmos. Environ., 44, 1904-1912, 2010.

Schaap, M., Otjes, R. P., and Weijers, E. P.: Illustrating the benefit of using hourly monitoring data on secondary inorganic aerosol and its precursors for model evaluation, Atmos. Chem. Phys., 11, 11041–11053, doi10.5194/acp-11-11041-2011, 2011.

Schättler, U., Doms, G., and Schraff, C.: A description of the nonhydrostatic regional COSMO-model. Part VII: User's guide, Deutscher Wetterdienst, Offenbach, 135 pp., 2008.

Schell, B., Ackermann, I., Hass, H., Binkowski, F., and Ebel, A.: Modelling the formation of secondary organic aerosol within a comprehensive air quality model system, J. Geophys. Res., 106, 28275–28293, 2001.

Seinfeld, J. H. and Pandis, N.: Atmospheric Chemistry and Physics: From Air Pollution to Climate Change. From Air Pollution to Climate Change, John Wiley and Sons, Inc., New York, 1326 pp., 1998.

Solazzo, E., Biancini, R., Pirovano, G., Matthias, V., Vautard, R., Moran, M. D., Appel, K. W., Bessagnet, B., Brandt, J., Christensen, J. H., Chemel, C., Coll, I., Ferreira, J., Forkel, R., Francis, X. V., Grell, G., Grossi, P., Hansen, A. B., Miranda, A. I., Nopmongcol, U., Prank, M., Sartelet, K. N., Schaap, M., Silver, J. D., Sokhil, R. S., Vira, J., Werhahn, J., Wolke, R., Yarwood, G., Zhang, J., Rao, S. T., and Galmarini, S.: Operational model evaluation for particulate matter in Europe and North America in the context of AQMEII, Atmos. Environ., 53, 75–92, 2012.

Stern, R., Yamartino, R., and Graff, A.: Analyzing the response of a chemical transport model to emissions reductions utilizing various grid resolutions. In: Twenty-eighth ITM on Air Pollution Modelling and its Application, Leipzig, Germany, 15–19 May 2006, 2006.

Stern R., Builtjes, P., Schaap, M., Timmermans, R., Vautard, R., Hodzic, A., Memmesheimer, M., Feldmann, H., Renner, E., Wolke, R., and Kerschbaumer, A.: A model inter-comparison study focussing on episodes with elevated PM_{10} concentrations, Atmos. Environ., 42, 4567–4588, 2008.

Tarrasón, L., Johnson, J.E., Fagerli, H., Benedictow, A., Wind, P., Simpson, D., Klein, H.: EMEP Status Report 1/2003 – Part III: Source-Receptor Relationships, Transboundary acidification, eutrophication and ground level ozone in Europe, Norwegian Meteorological Institute, Oslo, 2003.

Thunis, P., Cuvelier, C., Roberts, P., White, L., Post, L., Tarrasón, L., Tsyro, S., Stern, R., Kerschbaumer, A., Rouil, L., Bessagnet, B., Builtjes, P., Schaap, M., Boersen, G., and Bergstroem, R.: Evaluation of a Sectoral Approach to Integrated Assessment Modelling including the Mediterranean Sea, Eurodelta II report, Joint Research Center, Ispra, Italy, 2008.

Tsimpidi, A. P., Karydis, V. A., and Pandis, S. N.: Response of inorganic fine particulate matters to emission changes of SO_2 and NH_3: the Eastern United States as a case study, J. Air Waste Manage., 57, 1489–1498, 2007.

UBA: Manual for Quality Assurance (in German), Texte 28/04, ISSN 0722-186X, Umweltbundesamt – Berlin, Fachgebiet II 5.6, 536 pp., 2004.

UBA: Auswertung der Luftbelastungssituation 2009. Fachgebiet II 4.2 Beurteilung der Luftqualität, Umweltbundesamt, Dessau-Roßlau, Germany, 2010.

van Dingenen, R., Raes, F., Putaud, J. P., Baltensperger, U., Brüggemann, E., Charron, A., Facchini, M. C., Decesari, S., Fuzzi, S., Gehrig, R., Hansson, H. C., Harrison, R. M., Hüglin, Ch., Jones, A. M., Laj, P., Lorbeer, G., Maenhaut,W., Palmgren, F., Querol, X., Rodríguez, S., Schneider, J., ten Brink, H., Tunved, P., Tørseth, K., Wehner, B., Weingartner, E., Wiedensohler, A., and Wåhlin, P. A.: European Aerosol Phenomenology I: Physical characteristics of particulate matter at kerbside, urban, rural and background sites in Europe. Atmos. Environ., 38, 2561–2577, 2004.

Van Jaarsveld, J. A.: The Operational Priority Substances model, description and validation of OPS-Pro 4.1, RIVM report 500045001/2004, Bilthoven, The Netherlands, 2004.

Vautard, R., Schaap, M., and Bergström, R.: Skill and uncertainty of a regional air quality model ensemble, Atmos. Environ., 43, 4822–4832, 2009.

Walcek, C. J.: Minor flux adjustment near mixing ratio extremes for simplified yet highly accurate monotonic calculation of tracer advection, J. Geophys. Res., 105, 9335–9348, 2000.

Weijers, E. P., Schaap, M., Nguyen, L., Matthijsen, J., Denier van der Gon, H. A. C., ten Brink, H. M., and Hoogerbrugge, R.: Anthropogenic and natural constituents in particulate matter in the Netherlands, Atmos. Chem. Phys., 11, 2281–2294, doi10.5194/acp-11-2281-2011, 2011.

West, J. J., Ansari, A. S., and Pandis, S. N.: Marginal $PM_{2.5}$: Nonlinear Aerosol Mass Response to

Sulphate Reductions in the Eastern United States, J. Air Waste Manage., 49, 1415–1424, 1999.

Wichink Kruit, R. J., Van Pul, W. A. J., Sauter, F. J., Van den Broek, M., Nemitz, E., Sutton, M. A., Krol, M., and Holtslag, A. A. M.: Modeling the surface-atmosphere exchange of ammonia, Atmos. Environ., 44, 945–957, 2010.

Chapter 5

Paper III - Dynamic model evaluation for secondary inorganic aerosol and its precursors over Europe between 1990 and 2009

S. Banzhaf (1), M. Schaap (2), R. Kranenburg (2), A. M. M. Manders (2), A. J. Segers (2), A. H. J. Visschedijk (2), H. A. C. Denier van der Gon (2), J. J. P. Kuenen (2), E. van Meijgaard (3), L. H. van Ulft (3) , J. Cofala (4) and P. J. H. Builtjes (1/2)

(1) Institut für Meteorologie, Freie Universität Berlin, Carl-Heinrich-Becker Weg 6-10, 12165 Berlin, Germany
(2) TNO, Department Climate, Air Quality and sustainability, Princetonlaan 6, 3508 TA Utrecht, The Netherlands
(3) KNMI, De Bilt, The Netherlands
(4) IIASA, Laxenburg, Austria

submitted to Geoscientific Model Development.

Abstract

In this study we present a dynamic model evaluation of the chemistry transport model (CTM) LOTOS-EUROS to analyse the ability of the model to reproduce observed non-linear responses to emission changes and interannual variability of secondary inorganic aerosol (SIA) and its precursors over Europe from 1990 to 2009. The 20 year simulation was performed using a consistent set of meteorological data provided by the regional climate model RACMO2. Observations at European rural background sites have been used as reference for the model evaluation. To ensure the consistency of the used observational data stringent selection criteria were applied including a comprehensive visual screening to remove suspicious data from the analysis. The LOTOS-EUROS model was able to capture a large part of the day-to-day, seasonal and interannual variability of SIA and its precursors' concentrations. The dynamic evaluation has shown that the model is able to simulate the declining trends observed for all considered sulphur and nitrogen components following the implementation of emission abatement strategies for SIA precursors over Europe. Both, the observations and the model show the largest part of the decline in the 1990's while smaller concentration changes and an increasing number of non-significant trends are observed and modelled between 2000-2009. Furthermore, the results confirm former studies showing that the observed trends in sulphate and total nitrate concentrations from 1990 to 2009 are significantly lower than the trends in precursor emissions and precursor concentrations. The model captured these non-linear responses to the emission changes well. Using the LOTOS-EUROS source apportionment module trends in formation efficiency of SIA have been quantified for four European regions. The exercise has revealed a 20-50% more efficient sulphate formation in 2009 compared to 1990 and an up to 20% more efficient nitrate formation per unit NO_x emission, which added to the explanation of the non-linear responses. However, we have also identified some weaknesses to the model and the input data. LOTOS-EUROS underestimates the observed NO_2 concentrations throughout the whole time period, while it overestimates the observed NO_2 concentration trends. Moreover, model results suggest that the emission information of the early 1990's used in this study needs to be improved concerning magnitude and spatial distribution.

5.1 Introduction

Atmospheric input of sulphur and nitrogen components may decrease biodiversity in vulnerable terrestrial and aquatic ecosystems through eutrophication and acidification of soils and fresh water (Bobbink et al., 1998). The major sources of sulphur and reactive nitro-

gen in the atmosphere are the emissions of sulphur dioxide, nitrogen oxides and ammonia through fossil fuel combustion and agricultural activities. Although these primary gases may themselves be removed from the atmosphere by dry deposition or rainout, they are the precursor gases for secondary inorganic aerosol (SIA). The latter provide a means for long-range transport of these components on a continental scale causing negative ecosystem impacts far away from their major source areas. In addition, SIA contributes a large portion of particulate matter concentration throughout the European domain (Putaud et al., 2010). Especially ammonium nitrate concentrations are shown to be particularly enhanced during days with PM_{10} concentrations up or above the EU daily limit value (e.g. Weijers et al., 2011). Moreover, SIA are involved in climate change by affecting the radiation balance of the earth (Forster et al., 2007). Recent studies show that short term climate mitigation aimed at reducing black carbon may be effective, provided that the climate impact of the co-emitted SIA precursors does not cause a net cooling impact (Bond et al., 2013). Hence, a thorough understanding of the SIA budget is required to inform policy makers and to devise mitigation strategies that are effective for biodiversity, climate change and human health.

To combat the adverse impacts on biodiversity and human health a series of international conventions and agreements were implemented. The Convention on Long-range Transboundary Air Pollution was adopted in 1979 and the related Gothenburg Protocol establishing emission ceilings for sulphur, NO_x, VOCs and ammonia for 2010 negotiated by the EU Member States together with Central and Eastern European countries, the United States and Canada was accepted in 1999 (UNECE, 1999). The National Emissions Ceiling Directive (NECD 2001/81/EC) was introduced in 2001 (EC, 2001) setting national emission ceilings for the EU countries for 2010 and 2020. The implemented mitigation measures have led to significant emission reductions (Grennfelt and Hov, 2005). SOx emissions have decreased by 75%, NO_x emissions by 42% and NH_3 emissions by 28% in the EEA-32 group of countries from 1990-2010 (EEA, 2012). As part of the conventions air pollution monitoring networks have been implemented over Europe providing a long-term observation facility to be able to assess the effectiveness of the implemented air quality management. Although the substantial emission reductions of SO_2, NO_x and NH_3 are largely reflected in the trends of pollutant concentrations and wet deposition fluxes, the responses were found to be non-linear (e.g. Løvblad et al., 2004; Fagerli and Aas, 2008; Tørseth et al., 2012). These studies highlighted that for SIA and its precursors the implemented emission mitigation measures did not completely meet the expected concentration reduction. Hence, understanding of the non-linear responses is important to be able to provide robust policy support.

Chemistry transport models (CTMs) are used to analyse potential emission reduction

strategies and quantify their effectiveness. Before the CTMs can be used to inform policy development they need to be evaluated. Dennis et al. (2010) introduced a comprehensive evaluation framework in which four types of model evaluation are identified: operational, diagnostic, dynamical and probabilistic evaluation. Operational model evaluations have been performed within a huge number of studies using standard statistical and graphical analysis to determine how the model results compare with observations (e.g. Appel et al., 2011, Thunis et al., 2012). Diagnostic model evaluation, focussing on the description of an individual process or component in the model has also been subject of many studies (e.g. Fahey and Pandis, 2003; Redington et al., 2009; Banzhaf et al., 2012). Recently, probabilistic or ensemble based evaluation has gained popularity as the ensemble mean of a group of models shows mostly the best model performance in comparison to observations (Vautard et al., 2007; McKeen et al., 2005). Dynamic model evaluations (=analysis of the response to emission changes/influence of meteorology) have only been performed in a few studies so far (e.g. Berglen et al., 2007).

CTMs need to be able to capture non-linear responses of the emission-concentration and emission-deposition relationship as well as interannual variability over the last 15-20 years to provide confidence in the use of CTMs for regulatory purposes (Civerolo et al., 2010). Colette et al. (2011) investigated the capability of six state-of-the-art CTMs to reproduce air quality trends and interannual variability of ozone, NO_2 and PM_{10} for the time period of 10 years from 1998-2007. They concluded that the models captured most of the important features to justify their implementation for future projections of air quality provided that enough attention is given to their underestimation of interannual variability. Fagerli and Aas (2008) found that the EMEP model's response for nitrogen in air and precipitation to emission changes over Europe from 1980-2003 is reasonable. The results indicated a lack of trends in total nitrate (TNO_3: sum of aerosol nitrate and gaseous nitric acid) concentrations despite NO_x emission reductions and it was concluded from the model simulations that this non-linear behaviour can partly be attributed to a shift in the equilibrium between nitric acid and ammonium nitrate towards particulate phase, which was caused by SO_2 emission reductions. However, the model simulations could not be performed using a consistent meteorological data set for all simulated years. Civerolo et al. (2010) performed an 18-year CMAQ simulation (1988-2005) over the north-eastern United States enabling the investigation of spatial patterns and seasonal variations, but also on long-term trends of sulphate and nitrate in the presence of emissions changes and meteorological variability. The results suggested that the modelling system largely captured the long-term trends in sulphur and nitrogen compounds. While the seasonal changes in sulphur compounds were also captured, the model did not reproduce the average seasonal variation or spatial patterns in nitrate.

Former studies suggest that the non-linear response of pollutant concentrations to emission changes can be attributed to the differing magnitude of emission reduction for the different substances (Løvblad et al., 2004; Fagerli and Aas, 2008) inducing shifts in the atmospheric chemistry and equilibrium between gas- and particulate phase, which determine the gas to particle conversion. These non-linearities have been also identified in short term modelling studies that focus on the sensitivity of SIA formation to precursor emission reductions (e.g. Banzhaf et al., 2013; Erisman and Schaap, 2004; Redington et al., 2009; Derwent et al., 2009). State of the art labelling approaches (Yarwood et al., 2007; Wagstrom et al., 2008) can be applied to track the source allocation for secondary aerosols and its precursor gases to study the response of atmospheric chemistry to emission changes. However, long-term simulations including a source apportionment have not yet been performed due to the high computational burden. Kranenburg et al. (2013) introduced a source apportionment module for the operational CTM LOTOS-EUROS, which enables long-term simulations with source attribution to investigate possible trends in the gas to particle formation efficiency that accompanied the changes in emission levels over time. We aim to evaluate the LOTOS-EUROS model for its ability to model the trends in SIA concentrations and, at the same time, investigate the non-linearity in SIA formation. In this study a model run of 20 years from 1990 to 2009 was performed with a horizontal grid resolution of 0.50° longitude × 0.25° latitude over Europe using the CTM LOTOS-EUROS (section 5.2.1.1). The model explicitly accounts for cloud chemistry and aerosol thermodynamics. The model run is based on emissions for 1990, 1995, 2000, 2005 and 2010 provided by IIASA (section 5.2.1.2) and a consistent 3 hourly meteorological data set from 1990 to 2009 obtained from the regional climate model RACMO2 (section 5.2.1.2) of the Royal Netherlands Meteorological Institute (KNMI). The modelled concentrations of SIA and its precursors are compared to observations at rural background sites (section 5.2.2). By means of an operational (section 5.3.1) and a dynamic evaluation (section 5.3.2) we identify shortcomings and limitations of the model system and input data that need to be improved or considered when using the applied set up for future emission scenarios. In order to enable the analysis of trends in gas to particle conversion and residence time of the involved species the source apportionment module of LOTOS-EUROS (section 5.2.1) has been used to trace the amount of SIA formed per unit emission of SO_2, NO_x and NH_3 for 4 different regions over Europe from 1990-2009 (section 5.3.4). The results are discussed and conclusions are drawn in section 5.4.

5.2 Methods and data

This investigation focuses on SIA (SO_4, NO_3 and NH_4) and its precursors (SO_2, NO_2 and NH_3) over the time period 1990 to 2009. Although the focus is on this 20 year long period we have also investigated the trends in concentrations for the shorter time periods 1995-2009 and 2000-2009 because emission reductions did not proceed linearly and in line with each other from 1990-2009. By considering several time periods we could assess the sensitivity of the trend to the different time periods. Furthermore, the amount of available observations increased for the later periods, which made a broader assessment of the results possible.
In the following subsections the applied model and model set-up, the used observations and the statistic tools we have used to evaluate the model and calculate and assess the observed and modelled trends are described.

5.2.1 Simulation description

5.2.1.1 Model description LOTOS-EUROS

LOTOS-EUROS (LOng Term Ozone Simulation - EURopean Operational Smog) is a 3D CTM. The off-line Eulerian grid model simulates air pollution concentrations in the lower troposphere solving the advection-diffusion equation on a regular lat-lon-grid with variable resolution over Europe (Schaap et al., 2008). In this study, model version 1.8 was used.
The vertical transport and diffusion scheme accounts for atmospheric density variations in space and time and for all vertical flux components. The vertical grid is based on terrain following vertical coordinates and extends to 3.5 km above sea level. The model uses a dynamic mixing layer approach to determine the vertical structure, i.e. the vertical layers vary in space and time. The layer on top of a 25 m surface layer follows the mixing layer height, which is obtained from the meteorological input data that is used to force the model. The height of the two reservoir layers is determined by the difference between model top at 3.5 km and mixing layer height. If the mixing layer extends near or above 3.5 km, the top of the model exceeds the 3.5 km according to the above-mentioned description. The horizontal advection of pollutants is calculated applying a monotonic advection scheme developed by Walcek et al. (2000).
Gas-phase chemistry is simulated using the TNO CBM-IV scheme, which is a condensed version of the original scheme (Whitten et al, 1980). Hydrolysis of N2O5 is explicitly described following Schaap et al. (2004). LOTOS-EUROS explicitly accounts for cloud chemistry computing sulphate formation as a function of cloud liquid water content and

cloud droplet pH as described in Banzhaf et al. (2012). For Aerosol chemistry LOTOS-EUROS features the thermodynamic equilibrium module ISORROPIA2 (Fountoukis and Nenes, 2007). Dry Deposition fluxes are calculated following a resistance approach as described in (Erisman et al, 1994). Furthermore, a compensation point approach for ammonia is included in the dry deposition module (Wichink Kruit et al., 2012). The wet deposition module is based on precipitation rates using simple scavenging coefficients for the below cloud scavenging of gases (Schaap et al, 2004) and particles (Simpson et al, 2003).
In LOTOS-EUROS, the temporal variation of the emissions is represented by monthly, day-of-the-week and hourly time factors that break down the annual totals for each source category. An included biogenic emission routine is based on detailed information on tree species over Europe (Koeble and Seufert, 2001). The emission algorithm is described in Schaap et al. (2009) and is very similar to the simultaneously developed routine by Steinbrecher et al. (2009). Sea salt emissions are described using Martensson et al. (2003) for the particles < 1 μm and Monahan et al. (1986) for the coarser particles.
LOTOS-EUROS includes a source apportionment module, which enables tracking the origin of the modelled concentrations for different tracers. Using a labelling technique the module calculates the contribution of specified sources for all model grid cells and time steps. The contributions per label are calculated as fractions of the total tracer concentration. The source apportionment module is extensively described in Kranenburg et al. (2013).
The LOTOS-EUROS model has participated in several international model inter comparison studies addressing ozone (Hass et al, 1997; Van Loon et al, 2007; Solazzo et al., 2012a) and particulate matter (Cuvelier et al, 2007; Hass et al, 2003; Stern et al, 2008; Solazzo et al., 2012b) and shows comparable performance to other European models.

5.2.1.2 Model setup

A model run of 20 years from 01.01.1990 to 31.12.2009 has been performed on a domain covering Europe (35°N-70°N; 10°W-40°E) with a horizontal resolution of 0.50° longitude $\times$ 0.25° latitude on a rectangular regular latitude-longitude grid (ca. 25 $\times$ 25 km^2). As described above the lowest dynamic layer is the mixing layer, taken from the meteorological input.
The simulation was forced with a consistent meteorological data set from 1990 to 2009 obtained from the regional climate model RACMO2 (Lenderink et al., 2003; Van Meijgaard et al., 2008) of the KNMI. At the boundaries the simulation was driven by meteorology from ERA-Interim reanalysis (Dee et al., 2011). RACMO2 has a horizontal resolution of 0.44° with 114 points distributed from 25.04°W to 24.68°E longitude and 100 points

from 11.78°S to 31.78°N latitude in the rotated grid. The South Pole is rotated to 47°S and 15°E. In the vertical, 40 pressure levels were used. As described in Manders et al. (2012) the horizontal projection of RACMO2 fields on the LOTOS-EUROS grid was carried out by bi-linear interpolation. The vertical projection of RACMO2 profiles on the much coarser LOTOS-EUROS vertical grid was achieved by mass-weighted averaging of those RACMO2 model layers that were fully or partially contained in each of the LOTOS-EUROS model layers. At the applied resolution RACMO2 uses a model time step of 15 min and output for coupling with LOTOS-EUROS was generated every three hours. RACMO2 has been included in ensemble studies with other regional climate models (Kjellström and Giorgi, 2010; Kjellström et al., 2010; Vautard et al., 2013; Kotlarski et al., 2014) and has been successfully applied to force LOTOS-EUROS in earlier studies (Manders et al., 2011; Manders et al., 2012; Mues et al., 2013).

Lateral boundary conditions in LOTOS-EUROS were taken from climatological background concentrations for gases and aerosols. Some aerosols species, heavy metals and pops are set to constant at the boundaries. The climatology fields did not include wind-blown dust going back to 1990. Hence, dust from e.g., wind erosion, agricultural land management and resuspension by road transport has been neglected, as it does not contribute to the here investigated substances. For the interpretation of the model results we need to keep in mind that there are no trends in boundary conditions over the investigated 20 year period.

The emissions applied in this study were provided by the International Institute for Applied Systems Analysis (IIASA). The data was generated using RAINS (1990-2000) and GAINS (2000-2010) model output. A description of the RAINS model and the GAINS model can be found in Amann et al. (1999) and Amann et al. (2011), respectively. Annual total emissions were provided per country, per sector and per SNAP (Selected Nomenclature for Air Pollutants) code for 1990, 1995, 2000, 2005 and 2010. A linear interpolation was performed to fill in the emissions of the years within the delivered ones. Figure 5.1a shows the trends in SO_2, NO_x and NH_3 emissions in the EU-27 member States including Norway and Switzerland (= EU-27+) for 1990 to 2010 in % with 1990 as reference derived from the applied final emission inventory. The emissions have decreased over Europe for all considered components. The slope of the decrease has been computed using a standard linear least square method. Most emission reduction was achieved for SO_2 with a negative trend of -3.9% a^{-1} (a: annum) leading to a decrease of more than 70% from 1990 to 2010. NO_x emissions have been decreased by somewhat less than 50% in the same time period (-2.52% a^{-1}) followed by NH_3 emissions with a decrease of somewhat less than 20% from 1990 to 2009 (0.85% a^{-1}). In Figure 5.1a we present results for the emission trends since 1990 for the EU-27+ member States as a whole. While it is known that emission changes

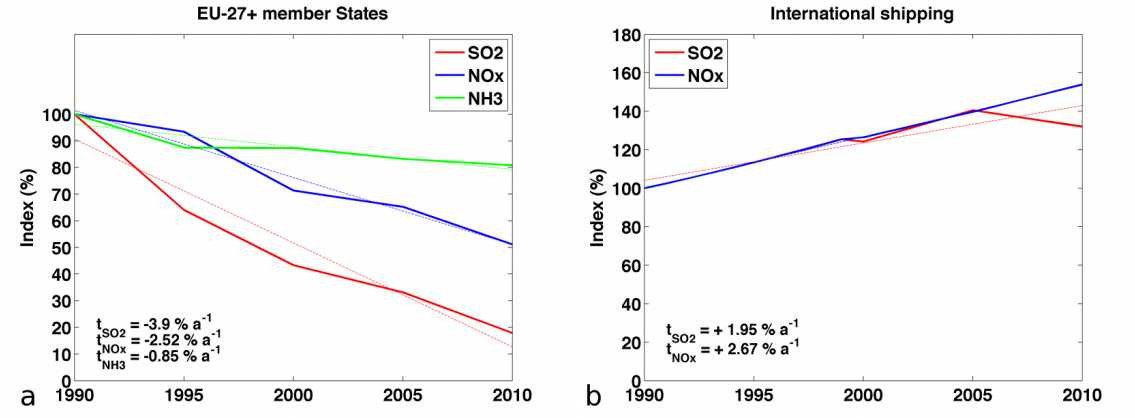

Figure 5.1 Emission trends of (a) SO_2, NO_x and NH_3 in the EU-27+ member States and (b) SO_2 and NO_x in International Shipping for 1990 to 2010 in % with 1990 as reference. The thin lines show the average trend computed over the entire period, the decrease per year is displayed as text.

from 1990 to 2009 differed significantly from region to region, precise information on the spatial distribution of the emissions for the early 90s is lacking. Hence, we used the TNO MACC (Denier van der Gon et al., 2010; Pouliot et al., 2012) spatial distribution of emissions for the year 2005 for the entire time period of investigation. Annual emissions from international shipping per sea and per sector were provided by the Centre on Emission Inventories and Projections (CEIP). Figure 5.1b shows the trends in SO_2 and NO_x International Shipping emissions for 1990 to 2010 in % with 1990 as reference. Included are the Baltic Sea, the North-East Atlantic Ocean, the North Sea, the Mediterranean Sea and the Black Sea. NO_x emissions have increased over the whole time period 1990 to 2009 (+2.67% a^{-1}) for all seas while SO_2 emissions (+1.95% a^{-1}) have increased from 1990 to 2005 and decreased thereafter due to improved fuel quality, especially in the Sulphur Emission Control Areas of the North Sea and the Baltic Sea.

In order to analyse the trends in gas to particle conversion and residence time of the involved species the LOTOS-EUROS source apportionment module was applied. We defined 5 labels for tracking 10 kilo tons (ktons) of SO_2, NO_x and NH_3 emissions from either one of these. The labels were defined to represent the following geographical areas:

1. The Netherlands and Belgium
2. Baltic Sea (international shipping)
3. Czech Republic
4. Romania
5. Rest

Ten ktons of precursor emission were chosen, as it is certainly smaller than the single country annual total emissions for 2009. Together with the simulation of each substance in each grid cell on hourly basis, the fractional contribution of each of the above labels to every substance, including sulphate, nitrate and ammonium, is calculated. By means of the latter the amount of SIA formed from the 10 ktons of precursor gases can be derived for each label and possible trends in gas to particle conversion within the time period 1990 to 2009 can be analysed.

5.2.2 Observations

In the following subsections we describe the in-situ surface observations that were used to evaluate the LOTOS-EUROS model and to derive the observed trends in SIA and its precursors concentrations (Section 5.2.2.1) and the observations used to compare to the meteorological input data provided by RACMO2 (Section 5.2.2.2).

5.2.2.1 Species concentrations

The European EMEP observational network is devised for trend assessment (EMEP/CCC, 2001; Hjellbrekke and Fjæraa, 2011). The EMEP data is validated through a quality assurance/quality control process involving the individual institutions responsible for the different sites and the EMEP-CCC as documented by several reports available on the EMEP website (www.emep.int). Data was downloaded from the EBAS repository (http://ebas.nilu.no/, download in autumn 2012). However, only a few selected stations per country are included in the network. In addition to the EMEP sites, the stations of AirBase (European AIR quality database), the public database of the European Environmental Agency (EEA), were added to the observational data set (http://airbase.eionet.europa.eu/, download in autumn 2012). The latter are not specifically devised for trend assessment but have been used in several studies on long-term trends (e.g. EEA, 2009; Colette et al., 2011; Wilson et al., 2012). The data reported to AirBase are quality controlled and checked prior to submission by the countries that provide the data.
This study is aimed to investigate the transboundary trend of concentrations in the European background following emission changes all over Europe from 1990-2009. Hence, only rural background stations are included in the applied observational data set. The analysis is based on daily observations. The consistency of the observational data set used for the trend assessment and the operational and dynamical model evaluation was ensured by the implementation of three selection criteria derived from the guidelines of the European Environmental Agency (EEA, 2009; Colette et al., 2011):

1. The annual coverage of data must be larger than 75%
2. With criterion No. 1 fulfilled, at least 80% of the annual time series must be available
3. Passing a visual screening of the data

For each time period (1990-2009, 1995-2009 and 2000-2009) a separate data subset of stations within the model domain (35°N-70°N; 10°W-40°E) was built based on the selection criteria described above. As the highest variability is expected in the beginning of each of the studied time periods only stations that could provide the requested 75% data coverage for the first year of the time period were included in the corresponding subset.
Finally a visual screening of the time series of daily observations for all species and at all stations that had passed the selection criteria described above was performed. Surprisingly many defective time series have been identified. The corresponding stations have been removed from the subsets. The most frequently reasons for removal from the data set were high detection limits throughout the time series leading to disappearing concentration regimes, high amounts of implausible outliers/peaks and constant value signals over long time periods. The data reliability is further discussed in section 5.4.
It was found that due to a lack of data the analyses of NH_3 observations could not be included in the study. However, total ammonia (TNH_4: sum of aerosol ammonium and gaseous ammonia) observations were included in the trend assessment as considerably more stations with TNH_4 observations than with NH_4 observations were available. The latter was also the case for TNO_3 and NO_3. Hence, the considered observed components within this study are SO_2, SO_4, NO_2, TNO_3 and TNH_4. In the Supplement, Figure 5.9 to Figure 5.11 show maps of the locations of the observational sites used for the analysis for the different components and the different time periods. Table 5.1 summarizes the number of stations for the different species and subsets before and after the visual screening. The number of discarded stations is highest for SO_2 and NO_2. For both components a large part of the considered stations are from AirBase passing through a less stringent quality control process than EMEP stations.
Due to a lack of long-term monitoring sites within Great Britain, France, Spain and the Mediterranean region within the monitoring networks used in this study the majority of sites for SO_2 and NO_2 observations is located within central Europe accompanied by several sites in northern and eastern Europe. For both components no southern European station and in the case of NO_2 no western European station was available for comparison for the 20 years period. For the time period 1995-2009 an increasing number of eastern and western European stations and in the case of SO_2 one southern European station passed the selection criteria. For TNO_3 and TNH_4 additionally to the lack of long-term observations in southern and western Europe a lack of observations in central Europe was

found and the majority of sites is located in northern and eastern Europe. Stations in ammonia hot spot regions like e.g. the Netherlands or the Po valley did not pass the data selection criteria for any of the time periods. Also for SO_4 no southern European station was available for 1990-2009. The available stations are distributed over Western, Eastern and Northern Europe with most stations being located in Northern Europe. For 1995-2009 central and eastern European stations and one southern European station could be included in the analysis. We would like to stress that the stations at which SO_2 and SO_4 concentrations are investigated may partly differ.
Finally, for the time period 2000-2009 few southern European stations could be included in the analysis of all considered components. Furthermore, Figure 5.12 in the Supplement shows for each component those stations that pass the data selection criteria for all considered time periods.

Table 5.1 Number of stations of the applied observational dataset per component and time period before and after the visual screening of the observed time series.

Species	Time period	Passed data availability criteria	Passed visual check of daily observations
SO_2	1990-2009	51	23
	1995-2009	88	40
	2000-2009	133	60
SO_4	1990-2009	15	15
	1995-2009	23	22
	2000-2009	28	28
NO_2	1990-2009	57	37
	1995-2009	98	64
	2000-2009	167	112
TNO_3	1990-2009	9	9
	1995-2009	9	9
	2000-2009	18	16
TNH_4	1990-2009	7	7
	1995-2009	8	8
	2000-2009	16	15

5.2.2.2 Meteorological observations

Selected parameters of the RACMO2 model are compared to observations to be able to assess the ability of the model to capture the observed meteorological seasonal, annual and interannual variability. For the evaluation, data of the European Climate Assessment and Dataset (ECA&D) project (Klok and Klein Tank, 2009) is applied. The project was

initiated by the European Climate Support Network (ECSN) and is funded by and coordinated at the KNMI. A compilation of daily observations obtained from climatological divisions of national meteorological and hydrological services, observatories and research centres throughout Europe and the Mediterranean are included in the database. The data series of observations is combined with quality control and analysis of extremes via climate change indices (Klein Tank et al., 2002).
Daily observed series of 4 parameters that affect atmospheric chemistry have been extracted from the dataset for the years 1990 to 2009 for evaluation purposes: Temperature (at 2 meter), relative humidity (at 2 meter), wind speed (at 10 meter) and precipitation. For each parameter a selection of stations was extracted so that, if available, central, northern, eastern, southern and western European stations were included in the analysis to also enable a regional consideration. For relative humidity no northern European stations could be included and western European stations were rare concerning observations of relative humidity and wind speed. In total 206 stations were selected for the evaluation of modelled temperature, 113 stations for the evaluation of modelled relative humidity, 246 stations for the evaluation of modelled wind speed and 240 stations for the evaluation of modelled precipitation. The observed station data is compared with model data at the nearest gridpoint.

5.2.2.3 Statistical measures and methods for evaluation and trend assessment

For the evaluation of the used meteorological input provided by RACMO2 and the resultant concentrations simulated by LOTOS-EUROS three statistical measures have been applied to assess the ability of the models to reproduce the observed values:

1. Correlation coefficient r

$$r = \frac{\sum_{i=1}^{n}(x_i - \overline{x})(y_i - \overline{y})}{\sqrt{\sum_{i=1}^{n}(x_i - \overline{x})^2 \sum_{i=1}^{n}(y_i - \overline{y})^2}} \tag{5.1}$$

2. Root mean square error (RMSE)

$$RMSE = \sqrt{\frac{1}{n}\sum_{i=1}^{n}(x_i - y_i)^2} \tag{5.2}$$

3. Bias

$$BIAS = \frac{1}{n}\sum_{i=1}^{n}(x_i - y_i) \tag{5.3}$$

where x is the model output vector and y its observation counterparts. Each vector has n elements and $\overline{x}$ and $\overline{y}$ represent their mean value. The correlation coefficient (Equation 5.1) has been applied to assess the simulated temporal variability and the RMSE (Equation 5.2) and bias (Equation 5.3) to assess the simulated absolute values. The evaluation of RACMO2 and LOTOS-EUROS fields is based on daily averages.
The trends in concentrations are computed using annual averages based on daily data. The slope is calculated using a standard linear least square method. Within this study we computed only linear trends and the computation of non-linear trends (Konovalov et al., 2010) or piecewise linear trends (Carslaw et al., 2011) has not been performed. To assess the significance of the trend a Mann-Kendall test at the 95% confidence level is performed (Kendall, 1976; Hipel and McLeod, 2005).

5.3 Results

5.3.1 Evaluation of model results

5.3.1.1 Evaluation of meteorological fields

The applied meteorological input data has been compared to observations to be able to assess the ability of RACMO2 to reproduce the observed meteorological annual, interannual and seasonal variability. In order to limit the length of this article only an abridgement of the performed evaluation is shown here. Four parameters that considerably impact atmospheric chemistry are shown: Temperature (at 2 meter), relative humidity (at 2 meter), wind speed (at 10 meter) and precipitation. The evaluation is based on daily data for the 20 years period. Table 5.2 summarizes the number of stations, the mean correlation coefficient, the observed mean and RMSE and bias. As an example Figure 5.2 shows the 60-days moving average of the four parameters averaged across all available German stations from 1990-2009. The 60-days moving average was chosen to be able to plot the whole time series in one graph and, at the same time, to be able to see variability in the time series. As the mean correlation coefficient of 0.97 in Table 5.2 shows the model captures very well the temporal distribution of temperature for the considered time period. Figure 5.2a shows that the interannual variability is simulated fairly well too. Warm summers like in 2003 and 2006 and cold winters like the one in 1995/1996 are well reproduced by RACMO2. However, the bias and also the corresponding graph in Figure 5.2 indicate a slight underestimation of the temperature during wintertime in central Europe. The performance of the model has also been assessed regionally for Northern, Eastern, Southern, Western and Central Europe separately (not shown here). The underestimation during wintertime was found to be most distinct for southern and least distinct for northern

Table 5.2 Statistical comparison between measured and modelled meteorological parameters using daily observations at European observational sites. The number of considered stations, mean correlation, observed mean, RMSE and bias are given.

Evaluation	Temperature	Relative humidity	Wind speed	Precipitation
Number of stations	206	113	246	240
Mean correlation	0.97	0.66	0.68	0.48
Observed mean	286.06 K	78%	3.82 m s^{-1}	1.82 mm
RMSE	2.82 K	11%	1.87 m s^{-1}	4.52 mm
Bias	-1.47 K	2 %	0.35 m s^{-1}	0.04 mm

Europe, which is consistent with findings in van Meijgaard et al. (2012) and Kotlarski et al. (2014).

As Figure 5.2b illustrates RACMO2 captures the interannual variability of the relative humidity at 113 European stations less well than that of the temperature. The latter was found to be most evident for southern Europe. Also the relative humidity is overestimated during wintertime, which is again most distinct for southern Europe and may be connected to the underestimation of the temperature during wintertime. Relative humidity is a difficult quantity to evaluate, in particular in areas or during episodes with high values of relative humidity ($> 95\%$). However, a mean correlation coefficient of 0.66 (Table 5.2) indicates that the observed temporal variability is satisfactorily simulated by the model.

The temporal variability of the wind speed is also satisfactorily simulated with a mean correlation coefficient of 0.68 over 246 European stations (Table 5.2). Figure 5.2c displays the mean 60 days moving average of wind speed for 59 German stations for the investigated time period. The graph indicates that although the timing is well simulated the model tends to overestimate the wind speed in central Europe. In central and eastern Europe the overestimation was found to be present throughout the whole year. In northern and southern Europe RACMO2 overestimates wind speed solely during wintertime while it tends to slightly underestimate wind speed during summertime.

Figure 5.2d shows the mean 60 days moving average of precipitation for 1990-2009 at 66 German stations. The figure shows that the interannual variability is modelled satisfactorily in central Europe although it is slightly underestimated. Dry years like 1996, 2003 and 2006 are well reproduced by the model. RACMO2 underestimates summertime precipitation in southern Europe while it tends to overestimate wintertime precipitation in northern and central Europe, which was also found by van Meijgaard et al. (2012) and Kotlarski et al. (2014). Generally, moving from daily to monthly or annual precipitation sums (not shown here) RACMO2 results compare better to the observed values. Mean

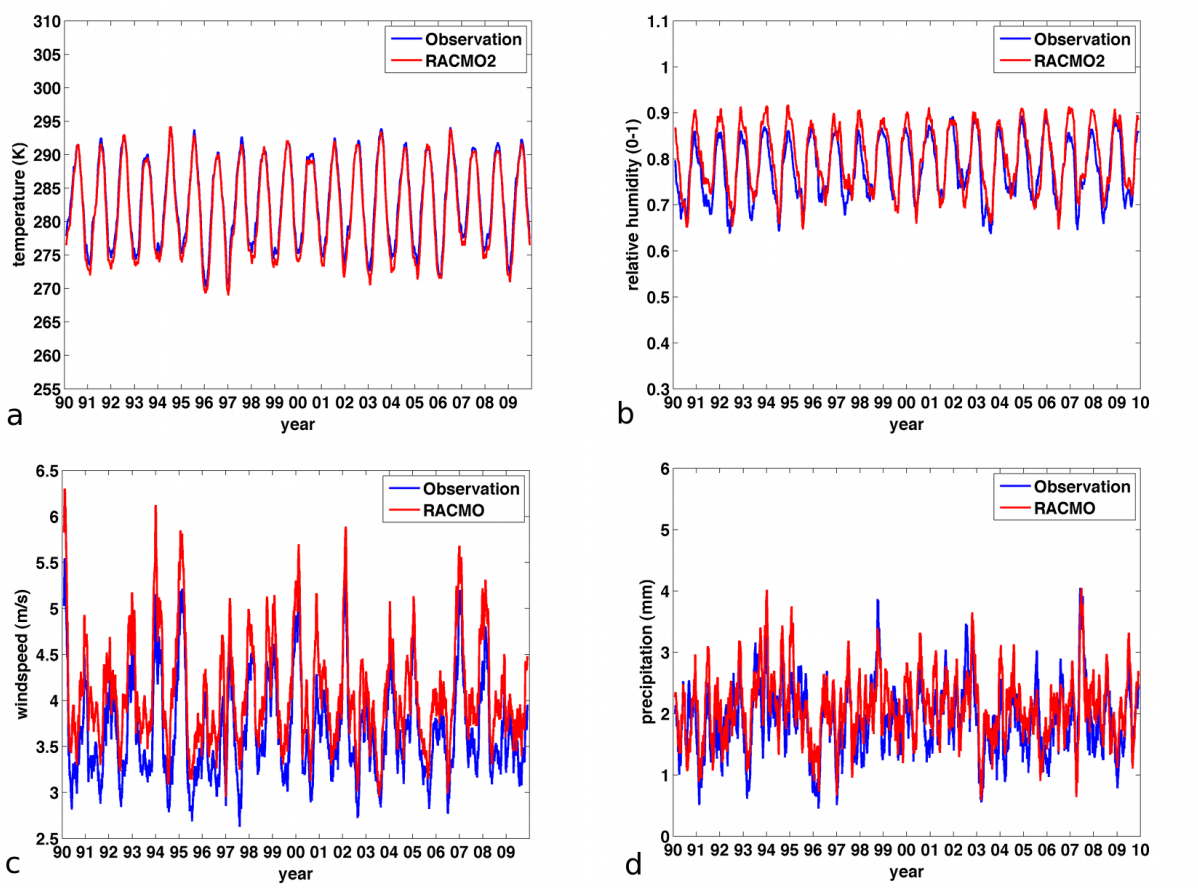

Figure 5.2 Mean 60 days moving average of (a) temperature, (b) relative humidity, (c) windspeed and (d) precipitation at 66, 61, 59 and 66 German observational sites, respectively, from 1990-2009.

correlation coefficient, RMSE and bias have been calculated at 240 European stations (Table 5.2). The mean correlation of 0.48 indicates that considering the high temporal variability of precipitation RACMO2 simulates the observed timing reasonably well.

For the CTM calculation it is more important to capture the occurrence of precipitation than to capture its intensity and duration with the meteorological driver as wet deposition is a very efficient removal process. Therefore, at each of the 240 stations it was investigated on which percentage of days of the 20 years period the model is able to simulate the observed rain occurrence (rain: yes; rain: no). In the following a correct modelled rain:yes or rain:no is referred to as 'hit'. To account for unphysical small amounts of drizzle that often occur in climate models, daily accumulated precipitation below 0.5mm was considered as no rain. The results are summarised in Table 5.3. At 205 out of 240 stations the model is able to correctly simulate the rain occurrence on more than 70% of the days from 1990-2009.

Although some shortcomings in the meteorological input fields were found the outcome of the evaluation of RACMO2 has shown that the model is capable of satisfactorily reproducing the observed magnitudes and meteorological annual, interannual and seasonal variability of the investigated parameters.

Table 5.3 Percentage of daily rain occurrence hits of the RACMO2 model from 1990 to 2009 at 240 European observational stations.

Hits	#stations
$h < 60\%$	0
$60\% \leq h < 70\%$	35
$70\% \leq h < 80\%$	156
$80\% \leq h < 90\%$	48
$h \geq 90\%$	1

5.3.1.2 Concentrations in air

Figure 5.3 shows for each component the 60-days moving average concentrations averaged across all available stations for the period 1990-2009. Besides the time series the average seasonal variation is given for this same 20 year time period. The summary of the statistical evaluation based on daily pairs of observed and measured concentrations is given in Table 5.4 for the 1990-2009, 1995-2009 and 2000-2009 time periods.
The modelled time series of SO_2 by LOTOS-EUROS underestimates the observed SO_2 concentrations (Figure 5.3a) in the period 1990-1997, while for later years there appears to be a small bias at these stations. Throughout the time series the year-to-year variability is captured well by the model, as is the seasonal variation. The concentrations of sulphate are systematically underestimated by LOTOS-EUROS throughout the whole period. The underestimation is most distinct from 1990-1997, which appears to be related to the underestimation of SO_2 in the same period. Analysis of the individual sites showed that the sites located in eastern and central Europe largely determine the underestimation for both components as northern European stations show much better comparison. The correlation coefficient of 0.5 for SO_2 for 1990-2009 suggests that the timing is not very well captured throughout the time period. Again a separation in time and region was detected. For stations in central and eastern Europe for the years 1990-1997 average correlation coefficients of 0.40 and 0.54 were found, whereas these increase to 0.54 and 0.69 for central and eastern Europe, respectively, for 1998-2009. Also for SO_4 the correlation coefficient is improved for the 1998 to 2009 time period (0.56) compared to the 1990 to 1997 time period (0.50). We connect the difference in the model performance for these

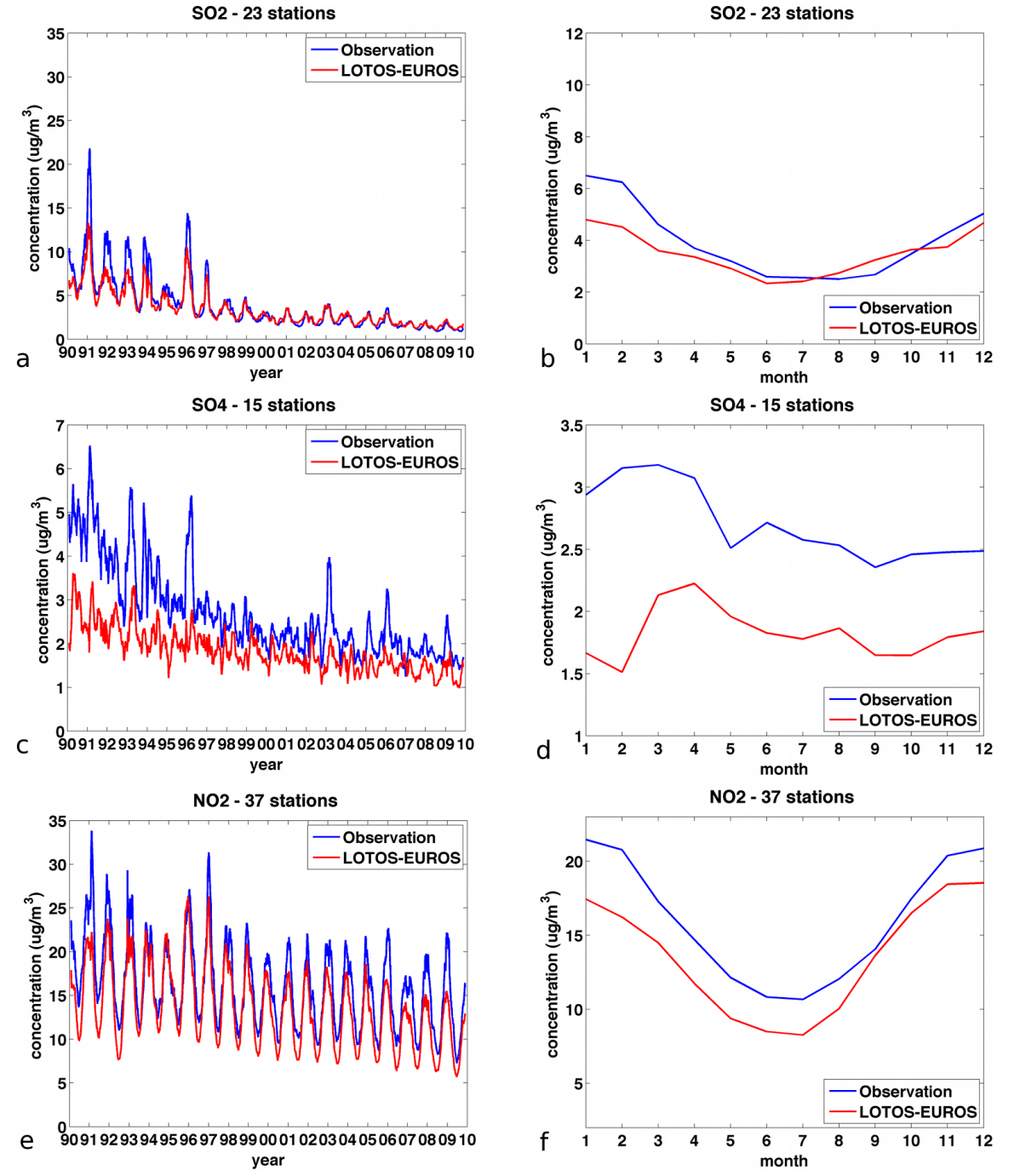
SO2 - 23 stations
Observation
LOTOS-EUROS
concentration (ug/m3)
year
a
SO2 - 23 stations
concentration (ug/m3)
month
b
SO4 - 15 stations
c
SO4 - 15 stations
d
NO2 - 37 stations
e
NO2 - 37 stations
f

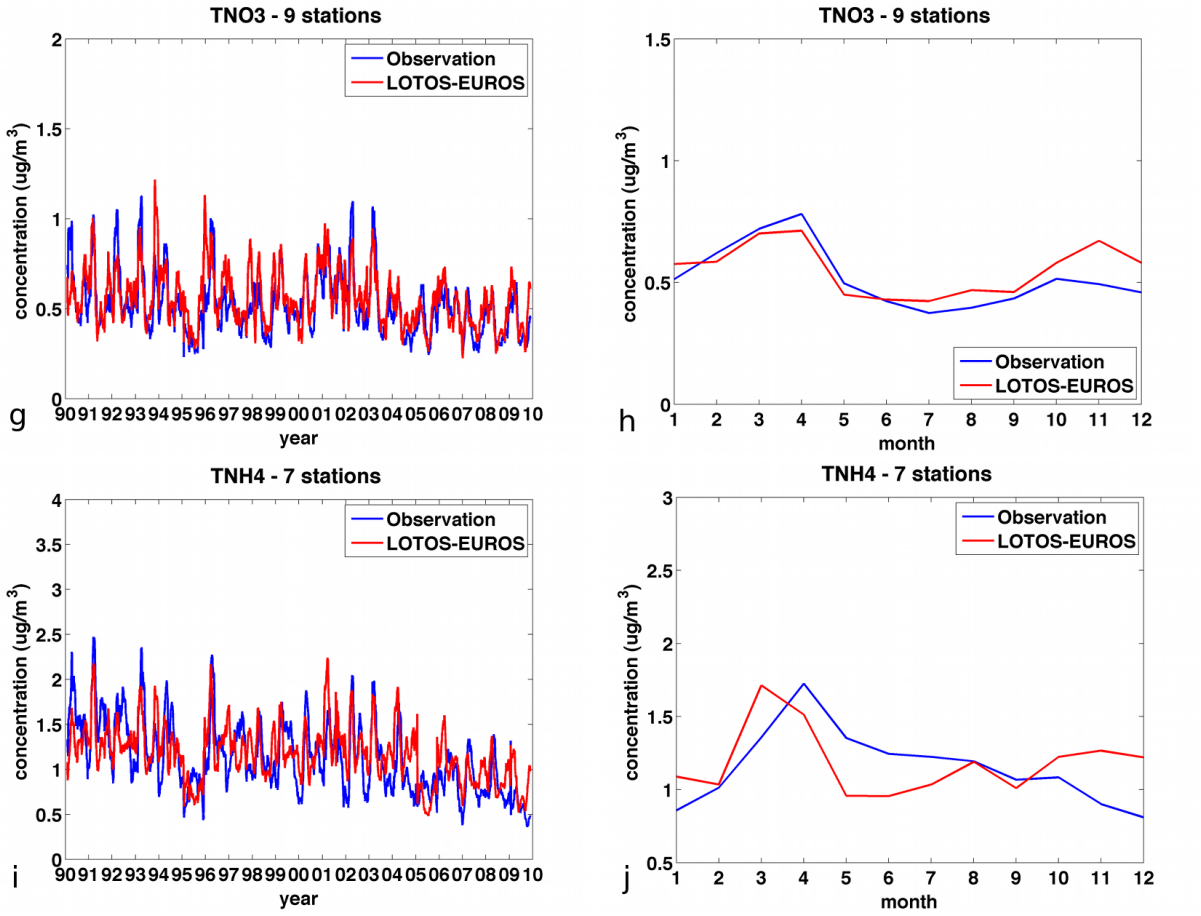

Figure 5.3 Mean 60 days moving average (left panel) and seasonal cycle (right panel) of (a-b) SO_2, (c-d) SO_4, (e-f) NO_2, (g-h) TNO_3 and (i-j) TNH_4 for the time period 1990-2009. The number of considered stations is given in the figure captions.

periods to the lack of a good representation of the change in emission structures in the power sector in eastern and parts of central Europe as a consequence of the fall of the Berlin wall and political changes associated with the liberalisation of the Eastern Bloc's authoritarian systems as discussed below.

A striking feature in the comparison for SO_4 (Figure 5.3c) is the inability of the model to reproduce the magnitude of several spring episodes that occurred in e.g. 1996, 2003 and 2006. Although for some of these episodes the model is able to capture the timing, it is not able to reproduce the peak values. These episodes are characterized by very stable conditions across central Europe and some have been studied in detail (e.g. Stern et al., 2008; Banzhaf et al., 2013). A model comparison by Stern et al. (2008) has shown that also other state of the art models were not able to simulate the peak values in early spring 2003.

On average, the model underestimates NO_2 concentrations by about 15%. Figure 5.3e

Table 5.4 Statistical comparison between measured and modelled concentrations using daily observations. The number of considered stations, mean correlation, observed mean, RMSE and bias are given for each component and each time period.

Period	Evaluation	SO_2	NO_2	SO_4	TNO_3	TNH_4
1990-2009	number of stations	23	37	15	9	7
	mean correlation	0.5	0.72	0.44	0.64	0.71
	observed mean (μg m^{-3})	3.86	15.97	2.77	0.56	1.35
	RMSE (μg m^{-3})	6.01	8.66	2.86	0.61	1.21
	Bias (μg m^{-3})	-0.44	-2.43	-0.88	0.04	0.03
1995-2009	number of stations	40	64	22	9	8
	mean correlation	0.59	0.67	0.57	0.64	0.64
	observed mean (μg m^{-3})	4	14.19	2.46	0.46	1.17
	RMSE (μg m^{-3})	6.49	8.58	2.27	0.54	1.05
	Bias (μg m^{-3})	-0.67	-2.58	-0.66	0.12	0.03
2000-2009	number of stations	60	112	28	16	15
	mean correlation	0.5	0.6	0.55	0.56	0.57
	observed mean (μg m^{-3})	3.34	14.12	2.16	0.6	1.38
	RMSE (μg m^{-3})	5.01	9.37	1.95	0.6	1.18
	Bias (μg m^{-3})	-0.69	-3.77	-0.58	0.12	0.21

shows that the overall bias is distinct in the first three years of the time series and becomes small in the years afterwards. After 2000 the bias between modelled and observed NO_2 starts to increase again and becomes increasingly larger towards 2009. The temporal correlation coefficient (>0.7) for these stations throughout the series and the good representation of the seasonal cycle illustrates that LOTOS-EUROS captures the day-to-day variability well. Also, the interannual variability is reproduced reasonably well.

As Figure 5.3g and h illustrate, total nitrate concentrations are simulated very well by LOTOS-EUROS. Other than for SO_4, some TNO_3 episodes are well captured by the model. The lower correlation coefficient for TNO_3 compared to NO_2 we attribute to a less strong seasonal variability and emission signal in the TNO_3 concentrations. In case of TNH_4 there is also a small bias and the model captures a large part of the observed variability. The major shortcoming in the TNH_4 modelling is clearly visible in the average seasonal cycle. The model overestimates TNH_4 concentrations during wintertime (Oct-Jan) and tends to underestimate during late spring and early summer. Moreover, the maximum concentration is modelled to be in March, whereas the observed maximum occurs in April. The lack of a good representation of the seasonal cycle in the ammonia emissions is a likely cause for this feature.

For the validation of the model more sites become available for the later time periods (see Section 5.2.2.1). Comparing the overall correlation coefficient, RMSE and bias for each time period in Table 5.4 shows that these are not generally improved for the later

time periods compared to those of 1990-2009. The reason is that more stations become available for eastern and also southern European stations, which in general show lower model skill (see e.g. Vautard et al., 2009). Analysis of the performance across the few stations that pass the data selection criteria for all three periods shows that the model results compare better to the observations for the later years than for the (early) 1990's (Table 5.5). Comparison between the components shows that the model skill for nitrogen components is larger than for the sulphur compounds.

Table 5.5 Statistical comparison between measured and modelled concentrations using daily observations at those stations that are available for all three periods. The number of considered stations and the mean correlation are given for each component and each time period.

Period	Evaluation	SO_2	NO_2	SO_4	TNO_3	TNH_4
all	number of stations	15	33	11	4	3
1990-2009	mean correlation	0.51	0.71	0.47	0.58	0.69
1995-2009	mean correlation	0.59	0.73	0.63	0.69	0.69
2000-2009	mean correlation	0.64	0.73	0.64	0.68	0.69

5.3.2 Trends in concentrations

The observed and modelled trends are illustrated in Figure 5.4, Figure 5.5 and Figure 5.6. Figure 5.4 shows boxplots of the absolute and relative observed and modelled trends for all components. Boxplots are used to provide a concise illustration of a higher amount of data points. We are aware that hence, for the components TNO_3 and TNH_4 a boxplot is not necessary for the time periods 1990-2009 and 1995-2009. The median trend for 7, 8 or 9 stations is robust but the calculation of the 25^{th} and 75^{th} percentile is of no significance. Being aware of the latter, boxplots for TNO_3 and TNH_4 have still been included for all time periods to be able to compare the trends to those of the other components. Table 5.6 summarizes the observed and modelled median trends for the three considered time periods.

Figure 5.5 shows scatter plots of the observed versus modelled trend for the studied components at the considered stations for the 3 different time periods. It is labelled in the graphs if the observed and/or modelled trends are significant (method used described in section 5.2.2.3): (+) implies that the observed and the modelled trends are significant, (o) implies that the observed trend is non-significant while the modelled trend is significant, (o) implies that the observed trend is significant while the modelled trend is non-significant and (o) implies that the observed and the modelled trends are non-significant.

Figure 5.6 shows the observed and modelled trends of the annual mean SO_4, TNO_3 and

TNH_4 concentrations, their 5^{th} and 95^{th} percentile and the corresponding trend lines. Solid lines refer to significant trends and dashed lines refer to non-significant trends (only found for the TNO_3 5^{th} percentile).

5.3.2.1 Observed trends

Figure 5.5 illustrates that the observed SO_2, SO_4 and NO_2 concentrations show significant negative trends at the majority of stations for the time periods 1990-2009 and 1995-2009. For NO_2 a significant positive trend for 1995-2009 was observed at two stations located in Estonia at the shore of the Baltic Sea. For TNO_3 and TNH_4 the majority of trends is significant negative for the 1990-2009 time period while for 1995-2009 the observed trends are non-significant at all stations (TNO_3) or at the majority of stations (TNH_4). We would like to stress again that for TNO_3 and TNH_4 the considered station locations are situated in northern and eastern Europe due to a lack of long-term observations in the other regions. The trends in TNO_3 in hot spot areas like the Netherlands may differ. For the time period 2000-2009 the observed trends are non-significant at the majority of stations for all considered components. Furthermore, the relative amount of stations with non-significant trends increases when moving from 1990-2009 (SO_2: 0%; SO_4: 0%; NO_2: 11%; TNO_3: 33%; TNH_4: 14%) to 1995-2009 (SO_2: 5%; SO_4: 18%; NO_2: 21%; TNO_3: 100%; TNH_4: 50%) to 2000-2009 (SO_2: 52%; SO_4: 86%; NO_2: 72%; TNO_3: 75%; TNH_4: 80%).

Figure 5.4 and Table 5.6 show that for all components the observed median absolute and relative negative trends decrease moving from 1990-2009 to 2000-2009 (absolute decrease in TNO_3 trends in the 3rd decimal place). For SO_2 and NO_2 the observed trends slightly decrease for 1995-2009 compared to 1990-2009 but decrease considerably for the time period 2000-2009. Comparing the observed absolute and relative trends in SO_4 concentrations to those of SO_2 shows that the trends in SO_4 are considerably lower. However, the relative trends for SO_4 concentrations are higher than those for NO_2, TNH_4 and TNO_3. For the absolute trends, the interquartile range, which is an indicator for the spread of the data, decreases for SO_2 and SO_4 when moving to later time periods although the number of stations increases while for NO_2 the interquartile range and therewith the spread of the distribution remains almost stable. This difference may be induced by the fact that the variation of emission changes from country to country is larger for nitrogen oxides compared to sulphur oxides (Løvblad et al., 2004).

Considering only those stations that fulfilled the selection criteria for all 3 time periods (not shown here) has shown that an increasing number of non-significant trends, the decrease of median absolute and relative trends and the decreasing (stable) spread of the trends for SO_2 and SO_4 (NO_2) when moving from 1990-2009 to 2000-2009 are also present

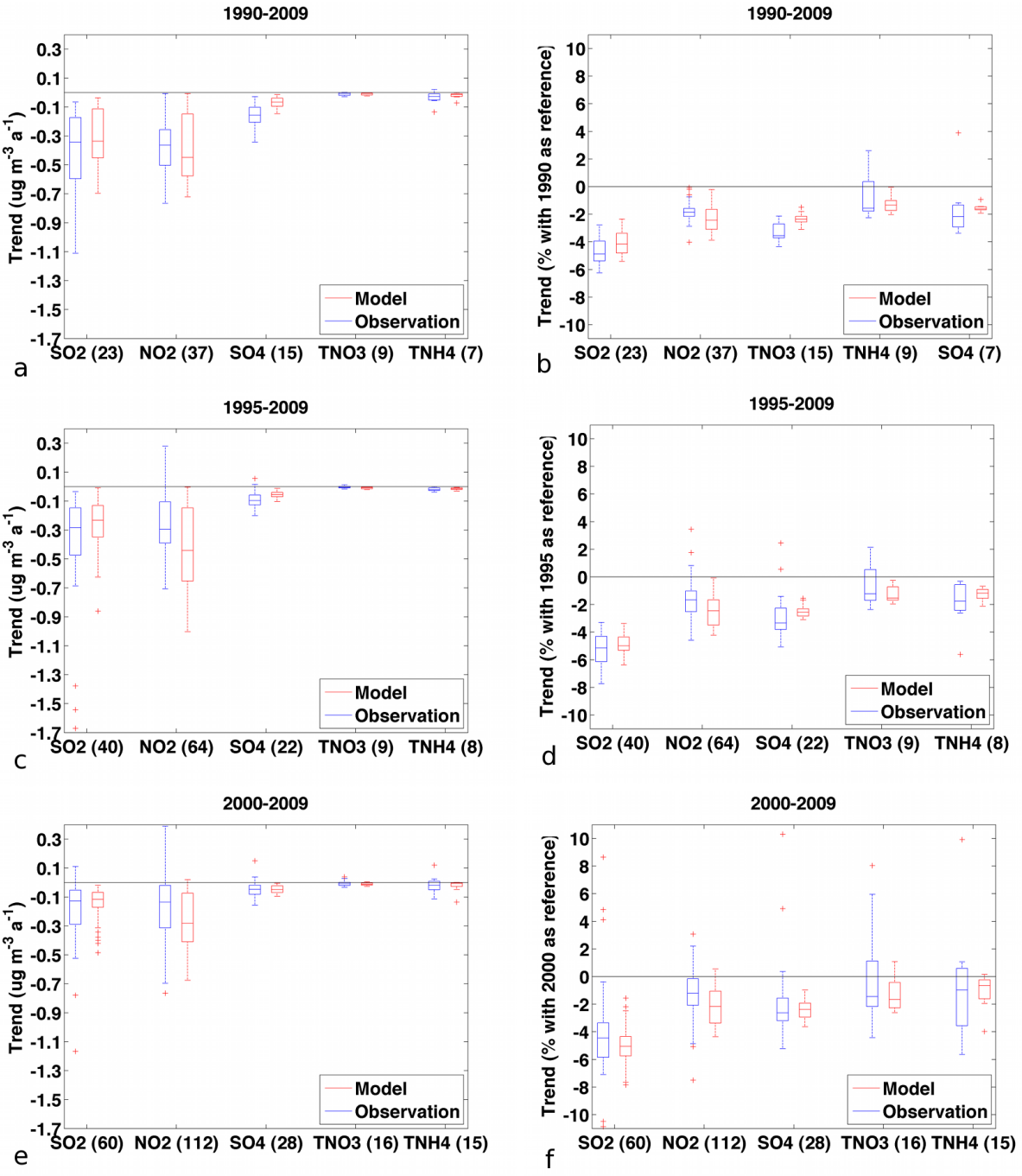

Figure 5.4 Boxplots of the absolute (left panel) and relative (right panel) observed (blue) and modelled (red) trends for the considered components and time periods.

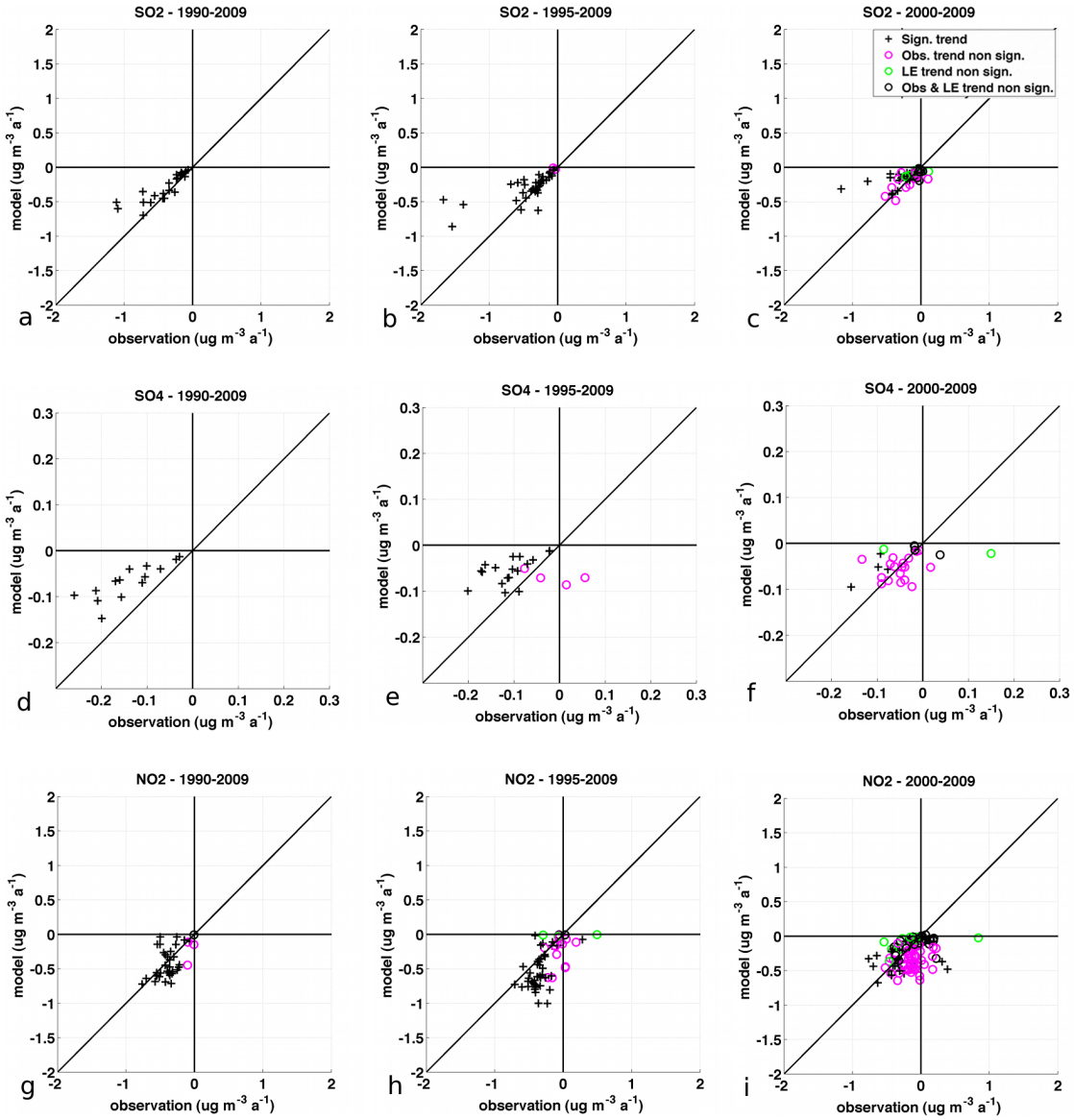
SO2 - 1990-2009
SO2 - 1995-2009
SO2 - 2000-2009
Sign. trend
Obs. trend non sign.
LE trend non sign.
Obs & LE trend non sign.
SO4 - 1990-2009
SO4 - 1995-2009
SO4 - 2000-2009
NO2 - 1990-2009
NO2 - 1995-2009
NO2 - 2000-2009
model (ug m-3 a-1)
observation (ug m-3 a-1)
a
b
c
d
e
f
g
h
i

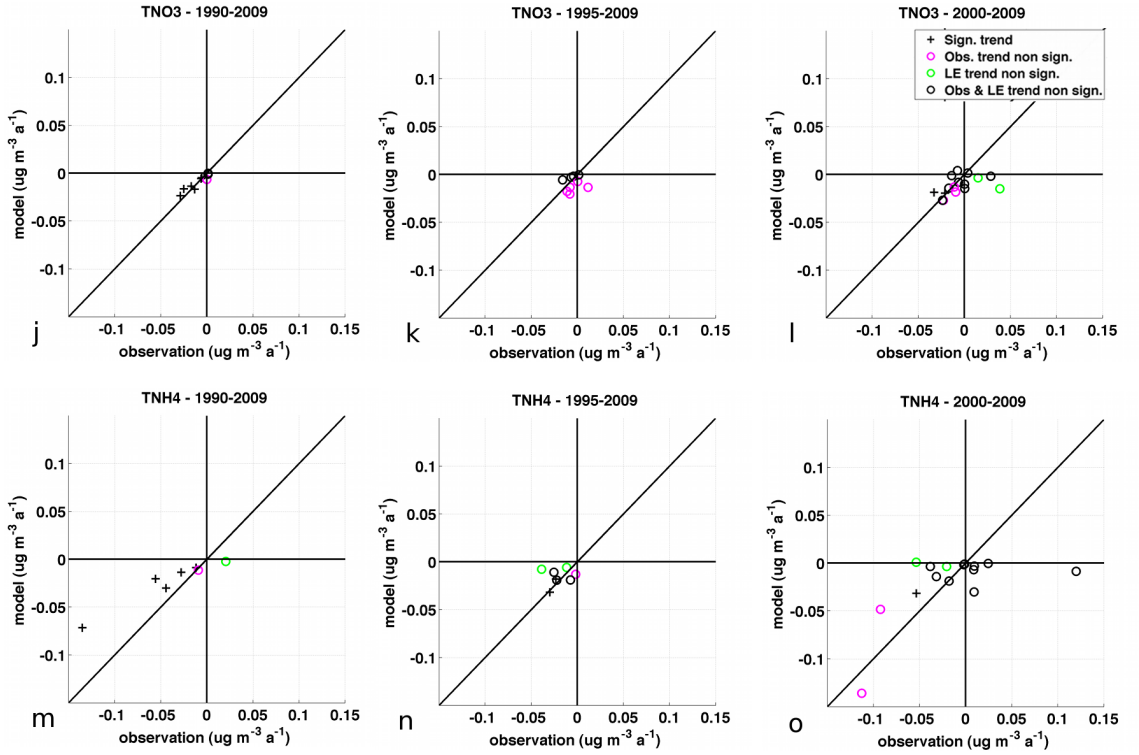

Figure 5.5 Scatter plots of the observed versus modelled trends for the studied components at the considered stations for the three different time periods. At each individual station the marker (described in the legend on the top right of the plot) indicates if the observed and/or modelled trend is significant following the Mann-Kendall test at a 95% confidence level.

when considering the same subset of stations.

5.3.2.2 Modelled trends and comparison to observed trends

As Figure 5.4 shows the model is able to well simulate the decrease in the absolute median negative trend for SO_2, SO_4 and NO_2 when moving from 1990-2009 to 1995-2009 to 2000-2009. As for the observed trends the model simulates only a slight decrease of the absolute negative median trend in SO_2, SO_4 and NO_2 concentration from 1990-2009 to 1995-2009 but a significant decrease from 1995-2009 to 2000-2009. Also, the model is able to reproduce the lower relative trends in observed SO_4 concentrations compared to those of SO_2 (see Figure 5.4b, 4d and 4f). Furthermore, the model is able to capture the decrease in the spread of the data distribution for SO_2 and SO_4 when moving from 1990-2009 to 1995-2009 to 2000-2009. However, the lower distance between upper and lower whisker and the lower or non-existent amount of outliers reveals that for both considered sulphur compounds the distribution of the modelled absolute and relative trends is less broad than that of the observed trends. This indicates that the modelled trends show a

Table 5.6 Number of stations and derived observed and modelled absolute (μg m^{-3} a^{-1}) and relative (% a^{-1}) median trends for the considered components and time periods.

Period	Evaluation	SO_2	NO_2	SO_4	TNO_3	TNH_4
1990-2009	number of stations	23	37	15	9	7
	Observed abs. median trend	-0.34	-0.36	-0.16	-0.01	-0.03
	Modelled abs. median trend	-0.34	-0.45	-0.07	-0.01	-0.01
	Observed rel. median trend	-4.88	-1.85	-3.55	-1.57	-2.18
	Modelled rel. median trend	-4.16	-2.44	-2.36	-1.33	-1.61
1995-2009	number of stations	40	64	22	9	8
	Observed abs. median trend	-0.28	-0.3	-0.1	-0.01	-0.02
	Modelled abs. median trend	-0.23	-0.44	-0.06	-0.01	-0.02
	Observed rel. median trend	-5.14	-1.67	-3.34	-1.23	-1.77
	Modelled rel. median trend	-4.98	-2.46	-2.57	-1.54	-1.18
2000-2009	number of stations	60	112	28	16	15
	Observed abs. median trend	-0.13	-0.14	-0.05	-0.01	-0.02
	Modelled abs. median trend	-0.12	-0.28	-0.05	-0.01	-0.01
	Observed rel. median trend	-4.45	-1.12	-2.63	-1.45	-0.98
	Modelled rel. median trend	-5.1	-2.17	-2.37	-1.66	-0.66

lower spatial variance over Europe than the observed trends. The latter is vice versa for NO_2 concentrations for which especially for the early time periods the interquartile range of the modelled absolute and relative trends is larger than that of the observed trends. The model simulates significant negative trends in SO_2, NO_2 and SO_4 concentrations at most station locations for 1990-2009 and 1995-2009 (see Figure 5.5), which coincides with the observed trends for these time periods. However, the model underestimates the negative trends in concentrations for SO_2 at several stations and for SO_4 at most stations (note that the stations at which SO_2 and SO_4 concentrations are investigated may partly differ) while it overestimates the negative trends in NO_2 concentrations at the majority of station locations. For all considered time periods the deviation of the modelled trends in SO_2, SO_4 and NO_2 concentrations from the observed trends were found to be most distinct at eastern European stations and stations in north-eastern Germany (e.g. the three outliers in Figure 5.5b correspond to trends at 2 stations in Czech Republic and one station in eastern Germany) and least distinct at northern European station locations. The findings from Figure 5.5 are also reflected in the median absolute and relative trends presented in Figure 5.4. Furthermore, the figure shows that for SO_2 and SO_4 the simulated trends improve considerably for the 2000-2009 compared to the earlier time periods while the trends in NO_2 are overestimated by the model throughout all time periods.

Figure 5.6a reveals that for SO_4 the strong observed negative trend is mostly driven by the high observed concentrations in the beginning of the 90s which could not be reproduced

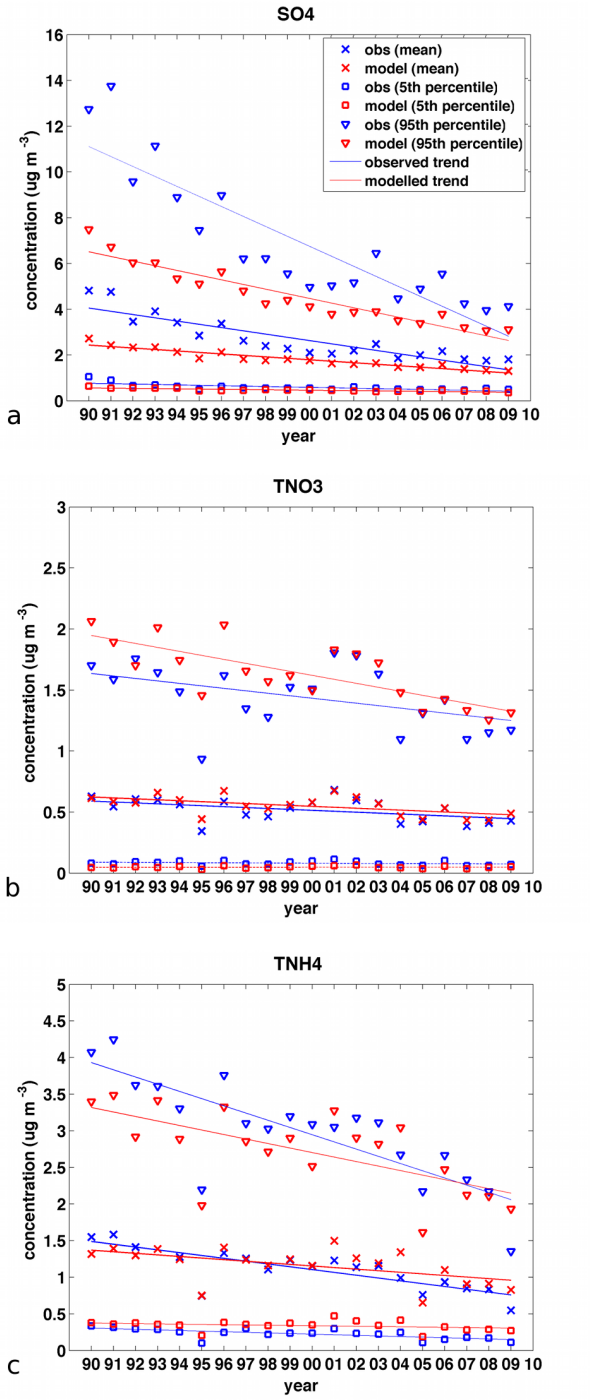

Figure 5.6 Observed (blue) and modelled (red) annual mean (crosses), 5^{th} percentile (squares) and 95^{th} percentile (triangles) and corresponding trend line of (a) SO_4, (b) TNO_3 and (c) TNH_4. Solid lines indicate a significant and dashed lines a non-significant trend.

by the model. The 5^{th} percentile, which represents the background concentrations, and its significant negative trend are well captured by the model. The negative trend of the 95^{th} percentile, which represents the high concentration range (the peak SO_4 concentrations), is significantly underestimated by the model. The model satisfactorily captures the temporal distribution of the interannual variability but there is a significant negative bias between modelled and observed value. This shows that the models inability to capture the observed trend in SO_4 is driven by the underestimation of the high range of concentrations.
Also for TNO_3 and TNH_4 shown in Figure 5.6b and Figure 5.6c the deviation from the observed values is most distinct in the 95^{th} percentile while the interannual variability is well simulated by the model. However, for both components but especially for TNO_3 the model compares considerably better to the observations than for SO_4. Also Figure 5.5 shows that the model well reproduces the low trends in TNO_3 concentrations at the majority of considered sites for all time periods while for TNH_4 the model tends to underestimate the observed concentration trends. Furthermore, for both components, TNO_3 and TNH_4, the increased relative number of non-significant trends when moving from the 1990-2009 to the 2000-2009 time period is well captured by the model at most stations. While for TNO_3 and TNH_4 concentrations the model captures the non-significance of trends at the majority of stations for the time period 2000-2009 the model underestimates the number of stations with observed non-significant concentration trends for SO_2, SO_4 and NO_2.

5.3.3 Sensitivity of resultant observed trends to data selection

Following the guidance of the European Environment Agency one of the data selection criteria listed in section 5.2.2.1 was that at least 80% of the annual time series of observations must be available at each site. In this section we would like to test the sensitivity of the resultant observed median trends to that selection criterion. Table 5.7 shows the number of stations and the observed median trends for all considered species for the selection criteria that at least 16 (= 80%), 17, 18, 19 or 20 years of the annual time series of observations must be available for the 1990-2009 time period. As already for the least stringent criterion we start with a small amount of stations for TNO_3 and TNH_4 concentrations and all stations are located in northern Europe, there is hardly any or no change in median trends when using a different number of available years for these components. For SO_2, NO_2 and SO_4 concentrations Table 5.7 shows that even though the sign is robust the selection criterion does impact the observed median trends as a result of a changing number of considered stations. The differences are smallest between choosing 16 or 17

years as selection criterion. The most stringent criterion of 20 years (=100%) significantly reduces the number of considered stations. Although the completeness of the time series increases the robustness of the trend assessment at the single stations, the overall assessment gets less representative for Europe as the number of stations is considerably lower.

Table 5.7 Number of stations and the corresponding observed median trend (μg m^{-3} a^{-1}) for different selection criteria varying the amount of required years of the annual time series.

1990-2009	SO_2		NO_2		SO_4		TNO_3		TNH_4	
#years	#stat.	Median trend	#stat.	Median trend	#stat.	Median trend	#stat.	Median trend	#stat.	Median trend
16	23	-0.343	37	-0.363	15	-0.156	9	-6×10^{-3}	7	-2.7×10^{-2}
17	21	-0.345	37	-0.363	14	-0.147	7	-6×10^{-3}	5	-2.7×10^{-2}
18	20	-0.302	36	-0.368	11	-0.11	6	-9×10^{-3}	3	-2.7×10^{-2}
19	14	-0.247	28	-0.368	9	-0.11	5	-6×10^{-3}	3	-2.7×10^{-2}
20	7	-0.234	12	-0.381	7	-0.101	3	-6×10^{-3}	3	-2.7×10^{-2}

5.3.4 Trends in SIA formation

In Figure 5.1a we have shown the relative emission decrease of SIA precursors based on the years 1990, 1995, 2000, 2005 and 2010 with 1990 as reference for the EU-27+ member States. A trend line is added for each component. Figure 5.7a and Figure 5.7b show the observed and modelled annual average concentrations of SO_2, NO_2, SO_4, TNO_3 and TNH_4 relative to the annual average concentration of 1990 at 23, 37, 15, 9 and 7 European stations, respectively, for the years 1990, 1995, 2000, 2005 and 2009. Trend lines are added for each component and the corresponding numbers are given at the lower left of each panel. Comparing Figure 5.7a and Figure 5.7b reveals that LOTOS-EUROS well simulates the observed relative trends. The curves for TNO_3 and TNH_4 demonstrate that the model is capable to capture meteorological variability. Together with the precursor emissions over land (Figure 5.1a) the observed concentrations of all considered components show negative trends for 1990 to 2009. The observed decrease in SO_2 concentrations is for the considered time period from 1990-2009 with -4.4% a^{-1} even larger than the corresponding decrease in SO_2 emissions (-3.9% a^{-1}). In contrast to SO_2, the decrease in observed SO_4 concentrations is with -3% a^{-1} less distinct and smaller than the decrease in SO_2 emissions. This non-linear effect is well reproduced by LOTOS-EUROS.

The LOTOS-EUROS source apportionment module was used to further investigate the observed and modelled non-linearity. Therefore 10 ktons of SO_2, NO_x and NH_3 emissions,

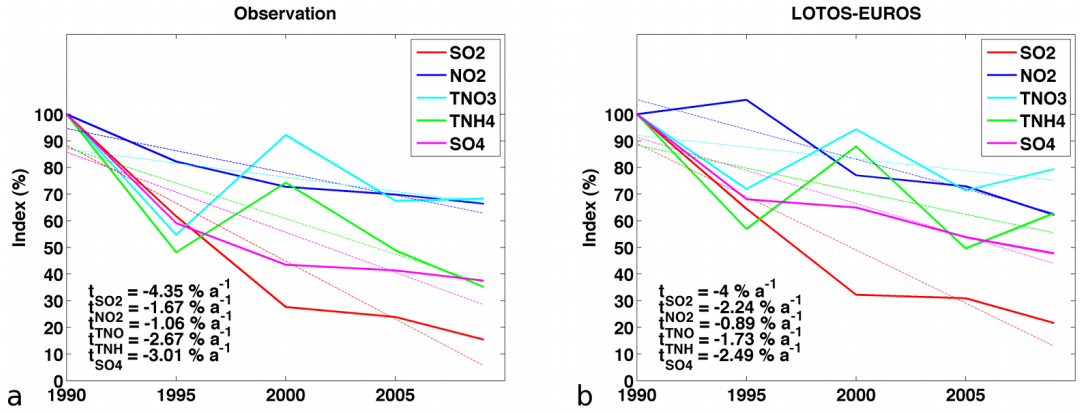

Figure 5.7 (a) Observed and (b) modelled annual average concentrations of SO_2, NO_2, SO_4, TNO_3 and TNH_4 relative to annual average concentrations of 1990 (solid lines) at 23, 37, 15, 9 and 7 European stations, respectively, for the years 1990, 1995, 2000, 2005 and 2009. Trends (in % a^{-1}) and the corresponding trend lines (dashed lines) are given for each component.

respectively, have been tracked for 1990 to 2009 for 4 different labels, which were chosen to be 4 different regions: The Netherlands and Belgium (NLBE), the Baltic Sea (BAS), Czech Republic (CZE) and Romania (ROM). By means of the labelling we can determine how much SIA was formed from the 10 ktons precursor emissions during the time period from 1990 to 2009. The results of the source attribution are presented in Figure 5.8. Figure 5.8a shows the amount of sulphate (solid lines) formed from 10 ktons SO_2 emissions relative to the amount formed from 10ktons SO_2 emissions in 1990 for the different labels for 1990 to 2009. A trend line (dashed line) is added for all labels. For all considered regions the sulphate formation efficiency increases from 1990 to 2009. Following the Mann-Kendall Test at a 95% confidence level the positive trends are significant for all labels. To investigate if the identified increase is a matter of climate change we re-run the model for 1990, 1995, 2000 and 2009 using the emissions for the corresponding year but the meteorology of 2005. The results are added to Figure 5.8a as accordingly coloured dots for each label. Most dots are located on or close to the corresponding trend line. The latter indicates that the increase in sulphate formation efficiency is induced by the change in emissions from 1990 to 2009. The increase is most distinct for the region NLBE with a 61% more efficient sulphate formation in 2009 compared to 1990 followed by CZE (+60%), BAS (+31%) and ROM (+28%). The major driver for the increased sulphate formation efficiency in the model has been an increasing neutralisation of cloud acidity and thus pH over time as diagnosed from the model run.

Sulphate formation is a sink for SO_2 concentrations and therefore the increase in sulphate formation efficiency explains that the decrease in SO_2 concentrations is larger than expected solely from the decrease in SO_2 emissions. Figure 5.8b displays the decrease in

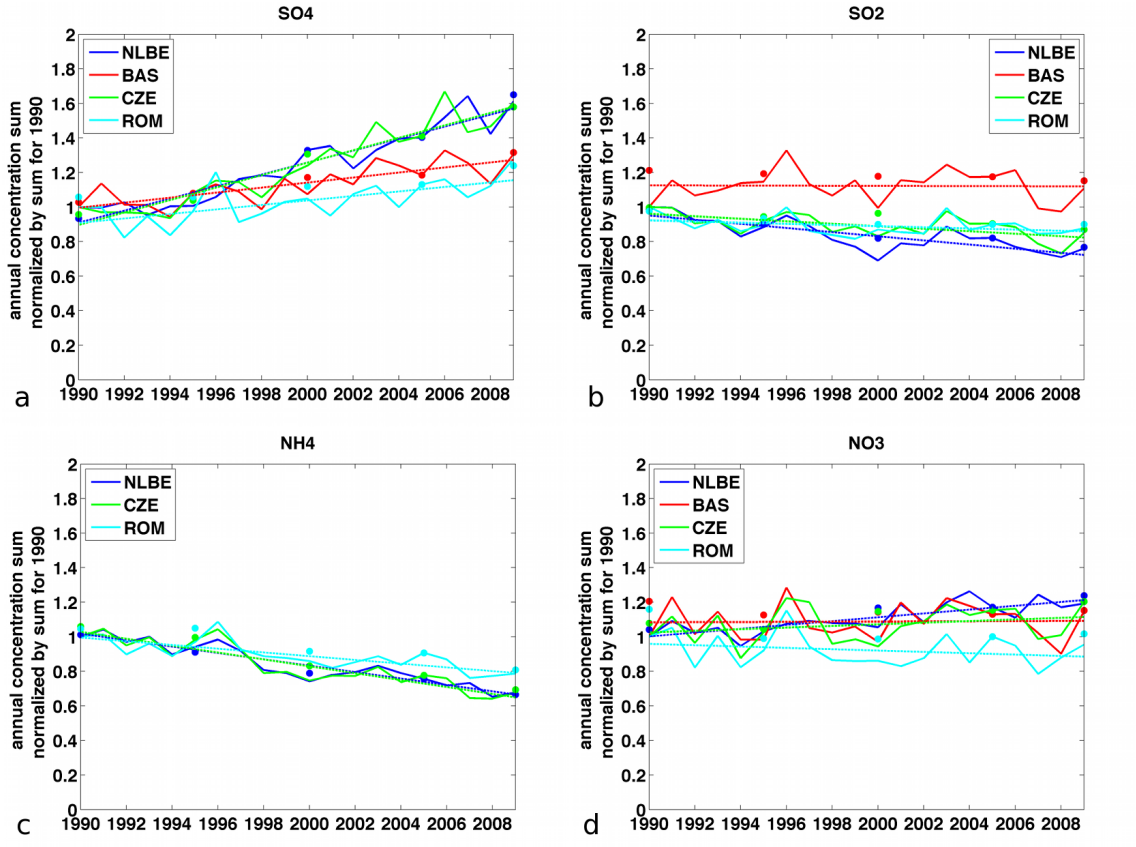

Figure 5.8 Amount of (a) sulphate, (c) ammonium and (d) nitrate (solid lines) formed from 10 ktons of SO_2, NH_3 and NO_2 emissions, respectively, relative to the amount formed in 1990, for the different labels as indicated by the colors, for the entire time period 1990 to 2009. Panel (b) shows the resultant SO_2 per unit SO_2 emission for each label for the 1990 to 2009 time period. The corresponding trend lines are presented as dashed lines. The dots denote results for the runs forced with 2005 meteorology.

SO_2 quantity per unit SO_2 emission showing a negative trend for the time period 1990 to 2009 for all considered labels. However, for the Baltic Sea (BAS) the trend from 1990 to 2009 is not significant following a Mann-Kendall Test at the 95% significance level.

Figure 5.8c reveals a decrease in ammonium formation per unit NH_3 emission for the labels NLBE, CZE and ROM with a reduction of -22% (ROM) to -33% (NLBE and CZE) for 2009 compared to 1990. Following a Mann-Kendall Test at the 95% significance level the trend is significant for these labels. BAS is not included in the figure as there is no NH_3 emission from shipping on the Baltic Sea.

The changes in nitrate formation efficiency from 1990 to 2009 are lower than for sulphate and ammonium (Figure 5.8d). A significant trend has been found for the label NLBE showing an increase in nitrate formation efficiency with an increase of +22% from 1990 to 2009. In the next section the results of the labelling exercise are further discussed.

5.4 Discussion and Conclusions

In this study we presented a dynamic model evaluation of the LOTOS-EUROS CTM to analyse the ability of the model to reproduce the non-linear responses to emission changes and inter-annual variability of SIA and its precursors over Europe from 1990 to 2009. This study presents the first evaluation of the model system over such a long time period. Below we discuss the major findings of the investigation as well as the lessons learned to further evaluate and improve the current study. The latter is important as this study could be seen as an exploratory exercise for the re-analysis of the 1990-2010 period with several model systems within the UNECE-EMEP taskforce on measurement and modelling (TFMM).

With respect to the study design we feel that the simulation of the whole period is a strong point as opposed to using one or several key meteorological years to study the impact of emission changes as it is difficult to choose a meteorological year that is representative for an average year throughout Europe. In addition, through the reanalysis with RACMO2 we have used a consistent set of meteorological data to drive the model for the whole period. The major activity needed to improve the study design is associated with the emission information for the early nineties. Improvements are especially needed for the eastern European countries. Emission estimates for 1990 are relatively uncertain (Granier et al., 2011) as much of the information currently used to estimate emissions is not available (at the same quality) for 1990. Moreover, we have simply used the spatial allocation of the TNO-MACC-2005 dataset and scaled the emission totals per sector back to those of 1990. As a result, the (spatial) representation of e.g. the industrial infrastructure and location of power plants, especially in eastern and parts of central Europe in the period 1990-2000 will not be correct as the infrastructure here during this period still resembled the pre-1990 period. The improvement needed here is highlighted by the higher underestimation of the (primary) pollutants and the lower model skill in the first years of the study period. One could use the spatial allocation of emission inventories built in the nineties to overcome these problems partly. Making a small compromise on the spatial resolution of the data may not be a large problem as model resolution does hardly affect the performance of CTMs for regional assessments (Schaap et al., in prep.).

Complementing the EMEP monitoring data with those of AIRBASE has increased the number of stations with valid time series, especially for the precursor gases. Our visual screening of the measurement data revealed that a large fraction of the stations with long time series were not useable as data quality was obviously an issue. The most frequent peculiarities were shifts in the concentration level, many implausible peaks of short duration, constant value signals over prolonged time periods or concentration regimes below

the detection limit. Most problems were associated to time series of sulphur dioxide. The number of defective time series was highest for the 1990's and decreases considerably towards 2009. The improved quality of observations may also contribute to the improved model performance for the more recent period. A lack of a long-term time series for southern and parts of western and eastern Europe hampered an evaluation across the full European domain. Furthermore, for concentrations of nitrate and ammonium there is a lack of observations with separation between gas- and aerosol-phase. Additional efforts for data mining within European countries could yield larger observational basis for evaluation of the time period. Moreover, generation of a centralized dataset for the specific purpose of evaluation long-term trends could be a means to improve the data quality by incorporation of expertise from the data providers.

The operational model evaluation showed that the day-to-day variability, as well as the seasonal and the inter-annual variability are satisfactorily simulated for all components. Within a multi-model trend assessment study Collette et al. (2011) presented the ability of 6 state of the art CTMs to simulate the seasonal cycle of amongst others SO_2, SO_4, NO_2, TNO_3 and TNH_4 concentrations at European rural background stations for the time period 1998-2007. A qualitative comparison of our model results to those presented in Collette et al. (2011) shows that LOTOS-EUROS performs comparatively well in simulating the observed seasonal cycles. Operational model evaluations within AQMEII (Solazzo et al., 2013) and EURODELTA (e.g. Vautard et al., 2009; Schaap et al., in prep.) showed that LOTOS-EUROS model skill is in line with those of models like EMEP and CHIMERE. Although LOTOS-EUROS was able to capture a large part of the observed variability in the considered sulphur and nitrogen compounds from 1990-2009, some shortcomings have been identified.

A systematic underestimation of sulphate concentrations is observed throughout the whole study. This could be connected to a lack of good representation of clouds, which is needed for the recently implemented cloud chemistry scheme (Banzhaf et al., 2012; Wichink Kruit et al., 2012). The method used to pass the information of the liquid water content vertical distribution from the vertically high resolved meteorological driver to LOTOS-EUROS running on 5 vertical layers may need further improvements. Furthermore, uncertainties in ammonia emissions (magnitude, space and time) may play an important role as ammonia provides the neutralising capacity of cloud droplets and constrains cloud water acidity. Cloud pH regulates the oxidation pathways of sulphur dioxide and therewith the formation efficiency of sulphate (Fowler et al., 2007). According to EMEP (2009) the uncertainty in magnitude of annual ammonia emission totals amounts about $\pm 30\%$ in Europe. Furthermore, the seasonal and diurnal variation in ammonia emissions are still uncertain and may differ regionally as a function of climatic conditions and in time

due to changing agricultural practices and regulations (Geels et al., 2012) which is not accounted for in most state of the art CTMs including LOTOS-EUROS. The underestimation of springtime episodes for sulphate connected to stable atmospheric conditions is observed in several years. In a case study for 2003 this feature was identified to be a common challenge for European CTMs as meteorological drivers tend to fail to represent these stable weather conditions satisfactorily (Stern et al., 2008).
Despite the mentioned shortcomings in the representation of the sulphur components, the model captures the non-linearity observed in the response to the emission changes. Investigating the observed trends at the EMEP monitoring sites between 1980 and 2009, Tørseth et al. (2012) showed that SO_2 trends indicate larger reductions than the reductions of SO_2 emissions while those of SO_4 concentrations are comparatively lower. These findings are very close to our analysis incorporating AIRBASE stations and earlier analyses by e.g. Løvblad et al. (2004). Fagerli and Aas (2008) presented an investigation on the observed trends of nitrogen from 1980-2003 at EMEP sites showing that the trends in TNO_3 concentrations were significantly lower than the trends in precursor emissions which matches the outcome of the here presented study. Using a source apportionment module trends in formation efficiency of SIA have been quantified adding to the explanation of the non-linearities described above. The exercise revealed an increase of sulphate formation efficiency and a decrease in ammonium formation efficiency for all regions considered. The major driver for the increased sulphate formation efficiency in the model was the increasing neutralisation of cloud acidity and thus pH over time. The modelled trend is supported by the observed increase in precipitation pH during the last decades (Løvblad et al., 2004; Tørseth et al., 2012). Hence, the pH dependent aqueous-phase sulphate formation by ozone is more effective (Redington et al., 2009; Banzhaf et al., 2012; 2013). In addition, the H_2O_2/SO_2 ratio increases which also leads to more efficient formation. Finally, the simultaneous NO_x and SO_2 emission reductions may lead to increased OH levels, which counteract the sulphate reduction as the rate of homogeneous oxidation of SO_2 is increased (Tarrasón et al., 2003; Derwent et al., 2009). The decrease in ammonium formation efficiency is related to the overall decrease in sulphate concentrations from 1990 to 2009, which leads to less ammonium sulphate formation. The strong decrease in sulphate concentrations from 1990-2009 increases the availability of ammonia for the formation of ammonium nitrate (Tarrasón et al., 2003; Fagerli and Aas, 2008). Hence, this could explain the change in nitrate formation efficiency for the Benelux region. Another reason for changes in the nitrate formation efficiency could be a change in the oxidant levels (Fowler et al., 2005; Fagerli and Aas, 2008). A decrease in NO_x emissions leads to a decrease of O3 titration and therewith to an increased rate of NO_2 to NO_3- conversion. The increased rate of NO_2 to NO_3- conversion could also be induced by higher

availability of oxidants that previously were consumed in the oxidation of SO_2 or other pollutants. A more detailed budget analysis is advised to study the changes in chemical regime.

Furthermore, LOTOS-EUROS underestimates the observed NO_2 concentrations on average by 15% throughout the whole time period. The underestimation is induced by modelled concentrations at central and eastern European stations while the model performs considerably better at northern European stations. Part of the underestimation may be explained by the measurement devices used in the networks. Oxidized nitrogen compounds such as HNO_3, PAN and other organic nitrates can significantly interfere with the measurements by contributing to the NO_2 signal (Steinbacher et al., 2007). In the beginning of the 90s again the uncertainties in the emission input may explain part of the bias in NO_2 concentrations. After 2000 the bias increases inducing an overestimation of the observed negative trend in NO_2 concentrations by the model. It has been investigated if the decrease in model performance after 2000 is connected to the increased NO_2/NO ratio of traffic emissions by comparing simulations with 3% and 20% direct NO_2 emissions from diesel fuelled vehicles. These runs showed a slight increase in the rural background close to large cities (up to 2 %), whereas in more remote areas NO_2 levels declined by about 0.5% due to the faster oxidation to nitric acid. Hence, this effect does not contribute to the mismatch between observed and modelled trends. The model inter-comparison study by Collette et al. (2011) has shown that 4 out of 6 models underestimate NO_2 concentrations at European rural background stations for the time period 1998-2007. Moreover, three of these models also show stronger trends than observed. A recent study using satellite retrieved NO_2 columns by OMI and in-situ data for the period 2005-2012 also showed lower trends in observations than in the European emission inventories (Curier et al., 2014). Hence, more research is needed to assess if the mismatch in the NO_2 trend is a model issue or if it can be attributed to too strong declines in the emission data.

The implemented emission abatement strategies for SIA precursors have led to concentration reductions over Europe even though for some secondary species the achieved concentration reduction is lower than corresponding precursor reductions would suggest. The LOTOS-EUROS model is able to capture most of the seasonal and interannual variability of SIA and its precursors' concentrations and their non-linear responses to emission changes for the time period 1990-2009. The largest part of the decline is observed in the 1990's. Smaller concentration changes and more non-significant trends are observed and modelled between 2000-2009. The smaller, non-significant trends between 2000-2009 do not necessarily imply that there is no trend present in the data, but only that we are not sure at the 95% confidence level (Nuzzo, 2014). It highlights that the validation of emission trends remains a challenge, in particular the ability to separate relatively smaller

trends from interannual variability (Koumoutsariset al., 2008; Voulgarakis et al., 2010). This study has revealed many interesting features and resulting research questions that can be approached making further use of the 20 years model simulation. Specific attention is needed to address the trends in NO_x and tackle the underestimation in sulphate and other pollutants in eastern Europe. As a next step we will analyse the ability of the model to reproduce the trends modelled for ozone as new analyses have shown shifts in seasonal variability over time (Parrish et al., 2013). Moreover, trends in wet and dry deposition should be investigated to further complement the budget analysis. We have found that the trends for SIA are emission-driven. Next, a quantification of trends induced by meteorological variability as reported by Andersson et al. (2007) is planned. Furthermore, special attention in further investigations will be given to uncertainties in the emission input by performing sensitivity studies on emission timing (dependency on meteorology etc.).

In short, we presented a successful dynamic model evaluation of the LOTOS-EUROS CTM aimed at SIA formation in Europe between 1990 and 2009. In general, the model is able to capture the non-linearity as detected in the observations. A source apportionment analysis has confirmed that changes in the formation efficiency due to changes in the chemical regime are at the basis of this non-linearity.

Acknowledgements

This work was funded by TNO within the framework of the R&D Project 3710 63 246 -'PINETI' (Pollutant Input and Ecosystem Impact) - funded by the Federal Environment Agency (Umweltbundesamt, Germany). Further support was provided by Freie Universität Berlin. We would like to acknowledge the data providers in the ECA&D project. Klein Tank, A.M.G. and Co-authors, 2002. Daily dataset of 20th-century surface air temperature and precipitation series for the European Climate Assessment. Int. J. of Climatol., 22, 1441-1453. Data and metadata available at http://eca.knmi.nl. Surface observations were obtained through the AIRBASE (EEA) and EBAS (NILU) repositories.

References

Amann, M., Cofala, J., Heyes, C., Klimont, Z. and Schöpp, W.: The RAINS Model: A Tool for Assessing Regional Emission Control Strategies in Europe. Pollution Atmosphérique 4. Paris, France, 1999.

Amann, M., Bertok, I., Borken-Kleefeld, J., Cofala, J., Heyes, C., Höglund-Isaksson, L., Klimont, Z., Nguyen, B., Posch, M., Rafaj, P., Sandler, R., Schöpp, W., Wagner, F., Winiwarter, W.: Cost-effective control of air quality and greenhouse gases in Europe: Modelling and policy applications, Environ. Modell. and Softw., Vol. 26, pp. 1489-1501, 2011.

Andersson, C., Langner, J., Bergstrom, R.: Interannual variations and trends in air pollution over Europe due to climate variability during 1958-2001 simulated with a regional CTM coupled to the ERA-40 reanalysis, Tellus 59B, 77-98, 2007.

Appel, K. W., Gilliam, R. C., Davis, N., Zubrow, A., and Howard, S. C.: Overview of the Atmospheric Model Evaluation Tool (AMET) v1.1 for evaluating meteorological and air quality models, Environ. Modell. Softw., 26, 434-443, 2011.

Banzhaf S., Schaap M., Kerschbaumer A., Reimer E., Stern R., van der Swaluw E., Builtjes P.: Implementation and evaluation of pH-dependent cloud chemistry and wet deposition in the chemical transport model REM-Calgrid, Atmos. Environ., 49, 378-390, 2012.

Banzhaf, S., Schaap, M., Wichink Kruit, R.J., Denier van der Gon, H. A. C., Stern, R., and Builtjes, P. J. H.: Impact of emission changes on secondary inorganic aerosol episodes across Germany, Atmos. Chem. Phys., 13, 11675-11693, doi:10.5194/acp-13-11675-2013, 2013.

Berglen, T.F., Myhre, G., Isaksen, I.S.A., Vestreng, V., Smith, S.J.: Sulphate trends in Europe: are we able to model the recently observed decrease?, Tellus 59, 773, 2007.

Bobbink, R., Hornung, M., and Roelofs, J. M.: The effects of airborne pollutants on species diversity in natural and semi-natural European vegetation, J. Ecol., 86, 717-738, doi:10.1046/j.1365-2745.1998.8650717.x, 1998.

Bond, T.C., Doherty, S.J., Fahey, D.W., Forster, P.M., Berntsen, T., DeAngelo, B.J., Flanner, M.G., Ghan, S., Karcher, B., Koch, D., Kinne, S., Kondo, Y., Quinn, P.K., Sarofim, M.C., Schultz, M.G., Schulz, M., Venkataraman, C., Zhang, H., Zhang, S., Bellouin, N., Guttikunda, S.K., Hopke, P.K., Jacobson, M.Z., Kaiser, J.W., Klimont, Z., Lohmann, U., Schwarz, J.P., Shindell, D., Storelvmo, T., Warren, S.G., Zender, C.S.: Bounding the role of black carbon in the climate system: a scientific assessment. Journal of Geophysical Research e Atmospheres 118, 5380-5552, 2013.
Carslaw, D., Beevers, S., Westmoreland, E., Williams, M., Tate, J., Murrells, T., Stedman, J., Li, Y., Grice, S., Kent, A., and Tsagatakis, I.: Trends in NO_x and NO_2 emissions and ambient measurements in the UK, Defra, London, 2011.

Civerolo, K., Hogrefe, C., Zalewsky, E., Hao, W., Sistla, G., Lynn, B., Rosenzweig, C., Kinney, P.L.: Evaluation of an 18-year CMAQ simulation: seasonal variations and long-term temporal changes in sul-

fate and nitrate. Atmos. Environ. 44, 3745-3752, 2010.

Colette, A., Granier, C., Hodnebrog, Ø., Jakobs, H., Maurizi, A., Nyiri, A., Bessagnet, B., D'Angiola, A., D'Isidoro, M., Gauss, M., Meleux, F., Memmesheimer, M., Mieville, A., Rouil, L., Russo, F., Solberg, S., Stordal, F., and Tampieri, F.: Air quality trends in Europe over the past decade: a first multi-model assessment, Atmos. Chem. Phys., 11, 11657-11678, doi: 10.5194/acp-11-11657-2011, 2011.

Curier, R.L., Kranenburg, R., Segers, A.J.S., Timmermans, R.M.A., Schaap, M.: Synergistic use of OMI NO_2 tropospheric columns and LOTOS-EUROS to evaluate the NO_x emission trends across Europe. Remote Sensing of Environment, 2014. Accepted for publication.

Cuvelier C., Thunis P., Vautard R., Amann M., Bessagnet B., Bedogni M., Berkowicz R., Brandt J., Brocheton F., Builtjes P., Carnavale C., Coppalle A., Denby B., Douros J., Graf A., Hellmuth O., Hodzic A., Honoré C., Jonson J., Kerschbaumer A., de Leeuw F., Minguzzi E., Moussiopoulos N., Pertot C., Peuch V.H., Pirovano G., Rouil L., Schaap M., Stern R., Tarrasón L., Vignati E., Volta M., White L., Wind P., Zuber A.: CityDelta: A model intercomparison study to explore the impact of emission reductions in European cities in 2010. Atmos. Environ., 41, 189-207, 2007.

Dee, D.P., and 35 co-authors, 2011. The ERA-Interim reanalysis: configuration and performance of the data assimilation system. Q. J. R. Meteorol. Soc., 137, 553-597. doi: 10.1002/qj.828

Denier van der Gon, H. A. C., Visschedijk, A., van den Brugh, H., and Dröge, R.: F&E Vorhaben: Strategien zur Verminderung der Feinstaubbelastung - PAREST: A high resolution European emission data base for the year 2005, TNO-Report, TNO-034-UT-2010-01895-RPT-ML, Utrecht, 2010.

Dennis, R., Fox, T., Fuentes, M., Gilliland, A., Hanna, S., Hogrefe, C., Irwin, J., Rao, S.T., Scheffe, R., Schere, K., Steyn, D., Venkatram, A.: A framework for evaluating regional-scale numerical photochemical modeling systems. Environ. Fluid. Mech., 10, 471-489, 2010.

Derwent, R. G., Witham, C. J., Redington, A. L., Jenkin, M., Stedman, J, Yardley, R., and Hayman, G.: Particulate matter at a rural location in southern England during 2006: model sensitivities to precursor emissions. Atmos. Environ., 43, 689-696, 2009.

EC: Directive 2001/42/EC of the European Parliament and of the Council of 27 June 2001 on the assessment of the effects of certain plans and programmes on the environment, 2001.

EEA: Assessment of ground-level ozone in EEA member countries, with a focus on long-term trends, Technical report No. 7/2009, European Environment Agency, Copenhagen, 2009.

EEA: Air quality in Europe - 2012 report, EEA report No. 4/2012, European Environment Agency, Copenhagen, 2012.

EMEP: Transboundary, acidification, eutrophication and ground level ozone in Europe in 2007 EMEP August 2009, ISSN 1504-6192, 2009.

EMEP/CCC: Manual for sampling and chemical analysis, EMEP/CCC Report 1/95 (Last rev. 2001), Norwegian Institute for Air Research, Kjeller, 2001.

Erisman, J. W., van Pul, A., and Wyers, P.: Parametrization of surface-resistance for the quantification of atmospheric deposition of acidifying pollutants and ozone. Atmos. Environ., 28, 2595-2607, 1994.

Erisman, J. W. and Schaap, M.: The need for ammonia abatement with respect to secondary PM reductions in Europe. Environ. Pollut., 129, 159-163, 2004.

Fagerli, H. and Aas, W.: Trends of nitrogen in air and precipitation: Model results and observations at EMEP sites in Europe, 1980-2003, Environ. Pollut., 154, 448-461, 2008.

Fahey, K. M., and S. N. Pandis, Size-resolved aqueous-phase atmospheric chemistry in a three dimensional chemical transport model, J. Geophys. Res., 108 (D22), 4690, doi:10.1029/2003JD003564, 2003.

Forster, P., Ramaswamy, V., Artaxo, P., Berntsen, T., Betts, R., Fahey, D. W., Haywood, J., Lean, J., Lowe, D. C., Myhre, G., Nganga, J., Prinn, R., Raga, G., Schulz, M., and Van Dorland, R.: Changes in atmospheric constituents and in radiative forcing, in: Climate Change 2007: The Physical Science Basis, Contribution of Working Group I to the Fourth Assessment Report of the Intergovernmental Panel on Climate Change, edited by: Solomon, S., Qin, D., Manning, M., Chen, Z., Marquis, M., Averyt, K. B., Tignor, M., and Miller, H. L., Cambridge University Press, Cambridge, UK, and New York, USA, 2007.

Fountoukis C. and Nenes A.: ISORROPIAII: A computationally efficient thermodynamic equilibrium model for Kalium - Calcium - Magnesium - Ammonium - Sodium - Sulfate - Nitrate - Chloride - Water aerosols. Atmos. Chem. and Phys., 7 (17), 4639-4659, 2007.

Fowler, D., Müller, J., Smith, R. I., Cape, J. N., and Erisman, J.W.: Nonlinearities in source receptor relationships for sulfur and nitrogen compounds, Ambio., 34, 41-46, 2005.

Fowler, D., Smith, R., Müller, J., Cape, J. N., Sutton, M., Erisman, J. W., and Fagerli, H.: Long-term trends in sulphur and nitrogen deposition in Europe and the cause of nonlinearities, Water Air Soil Poll., 7, 41-47, 2007.

Geels, C., Andersen, H. V., Ambelas Skjøth, C., Christensen, J. H., Ellermann, T., Løfstrøm, P., Gyldenkærne, S., Brandt, J., Hansen, K. M., Frohn, L. M., and Hertel, O.: Improved modelling of atmospheric ammonia over Denmark using the coupled modelling system DAMOS, Biogeosciences, 9, 2625-2647, doi:10.5194/bg-9-2625-2012, 2012.

Granier, C., Bessagnet, B., Bond, T., D'Angiola, A., van der Gon, H. D., Frost, G. J., Heil, A., Kaiser, J. W., Kinne, S., Klimont, Z., Kloster, S., Lamarque, J.-F., Liousse, C., Masui, T., Meleux, F., Mieville, A., Ohara, T., Raut, J. C., Riahi, K., Schultz, M. G., Smith, S. J., Thompson, A., van Aardenne, J., van der Werf, G. R., and van Vuuren, D. P.: Evolution of anthropogenic and biomass burning emissions of air pollutants at global and regional scales during the 1980-2010 period, Climatic Change, 109, 163-190, doi: 10.1007/s10584-011-0154-1, 2011.

Grennfelt, P. and Hov, Ø.: Regional air pollution at a turning point. Ambio 34(1), 2-10, 2005.

Hass H. Builtjes P.J.H, Simpson D., Stern R.: Comparison of model results obtained with several European regional air quality models. Atmospheric Environment.,31, 3259-3279, 1997.

Hass, H., van Loon, M., Kessler, C., Stern, R., Matthijsen, J., Sauter, F., Zlatev, Z., Langner, J., Foltescu, V., and Schaap, M.: Aerosol Modelling: Results and Intercomparison from 15 European Regional-scale Modelling Systems, EUROTRAC-2 Special report, Eurotrac-ISS, Garmisch Partenkirchen, Germany, 2003.

Hipel, K. W. and McLeod, A. I.: Time Series Modelling of Water Resources and Environmental Systems, Elsevier, Amsterdam, 2005.

Hjellbrekke, A. G. and Fjæraa, A. M.: Data Report 2009, Acidifying and eutrophying compounds and particulate matter, Norwegian Institute for Air Research, Kjeller, EMEP/CCC-Report 1/2011, 2011.

Kendall, M. G.: Rank Auto Correlation Methods, 4 ed., Griffin, Oxford, 1976. Kjellström, E., and Giorgi F.: Introduction to the special issue on 'Regional climate model evaluation and weighting'. Clim. Res., 44, 117-119, 2010.

Kjellström E., Boberg F., Castro M., Christensen H.J., Nikulin G., Sánchez E.: Daily and monthly temperature and precipitation statistics as performance indicators for regional climate models. Clim. Res., 44, 135-150, 2010.

Klein Tank, A.M.G, Wijngaard, J.B., Können, G.P., Böhm, R., Demarée, G., Gocheva, A., Mileta, M., Pashiardis, S., Hejkrlik, L., Kern-Hansen, C., Heino, R., Bessemoulin, P., Müller-Westermeier, G., Tzanakou, M., Szalai, S., Pálsdóttir, T., Fitzgerald, D., Rubin, S., Capaldo, M., Maugeri, M., Leitass, A., Bukantis, A., Aberfeld, R., van Engelen, A.F.V., Forland, E., Mietus, M., Coelho, F., Mares, C., Razuvaev, V., Nieplova, E., Cegnar, T., Antonio López, J., Dahlström, B., Moberg, A., Kirchhofer, W., Ceylan, A., Pachaliuk, O., Alexander, L.V., Petrovic, P.: Daily dataset of 20th-century surface air temperature and precipitation series for the European Climate Assessment. International Journal of Climatology 22: 1441-1453, 2002.

Klok, E. J. and Klein Tank, A. M. G.: Updated and extended European dataset of daily climate observations, International Journal of Climatology, 29(8), 1182-1191, DOI:10.1002/joc.1779, 2009.

Koeble, R., Seufert, G.: Novel maps for forest tree species in Europe. Proceedings of the 539 conference 'a changing atmosphere', Sept 17-20, Torino, Italy, 2001.

Kotlarski, S., Keuler, K., Christensen, O. B., Colette, A., Déqué, M., Gobiet, A., Goergen, K., Jacob, D., Lüthi, D., van Meijgaard, E., Nikulin, G., Schär, C., Teichmann, C., Vautard, R., Warrach-Sagi, K., Wulfmeyer, V.: Regional climate modeling on European scales: A joint standard evaluation of the EURO-CORDEX RCM ensemble, Geosci. Model Dev. Discuss., 7, 217-293, doi:10.5194/gmdd-7-217-2014, 2014.

Konovalov, I. B., Beekmann, M., Richter, A., Burrows, J. P., and Hilboll, A.: Multi-annual changes of NO_x emissions in megacity regions: nonlinear trend analysis of satellite measurement based estimates, Atmos. Chem. Phys., 10, 8481-8498, doi:10.5194/acp-10-8481-2010, 2010.

Koumoutsaris, S., Bey, I., Generoso, S., and Thouret, V.: Influence of El Nino-Southern Oscillation on the interannual variability of tropospheric ozone in the northern midlatitudes, J. Geophys. Res., 113, D19301, doi:10.1029/2007JD009753, 2008.

Kranenburg, R., Segers, A.J., Hendriks, C., Schaap, M.: Source apportionment using LOTOS EUROS: module description and evaluation, Geosci. Model Dev., 6, 721-733, doi:10.5194/gmd-6-721-2013, 2013.

Lenderink G., Van den Hurk B., Van Meijgaard E., Van Ulden A. P., Cuijpers J.: Simulation of present-day climate in RACMO2: first results and model developments, KNMI technical report TR 252, De Bilt, The Netherlands, 2003.

Løvblad, G., Tarrasón, L., Tørseth, K., and Dutchak, S.: EMEP Assessment Part I: European Perspective. Norwegian Meteorological Institute, P.O. Box 43, N-313 Oslo, Norway, 2004.

Manders, A. M. M., van Ulft, B., van Meijgaard, E., and Schaap, M.: Coupling of the air quality model LOTOS-EUROS to the climate model RACMO, Dutch National Research Programme Knowledge for Climate Technical Report KFC/038E/2011, ISBN 978-94-90070-00-7, 2011.

Manders A.M.M., van Meijgaard E., Mues A.C., Kranenburg R., van Ulft L.H., Schaap M., 2012. The impact of differences in large-scale circulation output from climate models on the regional modeling of ozone and PM. Atmos. Chem. Phys., 12, 9441-9458, 2012.

Martensson E.M., Nilsson E.D., de Leeuw G., Cohen L.H., Hansson H.C.: Laboratory simulations and parameterization of the primary marine aerosol production. J. Geophys. Res. 108, 2003.

McKeen, S., Wilczak, J., Grell, G., Djalalova, I., Peckham, S., Hsie, E.-Y., Gong, W., Bouchet, V., Menard, S., Moffet, R., McHenry, J., McQueen, J., Tang, Y., Carmichael, G. R., Pagowski, M., Chan, A., Dye, T., Frost, G., Lee, P., and Mathur, R.: Assessment of an ensemble of seven real-time ozone forecasts over eastern North America during the summer of 2004, J. Geophys. Res. D Atmos., 110, 1-16, 2005.

Meijgaard E. van, van Ulft, L. H., van de Berg, W.J., Bosveld, F.C., van den Hurk, B.J.J.M., Lenderink, G., Siebesma, A.P.: The KNMI regional atmospheric climate model RACMO version 2.1, KNMI, Technical report, TR-302, 2008.

Meijgaard E. van, van Ulft, L.H, Lenderink, G., de Roode, S.R., Wipfler, L., Boers, R. and Timmermans, R.M.A.: Refinement and application of a regional atmospheric model for climate scenario calculations of Western Europe, Climate changes Spatial Planning publication: KvR 054/12, ISBN/EAN 978-90-8815-046-3, pp 44, 2012.

Monahan E.C., Spiel D.E., Davidson K.L.: A model of marine aerosol generation via whitecaps and wave disruption. In Oceanic Whitecaps and their role in air/sea exchange, edited by Monahan, E.C, and Mac

Niocaill, G., pp. 167-174, D. Reidel, Norwell, Mass., USA, 1986.

Mues, A., Manders, A., Schaap, M., van Ulft, L.H., van Meijgaard, E., Builtjes, P.: Differences in particulate matter concentrations between urban and rural regions under current and changing climate conditions, Atmos. Environ., 80, 232-247, 2013.

Nuzzo, R.: Scientific method: Statistical errors, Nature, 506, 150-152, doi:10.1038/506150a, 2014. Parrish, D.D., Law, K.S., Staehelin, J., Derwent, R., Cooper, O.R., Tanimoto, H., Volz Thomas, A., Gilge, S., Scheel, H.E., Steinbacher, M., Chan, E.: Lower tropospheric ozone at northern midlatitudes: changing seasonal cycle. Geophys. Res. Lett. 40, 1631-1636, 2013.

Pouliot, G., Pierce, T, Denier van der Gon, H. , Schaap, M., Nopmongcol, U., Comparing Emissions Inventories and Model-Ready Emissions Datasets between Europe and North America for the AQMEII Project. Atmospheric Environment (AQMEII issue) 53, 4-14, 2012.

Putaud, J.-P., Van Dingenen, R., Alastuey, A., Bauer, H., Birmili,W., Cyrys, J., Flentje, H., Fuzzi, S., Gehrig, R., Hansson, H.C., Harrison, R.M., Herrmann, H., Hitzenberger, R., Hüglin, C., Jones, A.M., Kasper-Giebl, A., Kiss, G., Kousa, A., Kuhlbusch, T.A.J., Löschau, G., Maenhaut, W., Molnar, A., Moreno, T., Pekkanen, J., Perrino, C., Pitz, M., Puxbaum, H., Querol, X., Rodriguez, S., Salma, I., Schwarz, J., Smolik, J., Schneider, J., Spindler, G., ten Brink, H., Tursic, J., Viana, M., Wiedensohler, A., Raes, F.: A European aerosol phenomenology - 3: physical and chemical characteristics of particulate matter from 60 rural, urban, and kerbside sites across Europe. Atmospheric Environment 44, 1308-1320, 2010.

Redington, A. L., Derwent, R. G., Witham, C. S., and Manning, A. J.: Sensitivity of modelled sulphate and nitrate aerosol to cloud, pH and ammonia emissions, Atmos. Environ., 43, 20, 3227-3234, 2009.

Schaap, M., van Loon, M., ten Brink, H.M., Dentener, F.D., Builtjes, P.J.H.: Secondary inorganic aerosol simulations for Europe with special attention to nitrate. Atmos. Chem. and Phys., 4, 857-874, 2004.

Schaap, M., Timmermans, R.M.A., Sauter, F.J., Roemer, M., Velders, G.J.M., Boersen, G.A.C., Beck, J.P., Builtjes, P.J.H.: The LOTOS-EUROS model: description, validation and latest developments, International Journal of Environment and Pollution, 32 (2), 270-289, 2008.

Schaap, M., Manders, A. A. M., Hendriks, E. C. J., Cnossen, J. M., Segers, A. J., Denier van der Gon, H. A. C., Jozwicka, M., Sauter, F. J., Velders, G. J. M., Matthijsen, J., and Builtjes, P. J. H.: Regional Modelling of Particulate Matter for the Netherlands, PBL report 500099008, Bilthoven, The Netherlands, 2009.

Schaap, M., Cuvelier, C., Bessagnet, B., Hendriks, C., Baldesano, J., Colette, A., Thunis, P., Karam, D., Fagerli, H., Graff, A., Kranenburg, R., Nyiri, A., Pay, M.T., RouÃ¯l, L., Schulz, M., Simpson, D., Stern, R., Terrenoire, E., Wind, P.: Performance of European chemistry transport models as function of horizontal resolution. To be submitted to Atmos. Chem. and Phys..

Simpson, D., Fagerli, H., Jonson, J. E., Tsyro, S., Wind, P., and Tuovinen, J.-P.: Transboundary Acidi-

fication, Eutrophication and Ground Level Ozone in Europe, Part 1: Unified EMEP Model Description, EMEP Report 1/2003, Norwegian Meteorological Institute, Oslo, Norway, 2003.

Solazzo, E., Bianconi, R., Vautard, R., Wyat Appel, K., Moran, M. D., Hogrefe, C., Bessagnet, B., Brandt, J., Christensen, J. H., Chemel, C., Coll, I., Denier van der Gon, H. A. C., Ferreira, J., Forkel, R., Francis, X. V., Grell, G., Grossi, P., Hansen, A. B., Jericevic, A., Kraljevic, L., Miranda, A. I., Nopmongcol, U., Pirovano, G., Prank, M., Riccio, A., Sartelet, K. N., Schaap, M., Silver, J. D., Sokhi, R. S., Vira, J., Werhahn, J., Wolke, R., Yarwood, G., Zhang, J., Rao, S. T., and Galmarini, S.: Model evalution and ensemble modelling of surface level ozone in Europe and North America in the context of AQMEII, Atmos. Environ., 53, 60-74, 2012a.

Solazzo, E., Bianconi, Pirovano, G., Matthias, V., Vautard, R., Moran, M. D., Wyat Appel, K., Bessagnet, B., Brandt, J., Christensen, J. H., Chemel, C., Coll, I., Ferreira, J., Forkel, R., Francis, X. V., Grell, G., Grossi, P., Hansen, A. B., Miranda, A. I., Nopmongcol, U., Prank, M., Sartelet, K. N., Schaap, M., Silver, J. D., Sokhi, R. S., Vira, J., Werhahn, J., Wolke, R., Yarwood, G., Zhang, J., Rao, S. T., and Galmarini, S.: Operation model evaluation for particulate matter in Europe and North America in the context of AQMEII. Atmos. Environ., 53, 75-92, 2012b.

Steinbacher, M., Zellweger, C., Schwarzenbach, B., Bugmann, S., Buchmann, B., Ordónez, C., Prévot, A. S. H., and Hueglin, C.: Nitrogen oxide measurements at rural sites in Switzerland: bias of conventional measurement techniques, J. Geophys. Res., 112, D11307, doi:10.1029/2006JD007971, 2007.

Steinbrecher, R., Smiatek, G., Koeble, R., Seufert, G., Theloke, J., Hauff, K., Ciccioli, P., Vautard, R., and Curci, G.: Intra- and inter-annual variability of VOC emissions from natural and semi-natural vegetation in Europe and neighbouring countries. Atmos. Environ., 43, 1380-1391, doi:10.1016/j.atmosenv.2008.09.072, 2009.

Stern, R., Builtjes, P., Schaap, M., Timmermans, R., Vautard, R., Hodzic, A., Memmesheimer, M., Feldmann, H., Renner, E., Wolke, R., and Kerschbaumer, A.: A model inter-comparison study focussing on episodes with elevated PM_{10} concentrations, Atmos. Environ., 42, 4567-4588, 2008.

Tarrasón, L., Johnson, J.E., Fagerli, H., Benedictow, A., Wind, P., Simpson, D., Klein, H.: EMEP Status Report 1/2003 - Part III: Source-Receptor Relationships, Transboundary acidification, eutrophication and ground level ozone in Europe, Norwegian Meteorological Institute, Oslo, 2003.

Thunis, P., Georgieva, E., and Pederzoli, A.: A tool to evaluate air quality model performances in regulatory applications, Environ. Model. Softw., 38, 220-230, doi:10.1016/j.envsoft.2012.06.005, 2012.

Tørseth K., Aas W., Breivik K., Fjæraa A.M., Fiebig M., Hjellbrekke A.G., Lund Myhre C., Solberg S., Yttri K.E.: Introduction to the European Monitoring and Evaluation Programme (EMEP) and observed atmospheric composition change during 1972-2009. Atmos. Chem. and Phys., 12, 5447-5481, 2012.

UNECE: The 1999 Gothenburg Protocol to Abate Acidification, Eutrophication and Ground level Ozone UNECE, Gothenburg, Report, 1999.

Van Loon M., Vautard R., Schaap M., Bergström R., Bessagnet B., Brandt J., Builtjes P. J. H., Christensen J. H., Cuvelier K., Graf A., Jonson J. E., Krol M., Langner J., Roberts P., Rouil L., Stern R., Tarrasón L., Thunis P., Vignati E., White L., Wind P.: Evaluation of long term ozone simulations from seven regional air quality models and their ensemble average, Atmos. Environ., 41, 2083-2097, 2007.

Vautard, R., van Loon, M., Schaap, M., Bergström, R., Bessagnet, B., Brandt, J., Builtjes, P. J. H., Christensen, J. H., Cuvelier, C. , Graff, A., Jonson, J. E., Krol, M., Langner, J., Roberts, P., Rouil, L. , Stern, R., Tarrasón, L., Thunis, P., Vignati, E., White, L., Wind, P.: Is regional air quality model diversity representative of uncertainty for ozone simulation? Geophysical Research Letters 33, L24818, doi:10.1029/2006GL027610, 2007.

Vautard, R., Schaap, M., Bergström, R., Bessagnet, B., Brandt, J., Builtjes, P. J. H., Christensen, J. H., Cuvelier, C., Foltescu, V., Graff, A., Kerschbaumer, A., Krol, M., Roberts, P., Rouil, L., Stern, R., Tarrasón, L., Thunis, P., Vignati, E., and Wind, P.: Skill and uncertainty of a regional air quality model ensemble, Atmos. Environ., 43, 4822-4832, 2009.

Vautard, R., Gobiet, A., Jacob, D., Belda, M., Colette, A., Déqué, M., Fernández, J., García-Díez, M., Goergen, K., Güttler, I., Halenka, T., Karacostas, T., Katragkou, E., Keuler, K., Kotlarski, S., Mayer, S., Meijgaard, E., Nikulin, G., Patarčić, M., Scinocca, J., Sobolowski, S., Suklitsch, M., Teichmann, C., Warrach-Sagi, K., Wulfmeyer, V., Yiou, P.: The simulation of European heat waves from an ensemble of regional climate models within the EURO-CORDEX project, Clim. Dyn., 41, 255-2575, doi:10.1007/s00382-013-1714-z, 2013.

Voulgarakis, A., N.H. Savage, O. Wild, P. Braesicke, P.J. Young, G.D. Carver, and J.A. Pyle: Interannual variability of tropospheric composition: The influence of changes in emissions, meteorology and clouds. Atmos. Chem. Phys., 10, 2491-2506, doi:10.5194/acp-10-2491-2010, 2010.

Wagstrom, K. M., Pandis, S. N., Yarwood, G., Wilson, G. M., Morris, R. E.: Development and application of a computationally efficient particulate matter apportionment algorithm in a three dimensional chemical transport model, Atmos. Environ., 42, 5650- 5659, 2008.

Walcek, C. J.,: Minor flux adjustment near mixing ratio extremes for simplified yet highly accurate monotonic calculation of tracer advection. Journal of Geophysical Research D: Atmosphere 105 (D7), 9335-9348, 2000. Weijers, E. P., Schaap, M., Nguyen, L., Matthijsen, J., Denier van der Gon, H. A. C., ten Brink, H. M., and Hoogerbrugge, R.: Anthropogenic and natural constituents in particulate matter in the Netherlands, Atmos. Chem. Phys., 11, 2281-2294, doi: 10.5194/acp-11-2281-2011, 2011.

Whitten, G., Hogo, H., and Killus, J.: The Carbon Bond Mechanism for photochemical smog, Environ. Sci. Technol., 14, 14690-14700, 1980.

Wichink Kruit, R., Schaap, M., Sauter, F., Van der Swaluw, E., Weijers, E.: Improving the understanding of secondary inorganic aerosol distribution over the Netherlands. TNO report TNO-060-UT-2012-00334, 2012.

Wilson, R. C., Fleming, Z. L., Monks, P. S., Clain, G., Henne, S., Konovalov, I. B., Szopa, S., and Menut,

L.: Have primary emission reduction measures reduced ozone across Europe? An analysis of European rural background ozone trends 1996-2005, Atmos. Chem. Phys., 12, 437-454, doi:10.5194/acp-12-437-2012, 2012.

Yarwood, G., Morris, R. E., and Wilson, G. M.: Particulate Matter Source Apportionment Technology (PSAT) in the CAMX photochemical grid model, Air Pollution Modeling and Its Application XVII, 478-492, Springer US, 2007.

Supplementary material to 'Dynamic model evaluation for secondary inorganic aerosol and its precursors over Europe between 1990 and 2009'

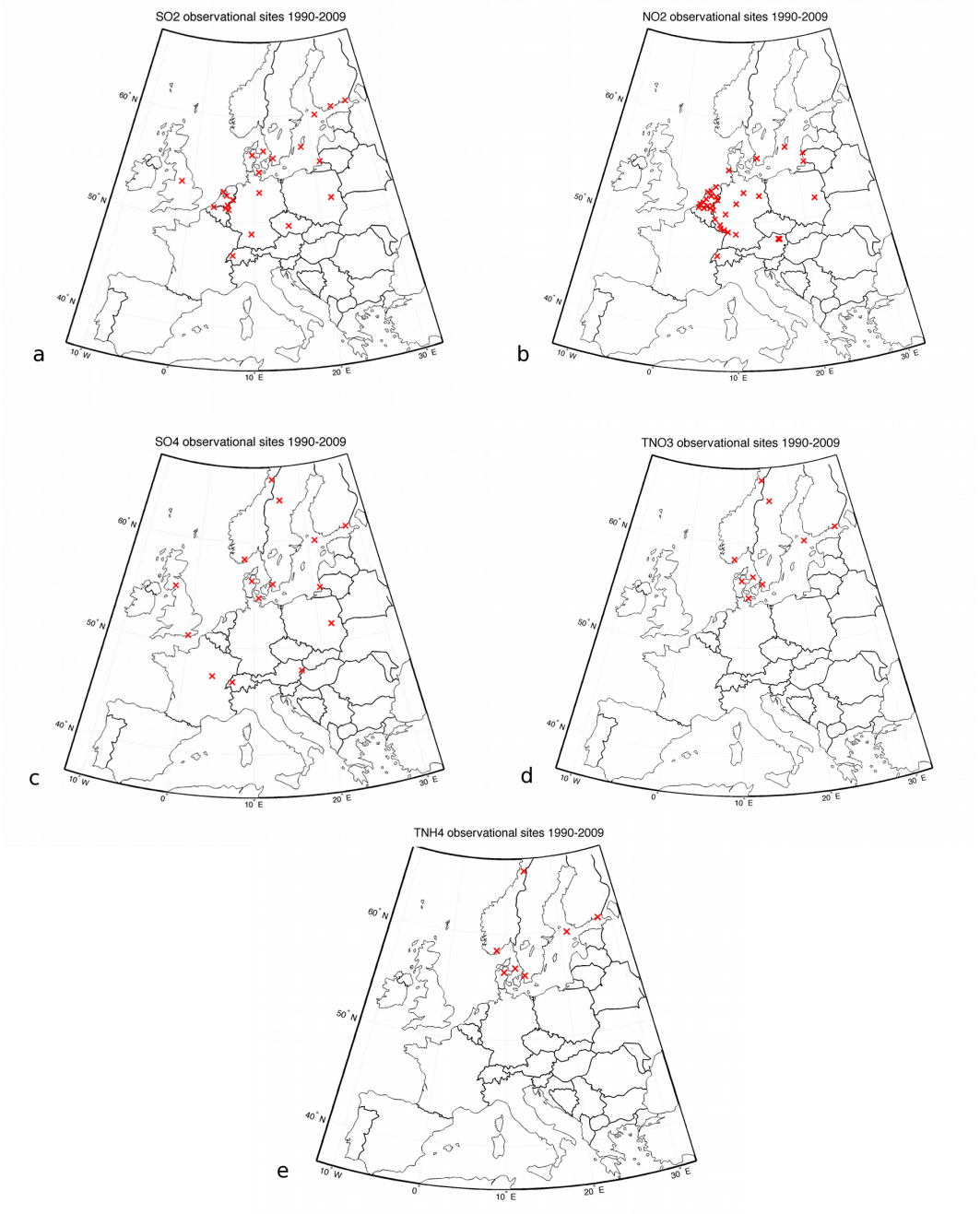

Figure 5.9 Locations of the observational sites used for the analysis of the different components for the 1990 to 2009 time period.

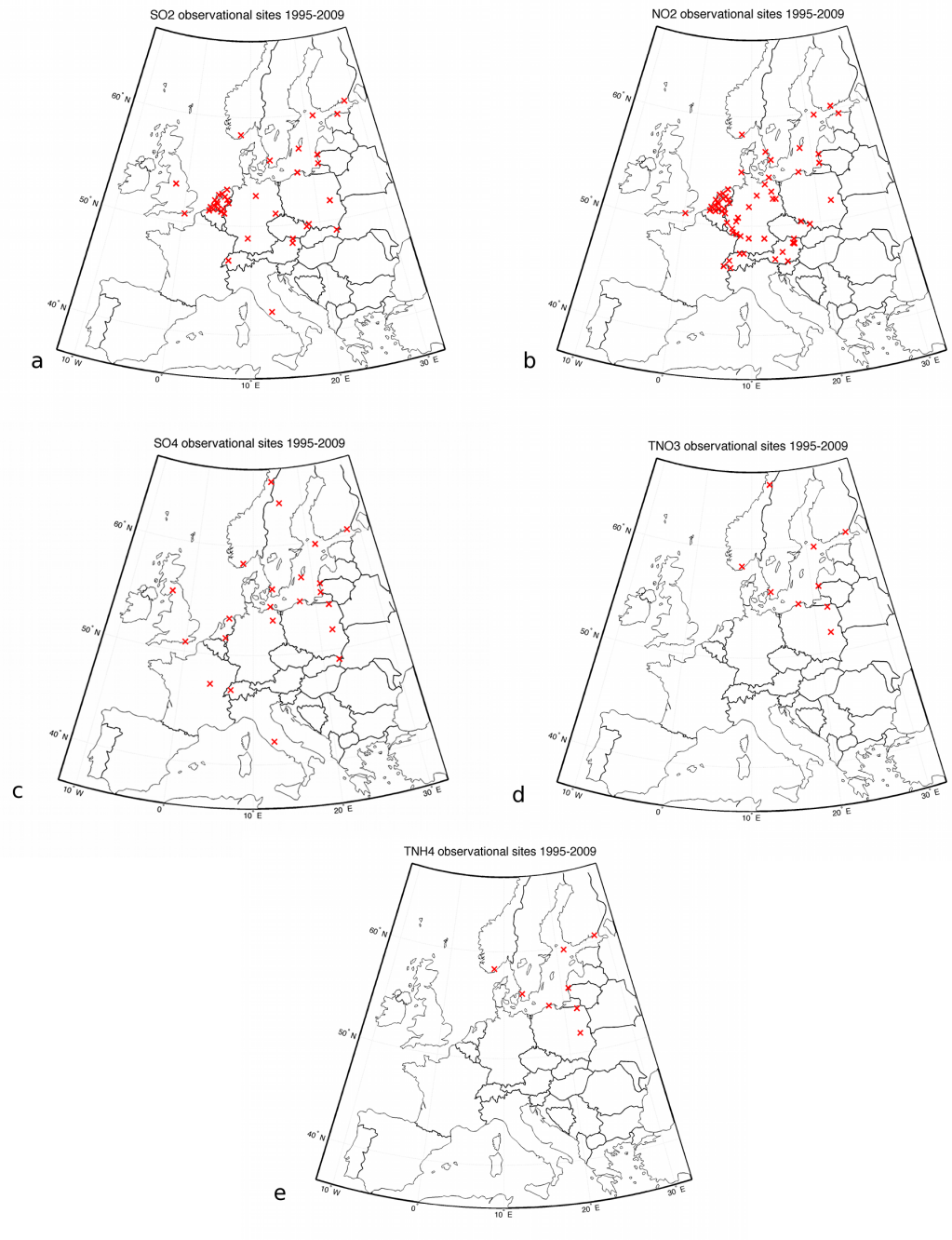

Figure 5.10 As Figure 5.9 for the 1995 to 2009 time period.

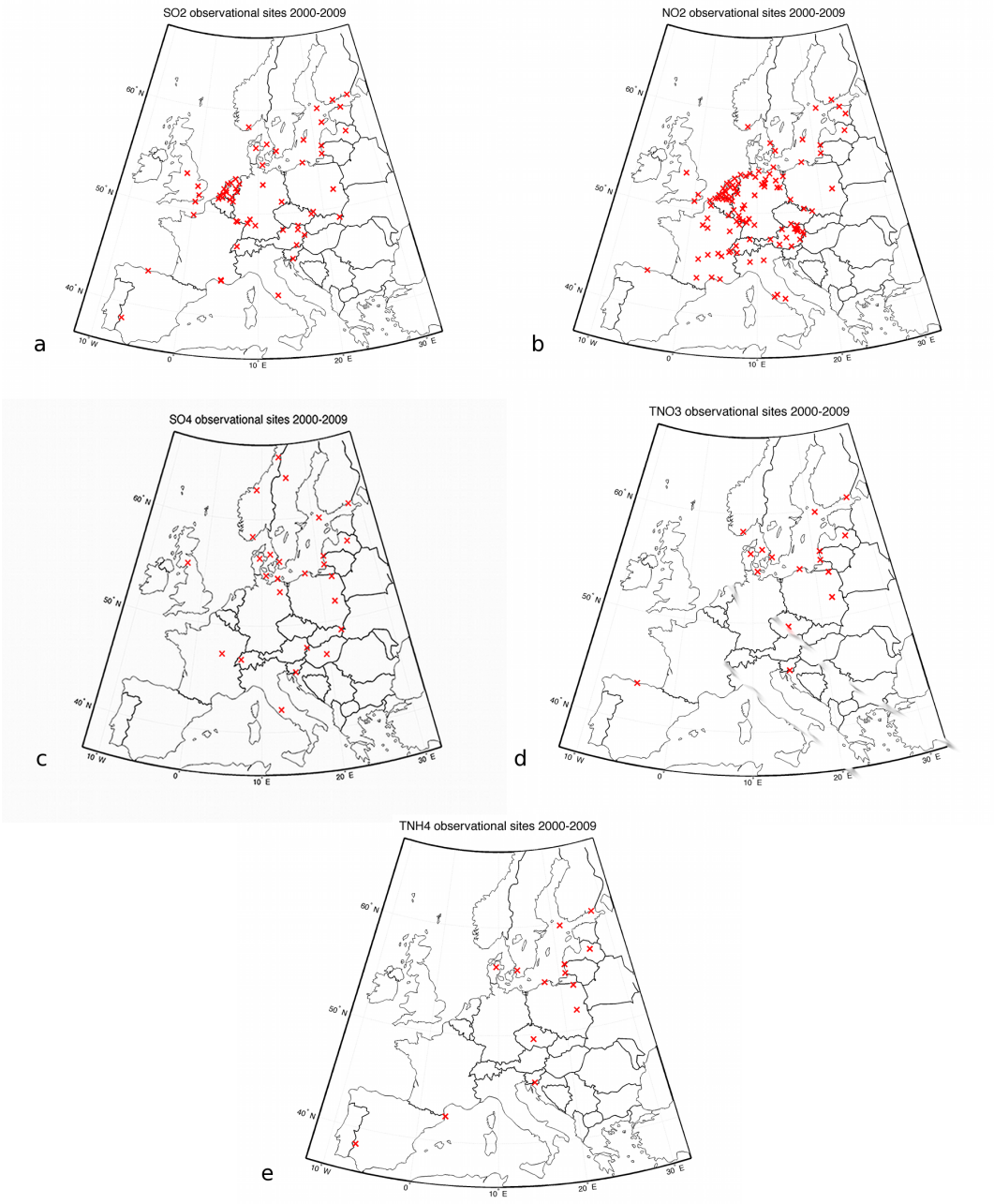

Figure 5.11 As Figure 5.9 for the 2000 to 2009 time period.

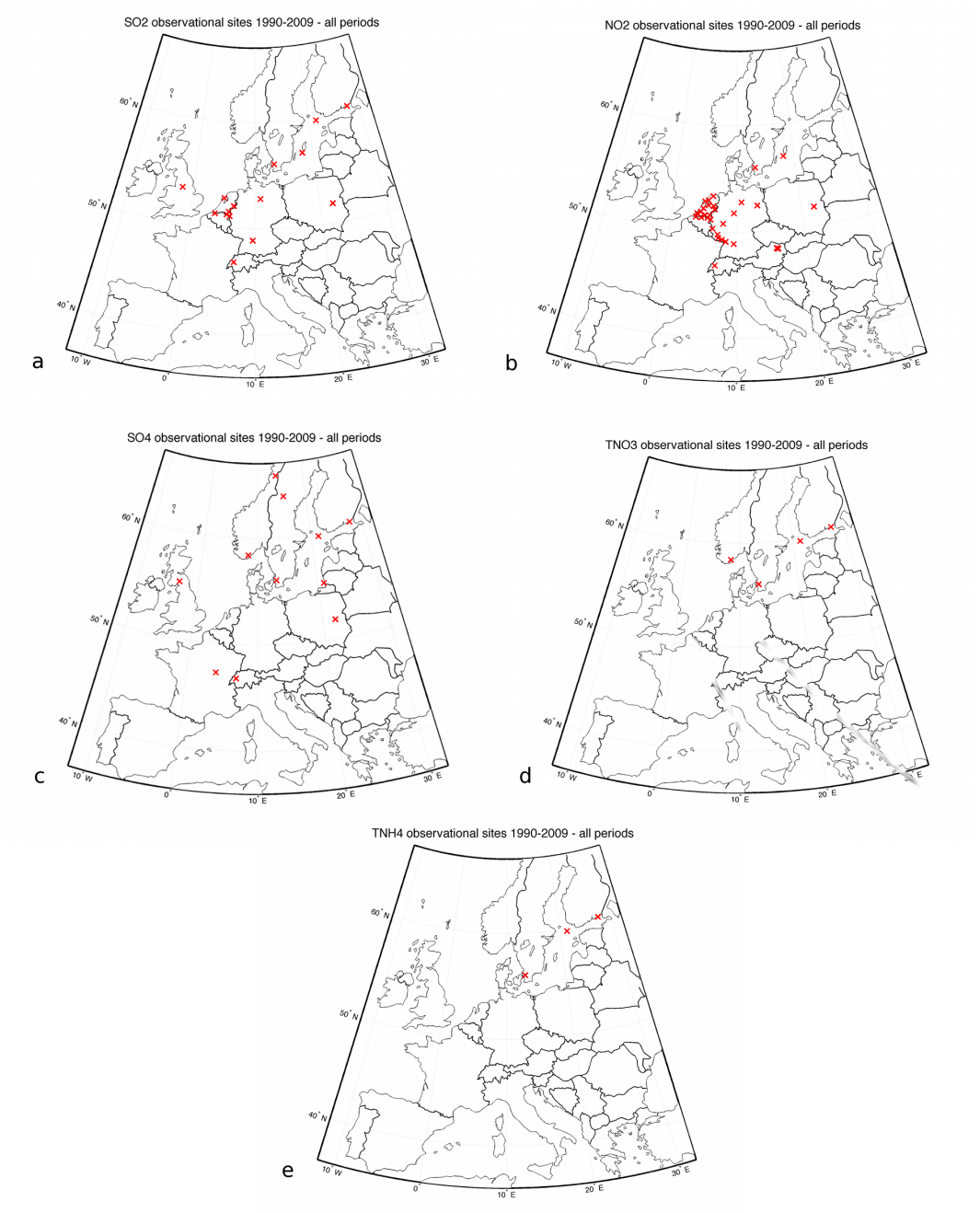

Figure 5.12 Locations of the observational sites used for the analysis of the different components when considering only those stations that pass the data selection criteria for all three periods.

Chapter 6

Overall conclusions and outlook

6.1 Overall conclusions

In the previous chapters the research aims and the research questions defined in section 1.7 have been addressed. Results on the improvement of the description of SIA formation and removal processes within a state-of-the-art CTM, the impact of the improved description on the model results, the observed and modelled responses of SIA to emission changes over Europe, and the ability of a state-of-the-art CTM to explain the non-linearity in the observed emission-concentration relationship have been presented. In the following the main conclusions from the previous chapters and the new elements that resulted from this study are summerised.

Within the study described in Chapter 3 an upgraded description of aqueous-phase chemistry and a new wet deposition scheme including cloud liquid water content dependent in-cloud scavenging and pH dependent droplet saturation have been implemented in the CTM RCG. A sensitivity study varying cloud and rain droplet pH has been performed and it was found that modelled air concentrations of SIA and its precursors as well as wet deposition fluxes of S and N are significantly affected by droplet pH variation within atmospheric ranges. Applying a droplet pH of 5.5 within the aqueous-phase chemistry and the gas wet scavenging scheme increased the modelled mean sulphate air concentrations by up to 10% compared to the base run (pH= 5) while the sulphur dioxide domain wet deposition sum increased by 110%. Furthermore it was found that the effect on sulphate formation in clouds in between precipitation events and prior to rain out dominates the impact of pH variations. While modelled burdens of S and reduced nitrogen were found to be sensitive to pH variations the oxidized nitrogen components showed negligible sensitivity.

As the sensitivity study revealed that droplet pH variations have a significant impact on resultant model air concentrations and wet deposition fluxes a model run using modelled

droplet pH has been performed and compared to a model run applying a constant pH of 5 and to observations. The results have shown that using a variable droplet pH improves the model performance concerning air concentrations and wet deposition fluxes of the investigated sulphur and nitrogen compounds. For sulphate and sulphur dioxide air concentrations the RMSE was reduced by 8% and 16%, respectively, for the investigation period in summer 2005. For the same time period the RMSE concerning SO_x wet deposition fluxes decreased by 16% when using modelled droplet pH. The results have revealed that applying a variable droplet pH is preferable to using a constant pH leading to better consistency concerning air concentrations and wet deposition fluxes. Within the study presented in Chapter 3 the first two research questions specified in section 1.7, concerning the improvement of the modelling of SIA within a state-of-the-art CTM and the sensitivity of model results to droplet pH variations have been addressed.

Using the improved RCG model system including modelled droplet pH two high PM episodes over Central Europe in spring 2009 have been analysed within the study presented in Chapter 4. These PM episodes had not been investigated prior to the study. Model simulations have been performed for a domain covering Europe (European domain) and a nested domain covering Germany (German domain). The model performed well in capturing the temporal variation of the PM_{10} and SIA concentrations and was successfully used to analyse the origin, development and characteristics of the investigated episodes. The two SIA episodes were found to be of different origin. For the first episode SIA was mainly formed outside the German domain while within the second episode the high SIA concentrations originated from local sources within the German domain.
Furthermore, sulphur dioxide, nitrogen oxides and ammonia emissions have been varied to study the response of modelled SIA concentrations and deposition fluxes of S and N to changes in precursor gas emissions during the investigated PM episodes. The response was found to be non-linear meaning that the reduction in SIA concentration and deposition fluxes of S and N and the reduction of precursor emissions are not one to one. The deviation from linearity was found to be lower for the total deposition fluxes than for SIA concentrations. Furthermore, the study has shown that incorporating explicit cloud chemistry in the model adds non-linear responses to the system and significantly modifies the response of modelled SIA concentrations and S and N deposition fluxes to changes in precursor emissions. When ammonia emissions are decreased, sulphate is reduced due to a reduced neutralisation of cloud acidity through the variable droplet pH approach, which is not accounted for when using constant droplet pH. Thus, using a modelled droplet pH accounts for an additional sulphate reduction, while the decrease in SIA concentrations results solely from a decrease in nitrate and ammonium concentrations when assuming a constant droplet pH.

The impact of national measures compared to European-wide mitigation efforts has been studied by means of several reduction scenarios with decreased SIA precursor emissions within the German domain only or within the European domain. The results indicate that important source areas are located upwind of Germany and long range transport adds a significant fraction to the locally formed SIA. Therefore, decreasing emissions on the European domain is more effective for all performed emission scenarios in reducing SIA concentration and total deposition fluxes within the German domain than reducing emissions on the German domain only. The latter confirms that a European-wide mitigation strategy is essential to achieve substantial pollutant concentration reductions. The analysis of the emission reduction scenario runs on the German domain revealed that sulphate and nitrate concentrations are only slightly reduced when reducing emissions of sulphur dioxide and nitrogen oxides simultaneously. In contrast, nitrate is significantly reduced when solely ammonia emissions are reduced. The results demonstrate that next to European-wide emission reductions additional national ammonia measures in Germany are more effective in reducing SIA concentrations and deposition fluxes than additional national measures on sulphur dioxide and nitrogen oxides.
Moreover, the potential of control strategies concerning SIA and PM reduction was found to be strongly connected to the specific emission regime of the investigated region. The results indicate that ammonia measures lead to highest SIA reduction in areas with moderate and low ammonia emission densities. In these regions SIA formation is limited by the availability of ammonia while in ammonia-rich areas SIA formation is limited by nitric acid. Following a reduction of ammonia in these nitric acid-limited regimes a sufficient amount of ammonia remains to neutralize the available nitric acid. Within the study presented in Chapter 4 the next four research questions specified in section 1.7, concerning the investigation of the origin, development and characteristics of PM_{10} episodes, as well as the sensitivity of modelled SIA levels to precursor emission changes, the impact of the improved cloud chemistry and wet scavenging descriptions on the modelled response and the effectiveness of different reduction scenarios on the European and the national domain have been addressed.

After studying the modelled responses of SIA concentrations to changes in precursor emissions a dynamic model evaluation of the CTM LOTOS-EUROS including the aqueous phase chemistry scheme developed in Chapter 3 has been performed over Europe from 1990 to 2009. The results are presented in Chapter 5. The ability of the model to reproduce the observed non-linear responses to emission changes and inter-annual variability of SIA and its precursors over Europe from 1990 to 2009 has been analysed. As emission reductions did not proceed linearly and in line with each other from 1990-2009, the time periods 1995-2009 and 2000-2009 have also been investigated to assess the sensitivity of

the trend to the different time periods. The 20 year simulation was performed using a consistent set of meteorological data provided by the regional climate model RACMO2. Observations at European rural background sites have been used as reference for the model evaluation. A visual screening of the measurement data has revealed that a large fraction of the stations with long time series were not useable as data quality was obviously an issue. The number of defective time series was found to be highest for the 1990s and decreased considerably towards 2009. Furthermore, a lack of a long-term time series for southern and parts of western and eastern Europe hampered an evaluation across the full European domain.

The study has shown that the LOTOS-EUROS model is able to capture a large part of the day-to-day, seasonal and interannual variability of SIA and its precursors' concentrations. Also, the analysis has revealed that the model is able to simulate the declining observed trends for all considered sulphur and nitrogen components following the implemented emission abatement strategies for SIA precursors over Europe. Both, the observations and the model show the largest part of the decline in the 1990s while smaller concentration changes and an increasing number of non-significant trends are observed and modelled between 2000-2009.

However, LOTOS-EUROS underestimates the observed nitrogen dioxide concentrations throughout the whole time period, while it overestimates the observed nitrogen dioxide concentration trends. Moreover, generally it was found that the model performs better in capturing the observed temporal variability and trends for the later time periods. The model results suggest that the emission information of the early 1990s used in this study needs to be improved concerning magnitude and spatial distribution. Furthermore, the improved quality of observations may also contribute to the improved model performance for the more recent time period.

The analysis of the results have confirmed former studies showing that the observed trends in sulphate and total nitrate concentrations from 1990 to 2009 are significantly lower than the trends in precursor emissions and precursor concentrations. The model well captured these non-linear responses to the emission changes. Using the LOTOS-EUROS source apportionment module trends in formation efficiency of SIA have been quantified for the four European regions 'Netherlands and Belgium', 'Baltic Sea', 'Czech Republic' and 'Romania'. The exercise has revealed a 20-50% more efficient sulphate formation in 2009 compared to 1990 for the considered regions. The major driver for the increased sulphate formation efficiency in the model has been an increasing neutralisation of cloud acidity and thus pH over time leading to a higher rate of aqueous phase oxidation of dissolved sulphur dioxide by ozone. Moreover, for the Benelux region a 20% more efficient nitrate formation per unit nitrogen oxides emission has been found. It is concluded that the

latter may be attributed to a shift in the equilibrium between nitric acid and ammonium nitrate towards particulate phase, caused by reduced sulphate concentrations from 1990 to 2009. An additional reason may be attributed to a change in the oxidant levels and a more detailed budget analysis is needed to further study the changes in chemical regime. However, by means of the source apportionment exercise, trends in formation efficiency of SIA have been quantified adding to the explanation of the non-linearities in the emission-concentration relationship of SIA and its precursor emissions. Herewith in Chapter 5, the remaining three research questions concerning the observed trends in SIA over Europe for different time periods between 1990 and 2009 and the ability of a state-of-the-art CTM to capture the observed trends and the corresponding non-linear responses to emission changes, as well as modelled trends in gas-to-particle conversion have been addressed.
Overall, the results have demonstrated that the explicit description of droplet pH has a significant impact on resultant model air concentrations and wet deposition fluxes and that modelling droplet pH is preferable to using a constant pH leading to better model consistency concerning air concentrations and wet deposition fluxes. The study has highlighted the non-linear response of modelled SIA concentrations and deposition fluxes of S and N to changes in precursor emissions. Incorporating explicit cloud chemistry in the model added non-linear responses to the system and significantly modified the models' response to precursor emission variations. Furthermore, the investigation has highlighted the important role of ammonia in the emission-concentration relationship as it drives the partitioning of nitrate between gas phase nitric acid and particulate ammonium nitrate and it constrains cloud droplet pH, which regulates the oxidation pathway of sulphur dioxide and therewith the formation efficiency of sulphate. Finally a dynamic model evaluation of the LOTOS-EUROS CTM aimed at SIA formation in Europe between 1990 and 2009 has shown that the model is able to capture the non-linearity in the emission-concentration relationship detected in the observations. Moreover, the performed source apportionment analysis has confirmed that changes in the formation efficiency due to changes in the chemical regime are at the basis of these non-linearities.
With this modelling study, added knowledge and an improved understanding has been obtained with respect to the non-linearity between emissions of N- and S-compounds and the resulting concentrations and deposition.

6.2 Outlook

CTMs provide fundamental information on the atmospheric aerosol burdens in combination with in-situ observations and remote sensing data. The models are important tools to investigate the interlinkages within and between atmospheric chemistry, physi-

cal processes and dynamics. The continuous model development and evaluation over the last decades have considerably improved the confidence in the CTM results. However, the models remain idealized tools exhibiting uncertainties. These could be related to missing compounds, processes and/or dependencies resulting in a further need of model development. Moreover, the model accuracy strongly depends on the accuracy of input parameter. Below, we discuss a few major research directions to expand on this thesis.

This study has highlighted the important role of ammonia in the emission-concentration relationship. However, among the precursor emissions, those of ammonia inherit the largest uncertainty in quantity, space and time and an improvement of the quality of ammonia emission inventories is needed. Furthermore, more knowledge on the ammonia emissions as function of ambient conditions, season and region throughout Europe and its consideration in the CTMs is needed. The latter could be implemented by developing a dynamical emission module taking into account regional specific factors and meteorology for the agricultural emission sector. Evaluation of such a model approach is a challenge as the availability of ammonia measurements is limited. This is especially the case for highly temporally resolved data.

In this respect, the recently discovered capability of advanced IR-sounders (e.g. Infrared Atmospheric Sounding Interferometer (IASI)) to probe atmospheric ammonia from satellite offers potential to contribute to the improvement of the emission inventories. As emission variability in space and time is generally important, all emission sectors should be included in the dynamical emission module.

An improved temporal and spatial ammonia emission information may also improve droplet pH calculation, which within this study was found to be sensitive to ammonia emission regimes. Also, the consideration of the effects of other buffering systems such as sea salt, mineral dust and organic components may further improve the droplet pH determination. Moreover, also organic compounds can be oxidised to organic acids, lowering cloud (and subsequently rain) water pH which is not accounted for within the droplet pH calculation. A follow up study focussing on improving the description of the chemistry of organics within the model should be performed.

The analyses of the 20 year LOTOS-EUROS run has revealed many interesting features and resulting research questions that should be addressed by means of the 20 years model simulation. Specific attention is needed to address the trends in nitrogen dioxide. The trend assessment could be improved by extending the study including long-term satellite measurements of nitrogen dioxide (e.g. derived from GOME and SCIAMACHY instruments). Furthermore, as nitrogen dioxide is a primary pollutant dominated by anthropogenic sources a close look at the emission data for Europe is needed. Traffic emissions dominate the emission total of nitrogen oxides in Europe and should be evaluated carefully.

Especially the verification if technological developments in engine technology (EURO 4 and 5 standards) delivered what they were aimed to and the assessment of the impact of using real world emission factors are necessary.

To further complement the budget analysis, trends in wet and dry deposition of sulphur and nitrogen compounds from 1990 to 2009 should be investigated. Unfortunately, the evaluation of modelled trends in dry deposition is not possible by the lack of observations. Furthermore, the analysis should be extended by investigating trends, and shifts in seasonal variability over time of ozone to gain insight on the changes in oxidant levels induced by the emission changes from 1990 to 2009.

Further attention should be given to the models' inability to reproduce high sulphate concentration episodes. These episodes are often observed during winter and spring under stagnant weather conditions characterized by low inversion heights, very stable conditions and low wind speeds. Previous studies have shown that prognostic weather prediction models that are used to force the CTMs tend to fail to represent these stable weather conditions satisfactorily. Further assessment and the improvement of the ability of the prognostic weather prediction models to simulate these weather conditions may contribute to an improved CTM performance during high concentration episodes.

This thesis has focussed on improving our knowledge on SIA formation and removal from the atmosphere. Hence, we focussed on SIA as constituent of particulate matter and a contributor to acid and nitrogen deposition fluxes. However, SIA is also involved in climate change by affecting the radiation balance of the earth. Recent studies have shown that short term climate mitigation aimed at reducing BC may only be effective provided that the climate impact of the co-emitted SIA precursors does not cause a net cooling impact. As ammonia constrains the concentration levels in the ammonium-sulphate-nitrate system, ammonia regimes also play a role with respect to sulphate and nitrate radiative forcing. The latter role of ammonia needs be addressed in future studies.

Appendix

Contribution to the Papers I, II and III:

The main topic of the study was formulated within the framework of the MAPESI project (BMU/UBA F&E-Vorhaben 370764200). The set-up of the study was developed by myself in discussions with colleagues at TNO. The literature study for the selection of a new wet deposition scheme was performed by myself. The improved process descriptions of aqueous-phase sulphate formation and wet scavenging were adapted to the RCG model system and implemented in the model by myself and in cooperation with TNO and RIVM. The chemistry transport model simulations used to address the scientific questions for Paper I and II were performed by myself at Freie Universität Berlin. The improved RCG routines were implemented in the LOTOS-EUROS model by colleagues at TNO in cooperation with myself. The simulations used in Paper III were prepared by myself but performed by colleagues at TNO. The literature studies, post processing of model and measurement data including plotting of figures and the analyses of results were mainly conducted by myself within all three papers. Discussion and interpretation of the results were done in cooperation with the colleagues at TNO. The papers were written by myself aided by the co-authors.

Publication list

Scientific articles

Banzhaf, S., Schaap, M., Kranenburg, R., Manders, A. M. M., Segers, A. J., Visschedijk, A. H. J., Denier van der Gon, H. A. C., Kuenen, J. J. P., van Meijgaard, E., van Ulft, L. H., Cofala, J. and Builtjes, P. J. H.: Dynamic model evaluation for secondary inorganic aerosol and its precursors over Europe between 1990 and 2009. Submitted to Atmospheric Chemistry and Physics, Mai 2014.

Wichink Kruit, R.J., Segers, A., Banzhaf, S., Kranenburg, R., Buitjes, P., Frommer, J., Greupel, M., Graff, A. and Schaap, M.: Assessment of nitrogen and sulfur deposition in Germany. To be submitted to Geoscientific Model Development.

Banzhaf, S., Schaap, M., Wichink Kruit, R.J., Denier van der Gon, H. A. C., Stern, R., and Builtjes, P. J. H.: Impact of emission changes on secondary inorganic aerosol episodes across Germany, Atmospheric Chemistry and Physics, 13, 11675-11693, 2013.

Banzhaf S., Schaap M. and Builtjes P.: Non-linear response of sulphur and nitrogen concentrations and deposition fluxes to emission changes. Air Pollution Modeling and its Application 22, 547-552, Springer, 2013.

Banzhaf, S., Schaap, M., Kerschbaumer, A., Reimer, E., Stern, R., van der Swaluw, E. and Builtjes, P.: Implementation and evaluation of pH-dependent cloud chemistry and wet deposition in the chemical transport model REM-Calgrid. Atmospheric Environment 49, 378-390, 2012.

Banzhaf, S., Schaap, M., Kerschbaumer, A., Reimer, E.,Stern, R., van der Swaluw, E. and Builtjes, P.: Wet Deposition: Model Development and Evaluation. Air Pollution Modeling and its Application 21, 459-465, Springer, 2011.

van der Swaluw, E., Schaap, M., Sauter, F., Banzhaf, S. and Manders, A.: Measuring and modeling wet deposition fluxes in the Netherlands and Europe. Air Pollution Modeling and its Application 21, 193-198, Springer, 2011.

Reports

Builtjes, P., Hendriks, E., Koenen, M., Schaap, M., Banzhaf, S., Kerschbaumer, A., Gauger, T., Nagel, H.-D., Scheuschner, T., Schlutow, A.: Erfassung, Prognose und Bewertung von Stoffeinträgen und ihren Wirkungen in Deutschland; Modelling of Air Pollutants and Ecosystem Impact (MAPESI). Abschlussbericht Förderkennzeichen (UFO-PLAN) 3707 64 200, Umweltbundesamt, 2011.

Presentations

Banzhaf, S., Schaap, M., Kranenburg, R., Manders, A. M. M., Segers, A. J., Visschedijk, A. H. J., Denier van der Gon, H. A. C., Kuenen, J. J. P., Hendriks, C. van Meijgaard, E., van Ulft, L. H., Cofala, J., Builtjes, P. J. H.: Can we explain the observed decrease in secondary inorganic aerosol and its precursors between 1990 and 2009 over Europe using LOTOS-EUROS? 9th International Conference on Air Quality, Garmisch-Partenkirchen, Germany, 24-28 March, 2014.

Banzhaf, S., Schaap, M., Wichink Kruit, R., Builtjes, P. J. H.: Modellierung der nassen und feuchten Deposition: Weiterentwicklung und Evaluation. Fachgespräch "Atmosphärische Deposition", Umweltbundesamt, Dessau, Germany, 10-11 Feb., 2014.

Banzhaf, S., Schaap, M., Kranenburg, R., Manders, A. M. M., Segers, A. J., Visschedijk, A. H. J., Denier van der Gon, H. A. C., Kuenen, J. J. P., Hendriks, C. van Meijgaard, E., van Ulft, L. H., Cofala, J., Builtjes, P. J. H.: Can we explain the observed decrease in secondary inorganic aerosol and its precursors between 1990 and 2009 over Europe using LOTOS-EUROS? 33rd ITM on Air Pollution Modelling and its Application, Miami, Florida USA, 26-30 Aug., 2013.

Banzhaf, S., Schaap, M., Wichink Kruit, R., Stern, R., Builtjes, P.: Response of PM_{10} concentrations across Germany to emission changes during PM_{10} episodes in spring 2009. 32nd ITM on Air Pollution Modelling and its Application, Utrecht, The Netherlands, 7-11 May, 2012.

Banzhaf, S., O'Connor, E.J., Schaap, M., Kerschbaumer, A., Builtjes, P.: Estimation of the impact of uncertainties in meteorological parameters on modelled concentrations and wet deposition fluxes. 11th EMS/10th ECAM, Berlin, Germany, 12-16 Sept., 2011.

Banzhaf, S., Schaap, M., Kerschbaumer, A., Reimer, E.,Stern, R., van der Swaluw, E., Builtjes, P.: Wet Deposition: Model Development and Evaluation. 31th ITM on Air Pollution Modelling and its Application, Torino, Italy, 27. Sept.- 01. Oct., 2010.

Banzhaf, S., Reimer, E., Kerschbaumer, A., Builtjes, P., Schaap, M., Stern R.: Simulation of Wet Deposition with the CTM REM-CALGRID using a diagnostic and a prognostic meteorological driver. 9th EMS/9th ECAM, Toulouse, France, 28 Sept.-02 Oct., 2009.

Banzhaf, S.: Parameterisation of vertical rain rate profiles for the meteorological driver of LOTOS and RCG. GLOREAM, Berlin, Germany, 28-30 Nov., 2007.

Posters

Kerschbaumer, A., Banzhaf, S., Builtjes, P.: Model Evaluation with respect to Deposition processes. 13th International Conference on Harmonisation within Atmospheric Dispersion Modelling for Regulatory Purposes, Paris, 1-4 June, 2010.

Banzhaf, S., Reimer, E., Kerschbaumer, A., Builtjes, P.: Wet deposition simulations based on meteorological objective analyses. EMS Annual Meeting, Amsterdam, 29. Sept.-03.Oct., 2008.

Danksagung

An dieser Stelle möchte ich mich gerne bei allen bedanken, die mich bei meiner Arbeit unterstützt haben.
Mein ganz besonderer Dank gilt Prof. Peter Builtjes für die Betreuung der Dissertation und die gemeinsame Projektarbeit innerhalb der letzten Jahre. Ich danke Dir für Dein Vertrauen, dass ich die Freiheit hatte weitgehend unabhängig und selbstständig zu arbeiten und dafür, dass Du immer für wissenschaftliche Diskussion und moralische Unterstützung erreichbar warst. Ich danke Dir auch für die Organisation meiner Aufenthalte bei der TNO in Utrecht, die die enge Zusammenarbeit mit den Kollegen bei TNO ermöglicht haben. Und vielen Dank, dass Du die Luftchemie an der FU nie aufgegeben hast.
My special thanks go to Martijn Schaap for your scientific guidance throughout this PhD and the many productive and motivating discussions. Thank you that you always managed to take time for the thorough reading and correction of the paper drafts. You have taught me a lot about writing scientific articles and I enjoy working with you.
Mein Dank gilt auch Andreas Kerschbaumer für die Zusammenarbeit zu Beginn meiner Arbeit und insbesondere die technische Unterstützung im Umgang mit RCG bis in die späten Abendstunden. Wenn Du nicht Adamello erschaffen hättest, hätte ich noch lange unter Windows gelitten.
Ich möchte mich auch bei meinen (ehemaligen) TrUmF Kollegen, insbesondere Eberhard Reimer, der mir die Arbeit bei TrUmF überhaupt erst ermöglicht hat, und Rainer Stern bedanken. Ich habe viel von Euch gelernt und freue mich Euch regelmäßig beim Stammtisch zu treffen.
Vielen Dank an Prof. Uwe Ulbrich für das Übernehmen des Zweitgutachtens und die stetige Unterstützung.
I would like to thank the air quality modelling group at TNO for their support and scientific input throughout this study. I always felt welcome and enjoyed the time in Utrecht with you.
Ich möchte mich auch bei Andrea Mues für die schöne gemeinsame Zeit im Büro und insbesondere für die bis heute sehr hilfreichen Tafelbeschriftungen bedanken.
Vielen Dank an das PINETI Projekt Konsortium, Thomas Scheuschner, Hans-Dieter Na-

gel, Markus Geupel, Jakob Frommer und insbesondere Roy Wichink Kruit für die gute und harmonische Zusammenarbeit innerhalb des Projektes und die vielen anregenden Diskussionen.
Vielen Dank auch an Thomas Bergmann für die viele und immer schnelle technische Hilfe.
Ich bedanke mich auch bei meiner immer wechselnden Mittagstischrunde, die stets für die perfekte Ablenkung zwischendurch sorgte.
Mein größter Dank jedoch gilt meiner Familie, insbesondere meinen Eltern Hermann und Ute und meinem Bruder Michael, meinem Freund Lionel und meinen Freunden, insbesondere Robinson, Max und Mareike, die mich uneingeschränkt unterstützt haben und immer an mich geglaubt haben und deren Rat ich nicht missen möchte.

Selbstständigkeitserklärung

Hiermit erkläre ich an Eides Statt, dass ich die vorliegende Arbeit selbstständig und ohne fremde Hilfe angefertigt, keine anderen als die angegebenen Quellen und Hilfsmittel benutzt und die den benutzten Quellen wörtlich oder inhaltlich entnommenen Stellen als solche kenntlich gemacht habe.
Diese Arbeit hat in gleicher oder ähnlicher Form noch keiner Prüfungsbehörde vorgelegen.

Sabine Banzhaf
Berlin, den 12.05.2014